EPIGENETIC REGULATION OF SOMATOSTATIN RECEPTORS IN NEUROENDOCRINE TUMORS

A Novel Therapeutic Approach?

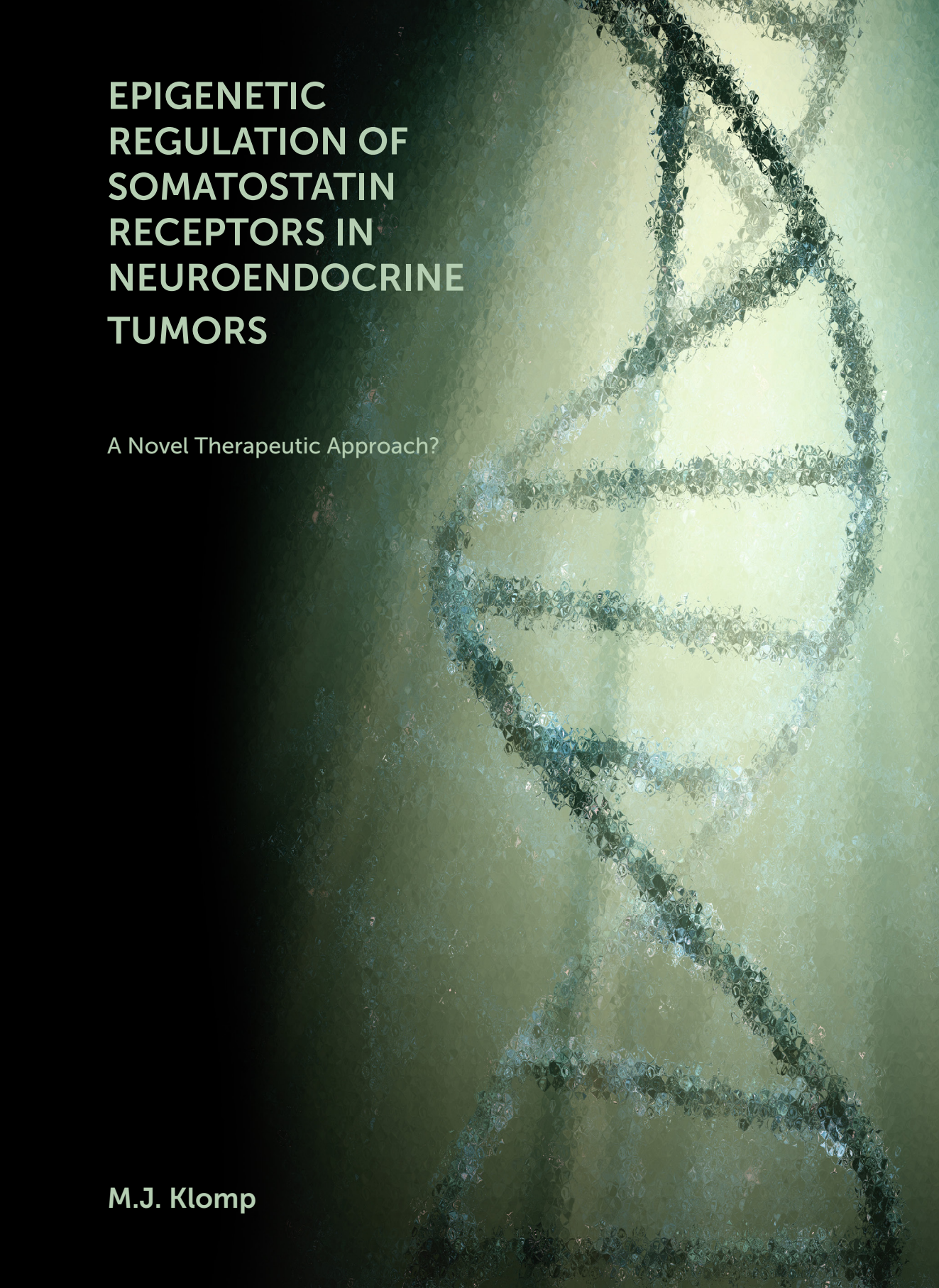

M.J. Klomp

Epigenetic Regulation of Somatostatin Receptors in Neuroendocrine Tumors

A novel therapeutic approach?

Maria Johanna Klomp

ISBN 978-94-6473-252-8

Cover design : Ilse Modder | www.ilsemodder.nl
Printed by: Proefschriften.nl

Epigenetic Regulation of Somatostatin Receptors in Neuroendocrine Tumors

A novel therapeutic approach?

Epigenetische regulatie van somatostatine receptoren in neuroendocriene tumoren

Een nieuwe therapeutische benadering?

Thesis

to obtain the degree of Doctor from the
Erasmus University Rotterdam
by command of the
rector magnificus

Prof. dr. A.L. Bredenoord

and in accordance with the decision of the Doctorate Board.
The public defence shall be held on

Friday 10 November 2023 at 10.30 hrs
by

Maria Johanna Klomp
born in 's-Hertogenbosch

Erasmus University Rotterdam

DOCTORAL COMMITTEE

PROMOTORS:

Prof. dr. L.J. Hofland

Prof. dr. C.W.G.M. Löwik

Prof. dr. ir. M. de Jong *

OTHER MEMBERS:

Prof. dr. J.W.M. Martens

Prof. dr. A.C. Dingemans

Dr. D.J. Vugts

COPROMOTOR:

Dr. S.U. Dalm

* In memoriam

TABLE OF CONTENTS

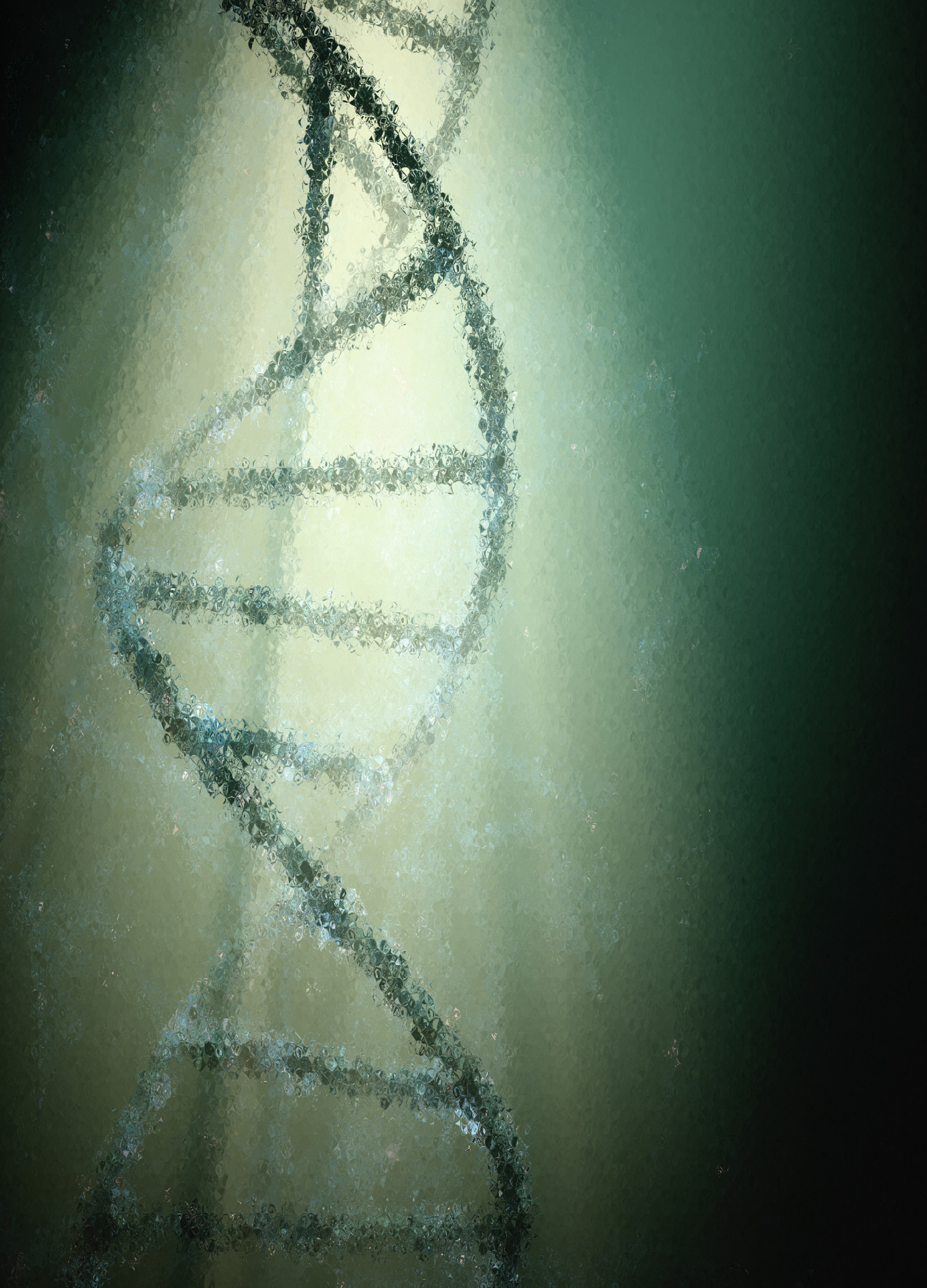

CHAPTER 1

General Introduction and Thesis Outline

Parts of this chapter are based on:

M.J. Klomp[1,2], S.U. Dalm[2], M. de Jong[2], R.A. Feelders[1], J. Hofland[1], L.J. Hofland[1].

[1] Department of Internal Medicine, Division of Endocrinology, Erasmus MC, 3015 GD Rotterdam, The Netherlands. [2] Department of Radiology & Nuclear Medicine, Erasmus MC, 3015 GD, Rotterdam, The Netherlands.

Reviews in Endocrine & Metabolic Disorders. 2021 Sep; 22(3):495-510

PART I

1. NEUROENDOCRINE TUMORS

Neuroendocrine tumors (NETs) and neuroendocrine carcinomas (NECs) together constitute neuroendocrine neoplasms (NENs), which arise from neuroendocrine cells found throughout the entire body and, consequently, represent a heterogeneous disease. NECs are characterized as poorly-differentiated grade 3 (G3) carcinomas with a Ki-67 index higher than 20% and more than 20 mitoses per 2 mm^2, and only represent 10-20% of all NENs. In contrast, NETs are well-differentiated and divided into grade 1 (G1), grade 2 (G2) and G3, characterized by a Ki-67 index and mitotic count per 2 mm^2 of, respectively, < 3% and < 2 for G1, 3-20% and 2-20 for G2, and > 20% and > 20 for G3 [1]. Both the tumor grade and disease stage, the latter assessed with the tumor, node and metastasis (TNM) staging system, are prognostic parameters and important in determining the disease management strategy [1, 2].

A population-based study of 64.971 patients [3], using the Surveillance, Epidemiology, and End Results (SEER) database, showed that the age-adjusted incidence of NETs increased over time, reaching 6.98 per 100.000 people in 2012. The reported incidence per 100.000 people per site of origin is 1.49 and 3.56 for lung and gastroenteropancreatic (GEP) sites, respectively, of which the small intestine, rectum and pancreas are the most abundantly reported sites for NETs within the GEP tract. In addition to classifications based on the primary tumor site, tumor grade and disease stage, NETs can be classified into non-functional and functional NETs. NETs demonstrating increased hormone secretion (e.g. serotonin and insulin) resulting into clinical symptoms are referred to as functional NETs. For example, functional small intestinal NETs (SI-NET) can cause carcinoid syndrome associated with complaints as diarrhea and flushing [4].

In contrast to the above-mentioned differences in NETs (i.e. site of origin, tumor grade, disease stage and whether or not hormone secreting), NETs also share similarities such as the expression of specific neuroendocrine markers (e.g. chromogranin A and synaptophysin). Furthermore, NETs frequently overexpress somatostatin receptors (SSTRs) [5, 6].

2. SOMATOSTATIN RECEPTORS

SSTRs are a family of G protein-coupled receptors, of which different subtypes exist, named SSTR1, SSTR2, SSTR3, SSTR4 and SSTR5. Alternative splicing of SSTR2 RNA generates two splice variants: SSTR2a and SSTR2b which differ in length. SSTRs can be activated by the neuropeptide somatostatin (SST), of which two isoforms are known, somatostatin-14 (SST-14) and somatostatin-28 (SST-28), both having high affinity for SSTRs [7, 8]. SST is produced by different organs in both the central nervous system, e.g. hypothalamus, and in other organs including pancreas, stomach and intestine. It is synthesized in response to multiple biological signals, for instance neurotransmitters, hormones and neuropeptides [9]. SSTR-expressing cells are found abundantly in human tissues, such as the brain, pituitary and the gastrointestinal tract [10]. The downstream pathways, activated by binding of SST to SSTRs,

are involved in regulating multiple physiological processes, i.e. inhibition of hormone secretion and cell proliferation, and induction of apoptosis [11, 12].

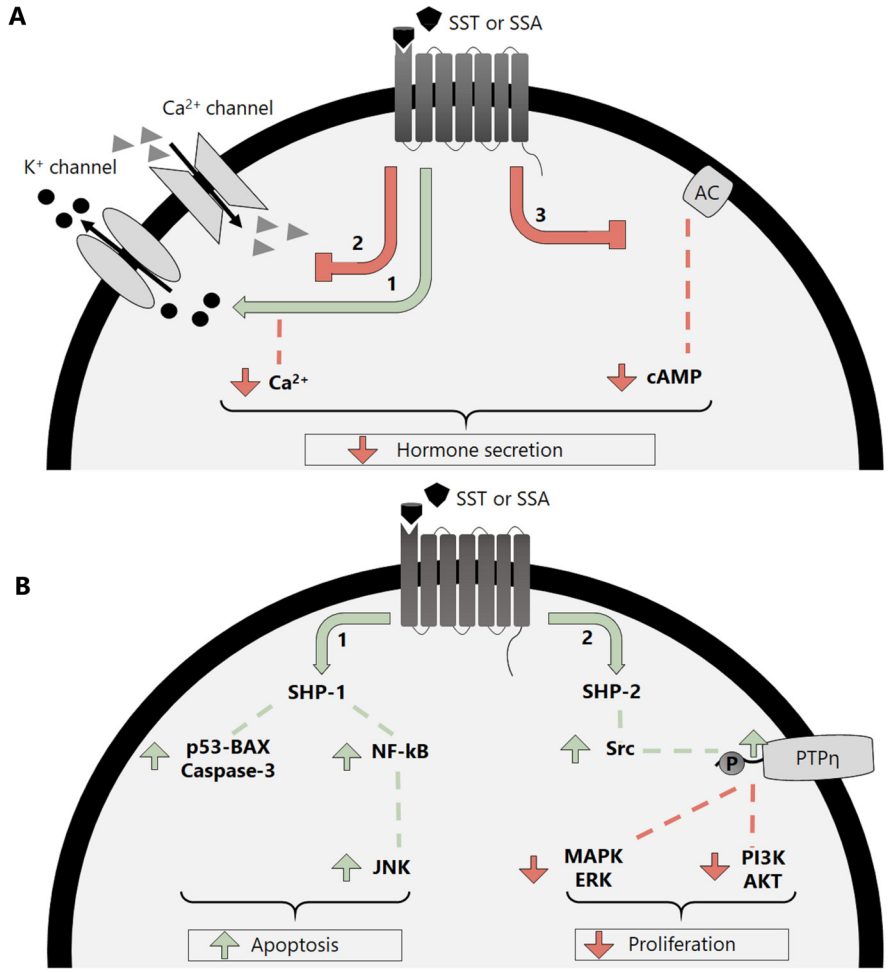

Figure 1. (A) Upon binding of somatostatin (SST) or somatostatin analogue (SSA), (1,2) K^+ channels are activated and Ca^{2+} channels are inhibited, resulting in decreased Ca^{2+} levels, and (3) adenylyl cyclase (AC) activity is inhibited thereby reducing intracellular cAMP levels. This results in inhibition of hormone secretion. **(B)** Activation of the SST-system also results in anti-tumoral activity: (1) SHP-1 is activated, thereby increasing pro-apoptotic and reducing anti-apoptotic proteins, and (2) SHP-2 is activated which results in activation of PTPη by Src-mediated phosphorylation. PTPη causes inhibition of pathways physiologically involved in cell proliferation. In both figure A and B, effects induced by SSTR activation are indicated by green (enhanced) or red (reduced) arrows. Figure is taken from [13], and used with permission from the copyright owner.

SSTR-mediated anti-secretory effects are induced via two main pathways: (1) inhibition of adenylyl cyclase (AC) resulting in reduced levels of cyclic AMP (cAMP) and (2) activation of K^+-channels and inhibition of voltage-dependent Ca^{2+}-channels resulting in reduced intracellular Ca^{2+} levels (Figure 1A). Both the reduction of cAMP and Ca^{2+} results in hormone anti-secretory

effects. Moreover, upon binding of SST to SSTR, src-homology phosphatase (SHP) proteins are activated which are involved in regulating cell proliferation and apoptosis. SHP type-1 (SHP-1) is involved in inducing apoptosis by increasing pro-apoptotic proteins, such as the p53-Bax-caspase-3 pathway, and by increasing JNK expression resulting in inhibition of anti-apoptotic proteins (Figure 1B). SHP type-2 (SHP-2) activation results in Src activity, which phosphorylates PTPη. As a result, MAPK/ERK and PI3K/ AKT proteins will be inactivated, causing upregulation of proteins involved in inhibiting proliferation (Figure 1B).

In addition to its pivotal role in physiological processes, aberrant SSTR expression has also been reported in several types of cancers, including breast cancer [14], colorectal cancer [15], prostate cancer [16, 17] and larynx cancer [18]. For prostate cancer, it was demonstrated that SSTR2 and SSTR5 are mostly expressed, i.e. in 34.8% and 56.5% of the examined prostate cancer samples, respectively [17]. In contrast, SSTR1 was expressed abundantly in 90% of primary breast cancer tissues, whereas SSTR2 and SSTR5 were expressed in a lower number of cases, i.e. 34.4% and 44.4% , respectively [19]. Moreover, as previously mentioned, it is widely known that SSTRs, more specifically receptors of subtype 2, are highly expressed on NET cells. In a study performed by Mizutani et al. [20], *SSTR* mRNA levels were measured in 13 NET samples derived from several locations. It was shown that SSTR2 is expressed in all cases. In another study, examining 112 SI-NETs, 19 pancreatic NETs (PAN-NETs) and 42 NETs derived from other locations, it was demonstrated that 65%, 76%, 90%, 86% and 93% of all cases were recognized by the expression of SSTR1, SSTR2, SSTR3, SSTR4 and SSTR5, respectively [5]. Upon discriminating low and high expression levels, SSTR2 was expressed most frequently, i.e. 51% of the examined NETs demonstrated high SSTR2 levels. In this study, it was shown that especially PAN-NETs and SI-NETs were often characterized by the expression of SSTR2.

These high SSTR2 expression levels paved the way for SSTR2-targeted treatments in NETs, including treatment with unlabeled somatostatin analogues (SSAs) [21]. SSAs have potent anti-secretory effects and thereby reduce symptoms related to the overproduction of bioactive substances in a significant proportion of NET patients [22, 23]. In addition, various studies have demonstrated that SSAs have tumor growth inhibitory actions in NET patients. Octreotide long-acting release (LAR) and lanreotide autogel are both SSAs with high affinity for SSTR2 [24]. Patients with well-differentiated metastatic midgut NETs benefited from octreotide LAR treatment, as demonstrated in a placebo-controlled study in which 85 patients were enrolled. This study showed a significantly increased time to progression from 6 to 14.3 months in the control and octreotide LAR-treated group, respectively [25]. Similar, a phase III study with lanreotide autogel in metastatic enteropancreatic NET patients reported a significantly increased progression-free survival compared to the placebo group [26].

In addition to treatment with SSAs, the overexpression of SSTR2 on NET cells is also strongly exploited for nuclear theranostic approaches, which will be described in more detail in PART II of this chapter.

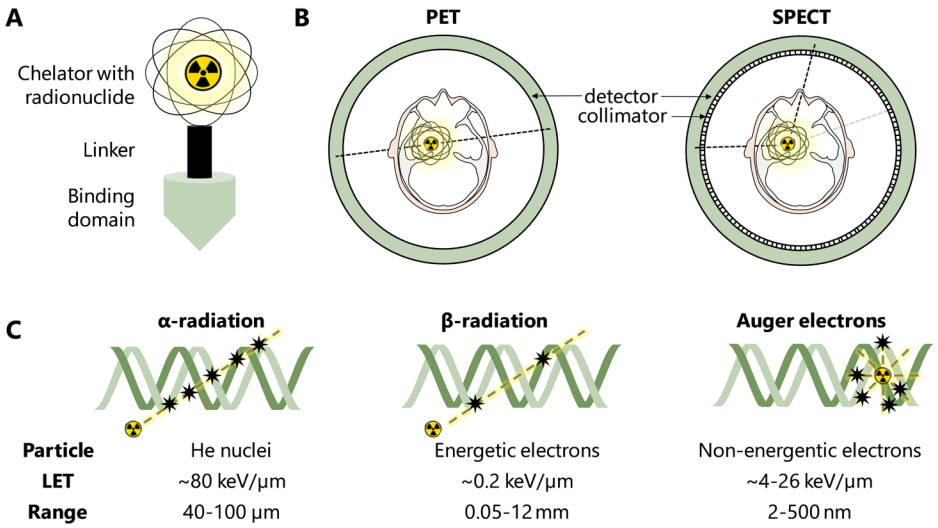

Figure 2. (A) Radiopharmaceuticals consist of a binding domain directed towards the biomarker of interest, a linker and chelator with a complexed radionuclide. (**B**) Schematic illustration of positron emission tomography (PET) and single-photon emission computed tomography (SPECT). **(C)** Alpha (α) particles, beta (β) particles and auger electrons have different biophysical properties characterized by differences in emitted particles, linear energy transfer (LET; keV/µm) and tissue penetration range (µm).

PART II

3. NUCLEAR IMAGING AND THERAPY

3.1. THERANOSTICS

The presence of biomarkers highly expressed on tumor cells (e.g. SSTR2 expression on NET cells) paved the way for targeted radionuclide imaging (diag*nostics*) and therapy (*thera*peutics), so called theranostics, for which radiopharmaceuticals are used. Such radiopharmaceuticals consist of a targeting moiety that binds with high affinity and specificity to the biomarker of interest. The radiopharmaceutical can have agonistic or antagonistic properties. Whereas antagonists bind to the biomarker without provoking physiologically downstream pathways, agonistic radiopharmaceuticals produce a similar response as the physiologically occurring activator. The targeting moiety of the radiopharmaceutical is, often via a linker, coupled to a chelator which can complex a radionuclide (Figure 2A). Radiopharmaceuticals can be applied for theranostic approaches, as the same (radio)pharmaceutical can be complexed to a radionuclide for diagnosis by nuclear imaging using positron emission tomography (PET) or single-photon emission computed tomography (SPECT), or a radionuclide suited for therapy (Table 1).

3.1.1. DIAGNOSTICS - PET VERSUS SPECT IMAGING

Nuclear imaging by PET or SPECT enables disease diagnosis and monitoring of therapy response (Figure 2B). For PET imaging, positron emitters (β^+) are used, e.g. copper-64 (^{64}Cu), gallium-68 (^{68}Ga), and terbium-152 (^{152}Tb) (Table 1). These radionuclides decay by the conversion of a proton into a neutron, thereby releasing a neutrino and a positron (e^+). These low-energy positrons annihilate with negatively charged electrons (e^-), thereby creating two gamma photons of 511 keV. As these gamma photons are emitted in opposite direction, accurate tumor detection and localization is possible [27-29]. For SPECT imaging, radioisotopes are used which directly emit gamma photons, e.g. indium-111 (^{111}In) and iodine-123 (^{123}I) (Table 1), thereby transitioning from a high energy state to a low energy state. Prior to reaching the rotating detectors, the photons have to pass a collimator (e.g. pinhole or parallel-hole collimators) enabling image reconstruction by providing positional information of the radiopharmaceutical [29, 30]. PET and SPECT both have advantages and disadvantages, e.g. the radioisotopes used for SPECT are easier to obtain and have longer half-lives than PET radioisotopes, however, the sensitivity of PET imaging is higher due to the absence of collimators [29].

Table 1. Relevant diagnostic and therapeutic radionuclides for theranostics approaches for NET patients.

	Diagnostic radionuclides				
	^{111}In*	**^{123}I**	**^{64}Cu**	**^{68}Ga**	**^{152}Tb**
$T_{1/2}$	2.80 d	13.2 h	12.7 h	67.7 m	17.5 h
E_γ (keV); I_γ (%)	245; 94 171; 91	159; 84			
$E_{\beta+}$ (keV); $I_{\beta+}$ (%)			278; 17	836; 88	1337; 8 1186; 6

	Therapeutic radionuclides						
	^{90}Y	**^{149}Tb**	**^{161}Tb**	**^{177}Lu****	**^{212}Pb**	**^{213}Bi**	**^{225}Ac**
$T_{1/2}$	64.1 h	4.1 h	6.9 d	6.7 d	10.6 h	45.6 m	10.0 d
$E_{\beta-}$ (keV); $I_{\beta-}$ (%)	932; 100		184; 5 174; 5 157; 65 138; 26	149; 79 111; 9 47; 12	171; 14 93; 82 41; 5	492; 67 320; 30	
E_α (keV); I_α (%)		3967; 17				5875; 2	5830; 51 5793; 18 5791; 9 5732; 8

** Auger electrons released from indium-111 (^{111}In) decay also have therapeutic potential. ** Gamma photons released from lutetium-177 (^{177}Lu) decay can be used for SPECT imaging. Abbreviations: $T_{1/2}$: half-life, m: minutes, h: hours, d: days, α: alpha-decay, β^+: beta$^+$-decay, β^-: beta$^-$-decay, γ: gamma-decay. Information is based on: [31].*

3.1.2. THERAPEUTICS – TARGETED RADIONUCLIDE THERAPY

In addition to nuclear imaging, radiopharmaceuticals can be used for targeted radionuclide therapy (TRT). Upon binding of the radiopharmaceutical to the respective biomarker present

on the tumor cells, DNA damage is induced possibly resulting in tumor cell death [32, 33]. DNA damage can be induced via several mechanisms. The main mechanism responsible for radiation-induced DNA damage results from the binding of the radiopharmaceutical to the biomarker expressed on the tumor cell itself. In addition to this, the cross-fire effect and bystander effect are involved in inducing DNA damage. As a result of cross-firing, cells are irradiated via the radiopharmaceutical taken up by neighboring cells. The bystander effect provokes signal-mediated effects in cells in close proximity of the irradiated cells, e.g. via signaling molecules, intercellular communication, and reactive oxygen and nitrogen species.

Various radionuclides, emitting different types of radiation, can be applied for therapeutic purposes, i.e. α-emitters (e.g. terbium-149 (^{149}Tb), bismuth-213 (^{213}Bi) and actinium-225 (^{225}Ac)), β-emitters (e.g. yttrium-90 (^{90}Y), terbium-161 (^{161}Tb), lutetium-177 (^{177}Lu) and lead-212 (^{212}Pb)) and auger electron emitters (e.g. ^{111}In) (Figure 2C, Table 1). These radionuclides differ in the emitted particles and herewith associated released energy, tissue penetration range and thus also in linear energy transfer (LET) [31, 33]. Due to these differences, the level of DNA damage that the radionuclides can induce varies between the different types of radiation [33, 34]. α-particles are characterized by a high LET, meaning that their energy, which is relatively high, is released over a short range. As a result, double-stranded DNA breaks can arise. Similar to α-particles, auger electrons induce mainly complex, double-stranded DNA breaks. On average 5 to 30 auger electrons per decaying atom are released, contributing to the complexity of the damage. However, since auger electrons have a short range, this only results in damage when the radionuclide is in close proximity of the DNA. Double-strand DNA breaks are relatively difficult to repair and, as a consequence, often lead to cell death. β-particles, on the other hand, are characterized by a lower LET, resulting in mainly single-stranded DNA breaks which are more easily repaired. However, if these breaks are not (correctly) repaired, this can in turn lead to the more complex double-stranded DNA breaks and cell death.

Currently, several targets are of interest for theranostic approaches. In addition to the SSTR2 on NET cells, the gastrin releasing peptide receptor overexpressed in prostate and breast cancer [35], and the prostate-specific membrane antigen overexpressed on prostate cancer [36] are also being explored for radionuclide theranostics. Moreover, in addition to biomarkers expressed on cancer cells, biomarkers on other cellular components of the tumor microenvironment, e.g. fibroblast activation protein-α expressed on cancer-associated fibroblasts and several biomarkers on macrophage (e.g. macrophage mannose receptor, translocator receptor and folate receptor-β) are being studied as targets for nuclear imaging and therapy [37]. Finally, specific altered processes of the tumor microenvironment (e.g. hypoxia, acidity and increased metabolism) are being exploited as targets.

3.2. THERANOSTIC APPROACH FOR NETs

Regarding SSTR2-targeted theranostics for NETs, several generations of radiolabeled SSAs have been developed over the last decades. First, the SSA octreotide was radiolabeled with iodine-123 (^{123}I), developing (^{123}I)-Tyr^3-octreotide, which was used for two-dimensional gamma camera scintigraphy [38, 39]. Improvements were made by the development of [^{111}In]In-DPTA^0-octreotide, also known as [^{111}In]In-pentetreotide or Octreoscan™, which was easier to produce, more widely available, and characterized by a longer half-life and a more beneficial renal clearance [40, 41]. As ^{111}In also emits auger electrons, the radiopharmaceutical was also tested as therapeutic radiopharmaceutical [42-44]. However, the aforementioned short range of the auger electrons hampered clinical responses. To overcome this, a shift was made to β-emitting radionuclides, which started with the development of [^{90}Y]Y-DOTA^0-Tyr^3-octreotide, also known as [^{90}Y]Y-DOTATOC [45-48]. The use of [^{90}Y]Y-DOTATOC was successful; for example Imhof et al. [49] reported a measurable decrease in the sum of the diameter of all tumor lesions in 29.7% of the patients, which correlated significantly with an increased survival. However, grade 4-5 permanent renal toxicity and grade 3-4 transient hematological toxicity were reported for, respectively, almost 10% and 13% of the treated patients [49]. To reduce the observed toxicity, research focused on the use of ^{177}Lu, a radionuclide with lower energy β-particles and a shorter tissue penetration range [50]. Next to the above, ^{177}Lu emits gamma photons which can be used for SPECT imaging and herewith for personalized dosimetry. This resulted in the development of [^{177}Lu]Lu-DOTA^0-Tyr^3-octreotide, also known as [^{177}Lu]Lu-DOTATOC. In a comparative cohort study in which [^{177}Lu]Lu-DOTATOC was compared to [^{90}Y]Y-DOTATOC, it was demonstrated that [^{177}Lu]Lu-DOTATOC significantly prolonged the survival for specific subgroups of patients, e.g. patients with low tumoral uptake of the radiopharmaceutical, solitary lesions and extra-hepatic lesions [51]. Whereas the safety profile in terms of renal toxicity was equal to that of [^{90}Y]Y-DOTATOC, the number of cases with severe transient hematological toxicity was lower using [^{177}Lu]Lu-DOTATOC. Further optimizations of the radiopharmaceutical resulted in the development of octreotate [52]. Radiolabeling of this molecule with ^{177}Lu led to [^{177}Lu]Lu-DOTA^0-Tyr^3-octreotate, also known as [^{177}Lu]Lu-DOTATATE, [^{177}Lu]Lu-oxodotreotide and Lutathera™ (Figure 3), which is characterized by a higher affinity for SSTR2 than its counterpart octreotide. Upon comparing [^{177}Lu]Lu-DOTATATE to [^{177}Lu]Lu-DOTATOC, it was shown that [^{177}Lu]Lu-DOTATATE is a more effective radiopharmaceutical for therapy due to its longer tumor residence time [53].

TRT using [^{177}Lu]Lu-DOTATATE, a treatment approach also known as peptide receptor radionuclide therapy (PRRT), was approved by the EMA in 2017 and the FDA in 2018 for the treatment of SSTR-positive GEP-NET patients [54]. The results of the NETTER-1 study, an open-labeled, randomized, controlled phase III trial, led to the approval of [^{177}Lu]Lu-DOTATATE for therapeutic purposes [55]. In this study, patients with advanced, inoperable, well-differentiated and SSTR-positive midgut NETs received four cycles of 7.4 GBq [^{177}Lu]Lu-DOTATATE intravenously eight weeks apart. It was reported that patients showed a clinically relevant

difference in median overall survival of 11.7 months in comparison to high-dose long-acting octreotide. Moreover, a favorable safety profile was described. Based on the positive results obtained with this SSTR2-targeting radiopharmaceutical, this treatment is now included in the EMSO Clinical Practice Guidelines for the management of SSTR2-positive GEP-NETs. PRRT is currently applied as either second- or third-line therapy after treatment with targeted drugs (i.e. SSAs, everolimus or sunitinib) and chemotherapy (i.e. capecitabine combined with temozolomide or streptozotocin combined with 5-fluorouracil), depending on the disease grade and stage [1].

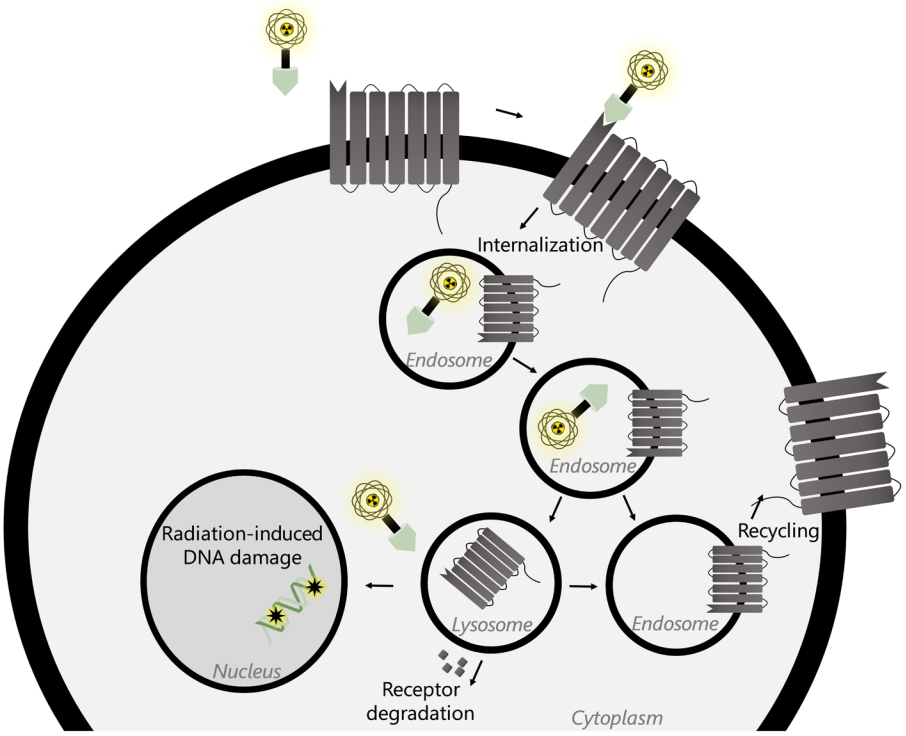

Figure 3. Upon binding of a SSTR2-targeting radiopharmaceutical with agonistic properties (e.g. [^{177}Lu]Lu-DOTATATE), the receptor-radiopharmaceutical complex is internalized. As a result of this, the radionuclide comes in close proximity of the DNA, causing radiation-induced DNA damage eventually resulting in tumor cell death. After internalization, the receptor itself is either recycled or degraded via endosomal and lysosomal trafficking.

Prior to PRRT, sufficient tumor uptake is confirmed by nuclear imaging. Currently, PET/CT is the preferred modality for patient selection using ^{68}Ga- or ^{64}Cu-radiolabeled SSAs, e.g. [^{68}Ga]Ga-DOTATATE [1]. The sensitivity of PET/CT is higher for detecting tumor lesions than scintigraphy [56], among others, due to a higher spatial resolution and a better target-to-background contrast [57]. However, due to the limited availability of PET tracers and scanners, SSTR scintigraphy (planar scans or SPECT/CT), e.g. using the radiopharmaceutical [^{111}In]In-DTPA^{0}-octreotide, can also be used for patient selection if PET/CT is not available [1, 57]. If a

tumoral uptake higher than the hepatic background uptake is confirmed, patients qualify for PRRT [58, 59].

Even though positive results are reported with SSTR2-targeting PRRT in NET patients, complete response rates are low (i.e. 1-2% complete response) and 12% of patients still demonstrate progressive disease after treatment [55, 60]. Moreover, resection, the only curative therapy option currently available [61], is only possible for the minority of NET patients due to the frequent presence of metastases at the time of diagnosis [62], further stressing the need for improved systemic treatments (e.g. PRRT). To overcome this need, multiple approaches are currently under investigation [63], e.g. the use of antagonists instead of agonist for increased radiopharmaceutical binding and herewith higher tumoral radiation dosages, the addition of an albumin binding domain to increase the blood circulation time and thus the tumor uptake of radiopharmaceuticals, the use of more cytotoxic α-emitting radionuclides in comparison to the β-emitting radionuclides or radiosensitizing tumor cells by inhibiting the DNA damage response. Finally, an exciting and novel approach is the attempt to upregulate SSTR2 expression by modulating the epigenetic regulation of the respective gene.

PART III

4. EPIGENETIC REGULATION

Cell-specific gene transcription is regulated by epigenetic modifications which are heritable during cell divisions. However, as the DNA sequence itself is not changed, these modifications are also characterized by their reversibility [64, 65]. Over the last years, epigenetic modifications have become an important field of interest, demonstrating their pivotal role in physiological processes, such as their role in cell differentiation and development [66]. Moreover, thorough investigations have demonstrated that the epigenetic machinery is also involved in the development of diseases, e.g. neurodevelopmental disorders and autoimmune diseases, as well as the development of cancer [67-70]. For its role in the development of cancer, the epigenetic machinery is involved in the activation of proto-oncogenes and/or inactivation of tumor suppressor genes, such as RB, P16 and BRCA1 [70]. Although epigenetic modifications can regulate gene expression at different levels, we will specifically focus on modifications targeting the DNA and the histones (Figure 4A).

One of the major epigenetic mechanisms regulating gene transcription are histone modifications. Specific histone-modifying enzymes can stimulate the formation of either condensed, inactive heterochromatin or decondensed, active euchromatin (Figure 4A). Acetylation and methylation of amino acids are the most frequently observed modifications at the N-terminal tails of the histones. Acetylation on lysine amino acids leads to a reduction of positive charges on the surface of histones, resulting in loss of interactions between DNA and histones. This in turn results in euchromatin formation which stimulates gene transcription. Histone acetyltransferases (HATs) and histone deacetylases (HDACs) are

responsible for the addition and removal of acetyl groups on lysine residues, respectively. Whereas histone acetylation is linked to transcriptional activation, histone methylation can either be repressive or activating. This depends on which lysine residue (K) on which histone (H3, H4) is modified, and the extent of methylation, i.e. di- or trimethylation (me2, me3). For example, H3K9me2/3, H3K27me2/3 and H4K20me3 are inhibiting histone methylation marks, and H3K4me2/3, H2K36me3 and H3K79me3 are known as important activating histone marks. The process of histone methylation is mediated by histone methyltransferases (HMTs) and histone demethylases (HDMs) [71, 72].

Another relevant epigenetic modification targets cytosine residues in the DNA. Methyl groups are transferred to the fifth carbon of the cytosine nucleobases by DNA methyltransferases (DNMTs) (Figure 4A, B). This process is mainly catalyzed by three enzyme subtypes, i.e. DNMT1, DNMT3a and DNMT3b. DNMT1, interacting with ubiquitin-like with PHD and RING finger domain (UHRF) proteins, is involved in maintaining methylation profiles during replication. DNMT3a and DNMT3b are both involved in *de novo* transfer of methyl groups. The catalytic activity of DNMT3a and DNMT3b is increased upon association with DNMT3L, which does not have catalytic activity on its own. DNA methylation often occurs on cytosine residues followed by guanine residues or in CpG islands which are frequently present within the promoter region. In response to DNA methylation, transcription factors are no longer able to bind. Moreover, specific inhibitory proteins bind to the DNA upon methylation resulting in repression of transcription, such as methyl-CpG-binding domain (MBD) proteins and zinc-finger proteins [73, 74].

Of note, there is a strong interplay between histone modifications and DNA methylation. For example, activating histone modifications prevent binding of DNMTs, thereby enhancing gene transcription. Moreover, DNMTs can interact with HMTs and HDAC, together stimulating the silenced heterochromatin state. Additionally, repressing MBD proteins interacting with methylated DNA are involved in regulating histone modifications, leading to transcriptional repression [73].

Based on the growing knowledge about the epigenetic machinery and its key role in gene transcription, drugs have been developed that target the enzymes involved in the abovementioned processes. DNA methyltransferase inhibitors (DNMTis, Figure 4C) and histone deacetylase inhibitors (HDACis, Figure 4D) both stimulate gene transcription, as these epigenetic drugs inhibit DNMTs and HDACs, respectively. There are several HDAC subtypes, leading to the development of subtype-specific HDACis. In short, based on both the homology with yeast HDACs and their function, human HDACs are divided in four classes; class I, II, III and IV, of which HDACs class II is subdivided in class IIa and IIb. The HDACis are targeting one or multiple classes, constituted of several HDAC proteins: epigenetic drugs targeting class I (HDAC1, 2, 3 and 8), class IIa (HDAC4, 5, 7 and 9), class IIb (HDAC6 and 10) and/or class IV (HDAC11) (Figure 4E) [75, 76].

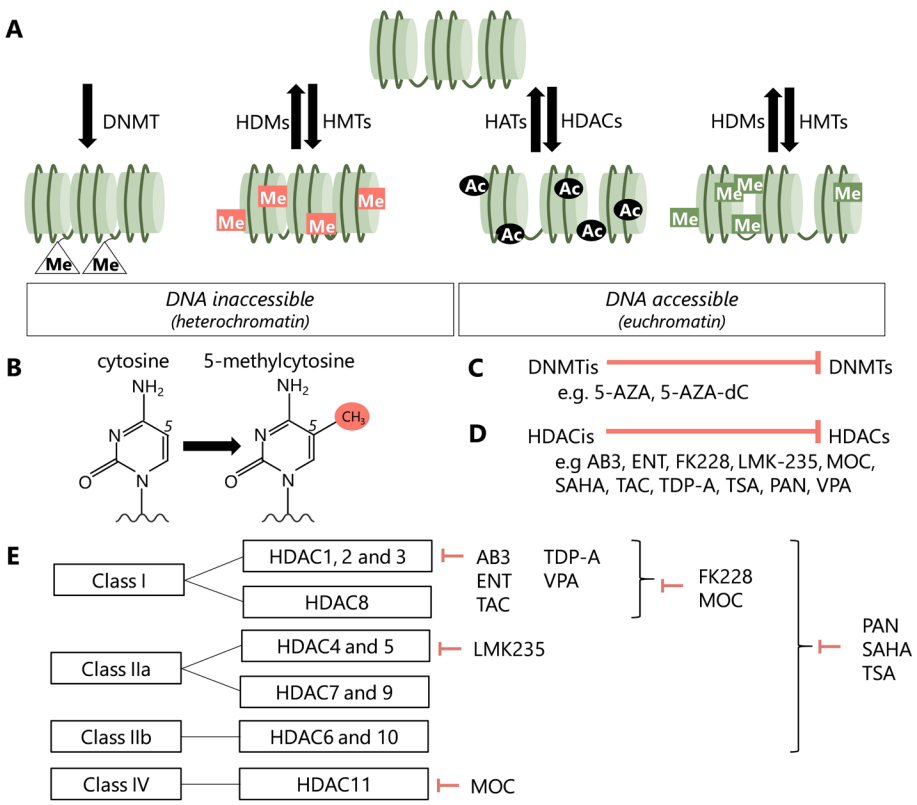

Figure 4. (A) Epigenetic modifications can modify both DNA and histones. DNA methylation and inactivating histone methylation stimulate heterochromatin, resulting in inaccessible DNA and therefore reduced gene transcription. Histone acetylation and activating histone methylation stimulate euchromatin, thereby stimulating gene transcription. Histone methylation can therefore both be inactivating and activating, depending on which lysine residue is modified on which histone. Examples of inactivating histone methylation marks (indicated in red) are H3K9me2/3, H3K27me2/3 and H4K20me3, and examples of activating histone methylation marks (indicated in green) are H3K4me2/3, H2K36me3 and H3K79me3. All epigenetic modifications are catalyzed by enzymes: (1) DNA methylation by DNMTs, (2) histone methylation marks by HMTs and HDMs, and (3) histone acetylation marks by HATs and HDACs. **(B)** DNMTs are involved in DNA methylation in which cytosine residues are converted into 5-methylcytosine residues. **(C,D)** Epigenetic drugs have been developed inhibiting certain groups of enzymes involved in epigenetic modifications, i.e. DNMTis and HDACis targeting DNMTs and HDACs, respectively, both stimulating transcriptionally active euchromatin. **(E)** HDACis often target multiple HDACs within HDAC class I, IIa, IIb and/or IV. AB3, entinostat (ENT), tacedinaline (TAC), thailandepsin-A (TDP-A) and valproic acid (VPA) target HDAC1, 2 and 3; romidepsin (FK228) targets all HDAC proteins within class I; LMK-235 targets HDAC4 and 5 within class IIa; panobinostat (PAN), vorinostat (SAHA) and trichostatin A (TSA) target HDAC proteins within class I, IIa and IIb; and mocetinostat (MOC) targets HDAC proteins in class I and IV [75, 77-80]. Figure is taken and adapted from [13].

Summarizing, DNMTis and HDACis can both be used to specifically target and change the epigenetic machinery and thus the epigenetic profile. These epigenetic drugs can therefore potentially modify gene expression and thus also protein expression levels in order to expand

current treatment options, including upregulation of SSTR2 for increased radiopharmaceutical uptake and PRRT efficacy in NET patients (Figure 5).

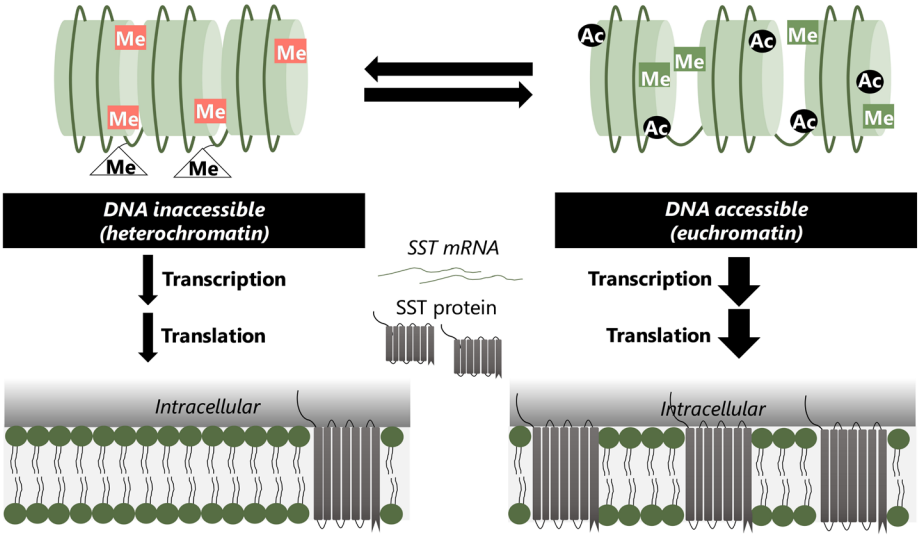

Figure 5. Activating histone marks, i.e. histone methylation on specific lysine residues (H3K4me2/3, H2K36me3 and H3K79me3) and histone acetylation (both indicated on the right side of the figure), stimulate euchromatin, resulting in more gene transcription. Epigenetic drugs can be used to stimulate euchromatin, in order to increase the expression of certain proteins. Thereby, it may be possible to increase the expression of targets for therapy, e.g. SSTR2 in NET patients with insufficient expression levels to qualify for PRRT. Figure is taken and adapted from [13].

5. EPIGENETIC REGULATION IN NETs

The important role of epigenetics in NET tissue has already been demonstrated in several clinical studies. In a cohort of PAN-NET patients, significant upregulation of multiple HDAC subtypes was reported, including HDAC3, nuclear HDAC4, nuclear and cytoplasmic HDAC5, cytoplasmic HDAC8, HDAC9, nuclear HDAC10 and HDAC11. More specifically, HDAC1, HDAC2, nuclear HDAC5 and HDAC11 were significantly elevated in high grade (G3) PAN-NETs in comparison to the expression levels found in low-grade PAN-NETs (G1 and G2). Further analysis showed that especially upregulation of nuclear HDAC5 was significantly associated with a reduced disease-free survival and overall survival [81]. Additionally, the HDACi entinostat (ENT) reduced the activity of proteins involved in the progression from primary to metastatic disease [82]. This suggests that histone acetylation marks could be a target for therapy. In line with changes in histone acetylation patterns, aberrant DNA methylation patterns have been described in NET tissue, emphasizing the important role of epigenetics in regulating gene expression involved in numerous processes such as cell cycle, cell death, cell growth and DNA repair [69, 83]. In an extensive review by Mafficini et al. [84], the genetic and epigenetic alterations in PAN-NETs and SI-NETs have been described. In this overview,

promoter hypermethylation of multiple genes was described, for instance hypermethylation of RASSF1A and CDKN2A, both being tumor suppressor genes involved in regulating cell cycle arrest, apoptosis and/or senescence. Additionally, inactivating mutations in HMTs were described, further suggesting deregulation of the epigenetic machinery.

Altogether, there is strong evidence that the epigenetic machinery is highly involved in the pathophysiology of NETs. It might even be speculated that this system is also involved in the regulation of SST and SSTR expression and signaling. Proper understanding of the epigenetic system in the regulation of SST/SSTRs, and more specifically SSTR2, could potentially open up possibilities to increase SSTR2 target expression and thus increase PRRT efficacy for NET patients.

THESIS OUTLINE

The aim of this thesis is to gain a better understanding of the role of the epigenetic machinery in regulating SSTR2 expression in NETs, and to use this knowledge to increase tumoral SSTR2 expression, ultimately resulting in a higher uptake of radiolabeled SSAs and a herewith associated improvement of SSTR2-targeted radionuclide imaging and therapy.

Chapter 2 reviews the role of the epigenetic machinery in controlling the expression of SSTRs and the neuropeptide SST, both in NETs and other types of cancer. Moreover, it provides an overview on how to modulate enzymes of the epigenetic machinery in order to alter the expression of SST and SSTRs.

In **Chapter 3**, we compared the effect of multiple HDACis on SSTR2 expression and [^{111}In]-DOTATATE uptake in three human NET cell lines (i.e. BON-1, H727 and GOT1). Moreover, the reversibility of the HDACi-induced effects was investigated, as well as the effect the HDACis have on the radiosensitivity of the NET cells.

In **Chapter 4**, the effect of HDACi valproic acid (VPA) was further evaluated *in vivo*. For this, the human small-cell lung cancer cell line NCI-H69 was used; a cell line characterized by relatively high baseline SSTR2 expression levels. It has been previously demonstrated that this cell line responds to PRRT and it is therefore frequently used in studies aiming to optimize SSTR2-targeted PRRT. Moreover, five other HDACis were screened in NCI-H69 tumor-bearing animals for inducing an increased SSTR2 expression level and enhanced uptake of radiolabeled SSA. Additionally, one of these HDACi was also tested in mice bearing a tumor derived from the BON-1 cell line, which is characterized by lower baseline SSTR2 expression levels than NCI-H69 cells. These latter two *in vivo* studies are described in **Chapter 5**.

In **Chapter 6**, we focused on finding correlations between SSTR2 expression and epigenetic marks in a subset of human SI-NET tissue samples, which included both histone modifications (i.e. acetylation and methylation) and DNA methylation profiles around the SSTR2 promoter. In parallel, a prospective clinical trial was performed aiming for an increased tumoral uptake of [^{68}Ga]Ga-DOTATATE after combination treatment with the HDACi VPA and the DNMTi hydralazine. This proof-of-concept study is described in **Chapter 7**.

REFERENCES

1. Pavel, M.; Öberg, K.; Falconi, M.; Krenning, E.P.; Sundin, A.; Perren, A.; Berruti, A.; clinicalguidelines@esmo.org, E.G.C.E.a. Gastroenteropancreatic neuroendocrine neoplasms: ESMO Clinical Practice Guidelines for diagnosis, treatment and follow-up. *Ann Oncol* **2020**, *31*, 844-860.
2. Özaslan, E.; Demir, S.; Karaca, H.; Güven, K. Evaluation of the concordance between the stage of the disease and Ki-67 proliferation index in gastroenteropancreatic neuroendocrine tumors. *Eur J Gastroenterol Hepatol* **2016**, *28*, 836-841.
3. Dasari, A.; Shen, C.; Halperin, D.; Zhao, B.; Zhou, S.; Xu, Y.; Shih, T.; Yao, J.C. Trends in the Incidence, Prevalence, and Survival Outcomes in Patients With Neuroendocrine Tumors in the United States. *JAMA Oncol* **2017**, *3*, 1335-1342.
4. Fernandes, C.J.; Leung, G.; Eads, J.R.; Katona, B.W. Gastroenteropancreatic Neuroendocrine Tumors. *Gastroenterol Clin North Am* **2022**, *51*, 625-647.
5. Qian, Z.R.; Li, T.; Ter-Minassian, M.; Yang, J.; Chan, J.A.; Brais, L.K.; Masugi, Y.; Thiaglingam, A.; Brooks, N.; Nishihara, R., et al. Association Between Somatostatin Receptor Expression and Clinical Outcomes in Neuroendocrine Tumors. *Pancreas* **2016**, *45*, 1386-1393.
6. Papotti, M.; Bongiovanni, M.; Volante, M.; Allìa, E.; Landolfi, S.; Helboe, L.; Schindler, M.; Cole, S.L.; Bussolati, G. Expression of somatostatin receptor types 1-5 in 81 cases of gastrointestinal and pancreatic endocrine tumors. A correlative immunohistochemical and reverse-transcriptase polymerase chain reaction analysis. *Virchows Arch* **2002**, *440*, 461-475.
7. Olias, G.; Viollet, C.; Kusserow, H.; Epelbaum, J.; Meyerhof, W. Regulation and function of somatostatin receptors. *J Neurochem* **2004**, *89*, 1057-1091.
8. Barnett, P. Somatostatin and somatostatin receptor physiology. *Endocrine* **2003**, *20*, 255-264.
9. Patel, Y.C. Somatostatin and its receptor family. *Front Neuroendocrinol* **1999**, *20*, 157-198.
10. Günther, T.; Tulipano, G.; Dournaud, P.; Bousquet, C.; Csaba, Z.; Kreienkamp, H.J.; Lupp, A.; Korbonits, M.; Castaño, J.P.; Wester, H.J., et al. International Union of Basic and Clinical Pharmacology. CV. Somatostatin Receptors: Structure, Function, Ligands, and New Nomenclature. *Pharmacol Rev* **2018**, *70*, 763-835.
11. Gatto, F.; Barbieri, F.; Arvigo, M.; Thellung, S.; Amarù, J.; Albertelli, M.; Ferone, D.; Florio, T. Biological and Biochemical Basis of the Differential Efficacy of First and Second Generation Somatostatin Receptor Ligands in Neuroendocrine Neoplasms. *Int J Mol Sci* **2019**, *20*.
12. Barbieri, F.; Bajetto, A.; Pattarozzi, A.; Gatti, M.; Würth, R.; Thellung, S.; Corsaro, A.; Villa, V.; Nizzari, M.; Florio, T. Peptide receptor targeting in cancer: the somatostatin paradigm. *Int J Pept* **2013**, *2013*, 926295.
13. Klomp, M.J.; Dalm, S.U.; de Jong, M.; Feelders, R.A.; Hofland, J.; Hofland, L.J. Epigenetic regulation of somatostatin and somatostatin receptors in neuroendocrine tumors and other types of cancer. *Rev Endocr Metab Disord* **2021**, *22*, 495-510.
14. Evans, A.A.; Crook, T.; Laws, S.A.; Gough, A.C.; Royle, G.T.; Primrose, J.N. Analysis of somatostatin receptor subtype mRNA expression in human breast cancer. *Br J Cancer* **1997**, *75*, 798-803.
15. Qiu, C.Z.; Wang, C.; Huang, Z.X.; Zhu, S.Z.; Wu, Y.Y.; Qiu, J.L. Relationship between somatostatin receptor subtype expression and clinicopathology, Ki-67, Bcl-2 and p53 in colorectal cancer. *World J Gastroenterol* **2006**, *12*, 2011-2015.
16. Hennigs, J.K.; Müller, J.; Adam, M.; Spin, J.M.; Riedel, E.; Graefen, M.; Bokemeyer, C.; Sauter, G.; Huland, H.; Schlomm, T., et al. Loss of somatostatin receptor subtype 2 in prostate cancer is linked to an aggressive cancer phenotype, high tumor cell proliferation and predicts early metastatic and biochemical relapse. *PLoS One* **2014**, *9*, e100469.
17. Werner, C.; Dirsch, O.; Dahmen, U.; Grimm, M.O.; Schulz, S.; Lupp, A. Evaluation of Somatostatin and CXCR4 Receptor Expression in a Large Set of Prostate Cancer Samples Using Tissue Microarrays and Well-Characterized Monoclonal Antibodies. *Transl Oncol* **2020**, *13*, 100801.
18. Stafford, N.D.; Condon, L.T.; Rogers, M.J.; MacDonald, A.W.; Atkin, S.L. The expression of somatostatin receptors 1 and 2 in benign, pre-malignant and malignant laryngeal lesions. *Clin Otolaryngol Allied Sci* **2003**, *28*, 314-319.

19. Zou, Y.; Tan, H.; Zhao, Y.; Zhou, Y.; Cao, L. Expression and selective activation of somatostatin receptor subtypes induces cell cycle arrest in cancer cells. *Oncol Lett* **2019**, *17*, 1723-1731.
20. Mizutani, G.; Nakanishi, Y.; Watanabe, N.; Honma, T.; Obana, Y.; Seki, T.; Ohni, S.; Nemoto, N. Expression of Somatostatin Receptor (SSTR) Subtypes (SSTR-1, 2A, 3, 4 and 5) in Neuroendocrine Tumors Using Real-time RT-PCR Method and Immunohistochemistry. *Acta Histochem Cytochem* **2012**, *45*, 167-176.
21. Stueven, A.K.; Kayser, A.; Wetz, C.; Amthauer, H.; Wree, A.; Tacke, F.; Wiedenmann, B.; Roderburg, C.; Jann, H. Somatostatin Analogues in the Treatment of Neuroendocrine Tumors: Past, Present and Future. *Int J Mol Sci* **2019**, *20*.
22. Ruszniewski, P.; Valle, J.W.; Lombard-Bohas, C.; Cuthbertson, D.J.; Perros, P.; Holubec, L.; Delle Fave, G.; Smith, D.; Niccoli, P.; Maisonobe, P., et al. Patient-reported outcomes with lanreotide Autogel/Depot for carcinoid syndrome: An international observational study. *Dig Liver Dis* **2016**, *48*, 552-558.
23. O'Toole, D.; Ducreux, M.; Bommelaer, G.; Wemeau, J.L.; Bouché, O.; Catus, F.; Blumberg, J.; Ruszniewski, P. Treatment of carcinoid syndrome: a prospective crossover evaluation of lanreotide versus octreotide in terms of efficacy, patient acceptability, and tolerance. *Cancer* **2000**, *88*, 770-776.
24. Appetecchia, M.; Baldelli, R. Somatostatin analogues in the treatment of gastroenteropancreatic neuroendocrine tumours, current aspects and new perspectives. *J Exp Clin Cancer Res* **2010**, *29*, 19.
25. Rinke, A.; Müller, H.H.; Schade-Brittinger, C.; Klose, K.J.; Barth, P.; Wied, M.; Mayer, C.; Aminossadati, B.; Pape, U.F.; Bläker, M., et al. Placebo-controlled, double-blind, prospective, randomized study on the effect of octreotide LAR in the control of tumor growth in patients with metastatic neuroendocrine midgut tumors: a report from the PROMID Study Group. *J Clin Oncol* **2009**, *27*, 4656-4663.
26. Caplin, M.E.; Pavel, M.; Ćwikła, J.B.; Phan, A.T.; Raderer, M.; Sedláčková, E.; Cadiot, G.; Wolin, E.M.; Capdevila, J.; Wall, L., et al. Lanreotide in metastatic enteropancreatic neuroendocrine tumors. *N Engl J Med* **2014**, *371*, 224-233.
27. Shukla, A.K.; Kumar, U. Positron emission tomography: An overview. *J Med Phys* **2006**, *31*, 13-21.
28. Ziegler, S.I. Positron Emission Tomography: Principles, Technology, and Recent Developments. *Nuclear Physics A* **2005**, *752*, 679-687.
29. Lu, F.M.; Yuan, Z. PET/SPECT molecular imaging in clinical neuroscience: recent advances in the investigation of CNS diseases. *Quant Imaging Med Surg* **2015**, *5*, 433-447.
30. de Kemp, R.A.; Epstein, F.H.; Catana, C.; Tsui, B.M.; Ritman, E.L. Small-animal molecular imaging methods. *J Nucl Med* **2010**, *51 Suppl 1*, 18S-32S.
31. *NuDat 3.0*. [cited 2022 04-12-2022]; Available from: https://www.nndc.bnl.gov/nudat3/.
32. Brady, D.; O'Sullivan, J.M.; Prise, K.M. What is the Role of the Bystander Response in Radionuclide Therapies? *Front Oncol* **2013**, *3*, 215.
33. Kassis, A.I. Therapeutic radionuclides: biophysical and radiobiologic principles. *Semin Nucl Med* **2008**, *38*, 358-366.
34. Reuvers, T.G.A.; Kanaar, R.; Nonnekens, J. DNA Damage-Inducing Anticancer Therapies: From Global to Precision Damage. *Cancers (Basel)* **2020**, *12*.
35. Mansi, R.; Nock, B.A.; Dalm, S.U.; Busstra, M.B.; van Weerden, W.M.; Maina, T. Radiolabeled Bombesin Analogs. *Cancers (Basel)* **2021**, *13*.
36. Ruigrok, E.A.M.; van Weerden, W.M.; Nonnekens, J.; de Jong, M. The Future of PSMA-Targeted Radionuclide Therapy: An Overview of Recent Preclinical Research. *Pharmaceutics* **2019**, *11*.
37. van der Heide, C.D.; Dalm, S.U. Radionuclide imaging and therapy directed towards the tumor microenvironment: a multi-cancer approach for personalized medicine. *Eur J Nucl Med Mol Imaging* **2022**.
38. Krenning, E.P.; Bakker, W.H.; Breeman, W.A.; Koper, J.W.; Kooij, P.P.; Ausema, L.; Lameris, J.S.; Reubi, J.C.; Lamberts, S.W. Localisation of endocrine-related tumours with radioiodinated analogue of somatostatin. *Lancet* **1989**, *1*, 242-244.

39. Lamberts, S.W.; Bakker, W.H.; Reubi, J.C.; Krenning, E.P. Somatostatin-receptor imaging in the localization of endocrine tumors. *N Engl J Med* **1990**, *323*, 1246-1249.
40. Bakker, W.H.; Albert, R.; Bruns, C.; Breeman, W.A.; Hofland, L.J.; Marbach, P.; Pless, J.; Pralet, D.; Stolz, B.; Koper, J.W., et al. [111In-DTPA-D-Phe1]-octreotide, a potential radiopharmaceutical for imaging of somatostatin receptor-positive tumors: synthesis, radiolabeling and in vitro validation. *Life Sci* **1991**, *49*, 1583-1591.
41. Krenning, E.P.; Kwekkeboom, D.J.; Bakker, W.H.; Breeman, W.A.; Kooij, P.P.; Oei, H.Y.; van Hagen, M.; Postema, P.T.; de Jong, M.; Reubi, J.C., et al. Somatostatin receptor scintigraphy with [111In-DTPA-D-Phe1]- and [123I-Tyr3]-octreotide: the Rotterdam experience with more than 1000 patients. *Eur J Nucl Med* **1993**, *20*, 716-731.
42. Krenning, E.P.; Kooij, P.P.; Bakker, W.H.; Breeman, W.A.; Postema, P.T.; Kwekkeboom, D.J.; Oei, H.Y.; de Jong, M.; Visser, T.J.; Reijs, A.E., et al. Radiotherapy with a radiolabeled somatostatin analogue, [111In-DTPA-D-Phe1]-octreotide. A case history. *Ann N Y Acad Sci* **1994**, *733*, 496-506.
43. Krenning, E.P.; Kooij, P.P.; Pauwels, S.; Breeman, W.A.; Postema, P.T.; De Herder, W.W.; Valkema, R.; Kwekkeboom, D.J. Somatostatin receptor: scintigraphy and radionuclide therapy. *Digestion* **1996**, *57 Suppl 1*, 57-61.
44. Valkema, R.; De Jong, M.; Bakker, W.H.; Breeman, W.A.; Kooij, P.P.; Lugtenburg, P.J.; De Jong, F.H.; Christiansen, A.; Kam, B.L.; De Herder, W.W., et al. Phase I study of peptide receptor radionuclide therapy with [In-DTPA]octreotide: the Rotterdam experience. *Semin Nucl Med* **2002**, *32*, 110-122.
45. Otte, A.; Jermann, E.; Behe, M.; Goetze, M.; Bucher, H.C.; Roser, H.W.; Heppeler, A.; Mueller-Brand, J.; Maecke, H.R. DOTATOC: a powerful new tool for receptor-mediated radionuclide therapy. *Eur J Nucl Med* **1997**, *24*, 792-795.
46. Otte, A.; Herrmann, R.; Heppeler, A.; Behe, M.; Jermann, E.; Powell, P.; Maecke, H.R.; Muller, J. Yttrium-90 DOTATOC: first clinical results. *Eur J Nucl Med* **1999**, *26*, 1439-1447.
47. Paganelli, G.; Zoboli, S.; Cremonesi, M.; Mäcke, H.R.; Chinol, M. Receptor-mediated radionuclide therapy with 90Y-DOTA-D-Phe1-Tyr3-Octreotide: preliminary report in cancer patients. *Cancer Biother Radiopharm* **1999**, *14*, 477-483.
48. Paganelli, G.; Zoboli, S.; Cremonesi, M.; Bodei, L.; Ferrari, M.; Grana, C.; Bartolomei, M.; Orsi, F.; De Cicco, C.; Mäcke, H.R., et al. Receptor-mediated radiotherapy with 90Y-DOTA-D-Phe1-Tyr3-octreotide. *Eur J Nucl Med* **2001**, *28*, 426-434.
49. Imhof, A.; Brunner, P.; Marincek, N.; Briel, M.; Schindler, C.; Rasch, H.; Mäcke, H.R.; Rochlitz, C.; Müller-Brand, J.; Walter, M.A. Response, survival, and long-term toxicity after therapy with the radiolabeled somatostatin analogue [90Y-DOTA]-TOC in metastasized neuroendocrine cancers. *J Clin Oncol* **2011**, *29*, 2416-2423.
50. Müller, C.; van der Meulen, N.P.; Benešová, M.; Schibli, R. Therapeutic Radiometals Beyond (177)Lu and (90)Y: Production and Application of Promising α-Particle, β(-)-Particle, and Auger Electron Emitters. *J Nucl Med* **2017**, *58*, 91S-96S.
51. Romer, A.; Seiler, D.; Marincek, N.; Brunner, P.; Koller, M.T.; Ng, Q.K.; Maecke, H.R.; Müller-Brand, J.; Rochlitz, C.; Briel, M., et al. Somatostatin-based radiopeptide therapy with [177Lu-DOTA]-TOC versus [90Y-DOTA]-TOC in neuroendocrine tumours. *Eur J Nucl Med Mol Imaging* **2014**, *41*, 214-222.
52. Kwekkeboom, D.J.; Kam, B.L.; van Essen, M.; Teunissen, J.J.; van Eijck, C.H.; Valkema, R.; de Jong, M.; de Herder, W.W.; Krenning, E.P. Somatostatin-receptor-based imaging and therapy of gastroenteropancreatic neuroendocrine tumors. *Endocr Relat Cancer* **2010**, *17*, R53-73.
53. Esser, J.P.; Krenning, E.P.; Teunissen, J.J.; Kooij, P.P.; van Gameren, A.L.; Bakker, W.H.; Kwekkeboom, D.J. Comparison of [(177)Lu-DOTA(0),Tyr(3)]octreotate and [(177)Lu-DOTA(0),Tyr(3)]octreotide: which peptide is preferable for PRRT? *Eur J Nucl Med Mol Imaging* **2006**, *33*, 1346-1351.
54. Hennrich, U.; Kopka, K. Lutathera(®): The First FDA- and EMA-Approved Radiopharmaceutical for Peptide Receptor Radionuclide Therapy. *Pharmaceuticals (Basel)* **2019**, *12*.

55. Strosberg, J.R.; Caplin, M.E.; Kunz, P.L.; Ruszniewski, P.B.; Bodei, L.; Hendifar, A.; Mittra, E.; Wolin, E.M.; Yao, J.C.; Pavel, M.E., et al. 177Lu-Dotatate plus long-acting octreotide versus high-dose long-acting octreotide in patients with midgut neuroendocrine tumours (NETTER-1): final overall survival and long-term safety results from an open-label, randomised, controlled, phase 3 trial. *The Lancet Oncology* **2021**, *22*, 1752-1763.
56. Cavicchioli, M.; Bitencourt, A.G.V.; Lima, E.N.P. (68)Ga-DOTATATE PET/CT versus (111)In-octreotide scintigraphy in patients with neuroendocrine tumors: a prospective study. *Radiol Bras* **2022**, *55*, 13-18.
57. Poletto, G.; Cecchin, D.; Sperti, S.; Filippi, L.; Realdon, N.; Evangelista, L. Head-to-Head Comparison between Peptide-Based Radiopharmaceutical for PET and SPECT in the Evaluation of Neuroendocrine Tumors: A Systematic Review. *Curr Issues Mol Biol* **2022**, *44*, 5516-5530.
58. Hope, T.A.; Abbott, A.; Colucci, K.; Bushnell, D.L.; Gardner, L.; Graham, W.S.; Lindsay, S.; Metz, D.C.; Pryma, D.A.; Stabin, M.G., et al. NANETS/SNMMI Procedure Standard for Somatostatin Receptor-Based Peptide Receptor Radionuclide Therapy with (177)Lu-DOTATATE. *J Nucl Med* **2019**, *60*, 937-943.
59. Hofman, M.S.; Lau, W.F.; Hicks, R.J. Somatostatin receptor imaging with 68Ga DOTATATE PET/CT: clinical utility, normal patterns, pearls, and pitfalls in interpretation. *Radiographics* **2015**, *35*, 500-516.
60. Brabander, T.; van der Zwan, W.A.; Teunissen, J.J.M.; Kam, B.L.R.; Feelders, R.A.; de Herder, W.W.; van Eijck, C.H.J.; Franssen, G.J.H.; Krenning, E.P.; Kwekkeboom, D.J. Long-Term Efficacy, Survival, and Safety of [(177)Lu-DOTA(0),Tyr(3)]octreotate in Patients with Gastroenteropancreatic and Bronchial Neuroendocrine Tumors. *Clin Cancer Res* **2017**, *23*, 4617-4624.
61. Zandee, W.T.; de Herder, W.W. The Evolution of Neuroendocrine Tumor Treatment Reflected by ENETS Guidelines. *Neuroendocrinology* **2018**, *106*, 357-365.
62. Singh, S.; Granberg, D.; Wolin, E.; Warner, R.; Sissons, M.; Kolarova, T.; Goldstein, G.; Pavel, M.; Öberg, K.; Leyden, J. Patient-Reported Burden of a Neuroendocrine Tumor (NET) Diagnosis: Results From the First Global Survey of Patients With NETs. *J Glob Oncol* **2017**, *3*, 43-53.
63. Minczeles, N.S.; Hofland, J.; de Herder, W.W.; Brabander, T. Strategies Towards Improving Clinical Outcomes of Peptide Receptor Radionuclide Therapy. *Curr Oncol Rep* **2021**, *23*, 46.
64. Kanwal, R.; Gupta, S. Epigenetic modifications in cancer. *Clin Genet* **2012**, *81*, 303-311.
65. Rodenhiser, D.; Mann, M. Epigenetics and human disease: translating basic biology into clinical applications. *Cmaj* **2006**, *174*, 341-348.
66. Skinner, M.K. Role of epigenetics in developmental biology and transgenerational inheritance. *Birth Defects Res C Embryo Today* **2011**, *93*, 51-55.
67. Lewis, E.M.; Kroll, K.L. Development and disease in a dish: the epigenetics of neurodevelopmental disorders. *Epigenomics* **2018**, *10*, 219-231.
68. Jeffries, M.A.; Sawalha, A.H. Autoimmune disease in the epigenetic era: how has epigenetics changed our understanding of disease and how can we expect the field to evolve? *Expert Rev Clin Immunol* **2015**, *11*, 45-58.
69. Finnerty, B.M.; Gray, K.D.; Moore, M.D.; Zarnegar, R.; Fahey Iii, T.J. Epigenetics of gastroenteropancreatic neuroendocrine tumors: A clinicopathologic perspective. *World J Gastrointest Oncol* **2017**, *9*, 341-353.
70. Sharma, S.; Kelly, T.K.; Jones, P.A. Epigenetics in cancer. *Carcinogenesis* **2010**, *31*, 27-36.
71. Maleszewska, M.; Kaminska, B. Is glioblastoma an epigenetic malignancy? *Cancers (Basel)* **2013**, *5*, 1120-1139.
72. Alaskhar Alhamwe, B.; Khalaila, R.; Wolf, J.; von Bulow, V.; Harb, H.; Alhamdan, F.; Hii, C.S.; Prescott, S.L.; Ferrante, A.; Renz, H., et al. Histone modifications and their role in epigenetics of atopy and allergic diseases. *Allergy Asthma Clin Immunol* **2018**, *14*, 39.
73. Moore, L.D.; Le, T.; Fan, G. DNA methylation and its basic function. *Neuropsychopharmacology* **2013**, *38*, 23-38.
74. Hervouet, E.; Peixoto, P.; Delage-Mourroux, R.; Boyer-Guittaut, M.; Cartron, P.F. Specific or not specific recruitment of DNMTs for DNA methylation, an epigenetic dilemma. *Clin Epigenetics* **2018**, *10*, 17.

75. Hessmann, E.; Johnsen, S.A.; Siveke, J.T.; Ellenrieder, V. Epigenetic treatment of pancreatic cancer: is there a therapeutic perspective on the horizon? *Gut* **2017**, *66*, 168-179.
76. Seto, E.; Yoshida, M. Erasers of histone acetylation: the histone deacetylase enzymes. *Cold Spring Harb Perspect Biol* **2014**, *6*, a018713.
77. Marek, L.; Hamacher, A.; Hansen, F.K.; Kuna, K.; Gohlke, H.; Kassack, M.U.; Kurz, T. Histone deacetylase (HDAC) inhibitors with a novel connecting unit linker region reveal a selectivity profile for HDAC4 and HDAC5 with improved activity against chemoresistant cancer cells. *J Med Chem* **2013**, *56*, 427-436.
78. Jang, S.; Yu, X.M.; Odorico, S.; Clark, M.; Jaskula-Sztul, R.; Schienebeck, C.M.; Kupcho, K.R.; Harrison, A.D.; Winston-McPherson, G.N.; Tang, W., et al. Novel analogs targeting histone deacetylase suppress aggressive thyroid cancer cell growth and induce re-differentiation. *Cancer Gene Ther* **2015**, *22*, 410-416.
79. Wang, C.; Henkes, L.M.; Doughty, L.B.; He, M.; Wang, D.; Meyer-Almes, F.J.; Cheng, Y.Q. Thailandepsins: bacterial products with potent histone deacetylase inhibitory activities and broad-spectrum antiproliferative activities. *J Nat Prod* **2011**, *74*, 2031-2038.
80. Boumber, Y.; Younes, A.; Garcia-Manero, G. Mocetinostat (MGCD0103): a review of an isotype-specific histone deacetylase inhibitor. *Expert Opin Investig Drugs* **2011**, *20*, 823-829.
81. Klieser, E.; Urbas, R.; Stattner, S.; Primavesi, F.; Jager, T.; Dinnewitzer, A.; Mayr, C.; Kiesslich, T.; Holzmann, K.; Di Fazio, P., et al. Comprehensive immunohistochemical analysis of histone deacetylases in pancreatic neuroendocrine tumors: HDAC5 as a predictor of poor clinical outcome. *Hum Pathol* **2017**, *65*, 41-52.
82. Alvarez, M.J.; Subramaniam, P.S.; Tang, L.H.; Grunn, A.; Aburi, M.; Rieckhof, G.; Komissarova, E.V.; Hagan, E.A.; Bodei, L.; Clemons, P.A., et al. A precision oncology approach to the pharmacological targeting of mechanistic dependencies in neuroendocrine tumors. *Nat Genet* **2018**, *50*, 979-989.
83. Di Domenico, A.; Wiedmer, T.; Marinoni, I.; Perren, A. Genetic and epigenetic drivers of neuroendocrine tumours (NET). *Endocr Relat Cancer* **2017**, *24*, R315-R334.
84. Mafficini, A.; Scarpa, A. Genetics and Epigenetics of Gastroenteropancreatic Neuroendocrine Neoplasms. *Endocr Rev* **2019**, *40*, 506-536.

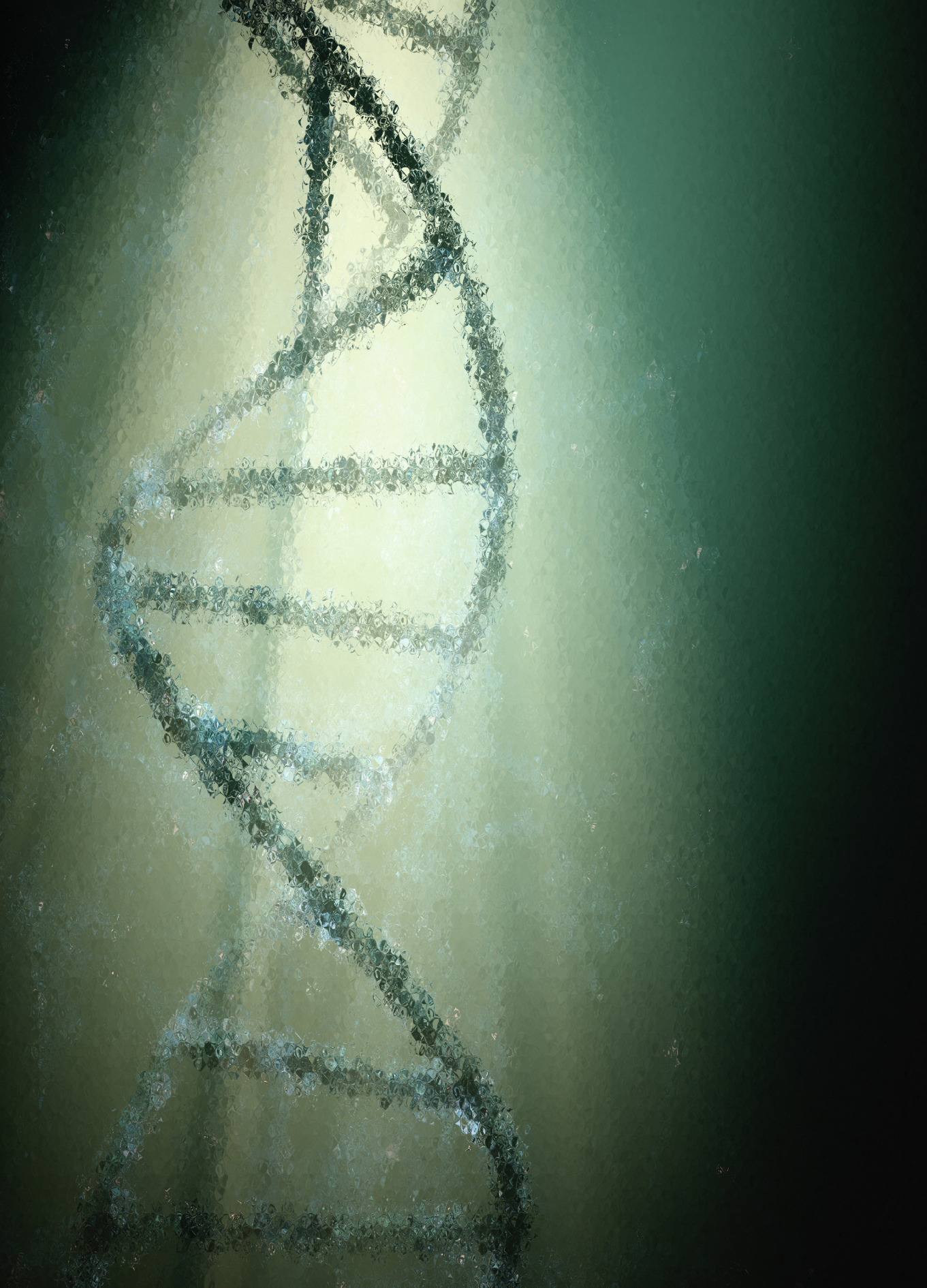

CHAPTER 2

Epigenetic Regulation of Somatostatin and Somatostatin Receptors in Neuroendocrine Tumors and other Types of Cancer

Based on:

M.J. Klomp[1,2], S.U. Dalm[2], M. de Jong[2], R.A. Feelders[1], J. Hofland[1], L.J. Hofland[1].

[1] Department of Internal Medicine, Division of Endocrinology, Erasmus MC, 3015 GD Rotterdam, The Netherlands. [2] Department of Radiology & Nuclear Medicine, Erasmus MC, 3015 GD, Rotterdam, The Netherlands.

Reviews in Endocrine & Metabolic Disorders. 2021 Sep; 22(3):495-510

ABSTRACT

Both somatostatin (SST) and somatostatin receptors (SSTRs) are proteins with important functions in both physiological tissue and in tumors, particularly in neuroendocrine tumors (NETs). NETs are frequently characterized by high SSTRs expression levels. SST analogues (SSAs) that bind and activate SSTR have anti-proliferative and anti-secretory activity, thereby reducing both the growth as well as the hormonal symptoms of NETs. Moreover, the high expression levels of SSTR type-2 (SSTR2) in NETs is a powerful target for therapy with radiolabeled SSAs. Due to the important role of both SST and SSTRs, it is of great importance to elucidate the mechanisms involved in regulating their expression in NETs, as well as in other types of tumors. The field of epigenetics recently gained interest in NET research, highlighting the importance of this process in regulating the expression of gene and protein expression. In this review we will discuss the role of the epigenetic machinery in controlling the expression of both SSTRs and the neuropeptide SST. Particular attention will be given to the epigenetic regulation of these proteins in NETs, whereas the involvement of the epigenetic machinery in other types of cancer will be discussed as well. In addition, we will discuss the possibility to target enzymes involved in the epigenetic machinery to modify the expression of the SST-system, thereby possibly improving therapeutic options.

Keywords: cancer; epigenetic regulation; neuroendocrine tumors; somatostatin; somatostatin receptor.

1. EPIGENETIC REGULATION OF SSTR

1.1. EPIGENETIC REGULATION OF SSTR IN NETs

As discussed in *Chapter 1*, somatostatin (SST) analogues (SSAs) are a cornerstone medical treatment modality for neuroendocrine tumors (NETs), targeting somatostatin type-2 receptors (SSTR2) which are often expressed at a high level in NETs. The genomic DNA of human *SSTR2* contains multiple transcription start sites (TSSs). Two TSSs are located 82–93 nucleotides upstream [1, 2] from the translation start codon with an initiation element *inr* in close proximity. This *inr* is involved in regulating gene transcription in the absence of a TATA-box as transcription factors are able to bind to the E-box present within this *inr* [3]. Another TSS is located further upstream and contains a CpG island [4]. As CpGs are often the target for epigenetic modifications, it is likely that epigenetic regulation is involved in controlling *SSTR2* gene expression via this TSS. This suggests that deregulation of the epigenetic machinery may also influence tumoral SSTR2 expression. To elucidate the role of epigenetic regulation in NET patients, different NET cell lines have been used. These include cell lines derived from pancreatic NETs (PAN-NETs, i.e. BON-1 and QGP-1), pulmonary NETs (i.e. NCI-H727), small-intestine (SI-NETs, i.e. GOT1) and medullary thyroid cancer (i.e. TT and MZ-CRC-1), which are all characterized by their own basal SSTR2 expression levels.

In PAN-NET cells lines BON-1 and QGP-1, both DNA methylation and histone modifications regulate SSTR2 expression. In comparison with other NET cell lines, BON-1 and QGP-1 cells are both characterized by relatively low SSTR2 expression levels. However, *SSTR2* mRNA levels are still relatively high compared to cell lines derived from other types of cancer [4]. QGP-1 cells demonstrated low *SSTR2* promoter methylation rates at only 2% in the 8 CpG islands examined [5]. Similar observations were made for the pancreatic BON-1 cells, characterized by slightly higher SSTR2 expression levels compared to QGP-1 cells. Low (~3%), or even unmeasurable levels of DNA methylation were found in the genomic region surrounding the TSS in BON-1 cells [4, 5]. The low levels of DNA methylation and relatively low SSTR2 expression levels could be related to the involvement of DNA methylation in other regions, as the above described studies only focus on specific areas in the promoter region. Torrisani et al. [4] showed an inverse association between the level of CpG island methylation and *SSTR2* mRNA levels within several cell lines, including the PAN-NET cell line BON-1. Additionally, transfection of a methylated *SSTR2* promoter in BON-1 cells induced silencing of the *SSTR2* promoter. This effect was caused by the absence of binding of transcription factor specificity protein-1, a protein involved in regulating the basal *SSTR2* promoter activity [4]. Together, these observations support the potential of *SSTR2* promoter methylation to suppress SSTR2 expression. Moreover, acetylation on histone 3 was present in both BON-1 and QGP-1 cells [6]. The involvement of histone acetylation was further confirmed by Veenstra et al. [5]. In conclusion, both DNA methylation and histone acetylation are likely involved in regulating SSTR2 expression, i.e. triggering heterochromatin and euchromatin, respectively.

The above-mentioned associations between epigenetic markers and SSTR2 expression levels suggest that epigenetic drugs could potentially stimulate SSTR expression in NET cells. The use of epigenetic drugs, such as DNA methyltransferase inhibitors (DNMTis) and histone deacetylase inhibitors (HDACis), may stimulate euchromatin, thereby promoting *SSTR2* gene transcription. This approach can especially be important for NET patients not eligible for SSTR2-mediated therapies due to insufficient or undetectable SSTR expression levels.

1.1.1. MODULATION OF SSTR EXPRESSION *IN VITRO* IN NET CELL LINES

Successful stimulation of SSTR2 through attenuation of methylation has been demonstrated in BON-1 cells by treatment with DNMTis 5-aza-2′-deoxycytidine (5-AZA-dC) or 5-azacitidine (5-AZA), as shown by significantly enhanced uptake of [^{68}Ga]Ga-DOTATOC [7]. Further analysis of 5-AZA-dC pretreatment demonstrated increased *SSTR2* mRNA and SSTR2 protein expression levels, which increased over time. Moreover, the uptake of [^{68}Ga]Ga-DOTATOC was clearly enhanced at human 5-AZA-dC therapeutic serum concentrations, whereas effects were barely observed at lower concentrations. Based on these data, a time- and dose-dependency was suggested. The efficacy of 5-AZA-dC in modulating SSTR2 expression is investigated in several other studies. A seven-day treatment schedule resulted in enhanced *SSTR2* mRNA expression levels in both BON-1 and QGP-1 cells using 100 nM and 50 nM, respectively. Receptor functionality was subsequently demonstrated with internalization studies using [^{125}I]I-[Tyr^{3}]octreotide, reporting a significantly increased 1.85-fold uptake in BON-1 cells [5]. In line with this, significantly increased SSTR2 protein levels in BON-1 cells after a 3 day exposure to 2.5 µM 5-AZA-dC were also observed in the study by Jin et al. [8]. However, in another study, it was demonstrated that a 3 day exposure to a lower dose of 5-AZA-dC (2 µM) had no significant effects on *SSTR2* mRNA expression levels in BON-1 cells [4]. As the experimental set-up is similar in terms of cell line and exposure time, the results support data the above mentioned of Taelman et al. [7] of a dose-dependent response. As both time- and dose-dependency are clearly suggested, a precise treatment regimen may be important parameter for study outcome.

In addition to DNA methylation, histone acetylation is also likely involved in regulating SSTR2. HDACis therefore also gained great interest as a novel therapeutic strategy to stimulate SSTR2 expression. Several HDACis have been tested in QGP-1 cells, which has led to contradictory results. Whereas Veenstra et al. [5] demonstrated increased internalization of radiolabeled SSAs after valproic acid (VPA) treatment, *SSTR2* mRNA levels were significantly decreased by 1 mM VPA. This indicated other modes of action, e.g. fast redirection of the receptor to the membrane after internalization, via yet unknown epigenetic mechanisms. Contrary to these findings, significantly increased *SSTR2* mRNA levels were reported after VPA treatment by Guenter et al. [9] when using a higher VPA dosage (4 mM). Other HDACis, such as romidepsin (FK228), vorinostat (SAHA) and AB3, provided similar results as significant upregulation was demonstrated on *SSTR2* mRNA expression level. Unfortunately, western blot analysis could not confirm SSTR2 upregulation in QGP-1 cells upon HDACi treatment [9]. In contrast to this,

the use of the HDACi LMK-235 provided more convincing results, as this treatment resulted in increased SSTR2 protein expression levels [6]. An epigenetic mechanism-of-action was confirmed by an augmented acetylation of histone 3 upon HDACi-treatment. Of note, LMK-235 has high affinity for histone deacetylase 4 (HDAC4) and histone deacetylase 5 (HDAC5) 5, both belonging to HDAC class IIa, whereas all the other tested HDACis either target multiple HDAC-classes or specifically target HDAC class I. This may suggest that HDAC4 and HDAC5 are highly involved in inducing euchromatin, thereby enabling *SSTR2* transcription in QGP-1 cells. The effects of HDACi-treatment in BON-1 cells were more consistent than the results in the QGP-1 cell line. A screen of several HDACis (i.e. scriptaid, dacinostat, panobinostat, trichostatin A (TSA), SAHA, phenylbutyrate, FK228 and tacedinaline (TAC)) demonstrated enhanced uptake of radiolabeled SSAs by BON-1 cells, reaching statistical significance for most HDACis [7]. Further analysis of cells treated with TAC demonstrated significantly increased *SSTR2* mRNA and SSTR2 protein expression levels. In line with these results, significantly increased *SSTR2* mRNA levels were described after TSA treatment by Torrisani et al. [4]. Furthermore, protein expression levels were significantly increased upon TAC treatment [8], specifically inhibiting HDAC1–3, further supporting the enhanced uptake described by Taelman et al. [7]. FK228, SAHA and AB3 were also able to enhance *SSTR2* mRNA significantly within 24 h, and even demonstrated increased protein expression levels after 48 h treatment [9]. Moreover, it was shown that upon LMK-235 treatment the level of acetylation on histone 3 was increased, providing a dose-dependent increase of SSTR2 protein after a one day treatment [6].

Furthermore, the effects of VPA in BON-1 cells were evaluated in various studies. VPA treatment resulted in an increased level of acetylation on histone 4, thereby confirming changes in the epigenetic machinery. In line with this, SSTR2b protein expression was increased [10]. This VPA-augmented *SSTR2* expression level was confirmed at mRNA level upon short- (24–28 h) and long-term (7 days) VPA treatment [5, 9, 11]. Furthermore, a 7.2-fold stimulated SSTR2 protein expression level was observed [9], while the functionality of increased SSTR2 expression was further confirmed by a significantly increased uptake of radiolabeled SSAs [5, 7]. Receptor functionality was also confirmed by an increased efficacy of camptothecin-somatostatin conjugates after VPA treatment, as demonstrated by reduced BON-1 cell proliferation [10]. These results suggest that SSTR2 expression is more easily modified in BON-1 cells than in QGP-1 cells, and the effects seem to be less dependent on the targeted HDAC classes.

In addition to PAN-NETs, the effect of HDACis was examined in both small intestinal (i.e. GOT1 and KRJ-I) and pulmonary (i.e. NCI-H727) NETs, characterized by variable SSTR2 expression levels. Expression levels in GOT1 cells exceed that of NCI-H727 cells, which are both characterized by higher expression levels compared to BON-1 and KRJ-I cells [8, 12]. Although there has been some debate about the origin of KRJ-I cells [13, 14], VPA treatment increased *SSTR2* mRNA levels in these cells [11]. Studies with the small intestinal cell line GOT1 are still limited. The effect of HDACi treatment was solely examined upon monotherapy with

either VPA [11] or TAC [8], resulting in a statistically significant ~2-fold increased SSTR2 protein expression level after TAC treatment, while no significant changes in mRNA expression were observed after VPA treatment. For comparison, a similar treatment schedule did change *SSTR2* significantly in BON-1 and KRJ-I cells.

In the pulmonary NET cell line NCI-H727, SSTR2 protein expression level was not changed significantly upon TAC treatment [8]. However, in another study, HDACis thailandepsin-A (TDP-A), FK228, SAHA, VPA and AB3 were able to increase *SSTR2* mRNA levels significantly when high dosages were used [15]. Western blot analysis confirmed over 2.5-fold upregulation in all conditions. Further examination of TDP-A-treated NCI-H727 cells demonstrated both receptor functionality and increased receptor-mediated uptake of [^{68}Ga]Ga-DOTATATE. Equal concentrations of TDP-A, FK228, SAHA, VPA, and AB3 showed SSTR2 protein upregulation in the TT medullary thyroid cancer cell line up to 3-fold, whereas these effects were not observed in the MZ-CRC-1 medullary thyroid cancer cell line. Of note, MZ-CRC-1 cells are characterized by high basal SSTR2 expression level compared to TT cells.

Studies have also focused on combining epigenetic treatments, e.g. the combination of DNMTis and HDACis. In BON-1 cells, the combination treatment of 5-AZA-dC and VPA had additive or synergetic effects as demonstrated by higher *SSTR2* mRNA levels and higher uptake of [^{125}I]I-[Tyr^3]octreotide compared to either monotherapy [5]. Moreover, this combination of epigenetic drugs also significantly increased [^{125}I]I-[Tyr^3]octreotide uptake in QGP-1 cells, while effects of both monotherapies didn't result in significant changes. In addition, combination of 5-AZA-dC and TAC gave synergistic effects as well, in terms of [^{68}Ga]Ga-DOTA-TOC uptake and cell survival [7]. A similar combination treatment of 5-AZA-dC and TAC was examined in the BON-1, NCI-H727 and GOT1 cell line by another research group, demonstrating significantly increased SSTR2 protein expression levels of 8.31-, 1.56- and 2.06-fold, respectively [8]. Additive effects were demonstrated for BON-1 cells, whereas this was not evidently observed for H727 and GOT1. Thus, the effects in H727 cells and GOT1 cells were less pronounced compared to results obtained with BON-1 cells.

Altogether these studies clearly suggest the involvement of the epigenetic machinery in the regulation of SSTR2 expression in NET cells. Although convincing results in QGP-1 were only induced upon LMK-235 treatment, results obtained with other cell lines suggest that especially NET cell lines with low (i.e. BON-1) or intermediate (i.e. NCI-H727 and TT cells) SSTR2 expression levels are susceptible to epigenetic drug treatment, whereas upregulation in NET cell lines with high SSTR2 expression levels is more limited (i.e. GOT1 and MZ-CRC-1 cells). This supports the concept of epigenetic therapy for NET patients with insufficient SSTR2 expression, thereby potentially making more patients eligible for treatment with (radiolabeled) SSAs. The studies described above are summarized in Table 1. Of note, DNMTis (i.e. 5-AZA-dC) and some of the HDACis (i.e. VPA, TAC, SAHA, FK228) have been tested in clinical trials. Based on published pharmacokinetic parameters, it can be concluded that the drug

concentrations used in the studies described above are within the same order of magnitude or even within the achievable human therapeutic range.

1.1.2. MODULATION OF SSTR EXPRESSION *IN VIVO* IN NET XENOGRAFT-MODELS

Based on the *in vitro* results discussed above, the effects of epigenetic drugs were also tested *in vivo* using NET-bearing mice. Direct anti-proliferative effects can be induced by HDACi treatment. Reduced xenograft growth was observed after AB3, VPA, TDP-A, FK229 and entinostat (ENT) treatment in BON-1, GOT1, TT and/or H-STS NET tumor-bearing mice, although statistical significance was not reached in all studies [10, 11, 16-19]. The combination treatment of VPA and camptothecin-somatostatin conjugate significantly reduced BON-1 tumor growth by 66%, compared to 17% and 42% for both monotherapies, respectively [10]. Tumors were not resected in this study and HDACi-upregulated SSTR2 expression was therefore not confirmed. Encapsulation of the HDACi TDP-A in micelles functionalized with either KE108 [17] or octreotide [19] reduced tumor volume with 92% and 74%, respectively. In both these studies, significant differences were found between the effects observed after treatment with TDP-A-loaded targeted micelles compared to TDP-A-loaded non-targeted micelles. Similar results were described for AB3-encapsulted KE108-functionalized micelles tested in medullary thyroid cancer TT xenografts [18]. According to the authors, the enhanced effects for TDP-A-loaded targeted micelles can be explained by the combination of both passive and active tumor targeting ability, i.e. enhanced permeation retention effect and efficient targeting of SSTRs, respectively. Unfortunately, tumors were not further analyzed to confirm changes in SSTR2 expression levels upon HDACi treatment. Although these data are not available, it may also be hypothesized that the enhanced effects upon treatment with TDP-A-loaded or AB3-loaded targeted micelles are caused by the fact that the HDACis are targeted to the SSTR2-expressing tumor cells, resulting in enhanced receptor expression due to HDACi-mediated changes in the epigenetic machinery. This SSTR2 upregulation may lead to increased therapeutic efficacy as more functionalized micelles will be targeted to the tumor cells. However, this hypothesis requires further investigations.

In the study published by Taelman et al. [7], it was demonstrated that 5-AZA-dC significantly increased the uptake of [^{68}Ga]Ga-DOTA-TOC in BON-1 tumor-bearing mice in a dose-dependent manner, resulting in increased tumor-to-background and tumor-to-kidney ratios. Moreover, a blocking study demonstrated SSTR-specific uptake after HDACi treatment, indicating SSTR-upregulation. As a result, tumors could be visualized using PET/CT-imaging modality. In addition to this study using a DNMTi, two studies have been published in which SSTR2 expression levels were examined by PET/CT-scans upon inhibition of HDAC class I proteins. For BON-1 tumor-bearing mice, significantly increased standard uptake values (SUVs) were observed on a PET/CT-scan after [^{68}Ga]Ga-DOTATATE injection when mice were pre-treated with FK228 [9]. A similar effect was observed in mice with NCI-H727 xenografts that were treated with TDP-A. This study showed a trend towards SSTR upregulation following

HDACi-treatment, although statistical significance was not reached due to differences in individual tumor size and uptake of [^{68}Ga]Ga-DOTATATE [15].

1.2. EPIGENETIC REGULATION OF SSTR IN OTHER CANCER TYPES

Studies focusing on other types of cancer showed that deregulation of SSTR is also often established by epigenetic mechanisms. For colorectal cancer (CRC), the *SSTR2* promoter was characterized by enhanced methylation levels, which was associated with reduced SSTR2 expression [20]. Similar results were obtained in head and neck squamous cell carcinomas (HNSCC). Here, higher methylation levels of SSTR1 were detected compared to adjacent normal mucosal tissue, which correlated with several clinicopathologic features [21]. This was confirmed in squamous cell carcinoma cell lines, exhibiting low *SSTR1* mRNA levels and high levels of promoter methylation in comparison to normal cell lines. In line with these results, increased methylation levels on CpG sites present within the *SSTR2* promoter region were also described for laryngeal squamous cell carcinomas [22]. Moreover, the *SSTR1* promoter was frequently methylated in Epstein-Barr virus (EBV) positive primary gastric cancer samples (67%), whereas this was not the case in EBV-negative primary gastric cancer samples [23]. In line with this result, *SSTR2, SSTR3* and *SSTR5* mRNA expression levels were also reported to be reduced in gastric cancer samples compared to paired normal gastric tissue [24]. For SSTR2, this was confirmed by Kim et al. [25] by a negative correlation between *SSTR2* methylation and gene expression in human gastric tumor tissue. In general, SSTR expression is reduced in cancer because of methylation of the promoter region. This suggests the involvement of the epigenetic machinery in deregulated SSTR expression in cancer. Epigenetic drugs can therefore potentially modulate SSTR expression and thus therapeutic opportunities.

1.2.1. MODULATION OF SSTR EXPRESSION *IN VITRO* AND *IN VIVO* IN OTHER TYPES OF CANCER

The involvement of the epigenetic machinery in other cancer types is further supported by studies aiming to increase SSTR expression using epigenetic drugs. The effect of VPA was evaluated in several human cell lines, i.e. hepatocellular carcinoma cells [26], small cell lung cancer cells [27] and cervical cancer cells [28, 29]. The epigenetic mechanism-of-action of VPA was confirmed by western blot analysis in hepatocellular carcinoma and lung cancer cells, as demonstrated by a decreased expression of HDAC4 protein and increased acetylation on histone 4. Likely as a result of this altered acetylation pattern, *SSTR2* was upregulated, i.e. a 20.6 and 7.4-fold increase, respectively. Therapeutic efficacy was increased in small cell lung cancer cells when VPA treatment was combined with camptothecin- or colchicine-somatostatin conjugates as shown by decreased cell growth *in vitro*. For cervical cancer cells, expression of *SSTR* subtypes were also changed upon VPA treatment. Here, VPA increased expression of *SSTR2*, *SSTR3* and *SSTR5* in a dose-dependent manner, while *SSTR1* expression levels were downregulated. The VPA-induced SSTR2 upregulation, resulted in enhanced effects of cytotoxic-somatostatin conjugates, both *in vitro* and *in vivo* [28, 29].

Table 1. Overview of *in vitro* studies with their main findings relevant for this review, focusing on modifying SSTR expression in NET cell lines using DNMTis or HDACis.

Cell types	Epidrug	Treatment Regiment	Main Findings	Ref
BON-1	Screen of several DNMTis and HDACis, e.g. 5-AZA-dC and TAC	75 g/mL 5-AZA-dC or 500 ng/mL TAC; time-dependency experiment (1–3 days)	- TAC and 5-AZA-dC increased the uptake of [^{68}Ga]Ga-DOTA-TOC most efficiently; *SSTR2* mRNA and SSTR2 protein expression levels were also significantly increased - Observed effects are time- and dose-dependent - Synergetic effects upon combination therapy in terms of [^{68}Ga]Ga-DOTA-TOC uptake and cell survival	[7]
BON-1 QGP-1	5-AZA-dC VPA	BON-1: 100 nM 5-AZA-dC and/or 2.5 mM VPA; 7 days QGP-1: 50 nM 5-AZA-dC and/or 1 mM VPA; 7 days	- Low *SSTR2* CpG island methylation around transcription start site; ~3% in BON-1, ~2% in QGP-1 - All treatments increased *SSTR2* mRNA levels and uptake of [^{125}I]I-[Tyr^3]octreotide significantly in BON-1; enhanced effects for combination therapy - *SSTR2* mRNA levels and uptake of [^{125}I]I-[Tyr^3]octreotide increased after combination therapy in QGP-1 - *T*reatment of QGP-1 with VPA decreased *SSTR2* mRNA levels and enhanced uptake of [^{125}I]I-[Tyr^3]octreotide non-significantly, suggesting other mechanisms of action - Histone acetylation more likely involved in regulating SSTR2 expression than histone methylation	[5]

Table 1 (continued). Overview of *in vitro* studies with their main findings relevant for this review, focusing on modifying SSTR expression in NET cell lines using DNMTis or HDACis.

BON-1 NCI-H727 QGP-1 GOT1	5-AZA-dC TAC	2.5 µM or 5.0 µM 5-AZA-dC and/or 2.5 µM or 5.0 µM TAC; 3 days	- SSTR2 protein expression levels in QGP-1 undetectable before and after HDACi treatment - Combination treatment induced statistically significant upregulation of SSTR2 protein expression in BON-1, GOT1 and NCI-H727; maximum increase of 8.31-fold in BON-1 - TAC significantly enhanced SSTR2 expression in BON-1 and GOT1; 5-AZA-dC in BON-1 and NCI-H727	[8]
BON-1	5-AZA-dC TSA	2 µM 5-AZA-dC and/or 150 nM TSA; 3 days	- *SSTR2* upstream promoter not methylated - Significantly upregulated *SSTR2* mRNA expression levels upon TSA and combination therapy - Statistically significant correlation between *SSTR2* mRNA expression and CpG island methylation in upstream promoter	[4]
BON-1 QGP-1	TDP-A SAHA VPA FK228 AB3	2 nM or 6 nM TDP-1, 1 µM or 3 µM SAHA, 1 mM or 4 mM VPA, 2 nM or 6 nM FK228 or 1 µM or 3 µM AB-3 1 day for RT-qPCR, 2 days for further analysis	- *SSTR2* mRNA levels significantly increased after 1 day treatment with 3 µM SAHA, 4 mM VPA, 6 nM FK228 and 3 µM AB3, in both BON-1 and QGP-1 - SSTR2 protein levels not evidently increased in QGP-1; maximum increase of 1.7-fold - SSTR2 protein levels clearly enhanced in BON-1; maximum increase of 7.2-fold - Increased functional SSTR2 density on cell surface for 6 nM FK228 in BON-1	[9]

Table 1 (continued). Overview of *in vitro* studies with their main findings relevant for this review, focusing on modifying SSTR expression in NET cell lines using DNMTis or HDACis.

BON-1 QGP-1	LMK-235	0.08 µM, 0.31 µM, 1.25 µM, 5.0 µM and 20 µM; 1 or 2 days	- Dose-dependent increased acetylation on histone 3 upon LMK-235 treatment - Dose-dependent increased SSTR2 protein level in BON-1 - SSTR2 protein levels detectable in QGP-1 after high concentration LMK-235 treatment	[6]
BON-1	VPA	2 mM or 4 mM; time-dependency experiment (3, 6, 18, 36 and 72 h)	- Time-dependent increased level of acetylation on histone 4 - Reduced activity of HDAC4 after chronic treatment - Increased SSTR2b and decreased SSTR1, SSTR3, SSTR4 and SSTR5 protein expression levels - VPA enhanced anti-proliferating effects of camptothecin-somatostatin conjugates	[10]
BON-1 KRJ-I GOT1	VPA	4 mM; 28 h	- Significantly increased *SSTR2* mRNA expression level in BON-1 and KRJ-I	[11]
NCI-H727 MZ-CRC-1 TT	TDP-A SAHA VPA FK228 AB3	2 nM or 6 nM TDP-1, 1 µM or 3 µM SAHA, 1 mM or 4 mM VPA, 2 nM or 6 nM FK228 or 1 µM or 3 µM AB-3 1 day for RT-qPCR, 2 days for further analysis	- *SSTR2* mRNA levels significantly increased in NCI-H727 after highest-dose HDACi treatment; VPA and TDP-A also increased expression at lower dose - SSTR2 protein levels evidently increased; minimum increase of 2.5-fold in NCI-H727 - TDP-A treatment significantly increased uptake of [^{68}Ga]Ga-DOTATATE in NCI-H727 - SSTR2 protein upregulated in TT after HDACi treatment; limited effects in MZ-CRC-1 which are characterized by higher basal SSTR2 expression levels compared to TT	[15]

The epigenetic machinery was also shown to be involved in the regulation of SSTR2 expression in pancreatic cancer cell lines. Upon epigenetic drug treatment with DNMTi 5-AZA-dC or HDACi TSA, *SSTR2* mRNA levels were increased, with even stronger upregulation observed for the combination treatment. These results suggest the involvement of both DNA methylation and histone acetylation [4]. The possibility to modulate *SSTR2* transcription by DNA methylation was confirmed by Gailhouste et al. [30], as *SSTR2* mRNA levels were upregulated after 5-AZA treatment, resulting in reduced cell growth upon treatment with SSAs. Upregulation of *SSTR4* and *SSTR5* was also reported in response to DNMTi treatment, thereby emphasizing the important role of DNA methylation in controlling the expression of several receptors within the SST-pathway.

SSTR5 expression in primary human laryngeal squamous cell carcinoma tissue demonstrated to be significantly lower compared to corresponding normal tissue. Low expression levels were confirmed in cell lines. Further analysis of these cancer cell lines demonstrated that methylation of exon 1 of the *SSTR5* gene is likely involved in downregulation of the protein. The involvement of histone modifications was also confirmed, as treatment with 5-AZA and/or TSA upregulated *SSTR5* mRNA expression levels. For the AMC-HN-8 cell line, the presence of active and inactive histone modifications in the *SSTR5* promoter were examined. Activating histone mark H3K4me3 was enriched upon 5-AZA-dC or combination treatment, activating histone mark H3K9ac was enriched upon TSA or combination treatment, and repressive histone mark H3K9me2 was decreased upon 5-AZA-dC or combination treatment. In this extensive study by Wang et al. [31], the involvement of both DNA methylation and histone modifications was therefore clearly demonstrated in the regulation of SSTR5 in laryngeal squamous cell carcinomas cell lines.

Moreover, 5-AZA-dC and TSA treatment increased *SSTR5* mRNA expression levels in a castration-resistant prostate cancer cell line [32]. Combining DNMTi and HDACi treatment had additive effects in this cell line in terms of *SSTR5* expression, whereas such effects were not observed in androgen-sensitive cell lines, suggesting cell type-specific responses. This cell type-specific response was further confirmed as 5-AZA-dC treatment was associated with *SSTR1* hypomethylation in androgen receptor-positive prostate cancer cell line, whereas this was not observed in an androgen-receptor negative prostate cancer cell line [33].

Data has also suggested the involvement of epigenetic mechanisms in the controlling SSTR2 expression in gastric cancer. In line with this, 5-AZA-dC and/or TSA treatment restored both *SSTR2* and *SSTR4* mRNA expression in 75% of the examined gastric cell lines, with the greatest effects observed upon combination therapy [25]. Upon comparing EBV-positive AGS gastric cancer cells and EBV-negative AGS gastric cancer cells, it was demonstrated that EBV-positive AGS cells are characterized by enhanced activity of DNMT3b and higher SSTR1 CpG island methylation levels. Further analysis showed that the viral latent membrane protein 2A (LMP2A), expressed upon EBV infection, is involved in DNMT3b upregulation. Treatment of EBV-positive AGS cells with 5-AZA-dC resulted in increased *SSTR1* mRNA levels. Of note, this

was not observed in the EBV-negative gastric cell line. The latter cell line is characterized by very low *SSTR1* CpG island methylation levels compared to EBV-positive AGS cells [23, 34]. This suggests that DNMTis are only efficient in enhancing SSTR levels in cells characterized by high DNA methylation levels.

Summarizing, these data demonstrated that, in line with the epigenetic regulation involved in SSTR2 expression in NETs, the epigenetic machinery plays an important role in the regulation of multiple SSTRs in other cancer types as well. Moreover, it is possible to increase SSTR expression in a number of cancer types by epigenetic drug treatment.

2. EPIGENETIC REGULATION OF SST IN CANCER

As discussed above, activation of SSTR by SST can induce several effects, e.g. inhibiting cell proliferation and hormone secretion, and promoting apoptosis. SST is therefore known has a protein with anti-proliferative and anti-secretory activity. This was further supported in a recently published paper, showing that knock out of SST in the BGC823 gastric cancer cell line resulted in an increased capacity for migration and invasion *in vitro* [35]. Due to its role, SST expression in cancer is evaluated extensively in order to find new biomarkers or to expand current therapeutic options. For NET patients, long-acting SSAs increase progression-free survival [36, 37], confirming the anti-proliferative activity of SST upon SSTR activation. In addition, preclinical studies showed that the SST-SSTR interaction has tumor suppressor activity in certain tumors [38]. This raises the question whether deregulation of SST expression in NETs has impact of NET function as well. However, to the best of our knowledge, no reports have been published yet about the epigenetic regulation of SST in NETs.

On the other hand, the regulation of SST expression in gastric cancer has been subject to research. SST knock-down experiments in the GES-1 cell line resulted in a lowering of cells in the G0/G1 phase, suggesting an important role of SST in cell proliferation [39]. Moreover, a high DNA methylation level of the SST promoter and its association with undetectable SST expression has been described in seven gastric cancer cell lines [40]. Li. et al. [41] confirmed *SST* promoter hypermethylation in gastric cancer tissue. However, the authors were unable to validate a reduction in *SST* mRNA expression in human tissue using 10 pairs of tumor and adjacent non-tumorous tissue ($p = 0.074$). Contradictory to this, reduced *SST* mRNA and SST protein expression levels have been described in gastric carcinoma samples throughout multiple studies using larger cohorts of patients. Reduced *SST* mRNA and SST protein expression levels thereby both correlated with increased *SST* DNA methylation levels [24, 40, 42].

For renal cell carcinomas, published results are equivocal. Ricketts et al. [43] demonstrated hypermethylation both in cell lines and in primary tissue samples. In these tissue samples, it was shown that tumor-specific hypermethylation of the *SST* promoter was associated with reduced *SST* mRNA expression levels. Contradictory, Morris et al. [44] reported promoter

hypermethylation only in renal cancer cell lines, whereas this was not observed in any of the analyzed primary renal cell carcinoma tissue samples.

The involvement of the epigenetic machinery in the regulation of SST has also been demonstrated in several studies focusing on colon cancer and CRC. CpG sites within the *SST* gene were hypermethylated in different stages of tumorous samples, i.e. 94%, 100%, 94% and 57% for adenomas with low-grade dysplasia, adenomas with high-grade dysplasia, CRC and metastatic-CRC, respectively [45]. Likely as a result of this observed hypermethylation in CRC, the *SST* mRNA level was decreased in CRC compared to normal tissue, as demonstrated with microarray data [46]. In a small pilot study with only 4 samples collected from patients with pre-neoplastic colorectal sessile serrated adenomas, *SST* hypermethylation was demonstrated in all examined patients [47]. These results indicate that, among others, the downregulation of SST may be involved in the development of CRC. In line with this, *SST* promoter methylation is increased in CRC, associating with reduced expression levels [20, 46, 48]. In agreement with the results observed in CRC samples, *SST* promoter methylation levels were also significantly increased when focused specifically on primary colon cancer samples compared to normal colonic mucosae, i.e. 88% versus 47%, respectively [49].

Limited information is available about the epigenetic regulation of SST in other types of cancer. *SST* promoter hypermethylation was shown in pancreatic PANC-1 cells. Here, CpG methylation rates of 96–98% were associated with extremely low *SST* mRNA levels [30]. Moreover, knockdown of DNMT1 increased *SST* expression, emphasizing the role of DNA methylation and thus the epigenetic machinery in the regulation of SST expression. Furthermore, analysis of glioblastoma multiforme tissue samples demonstrated both *SST* hypermethylation on CpG sites and a 80.5-fold downregulated *SST* expression level compared to control brain tissue [50]. *SST* hypermethylation has also been reported for human tissue derived from cervical cancer [51] and anal cancer [52], and both in cell lines and human tissue derived from esophageal carcinomas [53], gliomas [54] as well as HNSCC [21, 55, 56]. For esophageal carcinomas, gliomas and HNSCC, a negative correlation with mRNA expression was found. It has even been suggested that SST may be used as a methylation-based biomarker for the prognosis and/or diagnosis of HNSCC [55], CRC [20, 48], cervical [51] and anal cancer [52].

There is a possibility that the presence of endocrine cells in the examined tissues affect the outcome of these studies, for example the presence of enteroendocrine cells in control colorectal and CRC tissue. These endocrine cells are characterized by the expression of SST, and differences in the number of these cells in normal and tumor tissue, and thus the level of SST expression, may bias the conclusions focusing on downregulated SST expression levels in tumor tissue. However, *SST* hypermethylation, which is reported for several types of tumors, still suggests that SST, with its anti-proliferating and anti-secretory effects, is under the control of the epigenetic machinery. To the best of our knowledge, no data are available with respect to the role of histone acetylation within this process. In line with SSTR2 regulation, SST

expression can therefore be modified by the use of epigenetic drug inhibitors targeting DNA methylation, i.e. DNMTis.

2.1. MODULATION OF SST EXPRESSION *IN VITRO* AND *IN VIVO*

In vitro studies have demonstrated that the DNMTi 5-AZA-dC modulates SST expression. 5-AZA-dC has been shown to induce demethylation of the *SST* gene and/or concomitantly increased SST protein expression levels in cell lines derived from colon cancer [49], renal cell carcinoma [43] and esophageal cancer [53]. Similar results were observed in the PANC-1 pancreatic cancer cell line upon 5-AZA treatment [30]. Results were also confirmed *in vivo*. Subcutaneous inoculation of 5-AZA pre-treated cells in athymic nude mice resulted in reduced tumor growth. Moreover, 5-AZA treatment of PANC-1 xenograft-bearing mice induced a significant reduction in tumor volume. Examination of the resected tumors showed that *SST* mRNA levels were significantly increased after 5-AZA treatment. Moreover, the *SST* promoter was demethylated at CpG sites upon epigenetic drug treatment.

Additionally, in the AGS gastric cancer cell line, the effect of 5-AZA-dC was dose-dependent. A lower dose (1.6 µM; 3 days treatment) had no effect on *SST* mRNA levels in the AGS cell line [42], whereas a higher dose (5 µM; 3 days treatment) reduced *SST* DNA promoter methylation levels and restored mRNA expression to detectable levels. Combination treatment of 5-AZA-dC and TSA even further increased *SST* mRNA levels [40]. Studies with other gastric cancer cell lines showed higher *SST* mRNA levels upon 5-AZA-dC in a subset of the tested cell lines [42], suggesting cell line-specific responses. Cell line-specific responses were also reported for gliomas [54], only demonstrating *SST* upregulation upon 5-AZA-dC treatment in cell lines characterized by promoter hypermethylation. The glioma cell lines U251 and SF767 are characterized by 51.6% and 77.1% methylation of the *SST* promoter, respectively. Upon 5-AZA-dC treatment, *SST* mRNA levels were significantly increased. Of note, these effects were not observed in SF126 cells, characterized by only 14.2% methylation. This suggests that DNMTi are only effective in cell lines with high promoter methylation levels. Upon inducing SST expression, there was enrichment of activating histone marks H3Ac and H3K4me3, and reduction of inhibiting mark H2K9me3, suggesting an interplay between the promoter region and chromatin structure.

Altogether, several lines of evidence suggest that DNA methylation as well as histone modifications are involved in deregulated SST expression in various types of cancer. Moreover, *SST* expression can be modulated by the use of epigenetic drugs, thereby further supporting the involvement of the epigenetic machinery.

3. CONCLUSION

In conclusion, understanding of the epigenetic mechanisms involved in the regulation of the expression of the SST-system is important for both NETs and other tumor types. A detailed analysis of this system potentially opens up new possibilities to develop or improve treatment

options for different types of SSTR-expressing tumors, including NETs. Although studies clearly prove the involvement of epigenetics in the regulation of SSTRs and SST expression *in vitro*, more in-depth studies are required to confirm the ability to upregulate SSTR2 by using epigenetic drugs in vivo. Proper analysis to confirm the mechanism-of-action of epigenetic drugs are often lacking, e.g. examining histones profiles, immunohistochemistry, RT-qPCR and/or autoradiography to confirm increased SSTR expression.

Moreover, receptor-specificity should be determined after epigenetic drug treatment. Since most of the knowledge on the epigenetic regulation of the SST-system is derived from *in vitro* studies in cell lines and experimental tumor models, future studies should also focus on the role of epigenetic marks in determining SSTR expression in primary NET tissues from patients. Moreover, the safety profile of epigenetic drugs on healthy tissue should be assessed as these drugs may potentially upregulate physiological SSTR2 expression which possibly results in enhanced (radio)toxicity in non-targeted organs. Known and future insights in the epigenetic regulation of SST and SSTR in NETs may result in the development of epidrug-based treatment modalities aiming to increase SST and SSTR2 expression. Increased intra-tumoral SST expression may in turn lead to anti-secretory and anti-proliferative effects, whereas increased SSTR2 expression could improve tumor visibility with SSTR-scintigraphy and enhance tumor response to (radiolabeled) SSAs. This may in particular be beneficial for patients with low or insufficient SSTR expression. Moreover, future studies, also including safety, are required to define the optimal dose and treatment duration for mono- and combination therapy with DNMTis and/or HDACis.

ACKNOWLEDGEMENTS

We thank the Medical Library of the Erasmus MC for assisting with the literature search.

REFERENCES

1. Petersenn, S.; Rasch, A.C.; Presch, S.; Beil, F.U.; Schulte, H.M. Genomic structure and transcriptional regulation of the human somatostatin receptor type 2. *Mol Cell Endocrinol* **1999**, *157*, 75-85.
2. Xu, Y.; Berelowitz, M.; Bruno, J.F. Characterization of the promoter region of the human somatostatin receptor subtype 2 gene and localization of sequences required for estrogen-responsiveness. *Mol Cell Endocrinol* **1998**, *139*, 71-77.
3. Pscherer, A.; Dorflinger, U.; Kirfel, J.; Gawlas, K.; Ruschoff, J.; Buettner, R.; Schule, R. The helix-loop-helix transcription factor SEF-2 regulates the activity of a novel initiator element in the promoter of the human somatostatin receptor II gene. *Embo J* **1996**, *15*, 6680-6690.
4. Torrisani, J.; Hanoun, N.; Laurell, H.; Lopez, F.; Maoret, J.J.; Souque, A.; Susini, C.; Cordelier, P.; Buscail, L. Identification of an upstream promoter of the human somatostatin receptor, hSSTR2, which is controlled by epigenetic modifications. *Endocrinology* **2008**, *149*, 3137-3147.
5. Veenstra, M.J.; van Koetsveld, P.M.; Dogan, F.; Farrell, W.E.; Feelders, R.A.; Lamberts, S.W.J.; de Herder, W.W.; Vitale, G.; Hofland, L.J. Epidrug-induced upregulation of functional somatostatin type 2 receptors in human pancreatic neuroendocrine tumor cells. *Oncotarget* **2018**, *9*, 14791-14802.
6. Wanek, J.; Gaisberger, M.; Beyreis, M.; Mayr, C.; Helm, K.; Primavesi, F.; Jäger, T.; Di Fazio, P.; Jakab, M.; Wagner, A., et al. Pharmacological inhibition of class IIA HDACs by LMK-235 in pancreatic neuroendocrine tumor cells. *Int J Mol Sci* **2018**, *19*.
7. Taelman, V.F.; Radojewski, P.; Marincek, N.; Ben-Shlomo, A.; Grotzky, A.; Olariu, C.I.; Perren, A.; Stettler, C.; Krause, T.; Meier, L.P., et al. Upregulation of Key Molecules for Targeted Imaging and Therapy. *J Nucl Med* **2016**, *57*, 1805-1810.
8. Jin, X.F.; Auernhammer, C.J.; Ilhan, H.; Lindner, S.; Nölting, S.; Maurer, J.; Spöttl, G.; Orth, M. Combination of 5-fluorouracil with epigenetic modifiers induces radiosensitization, somatostatin receptor 2 expression, and radioligand binding in neuroendocrine tumor cells in vitro. *J Nucl Med* **2019**, *60*, 1240-1246.
9. Guenter, R.; Aweda, T.; Carmona Matos, D.M.; Jang, S.; Whitt, J.; Cheng, Y.-Q.; Liu, X.M.; Chen, H.; Lapi, S.E.; Jaskula-Sztul, R. Overexpression of somatostatin receptor type 2 in neuroendocrine tumors for improved Ga68-DOTATATE imaging and treatment. *Surgery* **2019**.
10. Sun, L.; Qian, Q.; Sun, G.; Mackey, L.V.; Fuselier, J.A.; Coy, D.H.; Yu, C.Y. Valproic acid induces NET cell growth arrest and enhances tumor suppression of the receptor-targeted peptide-drug conjugate via activating somatostatin receptor type II. *J Drug Targeting* **2016**, *24*, 169-177.
11. Arvidsson, Y.; Johanson, V.; Pfragner, R.; Wangberg, B.; Nilsson, O. Cytotoxic Effects of Valproic Acid on Neuroendocrine Tumour Cells. *Neuroendocrinology* **2016**, *103*, 578-591.
12. Li, S.C.; Martijn, C.; Cui, T.; Essaghir, A.; Luque, R.M.; Demoulin, J.B.; Castano, J.P.; Oberg, K.; Giandomenico, V. The somatostatin analogue octreotide inhibits growth of small intestine neuroendocrine tumour cells. *PLoS One* **2012**, *7*, e48411.
13. Hofving, T.; Arvidsson, Y.; Almobarak, B.; Inge, L.; Pfragner, R.; Persson, M.; Stenman, G.; Kristiansson, E.; Johanson, V.; Nilsson, O. The neuroendocrine phenotype, genomic profile and therapeutic sensitivity of GEPNET cell lines. *Endocr Relat Cancer* **2018**, *25*, 367-380.
14. Alvarez, M.J.; Yan, P.; Alpaugh, M.L.; Bowden, M.; Sicinska, E.; Zhou, C.W.; Karan, C.; Realubit, R.B.; Mundi, P.S.; Grunn, A., et al. Reply to 'H-STS, L-STS and KRJ-I are not authentic GEPNET cell lines'. *Nature Genetics* **2019**, *51*, 1427-1428.
15. Guenter, R.E.; Aweda, T.; Carmona Matos, D.M.; Whitt, J.; Chang, A.W.; Cheng, E.Y.; Liu, X.M.; Chen, H.; Lapi, S.E.; Jaskula-Sztul, R. Pulmonary Carcinoid Surface Receptor Modulation Using Histone Deacetylase Inhibitors. *Cancers (Basel)* **2019**, *11*.
16. Alvarez, M.J.; Subramaniam, P.S.; Tang, L.H.; Grunn, A.; Aburi, M.; Rieckhof, G.; Komissarova, E.V.; Hagan, E.A.; Bodei, L.; Clemons, P.A., et al. A precision oncology approach to the pharmacological targeting of mechanistic dependencies in neuroendocrine tumors. *Nat Genet* **2018**, *50*, 979-989.

17. Chen, G.; Jaskula-Sztul, R.; Harrison, A.; Dammalapati, A.; Xu, W.; Cheng, Y.; Chen, H.; Gong, S. KE108-conjugated unimolecular micelles loaded with a novel HDAC inhibitor thailandepsin-A for targeted neuroendocrine cancer therapy. *Biomaterials* **2016**, *97*, 22-33.
18. Jaskula-Sztul, R.; Chen, G.; Dammalapati, A.; Harrison, A.; Tang, W.; Gong, S.; Chen, H. AB3-Loaded and Tumor-Targeted Unimolecular Micelles for Medullary Thyroid Cancer Treatment. *J Mater Chem B* **2017**, *5*, 151-159.
19. Jaskula-Sztul, R.; Xu, W.; Chen, G.; Harrison, A.; Dammalapati, A.; Nair, R.; Cheng, Y.; Gong, S.; Chen, H. Thailandepsin A-loaded and octreotide-functionalized unimolecular micelles for targeted neuroendocrine cancer therapy. *Biomaterials* **2016**, *91*, 1-10.
20. Liu, J.; Li, H.; Sun, L.; Wang, Z.; Xing, C.; Yuan, Y. Aberrantly methylated-differentially expressed genes and pathways in colorectal cancer. *Cancer Cell Int* **2017**, *17*.
21. Misawa, K.; Misawa, Y.; Kondo, H.; Mochizuki, D.; Imai, A.; Fukushima, H.; Uehara, T.; Kanazawa, T.; Mineta, H. Aberrant methylation inactivates somatostatin and somatostatin receptor type 1 in head and neck squamous cell carcinoma. *PLoS One* **2015**, *10*.
22. Shen, Z.; Chen, X.; Li, Q.; Zhou, C.; Li, J.; Ye, H.; Duan, S. SSTR2 promoter hypermethylation is associated with the risk and progression of laryngeal squamous cell carcinoma in males. *Diagn Pathol* **2016**, *11*, 10.
23. Zhao, J.; Liang, Q.; Cheung, K.F.; Kang, W.; Lung, R.W.M.; Tong, J.H.M.; To, K.F.; Sung, J.J.Y.; Yu, J. Genome-wide identification of Epstein-Barr virus-driven promoter methylation profiles of human genes in gastric cancer cells. *Cancer* **2013**, *119*, 304-312.
24. Shi, X.; Li, X.; Chen, L.; Wang, C. Analysis of somatostatin receptors and somatostatin promoter methylation in human gastric cancer. *Oncol Lett* **2013**, *6*, 1794-1798.
25. Kim, H.J.; Kang, T.W.; Haam, K.; Kim, M.; Kim, S.K.; Kim, S.Y.; Lee, S.I.; Song, K.S.; Jeong, H.Y.; Kim, Y.S. Whole genome MBD-seq and RRBS analyses reveal that hypermethylation of gastrointestinal hormone receptors is associated with gastric carcinogenesis. *Exp Mol Med* **2018**, *50*, 156.
26. Sun, G.; Mackey, L.V.; Coy, D.H.; Yu, C.Y.; Sun, L. The histone deacetylase inhibitor vaproic acid induces cell growth arrest in hepatocellular carcinoma cells via suppressing notch signaling. *J Cancer* **2015**, *6*, 996-1004.
27. Sun, L.; He, Q.; Tsai, C.; Lei, J.; Chen, J.; Makcey, L.V.; Coy, D.H. HDAC inhibitors suppressed small cell lung cancer cell growth and enhanced the suppressive effects of receptor-targeting cytotoxins via upregulating somatostatin receptor II. *Am J Transl Res* **2018**, *10*, 545-553.
28. Franko-Tobin, L.G.; Mackey, L.V.; Huang, W.; Song, X.; Jin, B.; Luo, J.; Morris, L.M.; Liu, M.; Fuselier, J.A.; Coy, D.H., et al. Notch1-mediated tumor suppression in cervical cancer with the involvement of SST signaling and its application in enhanced SSTR-targeted therapeutics. *Oncologist* **2012**, *17*, 220-232.
29. Tsai, C.; Leslie, J.S.; Franko-Tobin, L.G.; Prasnal, M.C.; Yang, T.; Vienna Mackey, L.; Fuselier, J.A.; Coy, D.H.; Liu, M.; Yu, C., et al. Valproic acid suppresses cervical cancer tumor progression possibly via activating Notch1 signaling and enhances receptor-targeted cancer chemotherapeutic via activating somatostatin receptor type II. *Arch Gynecol Obstet* **2013**, *288*, 393-400.
30. Gailhouste, L.; Liew, L.C.; Hatada, I.; Nakagama, H.; Ochiya, T. Epigenetic reprogramming using 5-azacytidine promotes an anti-cancer response in pancreatic adenocarcinoma cells. *Cell Death Dis* **2018**, *9*.
31. Wang, B.; Zhao, L.; Chi, W.; Cao, H.; Cui, W.; Meng, W. Aberrant methylation-mediated downregulation of lncRNA SSTR5-AS1 promotes progression and metastasis of laryngeal squamous cell carcinoma. *Epigenetics Chromatin* **2019**, *12*.
32. Liu, Z.; Marquez, M.; Nilsson, S.; Holmberg, A.R. Incubation with somatostatin, 5-aza decitabine and trichostatin up-regulates somatostatin receptor expression in prostate cancer cells. *Oncol Rep* **2008**, *20*, 151-154.
33. Habeeb, N.M.A.W.-A.; Ho, L.T.; Olkhov-Mitsel, E., *Integrated analysis of epigenomic and genomic changes by DNA methylation dependent mechanisms provides potential novel biomarkers for prostate cancer*. Oncotarget. 2014: ncbi.nlm.nih.gov.

34. Zhao, J.; Cheung, K.F.; Kang, W.; Tong, J.H.; To, K.F.; Sung, J.J.; Yu, J. Somatostatin receptor 1, a novel EBV-driven CpG hypermethylated gene, contributes to the pathogenesis of EBV-associated gastric cancer. *Gastroenterology* **2011**, *140*, S349.
35. Chen, W.; Ding, R.; Tang, J.; Li, H.; Chen, C.; Zhang, Y.; Zhang, Q.; Zhu, X. Knocking Out SST Gene of BGC823 Gastric Cancer Cell by CRISPR/Cas9 Enhances Migration, Invasion and Expression of SEMA5A and KLF2. *Cancer Manag Res* **2020**, *12*, 1313-1321.
36. Rinke, A.; Muller, H.H.; Schade-Brittinger, C.; Klose, K.J.; Barth, P.; Wied, M.; Mayer, C.; Aminossadati, B.; Pape, U.F.; Blaker, M., et al. Placebo-controlled, double-blind, prospective, randomized study on the effect of octreotide LAR in the control of tumor growth in patients with metastatic neuroendocrine midgut tumors: a report from the PROMID Study Group. *J Clin Oncol* **2009**, *27*, 4656-4663.
37. Caplin, M.E.; Pavel, M.; Cwikla, J.B.; Phan, A.T.; Raderer, M.; Sedlackova, E.; Cadiot, G.; Wolin, E.M.; Capdevila, J.; Wall, L., et al. Lanreotide in metastatic enteropancreatic neuroendocrine tumors. *N Engl J Med* **2014**, *371*, 224-233.
38. Pyronnet, S.; Bousquet, C.; Najib, S.; Azar, R.; Laklai, H.; Susini, C. Antitumor effects of somatostatin. *Mol Cell Endocrinol* **2008**, *286*, 230-237.
39. Wu, J.; Gu, Y.; Xiao, Y.; Xia, C.; Li, H.; Kang, Y.; Sun, J.; Shao, Z.; Lin, Z.; Zhao, X. Characterization of DNA Methylation Associated Gene Regulatory Networks During Stomach Cancer Progression. *Front Genet* **2018**, *9*, 711.
40. Jackson, K.; Soutto, M.; Peng, D.; Hu, T.; Marshal, D.; El-Rifai, W. Epigenetic silencing of somatostatin in gastric cancer. *Dig Dis Sci* **2011**, *56*, 125-130.
41. Li, H.; Liu, J.W.; Liu, S.; Yuan, Y.; Sun, L.P. Bioinformatics-Based Identification of Methylated-Differentially Expressed Genes and Related Pathways in Gastric Cancer. *Dig Dis Sci* **2017**, *62*, 3029-3039.
42. Zhang, X.; Yang, J.J.; Kim, Y.S.; Kim, K.Y.; Ahn, W.S.; Yang, S. An 8-gene signature, including methylated and down-regulated glutathione peroxidase 3, of gastric cancer. *Int J Oncol* **2010**, *36*, 405-414.
43. Ricketts, C.J.; Morris, M.R.; Gentle, D.; Brown, M.; Wake, N.; Woodward, E.R.; Clarke, N.; Latif, F.; Maher, E.R. Genome-wide CpG island methylation analysis implicates novel genes in the pathogenesis of renal cell carcinoma. *Epigenetics* **2012**, *7*, 278-290.
44. Morris, M.R.; Gentle, D.; Abdulrahman, M.; Clarke, N.; Brown, M.; Kishida, T.; Yao, M.; Teh, B.T.; Latif, F.; Maher, E.R. Functional epigenomics approach to identify methylated candidate tumour suppressor genes in renal cell carcinoma. *Br J Cancer* **2008**, *98*, 496-501.
45. Patai, Á.V.; Valcz, G.; Hollósi, P.; Kalmár, A.; Péterfia, B.; Patai, Á.; Wichmann, B.; Spisák, S.; Barták, B.K.; Leiszter, K., et al. Comprehensive DNA Methylation Analysis Reveals a Common Ten-Gene Methylation Signature in Colorectal Adenomas and Carcinomas. *PLoS One* **2015**, *10*, e0133836-e0133836.
46. Leiszter, K.; Sipos, F.; Galamb, O.; Krenács, T.; Veres, G.; Wichmann, B.; Furi, I.; Kalmár, A.; Patai Á, V.; Tóth, K., et al. Promoter hypermethylation-related reduced somatostatin production promotes uncontrolled cell proliferation in colorectal cancer. *PLoS One* **2015**, *10*.
47. Patai Á, V.; Barták, B.K.; Péterfia, B.; Micsik, T.; Horváth, R.; Sumánszki, C.; Péter, Z.; Patai, Á.; Valcz, G.; Kalmár, A., et al. Comprehensive DNA Methylation and Mutation Analyses Reveal a Methylation Signature in Colorectal Sessile Serrated Adenomas. *Pathol Oncol Res* **2017**, *23*, 589-594.
48. Kok-Sin, T.; Mokhtar, N.M.; Ali Hassan, N.Z.; Sagap, I.; Mohamed Rose, I.; Harun, R.; Jamal, R. Identification of diagnostic markers in colorectal cancer via integrative epigenomics and genomics data. *Oncology reports* **2015**, *34*, 22-32.
49. Mori, Y.; Cai, K.; Cheng, Y.; Wang, S.; Paun, B.; Hamilton, J.P.; Jin, Z.; Sato, F.; Berki, A.T.; Kan, T., et al. A Genome-Wide Search Identifies Epigenetic Silencing of Somatostatin, Tachykinin-1, and 5 Other Genes in Colon Cancer. *Gastroenterology* **2006**, *131*, 797-808.
50. Zhang, M.; Lv, X.; Jiang, Y.; Li, G.; Qiao, Q. Identification of aberrantly methylated differentially expressed genes in glioblastoma multiforme and their association with patient survival. *Exp Ther Med* **2019**, *18*, 2140-2152.

51. Ongenaert, M.; Wisman, G.B.; Volders, H.H.; Koning, A.J.; Zee, A.G.; van Criekinge, W.; Schuuring, E. Discovery of DNA methylation markers in cervical cancer using relaxation ranking. *BMC Med Genomics* **2008**, *1*, 57.
52. van der Zee, R.P.; Richel, O.; van Noesel, C.J.M.; Novianti, P.W.; Ciocanea-Teodorescu, I.; van Splunter, A.P.; Duin, S.; van den Berk, G.E.L.; Meijer, C.J.L.M.; Quint, W.G.V., et al. Host Cell Deoxyribonucleic Acid Methylation Markers for the Detection of High-grade Anal Intraepithelial Neoplasia and Anal Cancer. *Clin Infect Dis* **2019**, *68*, 1110-1117.
53. Jin, Z.; Mori, Y.; Hamilton, J.P.; Olaru, A.; Sato, F.; Yang, J.; Ito, T.; Kan, T.; Agarwal, R.; Meltzer, S.J. Hypermethylation of the somatostatin promoter is a common, early event in human esophageal carcinogenesis. *Cancer* **2008**, *112*, 43-49.
54. Zhang, Z.; Tang, H.; Wang, Z.; Zhang, B.; Liu, W.; Lu, H.; Xiao, L.; Liu, X.; Wang, R.; Li, X., et al. MiR-185 targets the DNA methyltransferases 1 and regulates global DNA methylation in human glioma. *Mol Cancer* **2011**, *10*, 124.
55. Misawa, K.; Mima, M.; Imai, A.; Mochizuki, D.; Misawa, Y.; Endo, S.; Ishikawa, R.; Kanazawa, T.; Mineta, H. The neuropeptide genes SST, TAC1, HCRT, NPY, and GAL are powerful epigenetic biomarkers in head and neck cancer: A site-specific analysis. *Clin Epigenetics* **2018**, *10*.
56. Misawa, K.; Mochizuki, D.; Imai, A.; Endo, S.; Mima, M.; Misawa, Y.; Kanazawa, T.; Carey, T.E.; Mineta, H. Prognostic value of aberrant promoter hypermethylation of tumor-related genes in early-stage head and neck cancer. *Oncotarget* **2016**, *7*, 26087-26098.

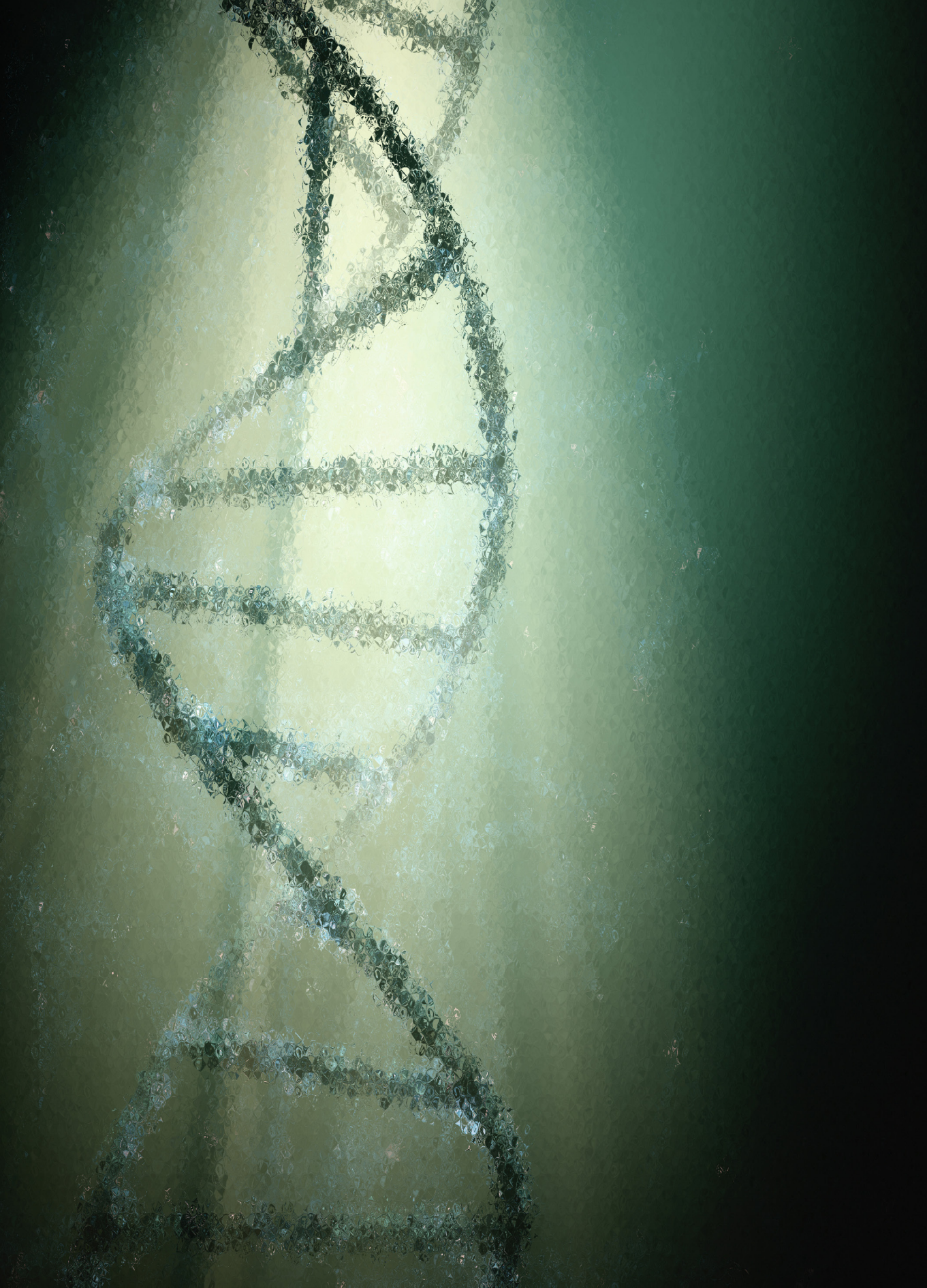

CHAPTER 3

Comparing the Effect of Multiple Histone Deacetylase Inhibitors on SSTR2 Expression and [^{111}In]In-DOTATATE Uptake in NET Cells

M.J. Klomp[1,2], S.U. Dalm[1], P.M. van Koetsveld[2], F. Dogan[2], M. de Jong[1], L.J. Hofland[2].

[1] Department of Radiology and Nuclear Medicine, Erasmus MC, 3015 GD, Rotterdam, The Netherlands. [2] Department of Internal Medicine, Division of Endocrinology, Erasmus MC, 3015 GD Rotterdam, The Netherlands.

Cancers (Basel). 2021 Sep 29;13(19):4905

ABSTRACT

The aim of this study was to increase somatostatin type-2 receptor (SSTR2) expression on neuroendocrine tumor (NET) cells using histone deacetylase inhibitors (HDACis), potentially increasing the uptake of SSTR2-targeted radiopharmaceuticals and subsequently improving treatment efficacy of peptide receptor radionuclide therapy (PRRT). Human NET cell lines BON-1, NCI-H727, and GOT1 were treated with HDACis (i.e., CI-994, entinostat, LMK-235, mocetinostat, panobinostat, or valproic acid (VPA); entinostat and VPA were the HDACis tested in GOT1 cells) to examine *SSTR2* mRNA expression levels and uptake of SSTR2-targeting radiotracer [^{111}In]In-DOTATATE. Reversibility of the induced effects was examined after drug-withdrawal. Finally, the effect of VPA on radiosensitivity was investigated. A strong stimulatory effect in BON-1, NCI-H727, and GOT1 cells was observed after HDACi treatment, both on *SSTR2* mRNA expression levels and [^{111}In]In-DOTATATE uptake. The effects of the HDACis were largely reversible over a period of seven days, demonstrating largest reductions within the first day. The reversibility profile of the induced effects suggests that proper timing of HDACi treatment is most likely essential for a beneficial outcome. In addition to increasing SSTR2 expression levels, VPA enhanced the radiosensitivity of all cell lines. In conclusion, HDACi treatment increased SSTR2 expression, and radiosensitivity was also enhanced upon VPA treatment.

Keywords: SSTR2; [^{111}In]In-DOTATATE; epigenetic drugs; histone deacetylase inhibitors; neuroendocrine tumors; peptide receptor radionuclide therapy; somatostatin type-2 receptors; upregulation.

1. INTRODUCTION

Neuroendocrine tumors (NETs) form a heterogeneous group of tumors which are often metastasized upon time of diagnosis. Unfortunately, treatment options for NETs are still limited [1]. The frequent overexpression of the somatostatin type-2 receptor (SSTR2) forms a pivotal target for therapy. Treatment with somatostatin analogues (SSAs) and the subsequent development of radiolabeled SSAs, i.e., [^{177}Lu]Lu-[DOTA-Tyr^3]octreotate ([^{177}Lu]Lu-DOTATATE) used for peptide receptor radionuclide therapy (PRRT), have both proven their efficacy in the treatment of NETs [2-4]. Unfortunately, complete responses after PRRT are still rare [4, 5]. Several promising approaches are under investigation to improve the efficacy of PRRT, such as SSTR2 upregulation using epigenetic drugs.

Varying SSTR2 expression levels among patients [6] and the absence of known mutations in the human SSTR2 gene, indicate that its expression may be regulated by epigenetic mechanisms, rather than genetic mutations. Previous studies have described an important role for epigenetic regulation in both NET pathogenesis and SSTR2 expression [7-10]. Due to the prominent role of epigenetics in this disease, it is hypothesized that epigenetic drugs will mainly target the tumor cells and, to a lesser extent, control tissue. By using synthetic inhibitors targeting the epigenetic machinery, it is possible to modify the epigenetic landscape. For the scope of this study, we focused only on histone acetylation. Histone deacetylase inhibitors (HDACis) specifically target histone deacetylases. Inhibition of these enzymes results in stimulation of the active euchromatin state, the state in which DNA is actively being transcribed. In short, the use of HDACis may modify the epigenetic profile in such a way that protein expression levels are increased [11, 12].

In this study, the aim was to thoroughly compare the effect of different HDACis targeting several classes of HDAC enzymes in three NET models: BON-1, NCI-H727, and GOT1 cells derived from pancreatic NET, lung carcinoid tumor, and midgut NET, respectively. We evaluated the effect of the selected HDACis on the different NET cell lines with respect to *SSTR2* mRNA expression levels and SSTR2 functionality using [^{111}In]In-DOTATATE uptake studies. Moreover, we analyzed reversibility profiles over time after HDACi withdrawal and investigated the radiosensitivity upon exposure to one of the HDACis.

2. MATERIALS AND METHODS

2.1. CELL CULTURE

The human pancreatic neuroendocrine tumor cell line BON-1 (kind gift of Dr. Townsend, University of Texas Medical branch, Galveston, TX, USA), the human pulmonary carcinoid cell line NCI-H727 (ATCC CRL-5815), and the human midgut neuroendocrine tumor cell line GOT1 (kind gift of Ola Nilsson, Sahlgrenska Cancer Center, University of Gothenburg, Sweden) were used in this study. BON-1 cells were cultured in DMEM/F-12 (1:1) supplemented with 10% (*v/v*) FCS, 2 mM L-glutamine, 1.25 mg/L fungizone, and 1 × 10^5 U/L penicillin; NCI-H727 cells were

cultured in RPMI medium 1640 + L-glutamine supplemented with 10% (*v/v*) FCS, 100 U/mL penicillin, and 100 µg/mL streptomycin, and; GOT1 cells were cultured in RPMI medium 1640 supplemented with 10% (*v/v*) FCS, 2 mM L-glutamine, 100 U/mL penicillin, 100 µg/mL streptomycin, 1.0 g/L insulin, 0.55 g/L transferrin, and 67 µg/L selenite. Once a week, BON-1 and NCI-H727 cells were trypsinized using 0.05% (*v/v*) trypsin + 0.53 mM EDTA and fresh medium was added on day four. GOT1 cells were trypsinized every two weeks using 0.05% (*v/v*) trypsin + 0.53 mM EDTA supplemented with DNAse (2 U/mL) with medium refreshment after one week.

2.2. HISTONE DEACETYLASE INHIBITORS

Six HDACis were tested in this study: valproic acid sodium salt (VPA; Sigma-Aldrich, Zwijndrecht, The Netherlands), entinostat (ENT; Sigma-Aldrich), CI-994 (Sigma-Aldrich), LMK-235 (AbMole Bioscience Inc., Brussels, Belgium), mocetinostat (MOC; Selleck Chemicals LCC, Breda, The Netherlands), and panobinostat (PAN; Selleck Chemicals LCC, Breda, The Netherlands). All HDACis were dissolved in 40% DMSO, except for VPA, which was dissolved in sterile aquadest. In all experiments, a final concentration of 0.4% DMSO or 1.0% aquadest was reached in the culture medium of treatment groups and vehicle controls. The tested HDACis were targeting HDACs, which are divided into several classes; class I (HDAC1, HDAC2, HDAC3, HDAC8), class IIA (HDAC4, HDAC5, HDAC7, HDAC9), class IIB (HDAC6, HDAC10), and class IV (HDAC11) [13]. PAN targeted class I, IIA, IIB; MOC targeted HDAC1, HDAC2, and HDAC3 in class I and HDAC11 in class IV; ENT, VPA, and CI-994 targeted HDAC1, HDAC2, and HDAC3 in class I and LMK-235 targeted HDAC4 and HDAC5 in class IIA [14, 15].

2.3. DOSE–RESPONSE CURVES AND DNA QUANTIFICATION

For all HDACis, dose–response studies based on a seven-day treatment schedule were performed. One day before HDACi treatment started, cells were plated in 24-well plates. Drug-supplemented medium was refreshed on day three and medium was removed on day seven. A cell growth assay was then performed by DNA quantification using Hoechst 33256 as previously described [16] with the adjustment of using 0.2% (*v/v*) Triton X-100 for cell lysis. For GOT1 cells, Quant-iT PicoGreen dsDNA reagent (Invitrogen, Breda, The Netherlands) was used. For this, Quant-iT PicoGreen dsDNA was diluted 120 times and 20 µL was added to each well. The absorbance was subsequently measured at excitation and emission wavelengths of 485 nm and 535 nm, respectively.

2.4. HDACi-TREATMENT REGIMEN

To study the effect of HDACis on SSTR2-expression, cells were plated in T75 flasks on day zero. HDACis were added on day one at their IC_{50} growth inhibitory concentrations and drug-supplemented medium was refreshed on day three. On day five, cells were trypsinized and plated for further analysis. Exactly four hours after cell plating, HDACis were added again. On day seven, samples were collected for analysis by RT-qPCR analysis (24-well plates) and for

internalization studies (12-well plates). For reversibility and radiosensitivity studies (24-well plates), culture periods were prolonged for another week in the absence and presence of HDACis, respectively.

2.5. mRNA ANALYSIS

For mRNA analysis, cells were lysed and subsequently incubated with oligo(dT)$_{25}$ dynabeads (Invitrogen, Breda, The Netherlands) to isolate poly-A$^+$ mRNA. Then, 23 µL H_2O was added for elution, and 10 µL poly-A$^+$ mRNA was used in the next steps. Poly-A$^+$ mRNA was converted into cDNA using the commercial RevertAid First Strand cDNA synthesis kit (Thermo Scientific, Breda, The Netherlands). To exclude the possibility of DNA contamination, cDNA was also prepared without the addition of RevertAid Reverse Transcriptase. Samples were diluted by adding 180 µL H_2O and RT-qPCR was performed. In short, 5 µL sample was mixed with 7.5 µL Taqman Universal PCR mastermix (Applied Biosystems, Breda, The Netherlands) supplemented with primers and probes. SSTR2 expression was determined relative to three housekeeping genes (HKGs). For analysis, the QuantStudio 7 Flex RT-qPCR system with QuantStudio Real-Time PCR software v1.5 was used. The number of copies for SSTR2 and all HKGs was calculated by the efficiency factor to the power of ΔCt (i.e., 40 minus measured Ct). Subsequently, the relative SSTR2 expression was calculated by dividing the number of SSTR2 copies by the geometric mean of all HKGs. Details on primers are represented in Table S1.

2.6. [^{111}In]In-DOTATATE RADIOLABELING

DOTATATE (Bachem AG, Budendorf, Switzerland) was radiolabeled with [^{111}In]$InCl_3$ (Curium Pharma, Petten, The Netherlands) with a molar activity of 50 MBq/nmol as previously described [17]. The radiochemical yield and radiochemical purity, measured using thin-layer chromatography and high-performance liquid chromatography, respectively, as previously described [17], were >95% and RCP > 90%, respectively.

2.7. [^{111}In]In-DOTATATE INTERNALIZATION STUDIES

Internalization studies were performed as previously described [18]. Cells were incubated with internalization medium (DMEM (1x)–GlutaMAX-I, 1% (wt/v) BSA, and 20 mM HEPES (pH 7.4)) supplemented with 10^{-9} M [^{111}In]In-DOTATATE (50 MBq/1 nmol), with or without 10^{-6} M unlabeled DOTATATE, for four hours. Following incubation, the excess unbound radiotracer was removed and the membrane-bound and internalized radioactivity were determined. For GOT1 cells, the protocol was slightly adjusted due to insufficient cell adherence. In each step, non-adherent cells were pelleted by centrifugation (3.5× *g*, 5 min) and combined with the attached cells. In addition, the total uptake was determined for GOT1 cells. To correct for possible differences in cell numbers, cell pellets of additional wells were collected and DNA content was measured with Hoechst 33258 using the same protocol described previously.

2.8. REVERSIBILITY

To determine the reversibility of HDACi-induced effects, drug-supplemented medium was removed on day seven. Cells were subsequently maintained in normal growth medium up to an additional period of seven days, with medium renewal after three days. Samples were collected one, three, and seven days after drug withdrawal and analyzed by RT-qPCR using the previously described method.

2.9. RADIOSENSITIVITY

HDACi-supplemented growth medium was refreshed on day seven and cells were irradiated up to 8 grays (Gy) using the RS320 (Xstrahl Live Sciences; 1.6554 Gy/min, 195 kV, 10 mA). On day eleven, HDACi-supplemented growth medium was refreshed again. Cells were fixated on day 14 using 10% (wt/v) trichloroacetic acid. Subsequently, plates were incubated with 0.5% (wt/v) sulforodamine B (SRB) solution. After incubation, the excess SRB solution was removed by washing plates with 1% (*v/v*) acetic acid and protein-bound dye was solubilized with 10 mM tris-base solution. Using a SpectraMax iD3 plate reader (Molecular Devices), the optical density was measured at 560 nm. For each plate, a background measurement was included.

2.10. STATISTICAL ANALYSIS

To estimate IC_{50} values, the obtained percentages were plotted using spline/LOWESS analysis using the point-to-point curve. For detecting correlations, the Pearson r^2 was determined. For all other analysis, results were calculated as percentage increase or decrease compared to the control situation. The resulting percentages were log-transformed. One-way ANOVA analysis using the Tukey post-hoc test was performed to detect significant differences between HDACi-treated cells. To detect differences in radiosensitivity and obtain IC_{50} values, a dose–response curve was plotted with variable slope. For all experiments, both biological and technical replicates were included. All results represent the mean ± SD of at least two independent biological replicates and at least three technical replicates; * $p < 0.05$, ** $p < 0.01$, *** $p < 0.001$, NS; non-significant. All statistical analyses were performed using GraphPad Prism 5 software.

3. RESULTS

3.1. NET CELL-LINE CHARACTERIZATION

SSTR2 expression levels were 0.0038 ± 0.0005, 0.0055 ± 0.0015, and 0.1468 ± 0.0248 (corrected for the geometric mean of three HKGs) in BON-1, NCI-H727, and GOT1 cells, respectively. Consistent with this, the internalized fraction of [^{111}In]In-DOTATATE was 6.99 ± 1.75 and 40.10 ± 9.78 percentage added dose per milligram DNA (%AD/mg DNA) in BON-1 and NCI-H727 cells, respectively. In line with mRNA expression levels, the total uptake in GOT1 cells was the highest: 405.04 ± 98.12% AD/mg DNA. *SSTR2* mRNA expression levels and uptake of radiolabeled [^{111}In]In-DOTATATE significantly correlated with an r^2 of 0.9958 ($p = 0.0413$) (Figure S1).

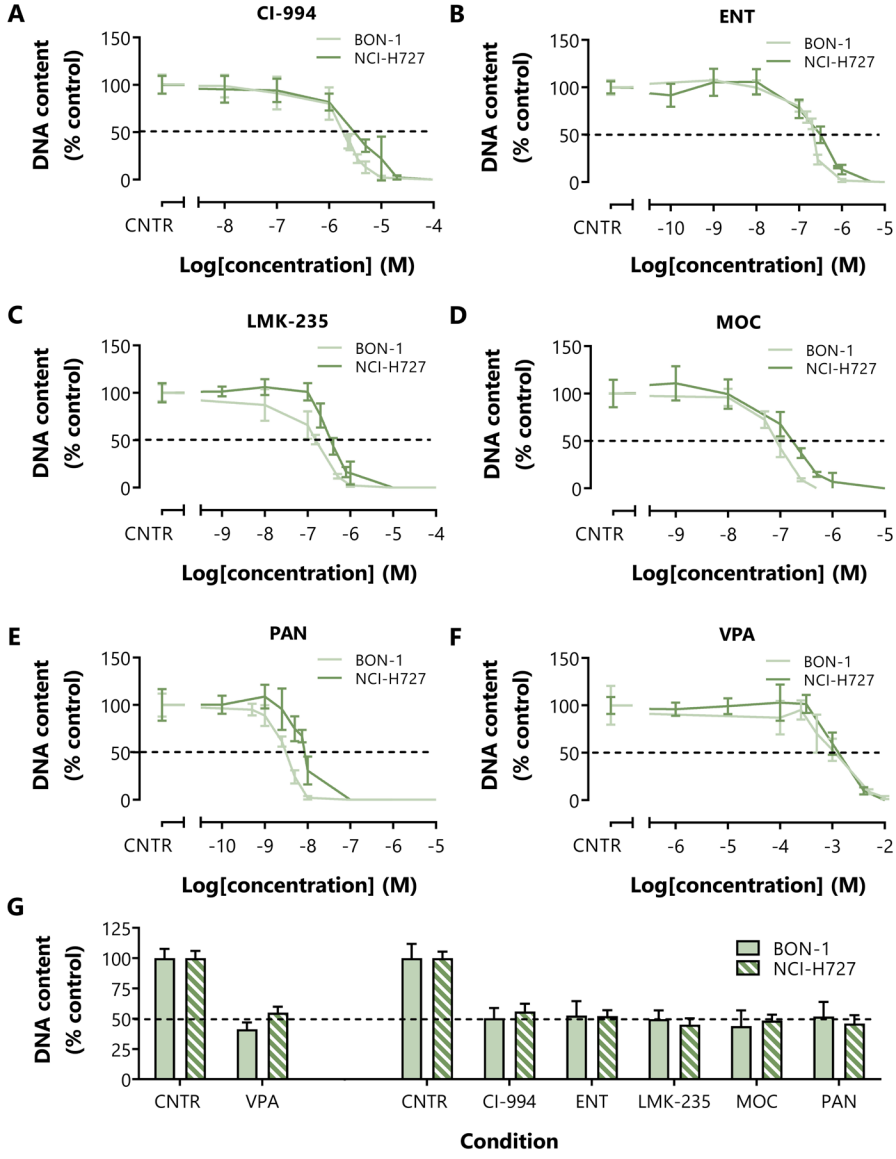

Figure 1. (A–F) Dose–response curves of six HDACis in BON-1 and NCI-H727 cells, represented in red and blue, respectively. **(G)** In order to include an experiment for further analysis, in which the effects of HDACis on *SSTR2* mRNA levels, uptake of [^{111}In]In-DOTATATE and radiosensitivity were evaluated, a proper reduction in DNA amount (i.e., approximately 50%) was confirmed as the internal control for each experiment. As HDACis were either dissolved in 40% DMSO or sterile aquadest, two vehicle-controls were included.

3.2. EFFECTS OF HDACis IN BON-1 AND NCI-H727 CELLS

BON-1 cells showed to be slightly more sensitive for HDACi treatment than NCI-H727 cells. The IC_{50} values on growth of BON-1 and NCI-H727 cells were, respectively, 1.85 µM and 3.05 µM for CI-994, 218 nM and 315 nM for ENT, 154 nM and 348 nM for LMK-235, 84.3 nM and 171 nM for MOC, 3.11 nM and 8.53 nM for PAN, and 1.12 mM and 1.31 mM for VPA (Figure 1A–F, Table S2). Treatment at these IC_{50} values demonstrated an expected inhibition of approximately 50% for all HDACis (Figure 1G).

In BON-1 cells, all HDACis significantly increased *SSTR2* mRNA expression levels ($p < 0.001$). CI-994, ENT, and PAN induced the strongest effects, i.e., a 3.07-, 3.13-, and 2.87-fold increase, respectively (Figure 2A). In line with this, uptake of [^{111}In]In-DOTATATE was significantly enhanced, i.e., 8.14-, 8.30-, and 7.54-fold, respectively (Figure 2B). Surprisingly, even though VPA had a relatively modest effect on the *SSTR2* mRNA expression level, the uptake of [^{111}In]In-DOTATATE after VPA was most pronounced, i.e., an 8.63-fold increase in uptake.

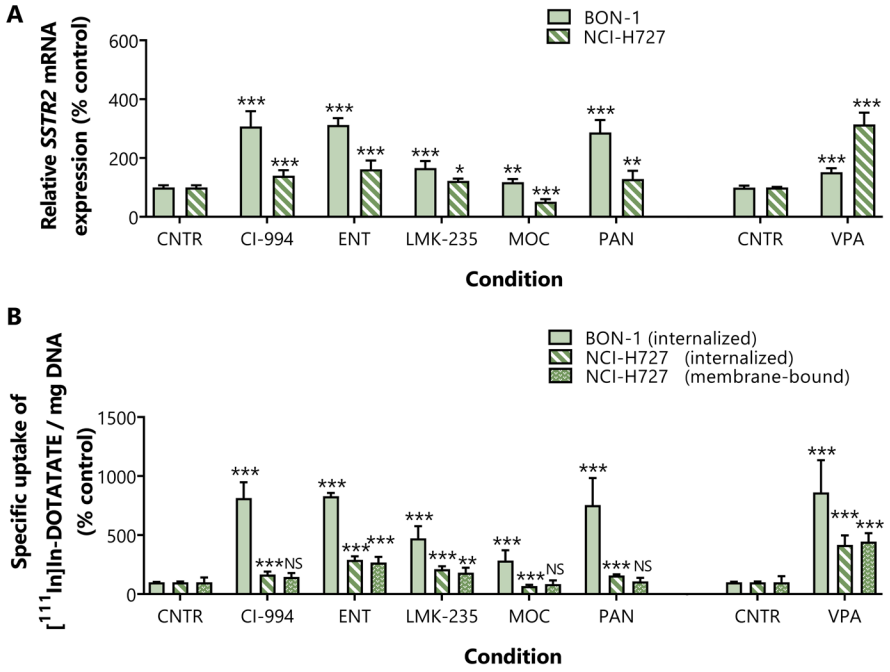

Figure 2. NET cells lines were treated for seven days with HDACis at the IC_{50} dose, and subsequently analyzed by **(A)** RT-qPCR (*SSTR2* mRNA) and **(B)** [^{111}In]In-DOTATATE uptake studies. For uptake studies, DNA was quantified to correct for differences in cell number at the start of the assay. Membrane-bound fractions for BON-1 are not shown as values were too low for accurate measurement. Results were normalized to vehicle-treated cells. * $p < 0.05$, ** $p < 0.01$, *** $p < 0.001$, NS; non-significant.

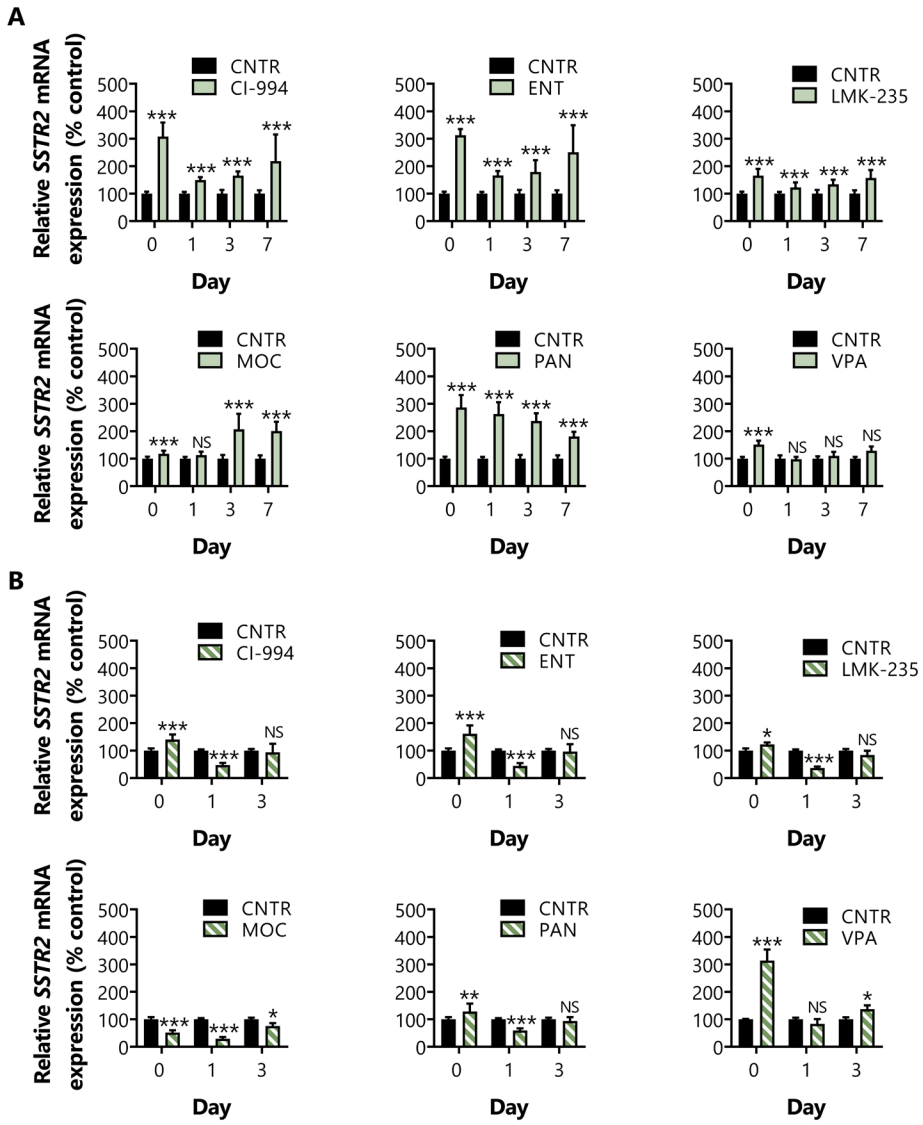

Figure 3. To determine reversibility of SSTR2 upregulation upon HDACi withdrawal, *SSTR2* mRNA levels were determined by RT-qPCR directly after treatment with HDACi at the IC_{50} dose (D0), and one (D1), three (D3), and seven days (D7) after HDACi withdrawal for BON-1 **(A)**, and at D0, D1, and D3 for NCI-H727 **(B)**. Results were normalized to vehicle-treated cells. * $p < 0.05$, ** $p < 0.01$, *** $p < 0.001$, NS; non-significant.

In NCI-H727 cells, the observed increases in percentage of internalized and membrane-bound fractions of [^{111}In]In-DOTATATE upon HDACi treatment followed similar patterns, demonstrated by a significant positive correlation ($r^2 = 0.9565$; $p = 0.0007$) (Figure S2A). Both the membrane and internalized fractions of radioactivity were most strongly increased upon VPA treatment: 4.16- and 4.45-fold, respectively. Internalization of [^{111}In]In-DOTATATE was also significantly increased after treatment with CI-994 (1.66-fold), ENT (2.91-fold), LMK-235

(2.10-fold), and PAN (1.58-fold). MOC slightly downregulated the uptake of [^{111}In]In-DOTATATE, i.e., 0.32-fold reduced uptake (Figure 2B). *SSTR2* mRNA expression levels followed an identical pattern (Figure 2A), resulting in a significant positive correlation between *SSTR2* mRNA expression levels and [^{111}In]In-DOTATATE uptake levels (r^2 = 0.9005; p = 0.0038) (Figure S2B). A statistically significant correlation was not reached in BON-1 cells (r^2 = 0.4534) (Figure S2C).

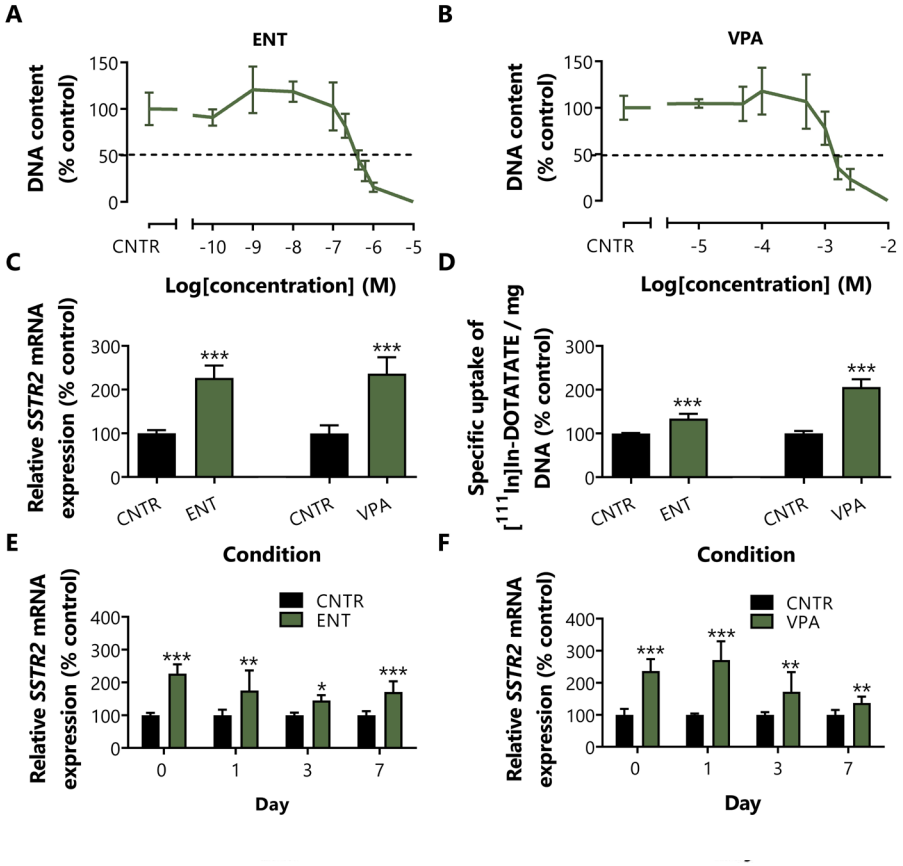

Figure 4. To examine the effect of HDACis in the GOT1 cell line, a dose–response curve was prepared for ENT **(A)** and VPA **(B)**. After a seven-day treatment with the IC_{50} dose, the increase in **(C)** *SSTR2* mRNA levels and **(D)** total uptake of radiolabeled SSAs were examined. **(E,F)** Reversibility profiles after HDACi withdrawal were evaluated by RT-qPCR directly after treatment (D0), and one (D1), three (D3), and seven days (D7) after HDACi withdrawal. Results in **(C–F)** were normalized to vehicle-treated cells. * p < 0.05, ** p < 0.01, *** p < 0.001.

3.3. REVERSIBILITY PROFILE OF SSTR2 EXPRESSION IN BON-1 AND NCI-H727 CELLS

Reversibility profiles of the effects of HDACis in BON-1 cells showed that control expression levels were not reached after treatment with CI-994, ENT, and LMK-235, i.e., 2.19-, 2.51-, and

1.57-fold increase seven days after drug withdrawal, respectively (Figure 3A). For these inhibitors, strong reductions within the first day after HDACi removal were observed. For PAN-treated cells, control levels were also not reached (1.81-fold increase). In these cells, a gradual downregulation of *SSTR2* expression over time was observed, suggesting a slow wash out of the effect of PAN on these cells. For MOC- and VPA-treated BON-1 cells, control levels were already reached after one day. At day three and day seven, a slight increase in *SSTR2* mRNA expression levels was observed in MOC treated cells, reaching significance for both time points.

In NCI-H727 cells, one day after VPA withdrawal control *SSTR2* mRNA expression levels were already observed (Figure 3B). Surprisingly, after three days, a small but significant upregulation was observed, i.e., 1.37-fold. For all other conditions, another reversibility pattern was observed. *SSTR2* expression levels were significantly reduced already one day after drug withdrawal, i.e., 0.53-, 0.55-, 0.63, 0.71-, and 0.43-fold for CI-994, ENT, LMK-235, MOC, and PAN, respectively. Generally, *SSTR2* mRNA expression levels reached control expression levels three days after drug removal. For MOC treatment, the only HDACi inducing *SSTR2* mRNA downregulation directly after treatment, control levels were not reached within this time frame.

3.4. EFFECTS OF HDACis IN GOT1 CELLS

Based on effects induced in BON-1 and NCI-H727 cells, the effects of ENT and VPA were examined in GOT1 cells. Measured IC_{50} values were 384 nM for ENT and 1.36 mM for VPA treatment (Figure 4A,B, Table S2). Both HDACis significantly increased *SSTR2* mRNA expression levels: 2.27- and 2.37-fold, respectively (Figure 4C). In line with this, also the total uptake of [^{111}In]In-DOTATATE was significantly enhanced, i.e., 1.34- and 2.06-fold, respectively (Figure 4D).

3.5. REVERSIBILITY PROFILE OF SSTR2 EXPRESSION IN GOT1 CELLS

Concordant with the observations in BON-1 and NCI-H727 cells, the effects of ENT and VPA gradually decreased over the seven-day period. However, control *SSTR2* mRNA expression levels were not reached within the examined time period (Figure 4D,E).

3.6. RADIOSENSITIZING EFFECTS UPON VPA TREATMENT

As VPA treatment induced strong and significant stimulatory effects on *SSTR2* mRNA expression and [^{111}In]In-DOTATATE uptake in all three NET cell lines, the effect of this HDACi was also examined in terms of radiosensitivity (Figure 5). Irradiated VPA-treated NET cells proliferated less than irradiated control cells. IC_{50} values were 4.39 Gy, 3.22 Gy, and 1.34 Gy for untreated BON-1, NCI-H727, and GOT1 cells, whereas VPA-treated cells had IC_{50} values of 2.82 Gy, 1.88 Gy, and 0.72 Gy, respectively, demonstrating a statistically significant increased sensitivity to external beam irradiation induced by VPA.

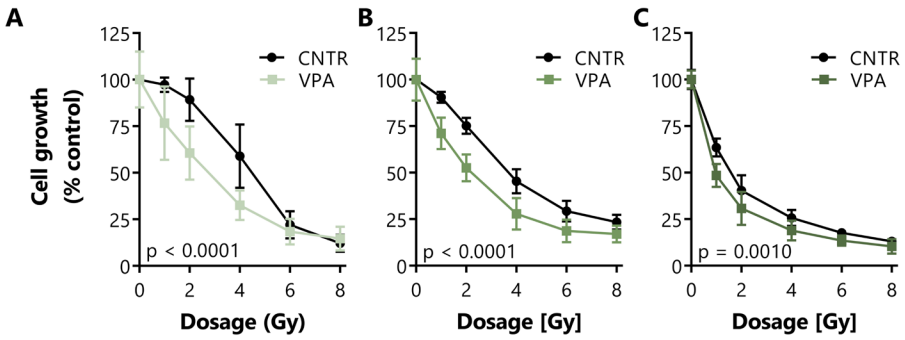

Figure 5. After a seven-day treatment with the IC_{50} dose, VPA-treated and untreated BON-1 **(A)**, NCI-H727 **(B)**, and GOT1 **(C)** cells were exposed to different dosages of irradiation using external beam radiation to investigate increased radiosensitivity.

4. DISCUSSION

As the number of complete responses in NET patients is limited after PRRT, therapy improvement is highly needed. For this reason, we focused on HDACi-induced SSTR2 upregulation in three NET cell-line models as a way of improving uptake of radiolabeled SSAs, and thereby possibly increasing treatment efficacy.

In line with our results, previous studies also reported on the effects of HDACi treatment, showing SSTR2 upregulation and/or increased uptake of radiolabeled SSAs in different NET models [16, 19-26]. However, the strength of our study was the use of HDACi-specific and cell line-based IC_{50} values allowing for a comparison of effects induced by HDACis targeting different classes of HDAC enzymes. Moreover, we investigated the induced effects in three frequently used NET cell-line models derived from different origins. Importantly, the established IC_{50} values of the HDACis were below or within the same order of magnitude as the therapeutic dose, indicating the clinical relevance of the used concentrations.

The effects induced by the HDACis clearly enhanced uptake of the radiolabeled SSA [^{111}In]In-DOTATATE, as well as *SSTR2* mRNA expression levels in both BON-1 and NCI-H727 cells. VPA and ENT induced the strongest effects in both cell lines. CI-994, targeting the same HDAC enzymes as VPA and ENT, also induced strong upregulation in BON-1 cells, suggesting that epigenetic modifiers targeting HDAC class I enzymes are strongly involved in SSTR2 transcription. Therefore, we expected that MOC, targeting both HDAC class I and class IV, would also enhance SSTR2 expression. However, only weak *SSTR2* upregulation and even downregulation was observed, suggesting that HDACis may have induced cell-specific responses.

The extent of receptor upregulation upon HDACi treatment on *SSTR2* mRNA expression level and uptake of [^{111}In]In-DOTATATE correlated significantly in NCI-H727 cells (r^2 = 0.9005). For

BON-1 cells, an r^2 of 0.4534 was obtained. This correlation was not statistically significant due to the potent effects of VPA treatment on the uptake of [^{111}In]In-DOTATATE, i.e., imbalance between mRNA and uptake levels. With the exception of this condition, all other conditions indicated that the enhanced uptake was caused by SSTR2 upregulation, instead of other mechanisms-of-actions, e.g., faster recycling of SSTR2 to the cell membrane after internalization. Next to the correlation between *SSTR2* mRNA expression levels and uptake of [^{111}In]In-DOTATATE, it has been demonstrated in literature that the uptake of radiolabeled SSTR2 analogue is associated with SSTR2 protein expression levels [27, 28]. We therefore hypothesized that HDACi treatment increased the uptake of [^{111}In]In-DOTATATE by upregulation of SSTR2 protein expression levels.

In our study, we also evaluated whether SSTR2 baseline expression levels were associated with the extent of HDACi-induced SSTR2 upregulation. In general, our results showed that the strongest effects were induced in BON-1 cells, e.g., 8.63-, 4.16-, and 2.06-fold increased uptake of [^{111}In]In-DOTATATE after VPA treatment in BON-1, NCI-H727, and GOT1 cells, respectively. This pattern was observed for the majority of HDACis, suggesting that there may have been a relationship between extent of receptor upregulation and SSTR2 baseline expression levels. In the study of Exner et al. [29], it was demonstrated that *SSTR2* mRNA expression levels of BON-1 and NCI-H727 cells are lower than or comparable to control pancreatic and ileum tissue, respectively. Since GOT1 has higher *SSTR2* mRNA expression, we hypothesized that these cells had more expression than control tissue. We thereby demonstrated that HDACis could upregulate SSTR2 expression in NET cell lines characterized by a broad range of baseline expression levels, with SSTR2 expression levels lower and higher than control tissue.

To the best of our knowledge, we are the first reporting on the reversibility of SSTR2 upregulation after HDACi withdrawal. As epigenetic histone modifications are part of a dynamic process and the resulting marks are therefore reversible, we hypothesized that SSTR2 expression levels would go back to baseline. In line with this, our results showed that effects induced by HDACi treatment were largely and rapidly reversible. Generally, the largest reductions were observed in the first day. One day after drug withdrawal in NCI-H727 cells, a significant reduction was observed in all conditions, which frequently resulted in *SSTR2* downregulation compared to control cells. We hypothesized that upon drug withdrawal, HDACi enzymes were over-activated, resulting in strong histone deacetylation and thus reduced SSTR2 expression levels. However, over a time course of three days, control expression levels were reached again. This quick reversibility upon HDACi withdrawal can provide guidance for the timing between HDACi administration and [^{177}Lu]Lu-DOTATATE injection in preclinical studies in order to obtain beneficial effects.

Based on our analysis, VPA induced the strongest effects on uptake of [^{111}In]In-DOTATATE in all three examined NET cell lines. Therefore, the effect of VPA on radiosensitivity was examined using external beam irradiation. Using external beam irradiation, the radiosensitizing effect was distinguished from other possible mechanisms, e.g., increased therapeutic effect as a

consequence of increased [^{177}Lu]Lu-DOTATATE uptake or a combination of these two. We observed that the radiosensitivity of all NET cell lines was significantly increased after VPA treatment. This is in line with earlier published data by Jin et al. [19] who showed a slightly increased radiosensitivity upon treatment of BON-1 and QGP-1 cells with CI-994. Similar results were demonstrated for several other cancer types [30-33]. This suggests that VPA may have a dual function; it increases both *SSTR2* mRNA expression levels and uptake of [^{111}In]In-DOTATATE, and it increases radiosensitivity towards PRRT. Another major advantage is that VPA is already used in a clinical setting, e.g., for treatment of epilepsy and psychiatric disorders [34, 35]. This HDACi can therefore be of great interest for its potency to upregulate SSTR2.

Although upregulation of the target receptor has already been demonstrated to be successful for improving radioligand therapy for NETs *in vitro* [36] and increasing uptake of radiolabeled somatostatin analogues *in vivo* [20, 22], the improved therapeutic effect on tumor growth *in vivo* is not established yet for upregulation of the target receptor in combination with [^{177}Lu]Lu-DOTATATE treatment. In prostate cancer, several approaches are under investigation to increase target expression levels, i.e., treatment with antiandrogen MDV3100 resulting in an increased uptake of radiolabeled PSMA-targeting antibody ^{64}Cu-J591 [37], and, more importantly, treatment with enzalutamide enhancing PSMA expression and thereby improving survival in xenograft models upon combination with PSMA antibody drug conjugates [38]. In contrast to the above-described study by DiPippo et al. [38], Lückerath et al. [39] did not show an increased therapeutic response after treatment with [^{177}Lu]Lu-PSMA617 in combination with enzalutamide which caused an increased PSMA expression. In the study of McDevitt et al. [40] a feed-forward loop was described in prostate cancer xenografts irradiated with [^{225}Ac]hu11B6, causing upregulation of the human kallikrein peptidase 2, which is targeted by hu11B6 itself. Therefore, the potential of a combinational therapy consisting of HDACi and [^{177}Lu]Lu-DOTATATE in NET models should be addressed in future preclinical studies. Moreover, *in vivo* studies are required to examine the effect of HDACi treatment on SSTR2 expression level itself. There are several variables which should be taken into account, e.g., HDACi dose, treatment duration, and frequency and route of administration. Moreover, the quick reversibility after HDACi withdrawal *in vitro*, as was observed in our study, indicates that timing between HDACi and DOTATATE injection may be an important factor in preclinical studies. With these *in vivo* studies, it is also important to determine tumor-to-background ratios, thereby taking into account the effect of HDACis on physiological tissues.

5. CONCLUSION

In conclusion, we demonstrated that SSTR2 upregulation by HDACi treatment was possible in NET cell lines of different origins, especially using HDACi specifically targeting class I HDACs, and with strongest effects observed in cells characterized by low SSTR2 baseline expression levels. Generally, the effects were rapidly and largely reversible within one day after HDACi withdrawal. This suggests that proper timing of HDACi treatment could be an important factor

in both preclinical and clinical settings. Future studies will provide definite answers about the potential for this combinational therapy in order to improve NET patient outcomes.

REFERENCES

1. Raphael, M.J.; Chan, D.L.; Law, C.; Singh, S. Principles of diagnosis and management of neuroendocrine tumours. *CMAJ* **2017**, *189*, E398-E404.
2. Rinke, A.; Müller, H.H.; Schade-Brittinger, C.; Klose, K.J.; Barth, P.; Wied, M.; Mayer, C.; Aminossadati, B.; Pape, U.F.; Bläker, M., et al. Placebo-controlled, double-blind, prospective, randomized study on the effect of octreotide LAR in the control of tumor growth in patients with metastatic neuroendocrine midgut tumors: a report from the PROMID Study Group. *J Clin Oncol* **2009**, *27*, 4656-4663.
3. Caplin, M.E.; Pavel, M.; Ćwikła, J.B.; Phan, A.T.; Raderer, M.; Sedláčková, E.; Cadiot, G.; Wolin, E.M.; Capdevila, J.; Wall, L., et al. Lanreotide in metastatic enteropancreatic neuroendocrine tumors. *N Engl J Med* **2014**, *371*, 224-233.
4. Strosberg, J.; El-Haddad, G.; Wolin, E.; Hendifar, A.; Yao, J.; Chasen, B.; Mittra, E.; Kunz, P.L.; Kulke, M.H.; Jacene, H., et al. Phase 3 Trial of ^{177}Lu-Dotatate for Midgut Neuroendocrine Tumors. *N Engl J Med* **2017**, *376*, 125-135.
5. Brabander, T.; van der Zwan, W.A.; Teunissen, J.J.M.; Kam, B.L.R.; Feelders, R.A.; de Herder, W.W.; van Eijck, C.H.J.; Franssen, G.J.H.; Krenning, E.P.; Kwekkeboom, D.J. Long-Term Efficacy, Survival, and Safety of [^{177}Lu-DOTA^{0},Tyr^{3}]octreotate in Patients with Gastroenteropancreatic and Bronchial Neuroendocrine Tumors. *Clin Cancer Res* **2017**, *23*, 4617-4624.
6. Okuwaki, K.; Kida, M.; Mikami, T.; Yamauchi, H.; Imaizumi, H.; Miyazawa, S.; Iwai, T.; Takezawa, M.; Saegusa, M.; Watanabe, M., et al. Clinicopathologic characteristics of pancreatic neuroendocrine tumors and relation of somatostatin receptor type 2A to outcomes. *Cancer* **2013**, *119*, 4094-4102.
7. Klieser, E.; Urbas, R.; Stättner, S.; Primavesi, F.; Jäger, T.; Dinnewitzer, A.; Mayr, C.; Kiesslich, T.; Holzmann, K.; Di Fazio, P., et al. Comprehensive immunohistochemical analysis of histone deacetylases in pancreatic neuroendocrine tumors: HDAC5 as a predictor of poor clinical outcome. *Hum Pathol* **2017**, *65*, 41-52.
8. Alvarez, M.J.; Subramaniam, P.S.; Tang, L.H.; Grunn, A.; Aburi, M.; Rieckhof, G.; Komissarova, E.V.; Hagan, E.A.; Bodei, L.; Clemons, P.A., et al. A precision oncology approach to the pharmacological targeting of mechanistic dependencies in neuroendocrine tumors. *Nat Genet* **2018**, *50*, 979-989.
9. Di Domenico, A.; Wiedmer, T.; Marinoni, I.; Perren, A. Genetic and epigenetic drivers of neuroendocrine tumours (NET). *Endocr Relat Cancer* **2017**, *24*, R315-R334.
10. Klomp, M.J.; Dalm, S.U.; de Jong, M.; Feelders, R.A.; Hofland, J.; Hofland, L.J. Epigenetic regulation of somatostatin and somatostatin receptors in neuroendocrine tumors and other types of cancer. *Rev Endocr Metab Disord* **2021**, *22*, 495-510.
11. Alaskhar Alhamwe, B.; Khalaila, R.; Wolf, J.; von Bülow, V.; Harb, H.; Alhamdan, F.; Hii, C.S.; Prescott, S.L.; Ferrante, A.; Renz, H., et al. Histone modifications and their role in epigenetics of atopy and allergic diseases. *Allergy Asthma Clin Immunol* **2018**, *14*, 39.
12. Parbin, S.; Kar, S.; Shilpi, A.; Sengupta, D.; Deb, M.; Rath, S.K.; Patra, S.K. Histone deacetylases: a saga of perturbed acetylation homeostasis in cancer. *J Histochem Cytochem* **2014**, *62*, 11-33.
13. Hadden, M.J.; Advani, A. Histone Deacetylase Inhibitors and Diabetic Kidney Disease. *Int J Mol Sci* **2018**, *19*, 2630.
14. Hessmann, E.; Johnsen, S.A.; Siveke, J.T.; Ellenrieder, V. Epigenetic treatment of pancreatic cancer: is there a therapeutic perspective on the horizon? *Gut* **2017**, *66*, 168-179.
15. Marek, L.; Hamacher, A.; Hansen, F.K.; Kuna, K.; Gohlke, H.; Kassack, M.U.; Kurz, T. Histone deacetylase (HDAC) inhibitors with a novel connecting unit linker region reveal a selectivity profile for HDAC4 and HDAC5 with improved activity against chemoresistant cancer cells. *J Med Chem* **2013**, *56*, 427-436.
16. Veenstra, M.J.; van Koetsveld, P.M.; Dogan, F.; Farrell, W.E.; Feelders, R.A.; Lamberts, S.W.J.; de Herder, W.W.; Vitale, G.; Hofland, L.J. Epidrug-induced upregulation of functional somatostatin type 2 receptors in human pancreatic neuroendocrine tumor cells. *Oncotarget* **2018**, *9*, 14791-14802.

17. de Blois, E.; Chan, H.S.; de Zanger, R.; Konijnenberg, M.; Breeman, W.A. Application of single-vial ready-for-use formulation of 111In- or 177Lu-labelled somatostatin analogs. *Appl Radiat Isot* **2014**, *85*, 28-33.
18. Dalm, S.U.; Nonnekens, J.; Doeswijk, G.N.; de Blois, E.; van Gent, D.C.; Konijnenberg, M.W.; de Jong, M. Comparison of the Therapeutic Response to Treatment with a 177Lu-Labeled Somatostatin Receptor Agonist and Antagonist in Preclinical Models. *J Nucl Med* **2016**, *57*, 260-265.
19. Jin, X.F.; Auernhammer, C.J.; Ilhan, H.; Lindner, S.; Nölting, S.; Maurer, J.; Spöttl, G.; Orth, M. Combination of 5-Fluorouracil with Epigenetic Modifiers Induces Radiosensitization, Somatostatin Receptor 2 Expression, and Radioligand Binding in Neuroendocrine Tumor Cells In Vitro. *J Nucl Med* **2019**, *60*, 1240-1246.
20. Taelman, V.F.; Radojewski, P.; Marincek, N.; Ben-Shlomo, A.; Grotzky, A.; Olariu, C.I.; Perren, A.; Stettler, C.; Krause, T.; Meier, L.P., et al. Upregulation of Key Molecules for Targeted Imaging and Therapy. *J Nucl Med* **2016**, *57*, 1805-1810.
21. Wanek, J.; Gaisberger, M.; Beyreis, M.; Mayr, C.; Helm, K.; Primavesi, F.; Jäger, T.; Di Fazio, P.; Jakab, M.; Wagner, A., et al. Pharmacological Inhibition of Class IIA HDACs by LMK-235 in Pancreatic Neuroendocrine Tumor Cells. *Int J Mol Sci* **2018**, *19*, 3128.
22. Guenter, R.; Aweda, T.; Carmona Matos, D.M.; Jang, S.; Whitt, J.; Cheng, Y.Q.; Liu, X.M.; Chen, H.; Lapi, S.E.; Jaskula-Sztul, R. Overexpression of somatostatin receptor type 2 in neuroendocrine tumors for improved Ga68-DOTATATE imaging and treatment. *Surgery* **2020**, *167*, 189-196.
23. Guenter, R.E.; Aweda, T.; Carmona Matos, D.M.; Whitt, J.; Chang, A.W.; Cheng, E.Y.; Liu, X.M.; Chen, H.; Lapi, S.E.; Jaskula-Sztul, R. Pulmonary Carcinoid Surface Receptor Modulation Using Histone Deacetylase Inhibitors. *Cancers (Basel)* **2019**, *11*, 767.
24. Torrisani, J.; Hanoun, N.; Laurell, H.; Lopez, F.; Maoret, J.J.; Souque, A.; Susini, C.; Cordelier, P.; Buscail, L. Identification of an upstream promoter of the human somatostatin receptor, hSSTR2, which is controlled by epigenetic modifications. *Endocrinology* **2008**, *149*, 3137-3147.
25. Arvidsson, Y.; Johanson, V.; Pfragner, R.; Wängberg, B.; Nilsson, O. Cytotoxic Effects of Valproic Acid on Neuroendocrine Tumour Cells. *Neuroendocrinology* **2016**, *103*, 578-591.
26. Sun, L.; Qian, Q.; Sun, G.; Mackey, L.V.; Fuselier, J.A.; Coy, D.H.; Yu, C.Y. Valproic acid induces NET cell growth arrest and enhances tumor suppression of the receptor-targeted peptide-drug conjugate via activating somatostatin receptor type II. *J Drug Target* **2016**, *24*, 169-177.
27. Miederer, M.; Seidl, S.; Buck, A.; Scheidhauer, K.; Wester, H.J.; Schwaiger, M.; Perren, A. Correlation of immunohistopathological expression of somatostatin receptor 2 with standardised uptake values in 68Ga-DOTATOC PET/CT. *Eur J Nucl Med Mol Imaging* **2009**, *36*, 48-52.
28. Yu, J.; Cao, F.; Zhao, X.; Xie, Q.; Lu, M.; Li, J.; Yang, Z.; Sun, Y. Correlation and Comparison of Somatostatin Receptor Type 2 Immunohistochemical Scoring Systems with 68Ga-DOTATATE Positron Emission Tomography/Computed Tomography Imaging in Gastroenteropancreatic Neuroendocrine Neoplasms. *Neuroendocrinology* **2021**, *112*, 358-369.
29. Exner, S.; Prasad, V.; Wiedenmann, B.; Grötzinger, C. Octreotide Does Not Inhibit Proliferation in Five Neuroendocrine Tumor Cell Lines. *Front Endocrinol (Lausanne)* **2018**, *9*, 146.
30. Kuribayashi, T.; Ohara, M.; Sora, S.; Kubota, N. Scriptaid, a novel histone deacetylase inhibitor, enhances the response of human tumor cells to radiation. *Int J Mol Med* **2010**, *25*, 25-29.
31. Li, H.; Ma, L.; Bian, X.; Lv, Y.; Lin, W. FK228 sensitizes radioresistant small cell lung cancer cells to radiation. *Clin Epigenetics* **2021**, *13*, 41.
32. Chen, X.; Wong, P.; Radany, E.; Wong, J.Y. HDAC inhibitor, valproic acid, induces p53-dependent radiosensitization of colon cancer cells. *Cancer Biother Radiopharm* **2009**, *24*, 689-699.
33. Munshi, A.; Kurland, J.F.; Nishikawa, T.; Tanaka, T.; Hobbs, M.L.; Tucker, S.L.; Ismail, S.; Stevens, C.; Meyn, R.E. Histone deacetylase inhibitors radiosensitize human melanoma cells by suppressing DNA repair activity. *Clin Cancer Res* **2005**, *11*, 4912-4922.
34. Nanau, R.M.; Neuman, M.G. Adverse drug reactions induced by valproic acid. *Clin Biochem* **2013**, *46*, 1323-1338.

35. Romoli, M.; Mazzocchetti, P.; D'Alonzo, R.; Siliquini, S.; Rinaldi, V.E.; Verrotti, A.; Calabresi, P.; Costa, C. Valproic Acid and Epilepsy: From Molecular Mechanisms to Clinical Evidences. *Curr Neuropharmacol* **2019**, *17*, 926-946.
36. Shah, R.G.; Merlin, M.A.; Adant, S.; Zine-Eddine, F.; Beauregard, J.M.; Shah, G.M. Chemotherapy-Induced Upregulation of Somatostatin Receptor-2 Increases the Uptake and Efficacy of ^{177}Lu-DOTA-Octreotate in Neuroendocrine Tumor Cells. *Cancers (Basel)* **2021**, *13*, 232.
37. Evans, M.J.; Smith-Jones, P.M.; Wongvipat, J.; Navarro, V.; Kim, S.; Bander, N.H.; Larson, S.M.; Sawyers, C.L. Noninvasive measurement of androgen receptor signaling with a positron-emitting radiopharmaceutical that targets prostate-specific membrane antigen. *Proc Natl Acad Sci U S A* **2011**, *108*, 9578-9582.
38. DiPippo, V.A.; Nguyen, H.M.; Brown, L.G.; Olson, W.C.; Vessella, R.L.; Corey, E. Addition of PSMA ADC to enzalutamide therapy significantly improves survival in in vivo model of castration resistant prostate cancer. *Prostate* **2016**, *76*, 325-334.
39. Lückerath, K.; Wei, L.; Fendler, W.P.; Evans-Axelsson, S.; Stuparu, A.D.; Slavik, R.; Mona, C.E.; Calais, J.; Rettig, M.; Reiter, R.E., et al. Preclinical evaluation of PSMA expression in response to androgen receptor blockade for theranostics in prostate cancer. *EJNMMI Res* **2018**, *8*, 96.
40. McDevitt, M.R.; Thorek, D.L.J.; Hashimoto, T.; Gondo, T.; Veach, D.R.; Sharma, S.K.; Kalidindi, T.M.; Abou, D.S.; Watson, P.A.; Beattie, B.J., et al. Feed-forward alpha particle radiotherapy ablates androgen receptor-addicted prostate cancer. *Nat Commun* **2018**, *9*, 1629.

SUPPLEMENTAL FIGURES AND TABLES

SUPPLEMENTAL FIGURE 1

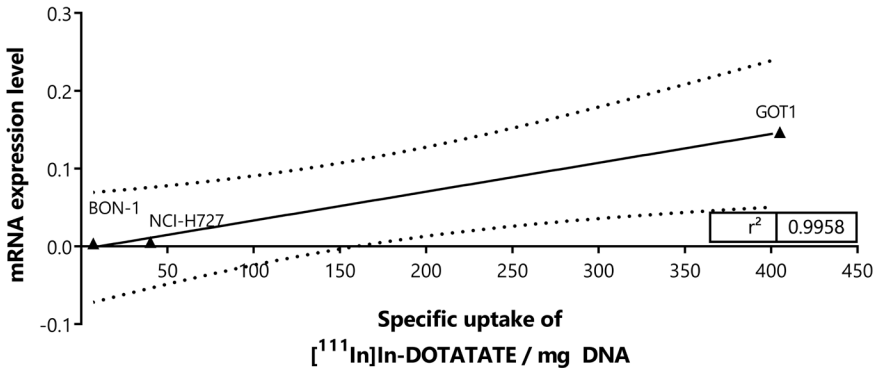

Figure S1. Pearson correlation analysis was performed by plotting basal *SSTR2* mRNA expression level in BON-1, NCI-H727 and GOT1 cells against corresponding uptake of [^{111}In]In-DOTATATE per milligram of DNA.

SUPPLEMENTAL FIGURE 2

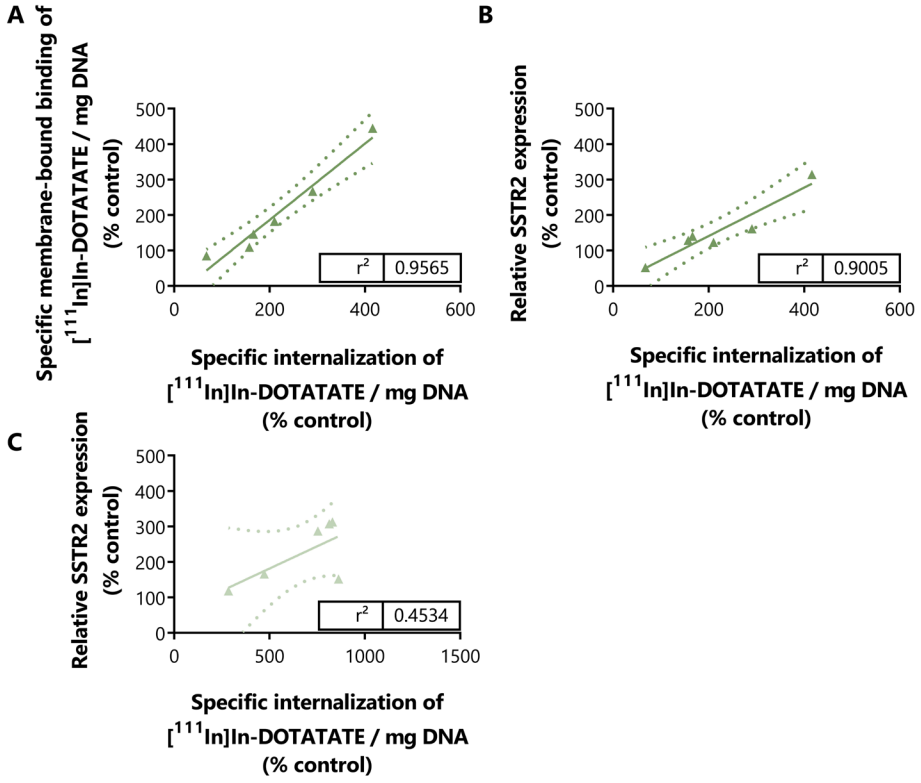

Figure S2. Pearson correlation analysis was performed by plotting the HDACi-enhanced [^{111}In]In-DOTATATE membrane-bound fraction to the increased internalized fraction in NCI-H727 cells (**A**), and by plotting the HDACi-enhanced [^{111}In]In-DOTATATE internalization levels against increased *SSTR2* mRNA expression levels in BON-1 (**B**) and NCI-H727 (**C**) cells.

SUPPLEMENTAL TABLE 1

Table S1. Primers used for RT-qPCR. HKG primers (Thermo Fisher Scientific) were diluted twenty times. For SSTR2, final concentration were 0.5 pM for both forward and reverse primers, and 0.1 pM for the SSTR2 probe (Sigma).

Gene	Primer information	Efficacy factor
GUSB	Hs00939627_m1	1.95
HPRT1	Hs02800695_m1	1.97
β-Actin	Hs01060665_g1	1.96
SSTR2	Forward: 5′-TCG GCC AAG TGG AGG AGA C Reverse: 3′-AGA GAC TCC CCA CAC AGC CA Probe: CCGGACGGCCAAGATGATCACC	1.91

SUPPLEMENTAL TABLE 2

Table S2. IC_{50} values on growth of BON-1, NCI-H727 and GOT1 cell lines, based on a seven day HDACi treatment period.

HDACi	BON-1	NCI-H727	GOT1
CI-994	1.85 µM	3.05 µM	ND
ENT	218 nM	315 nM	384 nM
LMK-235	154 nM	348 nM	ND
MOC	84.3 nM	171 nM	ND
PAN	3.11 nM	8.53 nM	ND
VPA	1.12 mM	1.31 mM	1.36 mM

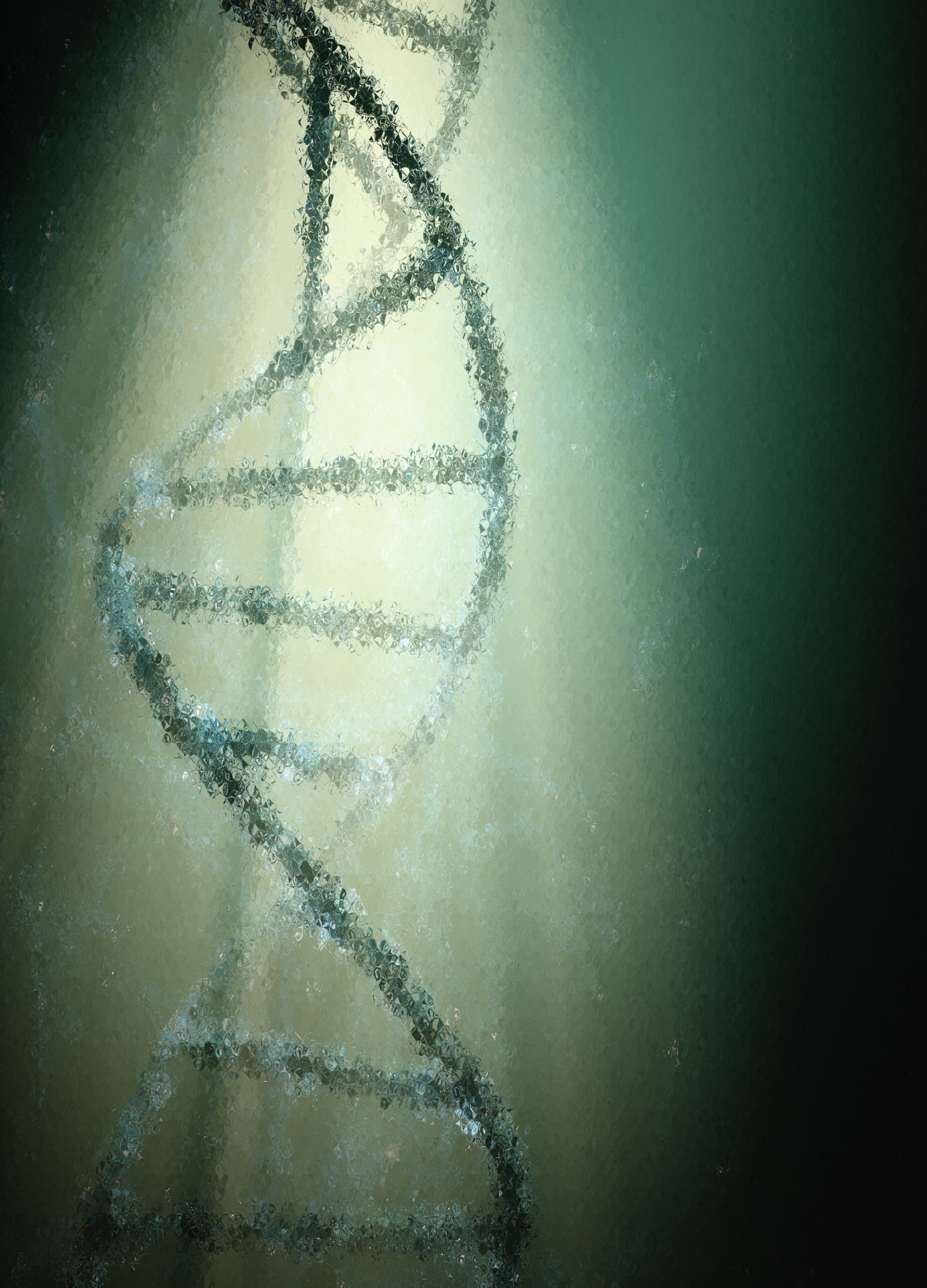

CHAPTER 4

The Effect of VPA Treatment on Radiolabeled DOTATATE Uptake: Differences Observed *In Vitro* and *In Vivo*

M.J. Klomp[1,2], L.J. Hofland[2], L. van den Brink[1], P.M. van Koetsveld[2], F. Dogan[2], C.M.A. de Ridder[1,3], D.C. Stuurman[1,3], M.C. Clahsen-van Groningen[3], M. de Jong[1], S.U. Dalm[1].

[1] Department of Radiology and Nuclear Medicine, Erasmus MC, 3015 GD Rotterdam, The Netherlands. [2] Department of Internal Medicine, Division of Endocrinology, Erasmus MC, 3015 GD Rotterdam, The Netherlands. [3] Department of Experimental Urology, Erasmus MC, 3015 GD, Rotterdam, The Netherlands. [4] Department of Pathology, Erasmus MC, 3015 GD, Rotterdam. The Netherlands.

Pharmaceutics. 2022 Jan 12; 14(1):173

ABSTRACT

Background: To improve peptide receptor radionuclide therapy (PRRT), we aimed to enhance the expression of somatostatin type-2 receptors (SSTR2) *in vitro* and *in vivo*, using valproic acid (VPA). **Methods:** Human NCI-H69 small-cell lung carcinoma cells were treated with VPA, followed by [^{111}In]In-DOTATATE uptake studies, RT-qPCR and immunohistochemistry analysis. Furthermore, NCI-H69 xenografted mice were treated with VPA or vehicle, followed by [^{177}Lu]Lu-DOTATATE injection. Biodistribution studies were performed, and tissues were collected for further analysis. **Results:** VPA significantly increased SSTR2 expression *in vitro*. In animals, a statistically significant increased [^{177}Lu]Lu-DOTATATE tumoral uptake was observed when VPA was administered eight hours before [^{177}Lu]Lu-DOTATATE administration, but increased tumor SSTR2 expression levels were lacking. The animals also presented significantly higher [^{177}Lu]Lu-DOTATATE blood levels, as well as an elevated renal tubular damage score. This suggests that the enhanced tumor uptake was presumably a consequence of the increased radiotracer circulation and the induced kidney damage. **Conclusions:** VPA increases SSTR2 expression *in vitro*. *In vivo*, the observed increase in tumoral [^{177}Lu]Lu-DOTATATE uptake is not caused by SSTR2 upregulation, but rather by other mechanisms, e.g., an increased [^{177}Lu]Lu-DOTATATE circulation time and renal toxicity. However, since both drugs are safely used in humans, the potential of VPA to improve PRRT remains open for investigation.

Keywords: peptide receptor radionuclide therapy; PRRT; somatostatin type-2 receptors; SSTR2; valproic acid; VPA; preclinical; histone deacetylase inhibitor; upregulation; epigenetics.

1. INTRODUCTION

Peptide receptor radionuclide therapy (PRRT) is an approved and efficient therapy for patients with somatostatin type-2 receptor (SSTR2) positive neuroendocrine tumors (NETs). For PRRT, the radiolabeled somatostatin analogue [^{177}Lu]Lu-[DOTA-Tyr^3]octreotate ([^{177}Lu]Lu-DOTATATE) is used, which binds with high affinity to the SSTR2 frequently overexpressed on NETs. Although SSTR2-mediated PRRT improved the progression-free survival of NET patients, complete responses are rare [1, 2]. Therefore, research is performed to improve PRRT outcomes via the upregulation of the target receptor SSTR2, using inhibitors which target the epigenetic machinery.

The efficacy of epigenetic drugs to increase SSTR2 expression has already been shown in multiple *in vitro* studies [3-12]. Both histone deacetylase inhibitors (HDACis) and DNA methyltransferase inhibitors (DNMTis) have been investigated. Valproic acid (VPA), an HDAC class I inhibitor, is one of the most studied inhibitors. VPA is clinically approved for the treatment of several neurologic disorders, facilitating clinical implementation [13]. Moreover, it was demonstrated in several NET cell lines, e.g., BON-1, NCI-H727 and GOT1, that VPA is superior to other HDACis with regard to SSTR2 upregulation [3-6]. However, to the best of our knowledge, the effect of VPA on SSTR2 expression and SSTR2-mediated radiotracer uptake has not been studied *in vivo* yet.

Therefore, the aim of this study was to examine the effects of VPA on SSTR2 expression levels *in vitro* and *in vivo*, using NCI-H69 human small-cell lung carcinoma cells. *In vitro*, we examined the effect of VPA treatment on SSTR2 expression level and [^{111}In]In-DOTATATE uptake, and we investigated whether this effect was time-dependent. Furthermore, we investigated the effect of a single VPA injection on tumor and physiological [^{177}Lu]Lu-DOTATATE uptake in NCI-H69 tumor-bearing mice.

2. MATERIALS AND METHODS

2.1. CELL CULTURE

NCI-H69 human small-cell lung carcinoma cells (ECACC) were sub-cultured once a week at a concentration of 180,000 cells/mL (T175 culture flask, 20 mL), and fresh medium was added on day four (30 mL). Cells were cultured up to 20 passages in a humidified atmosphere (37 °C, 5% CO_2) in RPMI medium 1640 + GlutaMAX-I (Gibco, Breda, The Netherlands) supplemented with 10% (*v/v*) fetal bovine serum (Gibco) and 5% (*v/v*) penicillin–streptomycin (Merck Life Science NV, Amsterdam, The Netherlands).

2.2. RADIOLABELING

DOTATATE (Bachem AG, Budendorf, Switzerland) was radiolabeled with [^{111}In]$InCl_3$ (Curium Pharma, Petten, The Netherlands) or ^{177}Lu (IDB Group, Baarle-Nassau, The Netherlands) with a molar activity between 60 and 200 MBq/nmol, and 50 MBq/nmol, respectively, as previously

described [14]. The radiochemical yield was > 95% and radiochemical purity was >90%, measured by thin-layer chromatography and high-performance liquid chromatography, respectively. For internalization studies over time, a mixture of gentisic acid and ascorbic acid (final concentration: 3.5 mM), and ethanol (final concentration: 7%) was added to maintain radiotracer stability (final volume: 140 µL) [14]. [^{111}In]In-DOTATATE was used for *in vitro* experiments, and [^{177}Lu]Lu-DOTATATE was used for *in vivo* studies, thereby taking possible future therapy studies requiring the use of [^{177}Lu]Lu-DOTATATE into consideration.

2.3. VPA TREATMENT

The IC_{50} value for VPA (Sigma-Aldrich) was determined based on a seven-day treatment. For this, 30,000 cells were plated in 24-well plates with normal growth medium, and VPA was added after 24 h at a final concentration between 10^{-2} M and 10^{-8} M for dose-response studies or at the IC_{50} dose for other experiments. VPA was dissolved in water, and untreated controls were vehicle-treated (final concentration of 1% H_2O). For dose–response studies, cell-growth medium and HDACi were refreshed on day four. Cells were then collected by centrifugation on day seven, and the amount of DNA was quantified by using Hoechst 33256 [6]. In short, cells were lysed with 0.2% (*v*/*v*) Triton X-100, and the DNA was sheared by sonification. Subsequently, the DNA concentration was determined after adding Hoechst 33256 and measuring the absorbance at an excitation and emission wavelength of 485 nm and 535 nm, respectively. Fluorescence of experimental samples was referenced to a standard curve of calf thymus DNA.

2.4. [^{111}In]In-DOTATATE INTERNALIZATION STUDIES OF VPA-TREATED CELLS

NCI-H69 cells were treated with VPA up to 48 h with the IC_{50} value to study the time-dependency of treatment. Internalization studies were performed 8, 16, 24, 40 and 48 h after start of VPA treatment as previously described [6], with implementation of minor adjustments. Two million cells were incubated with 1 mL of 1 nM [^{111}In]In-DOTATATE (60–200 MBq/nmol), with or without an excess of 1 µM unlabeled DOTATATE in RPMI medium 1640 + GlutaMAX-I supplemented with 1% (*w*/*v*) BSA and 20 mM HEPES (pH 7.4). Cells were incubated at 37 °C for two hours in 1.5 mL Safe-Lock Eppendorf tubes, washed twice with 1 mL cold phosphate-buffered saline (PBS) and subsequently pelleted by centrifugation (5 min, 0.9× *g*, 4 °C). The cell pellets were then measured in the gamma counter to determine the [^{111}In]In-DOTATATE uptake. To correct for differences in cell numbers that may occur as a consequence of washing steps, the DNA concentration of three spare samples was determined with Hoechst 33256, according to the protocol described above. These spare samples were also treated with either the vehicle (i.e., 0.1% H_2O) or HDACi.

2.5. RT-qPCR AND IMMUNOHISTOCHEMISTRY OF VPA-TREATED CELLS

SSTR2 expression levels were determined 24 h after VPA treatment by using RT-qPCR [6] and immunohistochemistry. For SSTR2 immunohistochemistry, cytospins were made (Rotofix 32A,

Hettich, Geldermalsen, The Netherlands) and samples were subsequently fixated with 2% paraformaldehyde (20 min, room temperature (RT)). After permeabilization with 0.1% (*v*/*v*) Triton X-100 in PBS (15 min, RT), samples were blocked with 1% (*w*/*v*) bovine serum albumin (BSA; 1 h, RT). Rabbit SSTR2 antibody (NeoBiotech, Maastricht, The Netherlands, NB-49-015, 1:100 dilution) was added (overnight, 4 °C), and Dako REAL EnVision detection system peroxidase/DAB$^+$, rabbit/mouse kit (Agilent Technologies, Amstelveen, The Netherlands) was used as secondary antibody (30 min, RT). Samples were counterstained with hematoxylin, mounted and visualized with the NanoZoomer 2.0 HT (Hamamatsu Photonics, Hamamatsu City, Japan). Afterward, the percentage of cells with positive staining was assessed on three random locations per slide, using a 10x magnification and the CellProfiler software (version 4.0.7), which is freely available to download at www.cellprofiler.org, accessed on 28 November 2021. The percentage of SSTR2 negative cells (Q0) and the extent of SSTR2 expression in the remaining cells were determined. For the latter, vehicle- and VPA-treated cells were pooled together, and the mean total intensity (MTI) of each SSTR2 positive cell was determined. Subsequently, the cells with the minimum and maximum MTI were recorded, and the difference between these two values was divided into four quartiles (Q1–Q4).

2.6. ANIMALS

All animal experiments were approved by the Animal Welfare Committee and were in accordance with European law. Male NMRI-Foxn1 nu/nu mice (5–8 weeks, Janvier) were housed under standard laboratory conditions (i.e., aseptic condition and 12 h light/dark cycle), given ad libitum access to water and food and acclimated for a week before the start of the experiment.

2.7. BIODISTRIBUTION STUDIES

Mice were subcutaneously injected on the right shoulder with NCI-H69 cells: 5 × 10^6 cells were injected in 100 µL containing 1/3 Matrigel (Corning, Amsterdam, The Netherlands) and 2/3 HBSS. Tumor size was measured twice a week with a caliper, and tumor volume was calculated by using the following formula: π/6 (tumor length * tumor width) ^ (3/2). Animals were divided into eight experimental groups based on body weight and tumor size (Supplementary Materials Table S1). After 18 days, mice were intraperitoneally injected with VPA (200 mg/kg or 400 mg/kg) or vehicle (0.9% NaCl). Four or eight hours after VPA injection, mice were intravenously injected with ~10 MBq/200 pmol/200 µL [^{177}Lu]Lu-DOTATATE (50 MBq/nmol) diluted in 1% (*w*/*v*) BSA in PBS (n = 5 per group). To determine the selectivity of [^{177}Lu]Lu-DOTATATE uptake, additional groups of mice received ~10 MBq/200 pmol/100 µL [^{177}Lu]Lu-DOTATATE (50 MBq/nmol) plus 4000 pmol/100 µL unlabeled DOTATATE intravenously in a single injection four hours after VPA (400 mg/kg) or vehicle (0.9% NaCl) administration (n = 4 per group).

Biodistribution studies were performed four hours after radiotracer injection. All collected organs were weighted and subsequently counted in the gamma-counter (Wallac Wizard 1480

automatic gamma counter; Perkin Elmer, Groningen, The Netherlands). The uptake of radioactivity was expressed as percentage injected dose per gram of tissue (% ID/g). Values were corrected for the amount of radioactivity left in the syringe and at the injection site (tail). For further analysis, several organs were either snap-frozen or formalin-fixed.

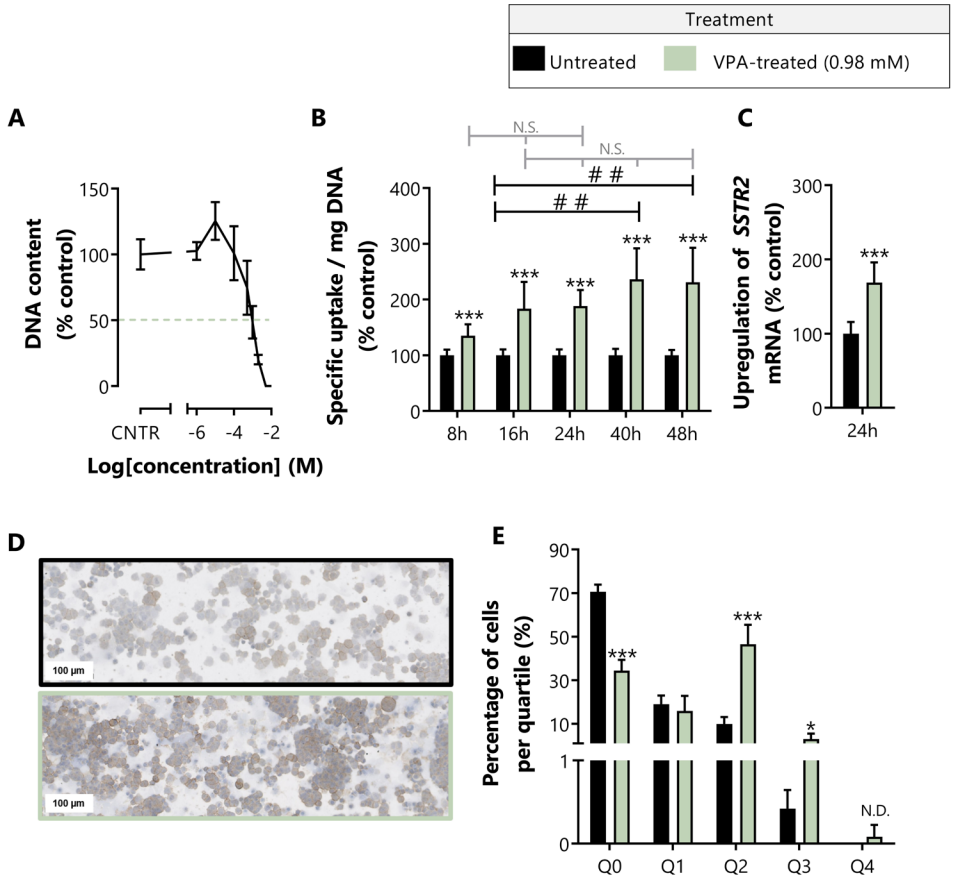

Figure 1. *In vitro* effects of VPA on SSTR2 expression The IC_{50} value of VPA in NCI-H69 cells was 0.98 mM **(A)**. To study the effect of VPA on SSTR2 expression, the uptake of [^{111}In]In-DOTATATE (per milligram DNA, expressed as percentage of control cells) **(B)**, *SSTR2* mRNA expression levels (expressed as percentage of control cells) **(C)** and SSTR2 protein expression levels **(D,E)** were examined. The percentage of SSTR2 negative cells (Q0) and the extent of SSTR2 intensity (Q1–Q4) were determined. To indicate significance for *t*-test results between vehicle- and VPA-treated cells, the following abbreviations and symbols were used: * $p < 0.05$; *** $p < 0.001$ and N.D. = non-determined (due to absence of vehicle-treated cells in Q4). For the one-way ANOVA results between different VPA-treated groups, the following abbreviations and symbols were used: ## $p < 0.01$ and N.S. = non-significant.

2.8. RT-qPCR AND IMMUNOHISTOCHEMISTRY OF TISSUE SAMPLES

To measure *SSTR2* mRNA expression levels, snap-frozen tissue was cryosectioned, mixed with lysis buffer and shortly centrifuged. The supernatant was used to determine mRNA expression

levels as previously described [6]. For SSTR2 immunohistochemistry, automated IHC, using the Ventana Discovery Ultra (Ventana Medical Systems Inc., Almere, The Netherlands), was used. Formalin-fixed paraffin-embedded sections (4 µm) were stained for SSTR2A, using a universal chromomap DAB detection Kit (#760-159, Ventana). In brief, following deparaffinization and heat-induced antigen retrieval with CC1 (#950-500, Ventana) for 92 min, the tissue samples were incubated with the SSTR2A antibody (Biotrend, Maastricht, The Netherlands, rabbit polyclonal, lot number D19803) in a 1:25 dilution for 60 min at 37 °C. Subsequently, tissue sections were incubated with secondary antibody omnimap anti-rabbit HRP (#760-4311, Ventana) for 20 min, followed by DAB detection. Incubation was followed by hematoxylin II counter-staining (#790-2208, Ventana) for eight minutes, after which tissue sections were exposed to a blue coloring reagent (#790-2037, Ventana) for eight minutes, according to the manufacturer's instructions. Stained sections were imaged and quantified by using the method described for the *in vitro* studies.

2.9. RENAL TUBULAR DAMAGE

Periodic Acid-Schiff Diastase (PAS+) staining (#860-014,Ventana) was performed by using the Ventana Special Stains Module (Ventana). In brief, formalin-fixed paraffin-embedded sections (3 µm) were deparaffinized and rehydrated by passage through a decreasing ethanol series. Then slides were incubated with PAS diastase for 12 min, followed by several washing steps. PAS periodic acid was added for four minutes at 50 °C, followed by PAS Schiffs for 20 min at 50 °C. Slides were counterstained with PAS hematoxylin for eight minutes. Every section was blindly scored by an experienced nephropathologist (M.C.C.v.G.) for tubular damage (10× magnification), using a 5-point scale, according to the following criteria: tubular dilatation, cast deposition, brush border loss and necrosis. Each parameter was graded in 10 fields with a score of 0–5: 0, no changes; 1, mild, <10%; 2, moderate, 10–25%; 3, severe, 25–50%; 4, very severe, 50–75%; and 5, extensive damage, >75%.

2.10. STATISTICS

In vitro analysis: A spline-LOWESS analysis with point-to-point curve was used to determine the IC_{50} value of VPA. Data for internalization studies and RT-qPCR were normalized to untreated cells and log-transformed. One-way ANOVA with a Tukey's multiple comparison test was used to detect differences in internalization studies; and to determine differences in RT-qPCR and IHC analysis, a *t*-test was used. All results represent the mean ± SD of at least two independent biological replicates and at least three technical replicates.

In vivo analysis: Biodistribution data (i.e., % ID/g tissue and tumor-to-background ratios) were log-transformed, and a one-way ANOVA with a Dunnett's multiple comparison test was performed to detect differences between experimental groups. For RT-qPCR results, a *t*-test was used to analyze the normalized and log-transformed data. A one-way ANOVA with a Dunnett's multiple comparison test was used to detect differences in IHC. All data results represent the mean ± SD.

All statistical analyses were performed by using GraphPad Prism 5 software.

3. RESULTS

3.1. EFFECTS OF VPA ON NCI-H69 CELLS *IN VITRO*

A seven-day cell-growth assay demonstrated that the IC_{50} value for VPA is 0.96 mM in NCI-H69 cells (Figure 1A). Treatment of NCI-H69 cells with the IC_{50} of VPA, followed by uptake studies, showed that the SSTR2-mediated uptake of [^{111}In]In-DOTATATE is fast and significantly increased after start of HDACi treatment (Figure 1B). Just eight hours after VPA administration, the uptake of [^{111}In]In-DOTATATE was 1.46-fold higher than the uptake measured in untreated cells. No statistical differences were observed between NCI-H69 cells treated with VPA for 16, 24, 40 and 48 h. For practical reasons, it was therefore decided to apply a 24 h VPA-treatment period for further experiments, characterized by a 1.88-fold increased [^{111}In]In-DOTATATE uptake compared to untreated cells.

RT-qPCR and immunohistochemical analyses were performed to study *SSTR2* mRNA and SSTR2 protein-expression levels after treating NCI-H69 cells for 24 h with VPA. *SSTR2* mRNA expression levels were significantly upregulated 1.69-fold compared to untreated cells (Figure 1C). In line with this, immunohistochemical analysis showed a clear increase in SSTR2 protein-expression levels (Figure 1D). Quantification of the total SSTR2 staining demonstrated a reduction in the number of SSTR2 negative cells (Q0), i.e., 70.6 ± 3.3% versus 34.4 ± 5.0% for untreated and VPA-treated cells, respectively. Furthermore, a significant increase in the percentage of cells in quartile two (Q2) and three (Q3) was observed after VPA treatment, suggesting an increase in the number of SSTR2-positive cells characterized by higher SSTR2 expression levels (Figure 1E).

3.2. EFFECTS OF VPA ON THE BIODISTRIBUTION OF [^{177}Lu]Lu-DOTATATE IN MICE BEARING NCI-H69 XENOGRAFTS

Biodistribution data showed that mice receiving VPA four hours prior to [^{177}Lu]Lu-DOTATATE administration had no significant increase in tumor uptake, i.e., 9.9 ± 3.3% ID/g, 10.2 ± 2.3% ID/g and 13.8 ± 2.2% ID/g for untreated, 200 mg/kg and 400 mg/kg VPA, respectively (Figure 2A). In line with this, the uptake of [^{177}Lu]Lu-DOTATATE did not change significantly in the majority of background organs of VPA-treated mice in comparison to untreated animals. A significant difference in radioactivity uptake was measured in the kidneys; [^{177}Lu]Lu-DOTATATE kidney uptake was lower after VPA treatment (Figure 2A), indicating a faster [^{177}Lu]Lu-DOTATATE excretion. Due to this reduction of radioactivity measured in the kidneys, the tumor-to-kidney ratio was significantly increased after VPA treatment, i.e., 1.8 ± 0.5, 6.5 ± 2.6 and 7.1 ± 5.8 for untreated, 200 mg/kg and 400 mg/kg VPA, respectively. In line with what was mentioned above, no significant differences in tumor-to-organ ratio were found for all other organs (Figure 2A and Figure S1A).

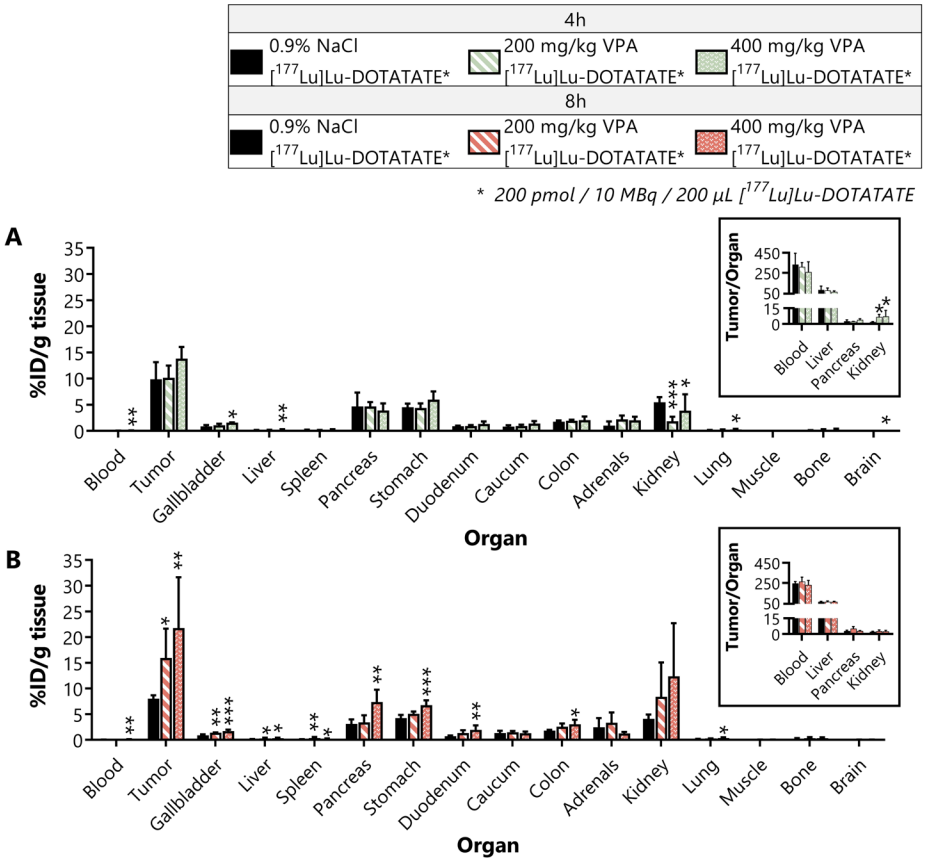

Figure 2. Biodistribution of [^{177}Lu]Lu-DOTATATE after VPA treatment [^{177}Lu]Lu-DOTATATE uptake expressed as percentage injected dose per gram tissue (% ID/g tissue) for animals injected with vehicle or VPA (200 mg/kg or 400 mg/kg) four (**A**) or eight (**B**) hours prior to [^{177}Lu]Lu-DOTATATE administration. For both treatment schedules, several tumor-to-organ ratios are depicted: * $p < 0.05$; ** $p < 0.01$; *** $p < 0.001$.

To determine whether [^{177}Lu]Lu-DOTATATE uptake was SSTR2-mediated after VPA treatment, vehicle or VPA (400 mg/kg) was administered four hours prior to radiotracer injection which was administered with an excess of unlabeled DOTATATE. A less efficient blocking of [^{177}Lu]Lu-DOTATATE uptake was demonstrated for VPA-treated mice compared to untreated animals, as shown by significantly increased levels of radioactivity measured in both tumor tissue and background organs of VPA-treated animals (Supplementary Materials Figure S2).

Contrary to the tumor uptake of animals pretreated with VPA four hours before [^{177}Lu]Lu-DOTATATE administration, the biodistribution data of mice injected with VPA eight hours before radiotracer injection demonstrated significantly increased [^{177}Lu]Lu-DOTATATE tumoral uptake. The tumor uptake was 15.9 ± 5.7% ID/g for 200 mg/kg and 21.7 ± 9.9% ID/g for 400 mg/kg VPA-treated mice compared to 8.0 ± 0.6% ID/g for untreated animals (Figure 2B). However, the physiological uptake of [^{177}Lu]Lu-DOTATATE was also significantly increased.

Whereas the lower dose of 200 mg/kg VPA only resulted in a statistically significant increased uptake in the gallbladder, liver and spleen, treatment with 400 mg/kg VPA also significantly increased the radiotracer uptake in pancreas, stomach, duodenum, colon and lungs. As a result of the increased physiological [^{177}Lu]Lu-DOTATATE uptake and the increased amount of radiotracer in the tumor, no differences in tumor-to-organ ratios were observed (Figure 2B and Supplementary Materials Figure S1B).

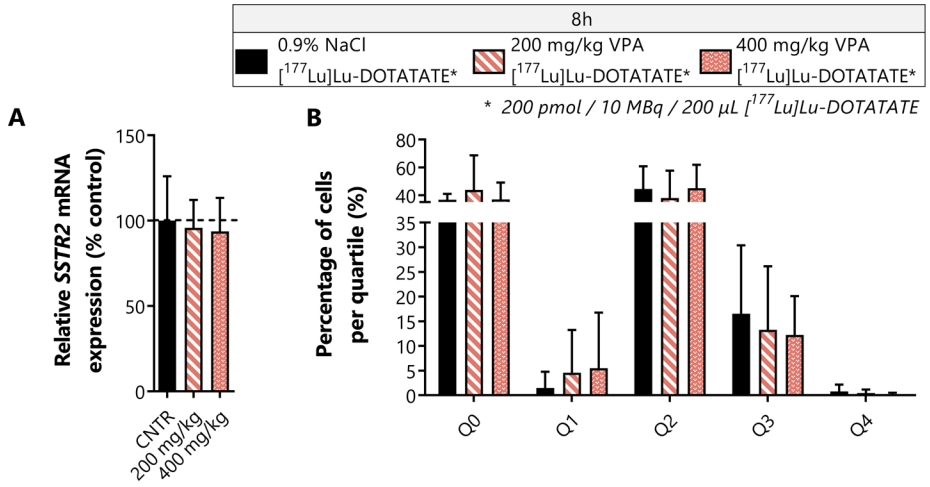

Figure 3. ***In vivo*** **tumoral SSTR2 expression levels after VPA-treatment** Tumors of NCI-H69 tumor-bearing mice injected with vehicle or VPA (200 mg/kg or 400 mg/kg) eight hours prior to [^{177}Lu]Lu-DOTATATE administration were analyzed for *SSTR2* mRNA expression levels **(A)** and SSTR2 protein-expression levels **(B)**. The percentage of SSTR2 negative cells (Q0) and the extent of SSTR2 intensity (Q1–Q4) were determined **(B)**.

Unexpectedly, we observed increased levels of [^{177}Lu]Lu-DOTATATE in the blood of VPA-treated mice compared to that of control animals. For mice injected with VPA or vehicle four hours prior to [^{177}Lu]Lu-DOTATATE administration, the radioactivity measured in the blood was 0.030 ± 0.001% ID/g, 0.033 ± 0.007% ID/g and 0.062 ± 0.028% ID/g for vehicle, 200 mg/kg and 400 mg/kg VPA-treated mice, respectively. For mice injected eight hours post VPA-administration, this was 0.033 ± 0.004% ID/g, 0.053 ± 0.010% ID/g and 0.085 ± 0.042% ID/g, respectively. The observed increase in radioactivity levels in the blood reached significance for the animals injected with 400 mg/kg VPA.

3.3. EFFECTS OF VPA ON SSTR2 EXPRESSION LEVELS IN TUMOR TISSUE OF NCI-H69 XENOGRAFTS

The increased blood radioactivity levels mentioned above suggest that there is an increased circulation time of [^{177}Lu]Lu-DOTATATE. This can potentially result in higher uptake levels of the radiotracer. To determine whether the increased tumor uptake observed in animals injected with VPA eight hours prior to [^{177}Lu]Lu-DOTATATE is a consequence of increased

SSTR2 expression or a potential effect of prolonged [^{177}Lu]Lu-DOTATATE circulation, *SSTR2* mRNA expression levels were measured in tumors of untreated and VPA-treated mice. No statistically significant differences in *SSTR2* mRNA expression levels were observed after VPA treatment (Figure 3A). Immunohistochemistry analysis for SSTR2 expression levels in tumor tissue confirmed the RT-qPCR results, demonstrating no evident increase in SSTR2 protein expression after VPA treatment (Figure 3B). In line with *SSTR2* mRNA expression levels measured in tumor tissue, the expression of *SSTR2* in spleen and liver, both showing an increased [^{177}Lu]Lu-DOTATATE uptake after VPA treatment, also showed no significant differences upon treatment (data not shown).

3.4. KIDNEY TUBULAR DAMAGE

To investigate possible mechanisms behind the increased [^{177}Lu]Lu-DOTATATE circulation time, the kidneys were analyzed because of the role of this organ in excretion of the radiotracer. The kidneys were scored for renal tubular damage (Figure 4A). In mice injected with [^{177}Lu]Lu-DOTATATE four hours after VPA or vehicle administration, where no significant increase in tumoral [^{177}Lu]Lu-DOTATATE uptake was observed, the renal tubular damage was limited, i.e., an average score of 0.2, 0.2 and 1.0 for untreated, 200 mg/kg and 400 mg/kg VPA-treated mice (Table 1). For these three experimental groups, no clear pattern was observed between the kidney damage score and the uptake of [^{177}Lu]Lu-DOTATATE (Figure 4B and Supplementary Materials Figure S3). However, 400 mg/kg VPA-treated mice receiving [^{177}Lu]Lu-DOTATATE in combination with an excess of unlabeled DOTATATE presented a high average renal tubular damage score of 3.5 (Table 1). In the majority of animals with a high tubular damage score, the uptake of [^{177}Lu]Lu-DOTATATE was increased in both tumors and physiological organs when compared to that of animals that were not pretreated with VPA and received an injection of [^{177}Lu]Lu-DOTATATE plus an excess of unlabeled DOTATATE (Figure 4B and Supplementary Materials Figure S3).

The kidneys of mice injected with the radiotracer eight hours post-VPA-administration, where a significant increased amount of [^{177}Lu]Lu-DOTATATE tumor uptake was observed, were also examined for kidney toxicity. All untreated animals received a damage score of 0, and the damage score for VPA-treated mice varied from 0 to 5. On average, the damage score was 1.6 for treatment with 200 mg/kg and 2.6 for 400 mg/kg VPA. A detailed overview of all damage scores can be found in Table 1. When correlating the renal tubular damage score and [^{177}Lu]Lu-DOTATATE uptake of several organs, it was demonstrated that high [^{177}Lu]Lu-DOTATATE uptake was often associated with high levels of renal tubular damage (Figure 4C and Supplementary Materials Figure S4).

4. DISCUSSION

The low number of complete responses after PRRT in NET patients with SSTR2 positive tumors shows the need for therapy improvement. The aim of this study was, therefore, to examine the

effect of the HDACi VPA on SSTR2 expression and radiotracer uptake. To do so, *in vitro* and *in vivo* studies were performed by using the SSTR2-expressing NCI-H69 cell line.

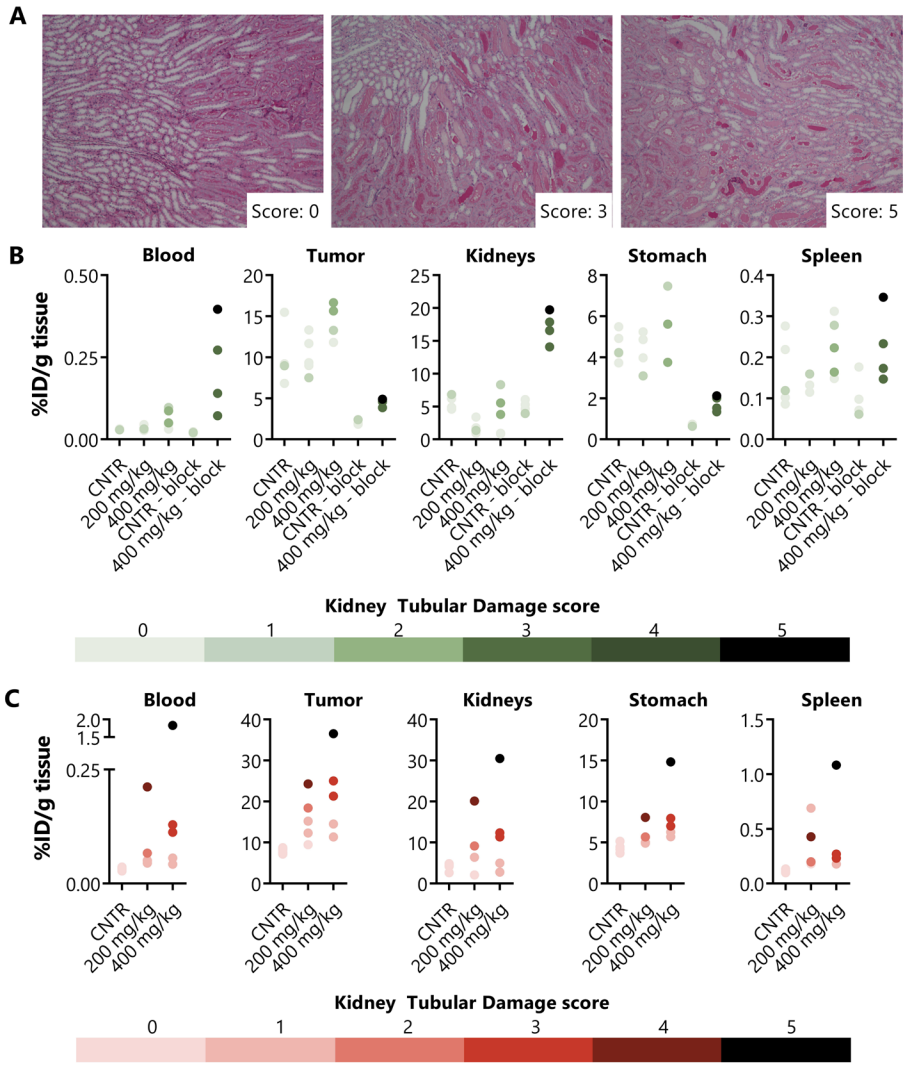

Figure 4. Biodistribution correlated with the observed renal-tubular-damage Kidneys were scored for renal tubular damage on a 5-point scale **(A)**. Biodistribution data were correlated with the renal tubular damage score for blood, tumor, kidneys, stomach and spleen of mice treated with vehicle or VPA (200 mg/kg or 400 mg/kg) four **(B)** or eight **(C)** hours prior to [^{177}Lu]Lu-DOTATATE administration. A color gradient is used to indicate the level of damage. Each data point in these graphs represents a mouse. For the uptake of [^{177}Lu]Lu-DOTATATE in kidneys, the average of both kidneys is plotted. Outliers based on % ID/g tissue are included in this figure.

The effect of class I-targeting HDACi VPA has been studied before, *in vitro*, in terms of increased uptake of radiolabeled DOTATATE, *SSTR2* mRNA expression levels and/or SSTR2

protein expression levels, using different NET cell models, i.e., BON-1, QGP1 and NCI-H727 [4, 5, 7, 11, 12]. We also studied the effect of VPA and several other HDACis in BON-1, NCI-H727 and GOT1 cells [6], showing the superior effects of VPA. Although convincing effects of VPA on SSTR2 expression levels have been described *in vitro*, an evaluation of its effect *in vivo*, including radiotracer uptake, is lacking.

Table 1. Tubular kidney damage scores (scale: 0–5) given to each experimental group.

	Tubular Kidney Damage Score					
	0	**1**	**2**	**3**	**4**	**5**
No VPA (4h)	4/5	1/5	-	-	-	-
200mg VPA (4h)	4/5	1/5	-	-	-	-
400mg VPA (4h)	2/5	1/5	2/5	-	-	-
No VPA (4h, block)	3/4	1/4	-	-	-	-
400mg VPA (4h, block)	-	-	-	3/4	-	1/4
No VPA (8h)	5/5	-	-	-	-	-
200mg VPA (8h)	1/5	2/5	1/5	-	1/5	-
400mg VPA (8h)	-	2/5	-	2/5	-	1/5

To examine the effect of VPA in a preclinical setting, we used the human small-cell lung carcinoma cell line NCI-H69. This model has high SSTR2 expression levels, and it is therefore frequently used in studies focusing on PRRT. First, we confirmed that there is an effect of VPA on SSTR2 expression levels *in vitro* in this model by demonstrating increased [^{111}In]In-DOTATATE uptake after VPA treatment. After 24 h, a 1.88-fold increased [^{111}In]In-DOTATATE uptake was measured. Moreover, mRNA analysis and immunohistochemistry demonstrated SSTR2 upregulation, thereby excluding other possible mechanisms of action.

It was demonstrated *in vitro* that the uptake of [^{111}In]In-DOTATATE is already significantly enhanced just eight hours after start of VPA treatment. For this reason, we hypothesized that VPA-induced effects arise quickly *in vivo* as well. This is further supported in the literature, where it is reported that there is an increase in acetylation on histones just two hours after VPA administration [15-17]. Moreover, these effects were observed after a single injection. Therefore, we decided to treat animals with a single VPA injection, quickly followed by [^{177}Lu]Lu-DOTATATE administration. As we have also demonstrated that effects are quickly reversible *in vitro* [6], we checked two timeframes between VPA and [^{177}Lu]Lu-DOTATATE injection, i.e., four and eight hours. Although we observed significant increased tumor uptake-values in mice treated with VPA eight hours prior to [^{177}Lu]Lu-DOTATATE administration, statistically significant increases in tumor-to-organ ratios were lacking. The absence of increased SSTR2 mRNA and protein expression levels, in combination with the increased amount of [^{177}Lu]Lu-DOTATATE in the blood of VPA-treated animals, suggested that the enhanced uptake is not caused by SSTR2 upregulation, but most likely by other mechanisms of action, such as an increased [^{177}Lu]Lu-DOTATATE circulation time.

To get insights in the possible mechanisms involved in an increased [^{177}Lu]Lu-DOTATATE circulation time, the renal tubular damage score was evaluated. It was shown that mice receiving VPA eight hours prior to [^{177}Lu]Lu-DOTATATE administration have increased renal damage. This damage most likely causes a slower excretion rate of the radiotracer, resulting in a longer circulation time. However, it remains to be investigated if the increased radiotracer circulation time induces renal damage, or that the renal damage is inducing a prolonged circulation time. Nonetheless, the observed increase in [^{177}Lu]Lu-DOTATATE circulation time can lead to an increased radiotracer uptake in both high (e.g., tumor, pancreas and stomach) and low (e.g., liver, spleen and lung) SSTR2-expressing organs.

Mice pretreated four hours prior to [^{177}Lu]Lu-DOTATATE administration did not demonstrate significantly increased [^{177}Lu]Lu-DOTATATE tumor uptake. In line with this, the renal tubular damage in this group was still limited. We therefore hypothesize that the extent of renal damage was not progressed enough to influence excretion at this time point. Mice following the same treatment regimen (400 mg/kg VPA, injected four hours prior to [^{177}Lu]Lu-DOTATATE administration), but also receiving an excess of unlabeled DOTATATE, are characterized by increased renal tubular damage in comparison to vehicle-treated animals receiving an excess of DOTATATE. We hypothesize that this may be caused by high DOTATATE concentrations damaging the kidneys that are already slightly affected by VPA and [^{177}Lu]Lu-DOTATATE combination treatment, radiation-induced nephrotoxicity as a consequence of high kidney-radiation dosages or a combination of these two. The radiation-induced toxicity can be a result of blocking the SSTR2 in the tumor and other physiological organs, leads to higher [^{177}Lu]Lu-DOTATATE renal exposure.

The exact mechanism behind the observed renal tubular damage cannot be determined from our data. The observed toxicity can either be a consequence of VPA monotherapy or the combination therapy of VPA and [^{177}Lu]Lu-DOTATATE. The observed toxicity cannot be an effect of [^{177}Lu]Lu-DOTATATE monotherapy, as vehicle-treated animals receiving only [^{177}Lu]Lu-DOTATATE do not demonstrate tubular damage. Furthermore, in a study by Svensson et al. [18], mice were injected with 90, 120 or 150 MBq [^{177}Lu]Lu-DOTATATE, which matched an absorbed dose in the renal cortex of 35, 47 and 58 Gy, respectively. The threshold dose value for tubular damage was determined to be approximately 24 Gy. Since animals were administered with only 10 MBq [^{177}Lu]Lu-DOTATATE and mice were sacrificed already four hours post-injection of the radiotracer, a kidney dose well below the threshold can be expected in our study, even in VPA-treated animals that received [^{177}Lu]Lu-DOTATATE plus an excess of unlabeled DOTATATE associated with a 3–4 times higher kidney uptake. When it comes to VPA, safety issues related to kidney function after a long-term VPA treatment period in rodents have previously been described [19-21]. However, to the best of our knowledge, renal toxicity has not been described after administration of a single VPA injection in animals, using the doses applied in our study. Nonetheless, the renal tubular damage of mice treated with VPA only has not been examined in this study, and we can therefore not draw firm

conclusions on the toxicity of VPA mono-treatment. Further research on this topic is required. Based on our data, the combination treatment and, thus, the interaction of the two drugs seems to be the most plausible explanation for the renal damage. We observed that animals receiving an excess of unlabeled DOTATATE after VPA treatment had an increased [^{177}Lu]Lu-DOTATATE kidney uptake, which, in turn, was associated with a higher kidney-damage score compared to control animals. This higher radioactivity uptake in the kidneys and the herewith higher radiation dose to this organ could potentially lead to radiation-induced kidney damage in animals treated with the combination of [^{177}Lu]Lu-DOTATATE and VPA, even though this radiotracer dosage seems safe when the excretion rate is not hampered. Moreover, our data indicate that VPA itself may contribute to the renal toxicity as a higher VPA dosage (400 mg/kg versus 200 mg/kg) or a longer treatment time (8 h versus 4 h) results in a more severe damage. This damage may be aggravated in combination with [^{177}Lu]Lu-DOTATATE, especially when a large amount of unlabeled DOTATATE is co-injected. We therefore hypothesize that it is likely that the interaction of VPA and [^{177}Lu]Lu-DOTATATE caused the renal toxicity observed in our study.

Even though the effect of VPA in the NCI-H69 cell model did not provide the desired effect *in vivo*, the potential of SSTR2 upregulation in response to other HDACis or DNMTis *in vivo* has been described previously. Two articles have been published studying the effect of HDACis by using NET-bearing mice [4, 5]. In these two studies, BON-1 and NCI-H727 tumor-bearing mice were treated with FK228 and TDP-A, respectively. After injection of [^{68}Ga]Ga-DOTATATE, the PET/CT-scan demonstrated increased standard uptake values after HDACi-treatment, reaching significance for FK228-treated animals. A more elaborative study is performed by Taelman et al. [3], showing statistically significant increased tumor uptake of [^{68}Ga]Ga-DOTATOC upon treatment with DNMTi decitabine in BON-1 tumor-bearing mice caused by an increase in SSTR2 protein-expression level. Moreover, the effect of decitabine treatment on [^{68}Ga]Ga-DOTATOC on physiological uptake was not significant. These results emphasize the potential value of combining epigenetic drugs and radiolabeled somatostatin analogues. Next to the HDACis used in the studies mentioned above [3-5], other HDACis have shown to be promising with regard to SSTR2 upregulation and increased SSTR2-targeting radiotracer uptake in *in vitro* studies, as was also described in our previous paper [6]. A next step can be to test these HDACis *in vivo* as well.

We hypothesize that the short half-life of VPA in mice of approximately 55 min may be a major factor preventing VPA from exerting its SSTR2-upregulating capacity [22]. This fast excretion can cause an insufficient tumoral VPA dose. To investigate if an insufficient tumoral dose is the cause of absent effects, VPA can be injected intratumorally. If this is proven to be effective for SSTR2 upregulation, effort could be made to increase the low tumoral VPA dose, e.g., by the use of a constant-rate infusion system, allowing for stable blood concentrations or by applying a tumor-targeting approach. This may support VPA to induce SSTR2 upregulation and, thus, increased [^{177}Lu]Lu-DOTATATE uptake. However, the renal damage observed in our study has to be kept in mind, and, in line with this, careful monitoring of potential renal toxicity

upon combination treatments, using VPA, is required in preclinical studies, also when VPA is administered differently and/or a lower dose is used. Moreover, although some very rare side effects affecting renal function have been described in humans as well [23], VPA is safely used for the treatment of neurological disorders [13]. Therefore, the potential of this combination therapy to improve PRRT outcomes in humans remains open for investigation.

5. CONCLUSION

In conclusion, VPA induced convincing SSTR2 upregulation in NCI-H69 cells *in vitro*. Although VPA is frequently studied for SSTR2 upregulation in NET cell lines showing positive results, our preclinical *in vivo* data demonstrated that a single VPA injection does not result in the desired effect in our mouse model. Although the radiotracer tumor uptake is increased in mice injected with VPA eight hours prior to [^{177}Lu]Lu-DOTATATE administration, this is not the result of SSTR2 upregulation, but most likely caused by other mechanisms, such as an increased [^{177}Lu]Lu-DOTATATE circulation time and renal toxicity. This observed damage is either the result of VPA monotherapy or, more likely, caused by an interaction between VPA and [^{177}Lu]Lu-DOTATATE. The absence of desired effects *in vivo* may be caused by insufficient tumoral VPA concentrations due to the short half-life of VPA. As higher VPA dosages are not possible due to the observed renal toxicity, VPA is not suitable to increase SSTR2 expression and, thus, PRRT efficacy in this model. However, since VPA rarely causes renal toxicity in humans and shows higher plasma protein binding and longer half-life, the effect of this HDACi on SSTR2 expression, the potentially increased [^{177}Lu]Lu-DOTATATE uptake and the herewith associated improved PRRT efficacy remains open for investigation in humans.

ACKNOWLEDGEMENTS

We would like to thank the Radiopharmaceutical Chemistry group (Radiology and Nuclear Medicine, Erasmus MC, The Netherlands) for radiolabeling of the tracers used in this study.

REFERENCES

1. Strosberg, J.; El-Haddad, G.; Wolin, E.; Hendifar, A.; Yao, J.; Chasen, B.; Mittra, E.; Kunz, P.L.; Kulke, M.H.; Jacene, H., et al. Phase 3 Trial of (177)Lu-ssttate for Midgut Neuroendocrine Tumors. *N Engl J Med* **2017**, *376*, 125-135.
2. Brabander, T.; van der Zwan, W.A.; Teunissen, J.J.M.; Kam, B.L.R.; Feelders, R.A.; de Herder, W.W.; van Eijck, C.H.J.; Franssen, G.J.H.; Krenning, E.P.; Kwekkeboom, D.J. Long-Term Efficacy, Survival, and Safety of [(177)Lu-DOTA(0),Tyr(3)]octreotate in Patients with Gastroenteropancreatic and Bronchial Neuroendocrine Tumors. *Clin Cancer Res* **2017**, *23*, 4617-4624.
3. Taelman, V.F.; Radojewski, P.; Marincek, N.; Ben-Shlomo, A.; Grotzky, A.; Olariu, C.I.; Perren, A.; Stettler, C.; Krause, T.; Meier, L.P., et al. Upregulation of Key Molecules for Targeted Imaging and Therapy. *J Nucl Med* **2016**, *57*, 1805-1810.
4. Guenter, R.; Aweda, T.; Carmona Matos, D.M.; Jang, S.; Whitt, J.; Cheng, Y.Q.; Liu, X.M.; Chen, H.; Lapi, S.E.; Jaskula-Sztul, R. Overexpression of somatostatin receptor type 2 in neuroendocrine tumors for improved Ga68-DOTATATE imaging and treatment. *Surgery* **2020**, *167*, 189-196.
5. Guenter, R.E.; Aweda, T.; Carmona Matos, D.M.; Whitt, J.; Chang, A.W.; Cheng, E.Y.; Liu, X.M.; Chen, H.; Lapi, S.E.; Jaskula-Sztul, R. Pulmonary Carcinoid Surface Receptor Modulation Using Histone Deacetylase Inhibitors. *Cancers (Basel)* **2019**, *11*, 767.
6. Klomp, M.J.; Dalm, S.U.; van Koetsveld, P.M.; Dogan, F.; de Jong, M.; Hofland, L.J. Comparing the Effect of Multiple Histone Deacetylase Inhibitors on SSTR2 Expression and [111In]In-DOTATATE Uptake in NET Cells. *Cancers (Basel)* **2021**, *13*, 4905.
7. Veenstra, M.J.; van Koetsveld, P.M.; Dogan, F.; Farrell, W.E.; Feelders, R.A.; Lamberts, S.W.J.; de Herder, W.W.; Vitale, G.; Hofland, L.J. Epidrug-induced upregulation of functional somatostatin type 2 receptors in human pancreatic neuroendocrine tumor cells. *Oncotarget* **2016**, *9*, 14791-14802.
8. Jin, X.F.; Auernhammer, C.J.; Ilhan, H.; Lindner, S.; Nölting, S.; Maurer, J.; Spöttl, G.; Orth, M. Combination of 5-Fluorouracil with Epigenetic Modifiers Induces Radiosensitization, Somatostatin Receptor 2 Expression, and Radioligand Binding in Neuroendocrine Tumor Cells In Vitro. *J Nucl Med* **2019**, *60*, 1240-1246.
9. Wanek, J.; Gaisberger, M.; Beyreis, M.; Mayr, C.; Helm, K.; Primavesi, F.; Jäger, T.; Di Fazio, P.; Jakab, M.; Wagner, A., et al. Pharmacological Inhibition of Class IIA HDACs by LMK-235 in Pancreatic Neuroendocrine Tumor Cells. *Int J Mol Sci* **2018**, *19*, 3128.
10. Torrisani, J.; Hanoun, N.; Laurell, H.; Lopez, F.; Maoret, J.J.; Souque, A.; Susini, C.; Cordelier, P.; Buscail, L. Identification of an upstream promoter of the human somatostatin receptor, hSSTR2, which is controlled by epigenetic modifications. *Endocrinology* **2008**, *149*, 3137-3147.
11. Arvidsson, Y.; Johanson, V.; Pfragner, R.; Wängberg, B.; Nilsson, O. Cytotoxic Effects of Valproic Acid on Neuroendocrine Tumour Cells. *Neuroendocrinology* **2016**, *103*, 578-591.
12. Sun, L.; Qian, Q.; Sun, G.; Mackey, L.V.; Fuselier, J.A.; Coy, D.H.; Yu, C.Y. Valproic acid induces NET cell growth arrest and enhances tumor suppression of the receptor-targeted peptide-drug conjugate via activating somatostatin receptor type II. *J Drug Target* **2016**, *24*, 169-177.
13. Nanau, R.M.; Neuman, M.G. Adverse drug reactions induced by valproic acid. *Clin Biochem* **2013**, *46*, 1323-1338.
14. de Blois, E.; Chan, H.S.; de Zanger, R.; Konijnenberg, M.; Breeman, W.A. Application of single-vial ready-for-use formulation of 111In- or 177Lu-labelled somatostatin analogs. *Appl Radiat Isot* **2014**, *85*, 28-33.
15. Dowdell, K.C.; Pesnicak, L.; Hoffmann, V.; Steadman, K.; Remaley, A.T.; Cohen, J.I.; Straus, S.E.; Rao, V.K. Valproic acid (VPA), a histone deacetylase (HDAC) inhibitor, diminishes lymphoproliferation in the Fas -deficient MRL/lpr(-/-) murine model of autoimmune lymphoproliferative syndrome (ALPS). *Exp Hematol* **2009**, *37*, 487-494.
16. Rouaux, C.; Panteleeva, I.; René, F.; Gonzalez de Aguilar, J.L.; Echaniz-Laguna, A.; Dupuis, L.; Menger, Y.; Boutillier, A.L.; Loeffler, J.P. Sodium valproate exerts neuroprotective effects in vivo through CREB-binding protein-dependent mechanisms but does not improve survival in an amyotrophic lateral sclerosis mouse model. *J Neurosci* **2007**, *27*, 5535-5545.

17. Qian, Y.R.; Lee, M.J.; Hwang, S.; Kook, J.H.; Kim, J.K.; Bae, C.S. Neuroprotection by valproic Acid in mouse models of permanent and transient focal cerebral ischemia. *Korean J Physiol Pharmacol* **2010**, *14*, 435-440.
18. Svensson, J.; Mölne, J.; Forssell-Aronsson, E.; Konijnenberg, M.; Bernhardt, P. Nephrotoxicity profiles and threshold dose values for [177Lu]-DOTATATE in nude mice. *Nucl Med Biol* **2012**, *39*, 756-762.
19. Gezginci-Oktayoglu, S.; Turkyilmaz, I.B.; Ercin, M.; Yanardag, R.; Bolkent, S. Vitamin U has a protective effect on valproic acid-induced renal damage due to its anti-oxidant, anti-inflammatory, and anti-fibrotic properties. *Protoplasma* **2016**, *253*, 127-135.
20. Raza, M.; Al-Bekairi, A.M.; Ageel, A.M.; Qureshi, S. Biochemical basis of sodium valproate hepatotoxicity and renal tubular disorder: time dependence of peroxidative injury. *Pharmacol Res* **1997**, *35*, 153-157.
21. Heidari, R.; Jafari, F.; Khodaei, F.; Shirazi Yeganeh, B.; Niknahad, H. Mechanism of valproic acid-induced Fanconi syndrome involves mitochondrial dysfunction and oxidative stress in rat kidney. *Nephrology (Carlton)* **2018**, *23*, 351-361.
22. Nau, H.; Zierer, R. Pharmacokinetics of valproic acid and metabolites in mouse plasma and brain following constant-rate application of the drug and its unsaturated metabolite with an osmotic delivery system. *Biopharm Drug Dispos* **1982**, *3*, 317-328.
23. Mahmoud, S.H.; Zhou, X.Y.; Ahmed, S.N. Managing the patient with epilepsy and renal impairment. *Seizure* **2020**, *76*, 143-152.

SUPPLEMENTAL FIGURES AND TABLES

SUPPLEMENTAL TABLE 1

	N	Body weight (g)	Tumor volume (mm^3)
No VPA (4 h)	5	34.1 ± 2.6	407.1 ± 201.3
200 mg/kg VPA (4h)	5	34.5 ± 1.7	419.2 ± 195.0
400 mg/kg VPA (4h)	5	35.4 ± 1.2	420.1 ± 197.6
No VPA (4 h, block)	4	34.2 ± 2.3	398.2 ± 221.7
400 mg/kg VPA (4 h, block)	4	35.0 ± 2.4	413.7 ± 236.4
No VPA (8 h)	5	35.7 ± 2.3	425.8 ± 237.7
200 mg/kg VPA (8h)	5	34.1 ± 1.1	419.6 ± 193.4
400 mg/kg VPA (8h)	5	34.6 ± 2.5	398.1 ± 203.8

Table S1. Animal characteristics Number of mice (n), body weight (g) and tumor volume (mm^3) of all experimental groups, measured one day before VPA and [^{177}Lu]Lu-DOTATATE administration. Body weight and tumor volume data are represented as mean ± standard deviation.

SUPPLEMENTAL FIGURE 1

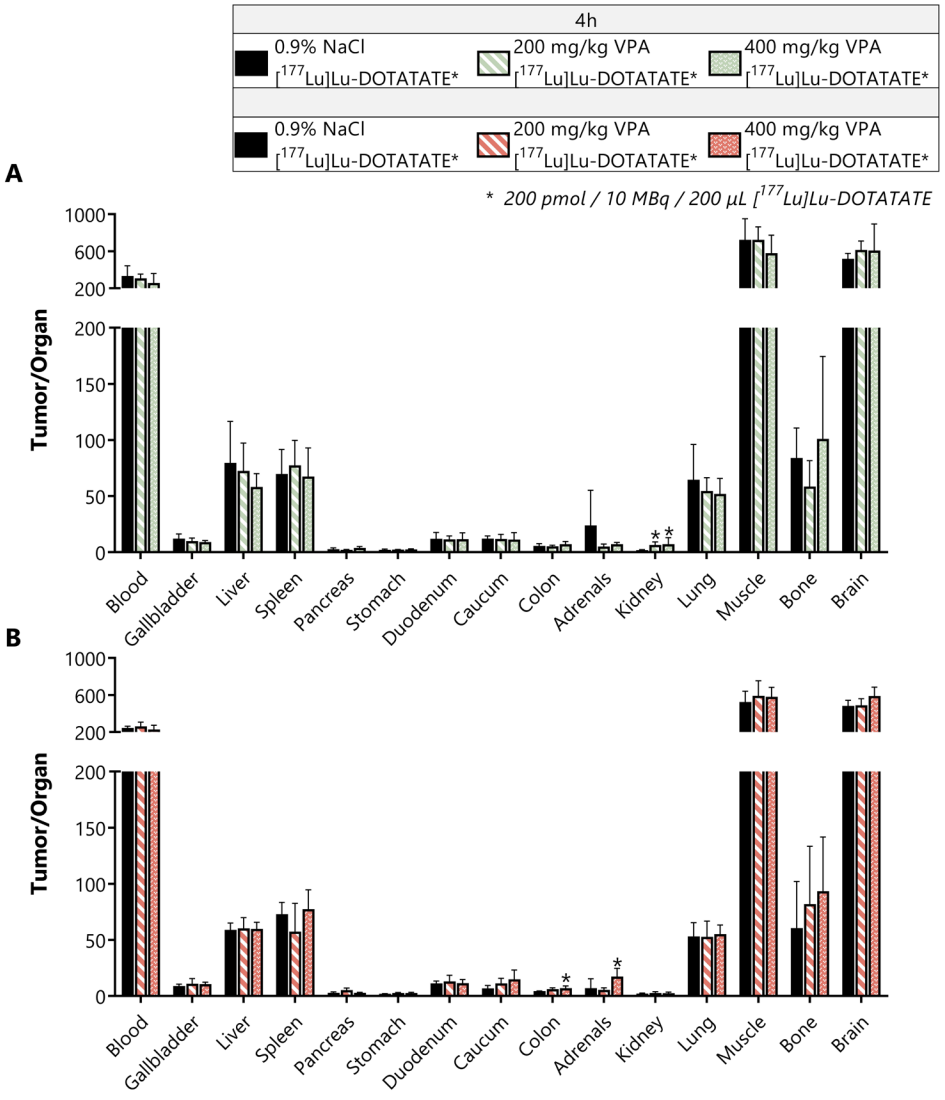

Figure S1. Tumor-to-organ ratios Tumor-to-organ ratios of mice treated with vehicle or VPA (200 mg/kg or 400 mg/kg) four (**A**) or eight (**B**) hours prior to [^{177}Lu]Lu-DOTATATE administration. All data are represented as mean ± standard deviation. * $p < 0.05$; ** $p < 0.01$; ***$p < 0.001$.

SUPPLEMENTAL FIGURE 2

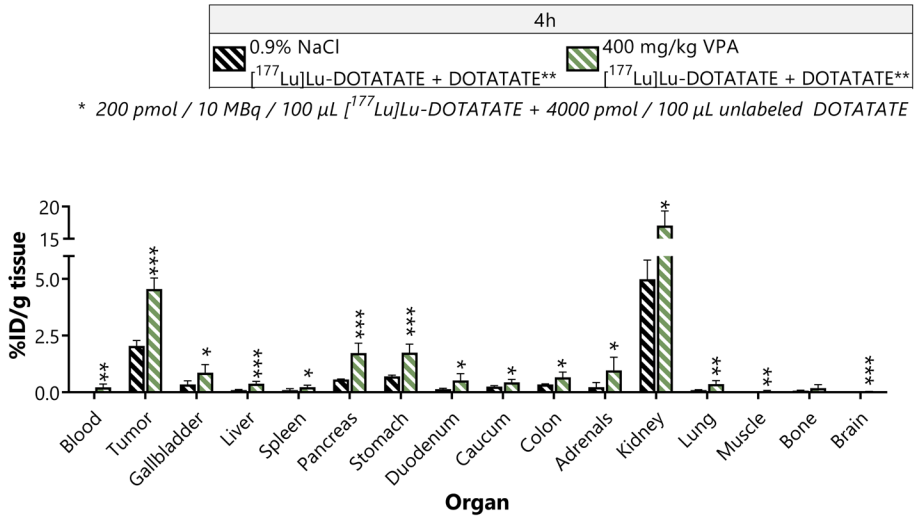

Figure S2. Biodistribution of [^{177}Lu]Lu-DOTATATE after VPA treatment in animals co-injected with an excess of unlabeled DOTATATE (block study) [^{177}Lu]Lu-DOTATATE uptake expressed as percentage injected dose per gram tissue (%ID/g tissue) for vehicle- and 400 mg/kg VPA-treated animals injected four hours prior to [^{177}Lu]Lu-DOTATATE administration in presence of an excess of unlabeled DOTATATE. * $p < 0.05$; ** $p < 0.01$; *** $p < 0.001$.

SUPPLEMENTAL FIGURE 3

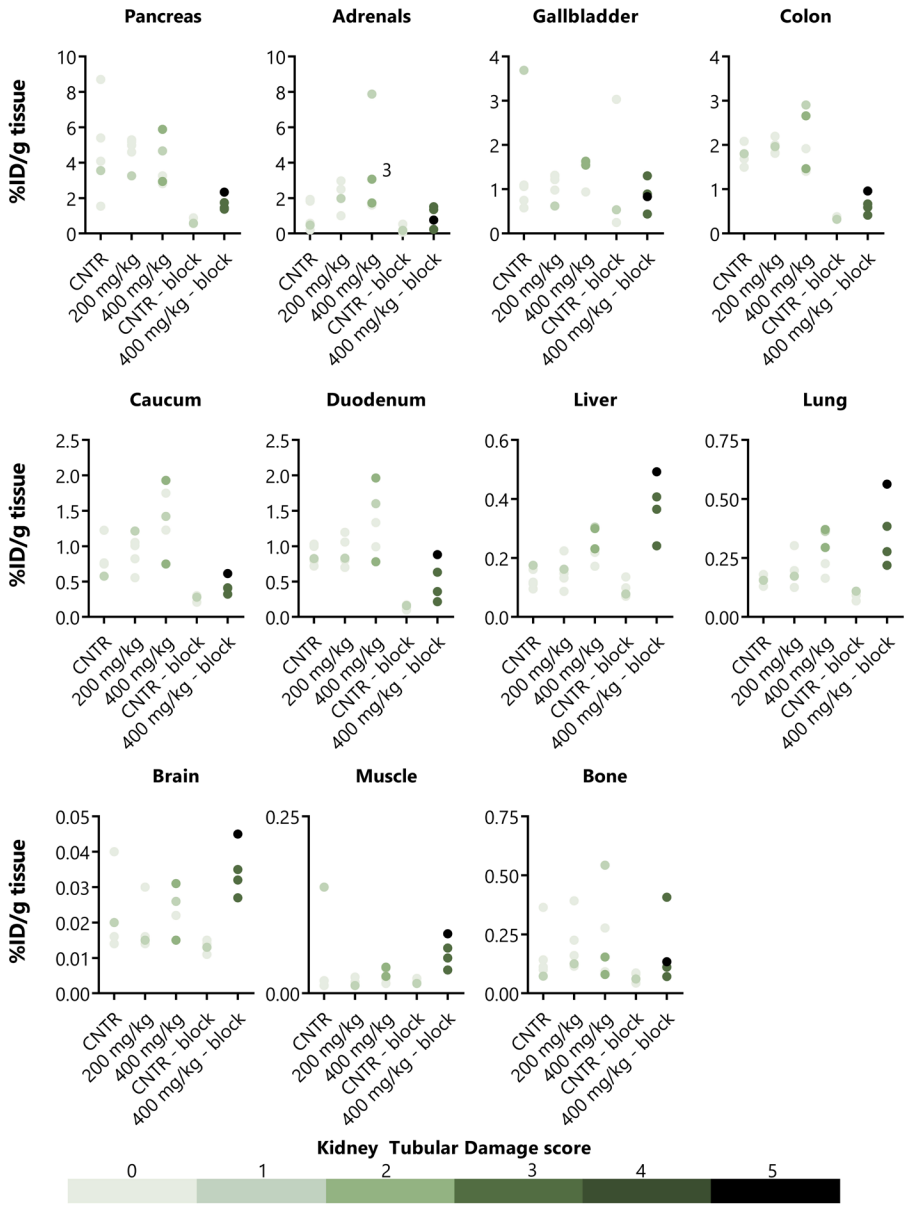

Figure S3. Biodistribution data correlated with the observed renal tubular damage (four hours) The renal tubular damage score of mice receiving VPA four hours prior to [^{177}Lu]Lu-DOTATATE dministration was correlated with the biodistribution data. A color gradient is used to indicate the level of renal tubular damage. Each data point in these graphs represents a mouse. Outliers based on %ID/g tissue are included in this figure.

SUPPLEMENTAL FIGURE 4

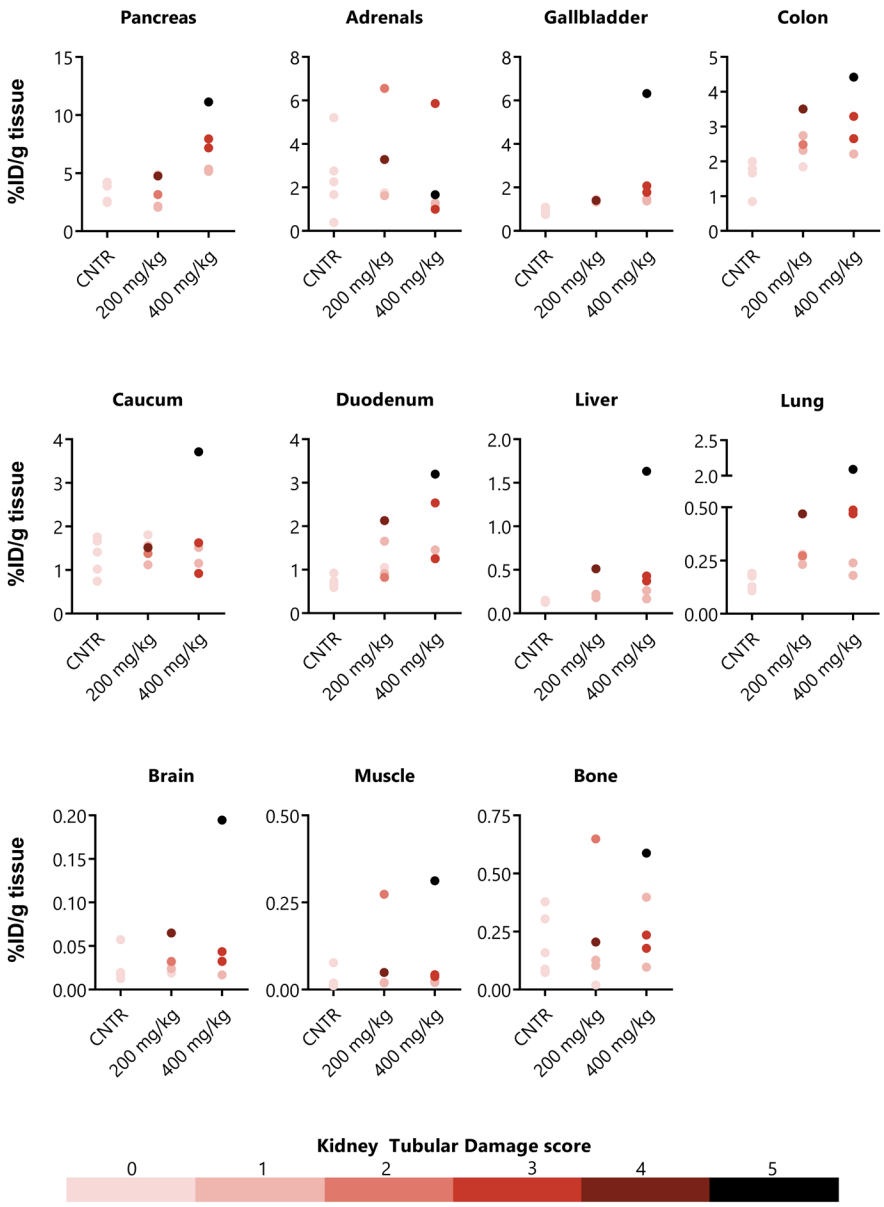

Figure S4. Biodistribution data correlated with the observed renal tubular damage (eight hours) The renal tubular damage score of mice receiving VPA eight hours prior to [^{177}Lu]Lu-DOTATATE administration was correlated with the biodistribution data. A color gradient is used to indicate the level of renal tubular damage. Each data point in these graphs represents a mouse. Outliers based on %ID/g tissue are included in this figure.

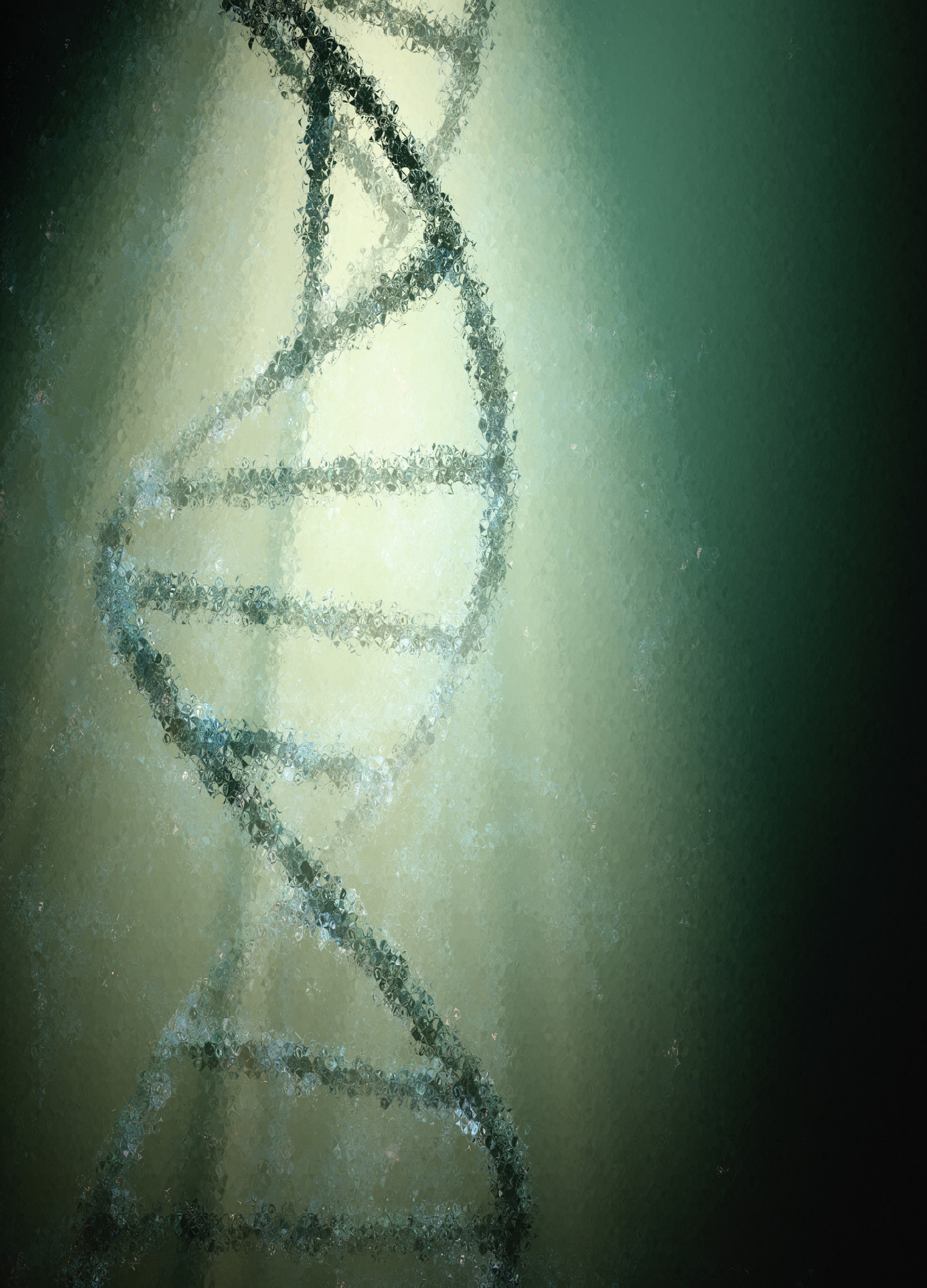

CHAPTER 5

Applying HDACis to Increase SSTR2 Expression and Radiolabeled DOTATATE Uptake: From Cells to Mice

M.J. Klomp[1,2], L. van den Brink[1], P.M. van Koetsveld[2], C.M.A. de Ridder[1,3], D.C. Stuurman[1,3], C.W.G.M. Löwik[1], L.J. Hofland[2], S.U. Dalm[1].

[1] Department of Radiology and Nuclear Medicine, Erasmus MC, 3015 GD Rotterdam, The Netherlands. [2] Department of Internal Medicine, Division of Endocrinology, Erasmus MC, 3015 GD Rotterdam, The Netherlands. [3] Department of Experimental Urology, Erasmus MC, 3015 GD, Rotterdam, The Netherlands.

Submitted in August 2023 to:
Life Sciences

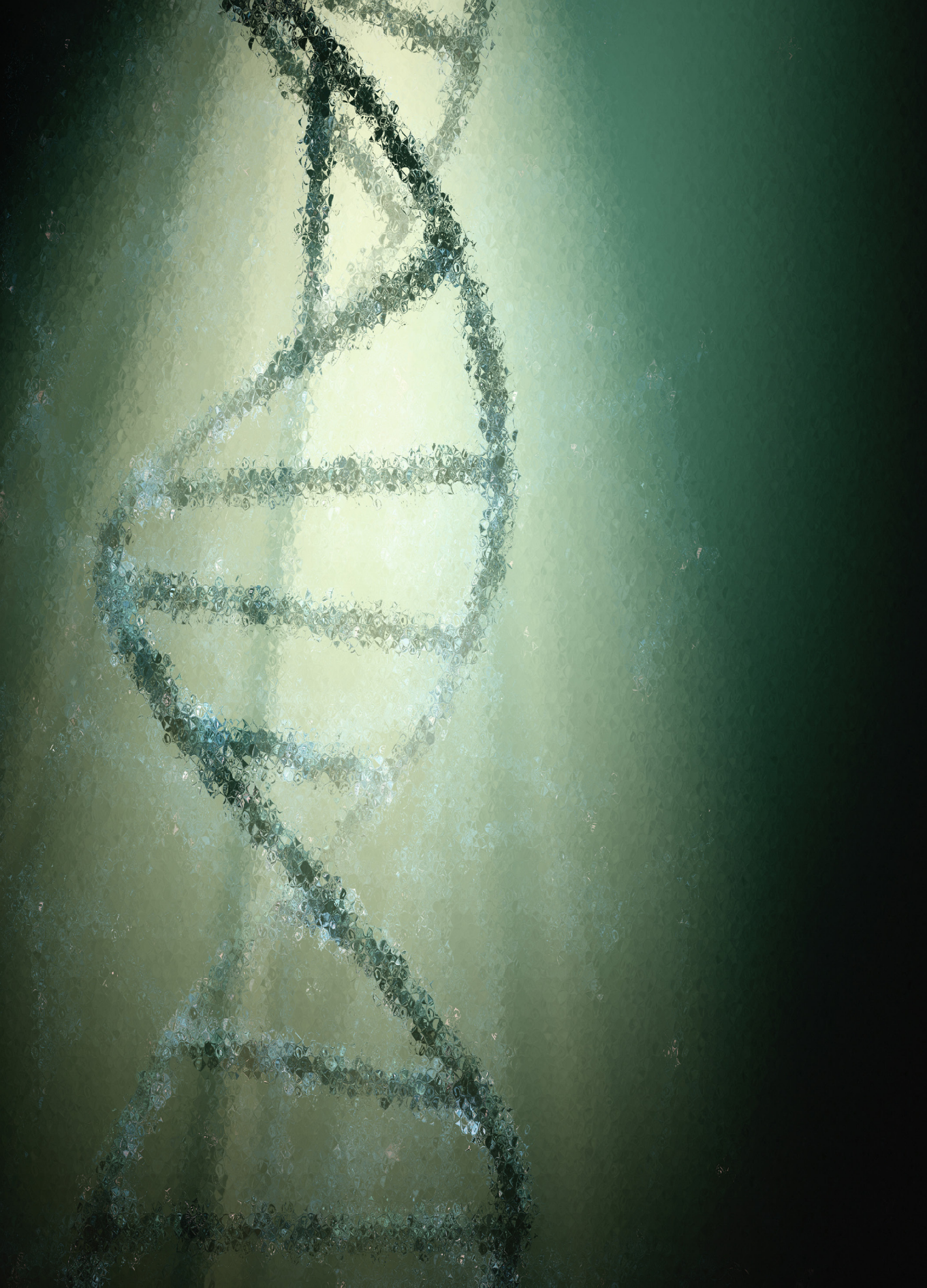

CHAPTER 6

Epigenetic Regulation of SSTR2 Expression in Small Intestinal Neuroendocrine Tumors

Based on[#]:

M.J. Klomp[1,2*], J. Refardt[1,3*], P.M. van Koetsveld[1], C. Campana[1,4], S.U. Dalm[2], F. Dogan[1], M.L.F. van Velthuysen[5], R.A. Feelders[1], W.W. de Herder[1], J. Hofland[1], L.J. Hofland[1].

[1] ENETS Center of Excellence, Department of Internal Medicine, Section of Endocrinology, Erasmus MC Cancer Institute, Rotterdam, The Netherlands. [2] ENETS Center of Excellence, Department of Radiology & Nuclear Medicine, Erasmus Medical Center, Rotterdam, The Netherlands. [3] ENETS Center of Excellence, Department of Endocrinology, University Hospital Basel, Basel, Switzerland. [4] Endocrinology Unit, Department of Internal Medicine and Medical Specialties, School of Medical and Pharmaceutical Sciences, University of Genova, Genova, Italy. [5] ENETS Center of Excellence, Department of Pathology, Erasmus Medical Center, Rotterdam, The Netherlands.

Frontiers in Endocrinology. 2023 May 8;14:1184436

[#] For this chapter, two adjustments were made. For uniformity, SST_2 was changed to SSTR2 and the radiotracer nomenclature has been adjusted. ***** Contributed equally to this work and share first authorship.

ABSTRACT

Background: Somatostatin receptor type 2 (SSTR2) expression is critical for the diagnosis and treatment of neuroendocrine tumors and is associated with improved patient survival. Recent data suggest that epigenetic changes such as DNA methylation and histone modifications play an important role in regulating SSTR2 expression and tumorigenesis of NETs. However, there are limited data on the association between epigenetic marks and SSTR2 expression in small intestinal neuroendocrine tumors (SI-NETs). **Methods**: Tissue samples from 16 patients diagnosed with SI-NETs and undergoing surgical resection of the primary tumor at Erasmus MC Rotterdam were analysed for SSTR2 expression levels and epigenetic marks surrounding the SSTR2 promoter region, i.e. DNA methylation and histone modifications H3K27me3 and H3K9ac. As a control, 13 normal SI-tissue samples were included. **Results**: The SI-NET samples had high SSTR2 protein and mRNA expression levels; a median (IQR) of 80% (70-95) SSTR2-positive cells and 8.2 times elevated SSTR2 mRNA expression level compared to normal SI-tissue (p = 0.0042). In comparison to normal SI-tissue, DNA methylation levels and H3K27me3 levels were significantly lower at five out of the eight targeted CpG positions and at two out of the three examined locations within the SSTR2 gene promoter region of the SI-NET samples, respectively. No differences in the level of activating histone mark H3K9ac were observed between matched samples. While no correlation was found between histone modification marks and SSTR2 expression, SSTR2 mRNA expression levels correlated negatively with DNA methylation within the SSTR2 promoter region in both normal SI-tissue and SI-NETs (p = 0.006 and p = 0.04, respectively). **Conclusion**: SI-NETs have lower SSTR2 promoter methylation levels and lower H3K27me3 methylation levels compared to normal SI-tissue. Moreover, in contrast to the absence of a correlation with SSTR2 protein expression levels, significant negative correlations were found between SSTR2 mRNA expression level and the mean level of DNA methylation within the SSTR2 promoter region in both normal SI-tissue and SI-NET tissue. These results indicate that DNA methylation might be involved in regulating SSTR2 expression. However, the role of histone modifications in SI-NETs remains elusive.

Keywords: DNA methylation, histone modifications, H3K27me3, H3K9ac, epigenetic, SI-NET

1. INTRODUCTION

Recent DNA sequencing studies have shown a very low mutation rate for well-differentiated neuroendocrine tumors (NETs) of all origins [1, 2]. Accordingly, epigenetic changes are likely the principal pathological drivers in the development and progression of NETs, especially in small intestinal NETs (SI-NETs) [3, 4]. Epigenetic changes affect gene expression without changing the DNA sequence and consist of DNA methylation and various histone modifications [3]. DNA methylation is a process in which cytosine residues within CpG islands, which are often located in gene promoter regions, are methylated, resulting in gene silencing. Histone modifications can lead to both transcriptional repression and transcriptional activation, depending on the type of epigenetic mark and its precise location, e.g., the activating histone mark H3K9Ac and the repressive histone mark H3K27me3 [5].

Several studies have uncovered a possible prognostic role for epigenetic marks in SI-NETs. For example, promoter methylation of the *RASSF1A* and *CTNNB1* genes was associated with extensive disease and poor overall survival in SI-NETs [6-8]. Another study was able to identify a panel of 21 genes with an altered DNA methylation profile resulting in changes in gene expression levels in the majority of the SI-NETs, thereby enabling to discriminate SINETs from other gastrointestinal tract malignancies and normal gastrointestinal tissue [2]. Histone modifications also contribute to tumorigenesis, with a small study demonstrating high expression of dimethylation on H3K4 in 93% of primary intestinal neuroendocrine carcinomas [9].

In accordance with the importance of epigenetic changes in tumorigenesis of NETs, research has also been focused on epigenetic drugs to improve diagnosis and therapy of NETs. As no genetic mutations in the somatostatin receptor subtype 2 (SSTR2) gene have been described, it has been suggested that the epigenetic machinery is strongly involved in regulating SSTR2 expression. SSTR2 is the most important molecular marker for NETs as functional imaging with radiolabeled somatostatin analogues is crucial for tumor staging. Furthermore, sufficient SSTR2 expression is the key element for treatment with unlabeled or radiolabeled somatostatin analogues [10]. Several *in vitro* and *in vivo* studies showed an increase in SSTR2 expression levels by decreasing DNA methylation and augmenting histone acetylation levels of the SSTR2 gene promoter region in human NET cell lines [11-17]. Although the majority of these studies have been performed using pancreatic NET cell lines, similar effects were also observed in the SI-NET cell line GOT1. Accordingly, one would expect correlations between epigenetic marks and SSTR2 expression levels in SI-NET tissues, i.e. inverse correlations of both DNA methylation levels and/or inhibiting histone marks with SSTR2 expression levels, and a positive correlation of SSTR2 expression with activating histone marks near the SSTR2 promoter region. However, so far, no such data have been described on SI-NETs. Therefore, the aim of this study was to investigate the role of DNA methylation as well as repressive and activating histone modifications (i.e. H3K27me3 and H3K9ac, respectively) in the regulation of SSTR2 expression of SI-NETs.

2. METHODS

2.1. SAMPLES

The selected samples consisted of fresh frozen tissue (FFT) material and formalin-fixed paraffin-embedded (FFPE) material of patients diagnosed with SI-NETs who underwent surgical resection of the primary tumor at the Erasmus MC Rotterdam, the Netherlands, and for which the diagnostic evaluation had been completed. Patients could refuse the use of their material, however, no specific consent was needed as long as patient anonymity is guaranteed. In total, 21 SI-NET and 13 normal SI-tissues samples were collected for evaluation. Whereas FFPE material was used for SSTR2 immunohistochemistry, FFT material was used for all other analyses. Prior to analyses, FFT was cut according to standard protocol, and hematoxylin and eosin staining was performed for quality control. Based on this staining, tumor cell content was measured by counting the number of cell nuclei and, subsequently, the tissues with less than 50% tumor cell content (n = 5) were excluded. Of the remaining 16 SI-NET samples, 9 had matching normal SI-tissue available.

2.2. IMMUNOHISTOCHEMISTRY

SSTR2 immunostaining was performed on 4 µm thick whole slide sections from FFPE embedded tissue blocks, on a validated and accredited automated slide stainer (Benchmark ULTRA System VENTANA Medical Systems, Tucson, AZ, USA) according to the manufacturer's instructions. Briefly, following deparaffinization and heat-induced antigen retrieval (pH 9.0), the tissue samples were incubated with rabbit anti-SST2A antibody (Biotrend; NB-49- 015-1ML, dilution 1:25) for 32 min at 37°C, followed by Optiview detection (#760-500 & #760-700, Ventana). Counterstain was done by hematoxylin II for 12 min and a blue colouring reagent for 8 min. Stained slides were scanned with the NanoZoomer 2.0 HT (Hamamatsu Photonics, Hamamatsu City, Japan) and both the percentage of SSTR2 positive cells and the intensity per area (intensity/area) were assessed using the CellProfiler software (version 4.0.7, www.cellprofiler.org) as previously described [18].

2.3. SSTR2 mRNA ANALYSIS

Tissues were lysed and incubated with Dynabeads oligo$(dT)_{25}$ (Invitrogen, Breda, The Netherlands) to isolate poly-A^+ mRNA, as described previously [17]. H_2O (23 µL) was added for elution, and 10 µL poly-A+ mRNA was used in the next steps. Poly-A+ mRNA was converted into cDNA using the commercial RevertAid First Strand cDNA synthesis kit (Thermo Scientific, Breda, Netherlands). cDNA was also prepared without the addition of RevertAid Reverse Transcriptase to exclude possible DNA contamination. Subsequently, samples were diluted by adding 180 µL H_2O. Afterwards 5 µL sample was mixed with 7.5 µL Taqman Universal PCR mastermix (Applied Biosystems, Breda, Netherlands) supplemented with primers and probes. SSTR2 expression was determined relative to the three housekeeping genes (HKGs) GUSB, HPRT1 and ACTB. Primer information can be found in Supplemental Table 1. For

analysis, the QuantStudio 7 Flex RT-qPCR system with QuantStudio Real-Time PCR software v1.5 was used. The number of copies for SSTR2 and all HKGs was calculated by the efficiency factor to the power of ΔCt (i.e., 40 minus measured Ct). Subsequently, the relative SSTR2 expression was calculated by dividing the number of SSTR2 copies by the geometric mean of all HKGs.

2.4. DNA ISOLATION, BISULFITE TREATMENT AND PYROSEQUENCING

DNA was isolated from the FFT samples according to protocol of the Genome Wizard DNA isolation kit (Promega Corporation, Madison, USA). For bisulfite conversion 1000 ng DNA was used with the Zymo Research EZ DNA Zymo kit according to the manufacturer's protocol (Zymo Research Corporation, Irvine, USA). Primer design was done with PyroMark Assay Design 2.0 (Qiagen N.V., Venlo, Netherlands). Bisulfite treated DNA was aliquoted and stored at -20°C. Pyrosequencing of bisulfite treated DNA was performed with the primers listed in Supplemental Table 1. PCR products were analysed on the PyroMark Q24 (Qiagen) with PyroMark Gold Q24 reagents (Qiagen) according to manufacturer's protocol. The eight CpG sites present in the SSTR2 promoter region were targeted, as these loci had been shown to be involved in the regulation of SSTR2 expression [19].

2.5. CHROMATIN IMMUNOPRECIPITATION

Chromatin immunoprecipitation (CHIP) analysis was performed on 11 SI-NET samples and 13 normal SI-tissue samples, of which seven samples were matched, measuring H3K27me3 and H3K9ac enrichment at three positions of the SSTR2 promoter region, i.e. the transcription start site (TSS) and two regions upstream of this location, allocated as -2 and -1. The fold-enrichment was calculated using the following formula: *efficiency factor* ^ ($CT_{\text{input adjusted}} - CT_{\text{immunoprecipitation}}$) x 100%, and subsequently divided by the fold-enrichment obtained with the IgG antibody. The used efficacy factors are 1.96, 1.99 and 2.00 for -2, -1 and TSS, respectively. A detailed protocol can be found in the Supplemental Appendix.

2.6. STATISTICS

Categorical data are presented as frequencies and percentages; quantitative data are reported as mean ± standard deviation (SD) or as median and interquartile range (IQR). To test for normality, the D'Agostino and Pearson test was used. For differences between SSTR2 expression levels in SI-NET and normal SI-tissue, a paired parametric t-test was performed. For differences in epigenetic marks, a Friedman test (matched, non-parametric One-Way ANOVA) was performed with a Dunn's multiple comparisons test. For correlation analysis, the data was log transformed to stabilize the variance, followed by Spearman correlation analysis. To test for uniform epigenetic modifications across the SSTR2 promoter region, a Spearman correlation matrix was performed on log-transformed data, using an adjusted p-value based on a Bonferroni correction. Differences were considered statistically significant at $p < 0.05$. Statistical evaluation was performed using GraphPad Prism version 9.0.0 (GraphPad Software).

3. RESULTS

3.1. PATIENT CHARACTERISTICS

Of the included 16 SI-NET samples, 9 (56%) came from male patients. Median age (IQR) was 61 years (54-66) at the time of tumor resection. The majority of samples were grade 1 tumors (12, 75%), while the remaining samples were low-grade 2 tumors. Nine (56%) patients had stage IV disease with lymph node metastases in 13 (81%), liver metastases in 8 (50%), bone metastases in 2 (13%) and peritoneal metastases in 4 (25%) patients. Ten (63%) patients suffered from hormonal syndrome, with 4 (25%) patients being pretreated with somatostatin analogues of which 2 (13%) were also treated with peptide receptor radionuclide therapy using [^{177}Lu]Lu-DOTATATE.

3.2. IMMUNOHISTOCHEMISTRY AND mRNA ANALYSES

Overall, the SI-NET samples showed high SSTR2 expression, with a median (IQR) percentage of positive cells of 80% (70-100) and an intensity/area of 0.262 (0.192-0.424) based on SSTR2 IHC, and a SSTR2/HKG ratio of 0.10 (0.05-0.14) based on the RT-qPCR analysis, Figures 1A–D. Results for one sample had to be excluded from SSTR2 IHC quantification due to insufficient eosinophilic counter-staining, hampering automated analysis. Analysis of the nine matched samples showed that SSTR2 mRNA expression levels of the SI-NET tissues were on average 8.2 times higher compared to that of normal SI-tissue with a median (IQR) SSTR2/HKG ratio of 0.05 (0.02-0.10) and 0.007 (0.005-0.009), p = 0.0042, for SI-NETs and normal SI-tissue, respectively, Figure 1E. No underlying factor such as gender, grade or stage for the wide range in expression could be identified. Also, no significant differences in SSTR2 mRNA or protein expression levels between treatment-naïve versus pretreated patients were observed (data not shown).

3.3. EPIGENETIC PROFILES OF SI-NET SAMPLES

Using the matched tissue samples, it was demonstrated that the epigenetic profiles of SI-NET tissues differ compared to normal SI tissues. In general, DNA methylation levels of the SSTR2 gene promoter of the SI-NET samples were relatively low and significantly lower at five out of the eight targeted CpG positions compared to what was observed in the normal SI-tissue, Figure 2A. For SI-NET samples, we observed a uniform DNA methylation across the SSTR2 promoter region, with each location, except position –1, showing a significant positive correlation with at least three other locations (Supplemental Table 2). Interestingly, position -1 showed a significant positive correlation with four positions in normal SI-tissue, whereas location 6 was not characterized by any significant correlation (Supplemental Table 3).

In addition to DNA methylation of the SSTR2 promoter region, differences were also found in histone methylation profiles. The enrichment of repressing epigenetic mark H3K27me3 was significantly lower in two out of the three locations in SI-NET tissue compared to the matched

normal SI-tissue, Figure 2B. No differences in the activating histone mark H3K9ac position were observed between matched samples, Figure 2C. Similar to the pattern observed for the DNA methylation profile, a uniform epigenetic profile was also demonstrated for the histone marks, i.e. a significant positive correlation between -2, -1 and TSS for both histone methylation and acetylation, Supplemental Tables 4, 5.

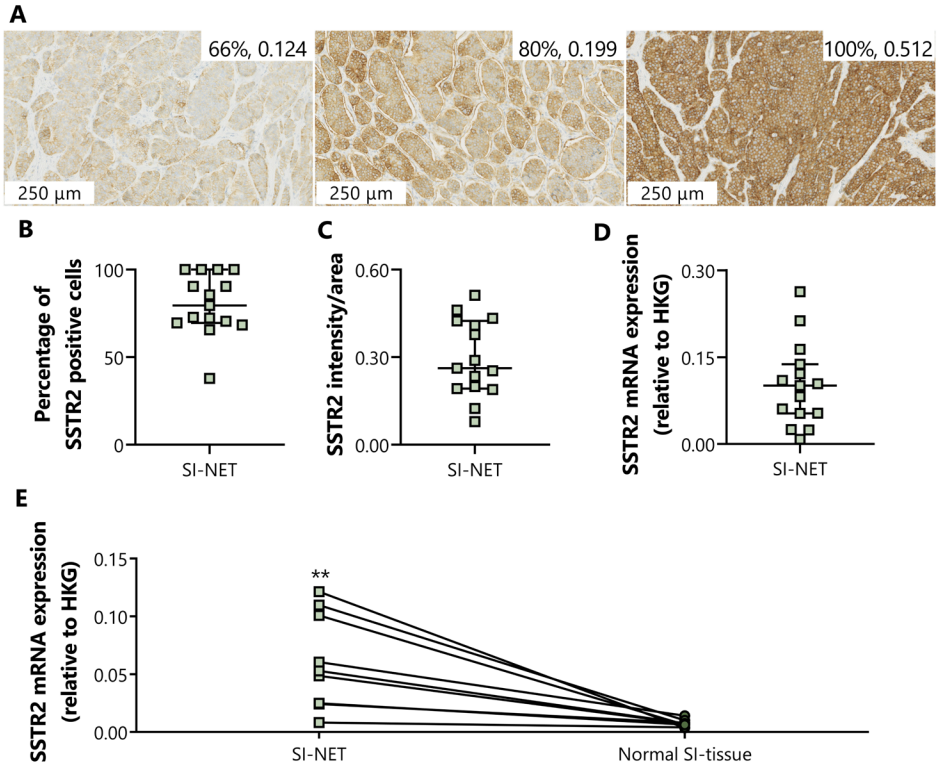

Figure 1. (**A**) Representative images of immunohistochemical SSTR2 staining. The numbers in the right upper corner represent the number of SSTR2 positive cells and the SSTR2 intensity/area. (**B**) The percentage of SSTR2 positive cells, (**C**) the SSTR2 intensity/area and (**D**) SSTR2 mRNA expression levels measured in small intestinal neuroendocrine tumor tissue, and (**E**) SSTR2 mRNA expression levels in small intestinal neuroendocrine tumor samples compared to paired normal small intestinal tissue. Data in (**B–D**) are presented as median with interquartile ranges. ** $p < 0.01$. SI-NET, small intestinal neuroendocrine tumor; normal SI-tissue, normal small intestinal tissue; SSTR2, somatostatin receptor subtype 2; HKG, housekeeping genes.

3.4. EPIGENETIC PROFILES AND SSTR2 EXPRESSION

To further evaluate the role of the epigenetic marks in regulating SSTR2 expression, the epigenetic modifications were correlated with the percentage of SSTR2 positive cells, the SSTR2 intensity/area and SSTR2 mRNA expression levels. SSTR2 mRNA expression levels correlated negatively with the mean level of DNA methylation of the SSTR2 promoter in the normal SI-tissue samples ($p = 0.006$, Figure 3A), reaching statistical significance (adjusted p-

value threshold of 0.006) for the individual CpG positions 1, 2 and 4 (rS = -0.79, -0.81 and -0.74; p = 0.002, 0.001 and 0.005, respectively). For the SI-NET samples, a statistically significant negative correlation was also found for SSTR2 mRNA expression levels and the mean level of DNA methylation of the SSTR2 promoter (p = 0.04), Figure 3B. However, using the adjusted p-value threshold of 0.006, no individual location showed a significant correlation, but a trend towards negative correlations was observed for location 1, 3, 4 and 5 (rS = -0.59, -0.58, -0.52 and –0.61; p = 0.019, 0.019, 0.040 and 0.013, respectively). No statistically significant correlations between the mean level of DNA methylation and the number of SSTR2 positive cells (p = 0.41) nor SSTR2 intensity/area (p = 0.21) were demonstrated in SI-NET tissues (Supplemental Figure 1).

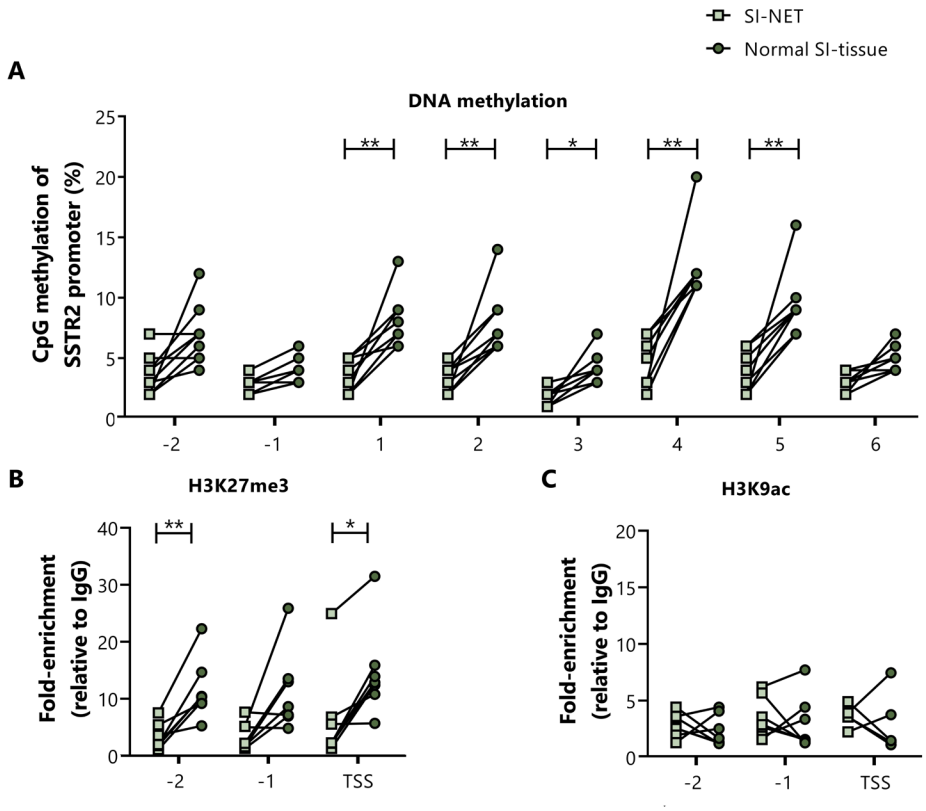

Figure 2. (**A**) Percentage of DNA methylation levels at different CpG positions of the SSTR2 gene promoter of small intestinal neuroendocrine tumor samples compared to matching normal small intestinal tissue. (**B, C**) Enrichment of H3K27me3 and H3K9ac on three locations in the SSTR2 promoter region (i.e. -2, -1 and TSS) in small intestinal neuroendocrine tumor samples compared to the matching normal small intestinal tissue. Data is presented as fold enrichment relative to IgG controls and log-transformed. * p < 0.05, ** p < 0.01. SI-NET, small intestinal neuroendocrine tumor; normal SI-tissue, normal small intestinal tissue; SSTR2, somatostatin receptor subtype 2.

A similar correlation analysis was performed with the mean level of histone mark enrichment on the three examined locations within the SSTR2 promoter region. In contrast to the

correlation found between the level of DNA methylation and SSTR2 mRNA expression in both normal SI-tissue and SI-NETs, no correlations were found in SI-NET samples between histone mark enrichment and SSTR2 mRNA expression levels (p = 0.33 and p = 0.43 for H3K27me3 and H3K9ac, respectively), Figure 4, nor with the percentage of SSTR2 positive cells (p = 0.54 and p = 0.89 for H3K27me3 and H3K9ac, respectively, Supplemental Figure 2) or the SSTR2 intensity/ area (p = 0.19 and p = 0.71 for H3K27me3 and H3K9ac, respectively, Supplemental Figure 2). Whereas correlations using the mean level of enrichment were lacking, correlations were also not found focusing for each individual location.

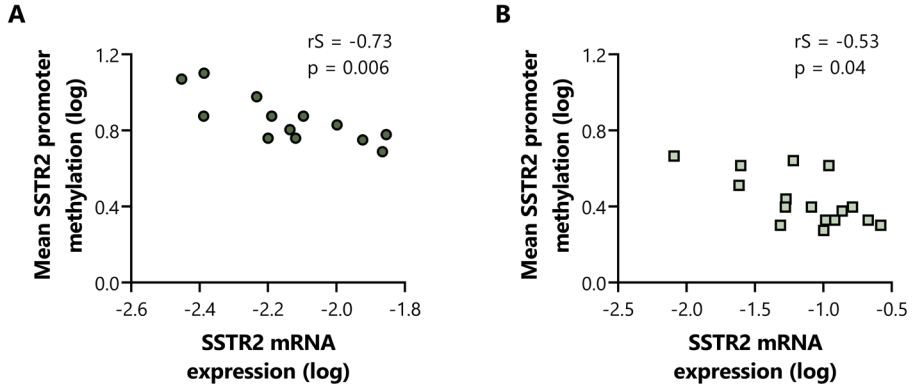

Figure 3. Correlation of the mean level of DNA methylation at CpG positions in the SSTR2 promoter region with SSTR2 mRNA expression levels in (**A**) normal small intestinal tissue and (**B**) small intestinal neuroendocrine tumor samples. Data are log-transformed. rS, Spearman r; SSTR2, somatostatin receptor subtype 2.

4. DISCUSSION

The aim of the current study was to investigate the association between DNA methylation, histone modifications and SSTR2 expression in SI-NET tissues. We showed that the SI-NET tissues had lower DNA and histone methylation levels compared to normal SI-tissue. Moreover, significant negative correlations were found between SSTR2 mRNA expression level and DNA methylation levels within the SSTR2 promoter region for both normal SI-tissue and SI-NETs.

Our results confirm that DNA methylation may play a role in SI-NET tumorigenesis. DNA methylation levels are significantly lower in the SI-NET samples compared to the adjacent normal SI-tissue, suggesting tumor induced changes in the epigenetic profile of the SSTR2 promoter region. In addition, we were able to show a clear negative correlation between the mean level of DNA methylation within the SSTR2 promoter and SSTR2 mRNA expression level in SINETs. Although significance was not reached after correcting for multiple testing, locations 1, 3, 4 and 5 seemed to be mostly involved in regulating SSTR2 expression. It cannot be excluded that a higher sample size might have led to significant results in one or multiple of these individual locations. Moreover, the heterogeneous character of SI-NET tissues could

have complicated the analysis [20]. The observed negative correlation is in line with previous research using NET cell lines showing compelling results demonstrating upregulation of SSTR2 expression following epigenetic treatment, and more specifically, DNA methyltransferase inhibitors [12, 21]. Moreover, a significant inverse correlation was found between DNA methylation – measured within an CpG island containing an upstream TSS for SSTR2 – and SSTR2 mRNA expression levels in a panel of 11 cell lines [19]. We did not only demonstrate a correlation between DNA methylation and SSTR2 mRNA in SI-NETs, a correlation was also found in normal SI-tissue. Surprisingly, location -1 was not correlated with any other positions in SI-NETs, whereas this was position 6 in normal SI-tissue. It is therefore possible that the epigenetic machinery responsible for DNA methylation is activated differently in normal SI-tissue and SI-NET tissue. Nevertheless, it should be considered that for a true comparison enterochromaffin cells should have been analysed instead of the normal SI-tissue.

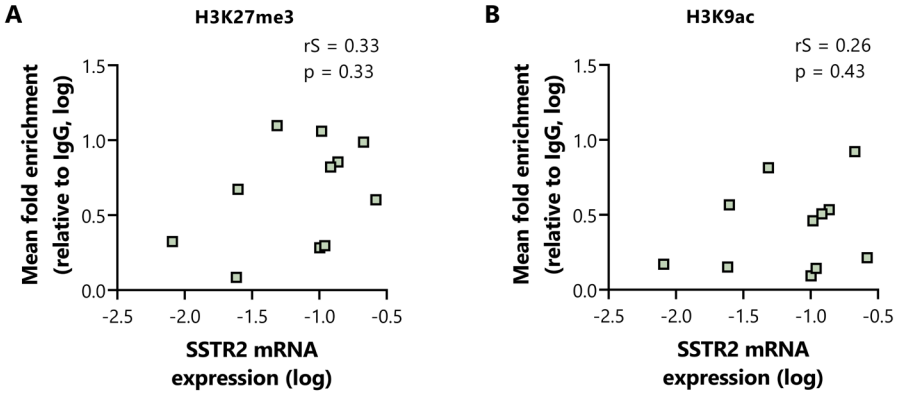

Figure 4. Correlation of SSTR2 mRNA expression levels with the fold enrichment of (**A**) H3K27me3 and (**B**) H3K9ac calculated as the mean enrichment on three locations within the SSTR2 promoter (i.e. -2, -1 and TSS) in the small intestinal neuroendocrine tumor samples. All data are presented as fold enrichment relative to IgG and data are log-transformed. rS, Spearman r; SSTR2, somatostatin receptor subtype 2.

While a correlation between DNA methylation and SSTR2 mRNA expression was found in the SI-NET tissues, this correlation was not found between DNA methylation levels and the percentage of SSTR2 positive cells, nor with the intensity/area. This might be due to the analyses performed; whereas mRNA and DNA methylation levels were determined based on the entire tumoral tissue including other cell types (e.g. fibrotic cells, endothelial cells), quantification of the SSTR2 IHC was purely based on the analysis of tumor cells. Also, while mRNA and DNA methylation were both studied from FFT, protein expression was quantified on FFPE samples, possibly introducing a sample bias. It would therefore have been of interest to perform western blot analysis on FFT material as well. Unfortunately, this analysis could not be performed due to the scarcity of tissue, and no statement can be made about possible correlations.

In contrast to the correlations found between SSTR2 mRNA and DNA methylation, no correlations were found between two widely studied histone modifications, i.e. activating (H3K9Ac) and repressive (H3K27me3) histone marks, and SSTR2 expression levels. Possibly other epigenetic histone modifications are involved that can alter SSTR2 gene expression, e.g. histone methylation at H3K9me2/3 (repressing), or at H3K4me1/2/3 and H3K36me3 (activating). Moreover, several lysine residues can be acetylated resulting in activation of gene transcription [22]. Accordingly, the use of antibodies for panacetylation on either histone 3 or histone 4 might be of interest, thereby evaluating histone modifications in a broader view.

Research is currently focusing on upregulating SSTR2 in NETs to improve diagnosis and treatment, but the available clinical data is ambiguous. Based on our findings, we would expect epigenetic drugs targeting the DNA methylation profile to be more effective in upregulating SSTR2 than drugs targeting the histone modifications. However, one trial involving nine patients with NETs from different origin and low baseline SSTR2 expression showed no SSTR2 upregulation upon epigenetic treatment with DNA methyltransferase inhibitor hydralazine combined with histone deacetylase (HDAC) inhibitor valproic acid [23]. Meanwhile, another small clinical trial involving five well-differentiated SINET patients with sufficient SSTR2 expression showed a minor but significant increase in radiolabelled somatostatin analogue uptake after treatment with the HDAC inhibitor vorinostat [24]. As discussed above, different histone marks could play a role in SSTR2 upregulation, thereby enabling SSTR2 upregulation in response to vorinostat. The opposing outcomes of these two clinical studies could also be due to differences in intratumoral drug levels or differences in tumor biology between NETs with low and high SSTR2 expression [25].

Our current study only focused on SI-NETs, and it is therefore unknown if our findings would have been similar in NETs of other origins. In line with our results, a correlation was found between the level of DNA methylation in the SSTR2 promoter and SSTR2 expression levels in pancreatic NETs [26]. In contrast, the direct role of histone marks in regulation SSTR2 in pancreatic NETs remains unclear. *In vitro* experiments using pancreatic NET cell lines, e.g. BON-1 and QGP-1, showed convincing effects of HDAC inhibitors on SSTR2 expression [17, 21, 23]. Moreover, elevated HDAC expression levels have been described in pancreatic NET tissues [27], together suggesting a possible role of histone acetylation in regulating SSTR2 expression in pancreatic NETs. However, despite these data, evidence for a direct association is lacking.

In conclusion, our study showed that well-differentiated SINETs have lower DNA and histone methylation levels on the SSTR2 promoter region compared to normal SI-tissue. A statistically significant correlation between SSTR2 mRNA expression and DNA methylation within the SSTR2 promoter region was observed in both normal SI-tissue and SI-NETs. Thus, while epigenetic factors seem to play an important role in SI-NET tumorigenesis, it is mainly DNA methylation that seems to be involved in regulating SSTR2. However, the role of histone modifications in regulating SSTR2 expression remains to be further elucidated.

ACKNOWLEDGMENTS

The authors thank the Colleagues of the Pathology Department (Erasmus Medical Center, Rotterdam, Netherlands) for performing the SSTR2 staining.

REFERENCES

1. Priestley, P.; Baber, J.; Lolkema, M.P.; Steeghs, N.; de Bruijn, E.; Shale, C.; Duyvesteyn, K.; Haidari, S.; van Hoeck, A.; Onstenk, W., et al. Pan-cancer whole-genome analyses of metastatic solid tumours. *Nature* **2019**, *575*, 210-216.
2. Karpathakis, A.; Dibra, H.; Pipinikas, C.; Feber, A.; Morris, T.; Francis, J.; Oukrif, D.; Mandair, D.; Pericleous, M.; Mohmaduvesh, M., et al. Prognostic Impact of Novel Molecular Subtypes of Small Intestinal Neuroendocrine Tumor. *Clin Cancer Res* **2016**, *22*, 250-258.
3. Di Domenico, A.; Wiedmer, T.; Marinoni, I.; Perren, A. Genetic and epigenetic drivers of neuroendocrine tumours (NET). *Endocr Relat Cancer* **2017**, *24*, R315-R334.
4. Scarpa, A. The landscape of molecular alterations in pancreatic and small intestinal neuroendocrine tumours. *Ann Endocrinol (Paris)* **2019**, *80*, 153-158.
5. Klomp, M.J.; Dalm, S.U.; de Jong, M.; Feelders, R.A.; Hofland, J.; Hofland, L.J. Epigenetic regulation of somatostatin and somatostatin receptors in neuroendocrine tumors and other types of cancer. *Rev Endocr Metab Disord* **2021**, *22*, 495-510.
6. Zhang, H.Y.; Rumilla, K.M.; Jin, L.; Nakamura, N.; Stilling, G.A.; Ruebel, K.H.; Hobday, T.J.; Erlichman, C.; Erickson, L.A.; Lloyd, R.V. Association of DNA methylation and epigenetic inactivation of RASSF1A and beta-catenin with metastasis in small bowel carcinoid tumors. *Endocrine* **2006**, *30*, 299-306.
7. Fotouhi, O.; Adel Fahmideh, M.; Kjellman, M.; Sulaiman, L.; Hoog, A.; Zedenius, J.; Hashemi, J.; Larsson, C. Global hypomethylation and promoter methylation in small intestinal neuroendocrine tumors: an in vivo and in vitro study. *Epigenetics* **2014**, *9*, 987-997.
8. Choi, I.S.; Estecio, M.R.; Nagano, Y.; Kim, D.H.; White, J.A.; Yao, J.C.; Issa, J.P.; Rashid, A. Hypomethylation of LINE-1 and Alu in well-differentiated neuroendocrine tumors (pancreatic endocrine tumors and carcinoid tumors). *Mod Pathol* **2007**, *20*, 802-810.
9. Magerl, C.; Ellinger, J.; Braunschweig, T.; Kremmer, E.; Koch, L.K.; Holler, T.; Buttner, R.; Luscher, B.; Gutgemann, I. H3K4 dimethylation in hepatocellular carcinoma is rare compared with other hepatobiliary and gastrointestinal carcinomas and correlates with expression of the methylase Ash2 and the demethylase LSD1. *Hum Pathol* **2010**, *41*, 181-189.
10. Refardt, J.; Hofland, J.; Kwadwo, A.; Nicolas, G.P.; Rottenburger, C.; Fani, M.; Wild, D.; Christ, E. Theranostics in neuroendocrine tumors: an overview of current approaches and future challenges. *Rev Endocr Metab Disord* **2021**, *22*, 581-594.
11. Veenstra, M.J.; van Koetsveld, P.M.; Dogan, F.; Farrell, W.E.; Feelders, R.A.; Lamberts, S.W.J.; de Herder, W.W.; Vitale, G.; Hofland, L.J. Epidrug-induced upregulation of functional somatostatin type 2 receptors in human pancreatic neuroendocrine tumor cells. *Oncotarget* **2016**, *9*, 14791-14802.
12. Taelman, V.F.; Radojewski, P.; Marincek, N.; Ben-Shlomo, A.; Grotzky, A.; Olariu, C.I.; Perren, A.; Stettler, C.; Krause, T.; Meier, L.P., et al. Upregulation of Key Molecules for Targeted Imaging and Therapy. *J Nucl Med* **2016**, *57*, 1805-1810.
13. Wanek, J.; Gaisberger, M.; Beyreis, M.; Mayr, C.; Helm, K.; Primavesi, F.; Jager, T.; Di Fazio, P.; Jakab, M.; Wagner, A., et al. Pharmacological Inhibition of Class IIA HDACs by LMK-235 in Pancreatic Neuroendocrine Tumor Cells. *Int J Mol Sci* **2018**, *19*.
14. Jin, X.F.; Auernhammer, C.J.; Ilhan, H.; Lindner, S.; Nolting, S.; Maurer, J.; Spottl, G.; Orth, M. Combination of 5-Fluorouracil with Epigenetic Modifiers Induces Radiosensitization, Somatostatin Receptor 2 Expression, and Radioligand Binding in Neuroendocrine Tumor Cells In Vitro. *J Nucl Med* **2019**, *60*, 1240-1246.
15. Guenter, R.; Aweda, T.; Carmona Matos, D.M.; Jang, S.; Whitt, J.; Cheng, Y.Q.; Liu, X.M.; Chen, H.; Lapi, S.E.; Jaskula-Sztul, R. Overexpression of somatostatin receptor type 2 in neuroendocrine tumors for improved Ga68-DOTATATE imaging and treatment. *Surgery* **2020**, *167*, 189-196.
16. Guenter, R.E.; Aweda, T.; Carmona Matos, D.M.; Whitt, J.; Chang, A.W.; Cheng, E.Y.; Liu, X.M.; Chen, H.; Lapi, S.E.; Jaskula-Sztul, R. Pulmonary Carcinoid Surface Receptor Modulation Using Histone Deacetylase Inhibitors. *Cancers (Basel)* **2019**, *11*.

17. Klomp, M.J.; Dalm, S.U.; van Koetsveld, P.M.; Dogan, F.; de Jong, M.; Hofland, L.J. Comparing the Effect of Multiple Histone Deacetylase Inhibitors on SSTR2 Expression and [(111)In]In-DOTATATE Uptake in NET Cells. *Cancers (Basel)* **2021**, *13*.
18. Campana, C.; van Koetsveld, P.M.; Feelders, R.A.; de Herder, W.W.; Iyer, A.M.; van Velthuysen, M.F.; Veenstra, M.J.; van den Dungen, E.S.R.; Franck, S.E.; Ferone, D., et al. Digital quantification of somatostatin receptor subtype 2a immunostaining: a validation study. *Eur J Endocrinol* **2022**, *187*, 399-411.
19. Torrisani, J.; Hanoun, N.; Laurell, H.; Lopez, F.; Maoret, J.J.; Souque, A.; Susini, C.; Cordelier, P.; Buscail, L. Identification of an upstream promoter of the human somatostatin receptor, hSSTR2, which is controlled by epigenetic modifications. *Endocrinology* **2008**, *149*, 3137-3147.
20. Samsom, K.G.; van Veenendaal, L.M.; Valk, G.D.; Vriens, M.R.; Tesselaar, M.E.T.; van den Berg, J.G. Molecular prognostic factors in small-intestinal neuroendocrine tumours. *Endocr Connect* **2019**, *8*, 906-922.
21. Veenstra, M.J.; van Koetsveld, P.M.; Dogan, F.; Farrell, W.E.; Feelders, R.A.; Lamberts, S.W.J.; de Herder, W.W.; Vitale, G.; Hofland, L.J. Epidrug-induced upregulation of functional somatostatin type 2 receptors in human pancreatic neuroendocrine tumor cells. *Oncotarget* **2018**, *9*, 14791-14802.
22. Alaskhar Alhamwe, B.; Khalaila, R.; Wolf, J.; von Bulow, V.; Harb, H.; Alhamdan, F.; Hii, C.S.; Prescott, S.L.; Ferrante, A.; Renz, H., et al. Histone modifications and their role in epigenetics of atopy and allergic diseases. *Allergy Asthma Clin Immunol* **2018**, *14*, 39.
23. Refardt, J.; Klomp, M.J.; van Koetsveld, P.M.; Dogan, F.; Konijnenberg, M.; Brabander, T.; Feelders, R.A.; de Herder, W.W.; Hofland, L.J.; Hofland, J. Effect of epigenetic treatment on SST(2) expression in neuroendocrine tumour patients. *Clin Transl Med* **2022**, *12*, e957.
24. Pollard, J.H.; Menda, Y.; Zamba, K.D.; Madsen, M.; O'Dorisio, M.S.; O'Dorisio, T.; Bushnell, D. Potential for Increasing Uptake of Radiolabeled (68)Ga-DOTATOC and (123)I-MIBG in Patients with Midgut Neuroendocrine Tumors Using a Histone Deacetylase Inhibitor Vorinostat. *Cancer Biother Radiopharm* **2021**, *36*, 632-641.
25. Refardt, J.; Zandee, W.T.; Brabander, T.; Feelders, R.A.; Franssen, G.J.H.; Hofland, L.J.; Christ, E.; de Herder, W.W.; Hofland, J. Inferior outcome of neuroendocrine tumor patients negative on somatostatin receptor imaging. *Endocr Relat Cancer* **2020**, *27*, 615-624.
26. Evans, J.S.; Beaumont, J.; Braga, M.; Masrour, N.; Mauri, F.; Beckley, A.; Butt, S.; Karali, C.S.; Cawthorne, C.; Archibald, S., et al. Epigenetic potentiation of somatostatin-2 by guadecitabine in neuroendocrine neoplasias as a novel method to allow delivery of peptide receptor radiotherapy. *Eur J Cancer* **2022**, *176*, 110-120.
27. Klieser, E.; Urbas, R.; Stattner, S.; Primavesi, F.; Jager, T.; Dinnewitzer, A.; Mayr, C.; Kiesslich, T.; Holzmann, K.; Di Fazio, P., et al. Comprehensive immunohistochemical analysis of histone deacetylases in pancreatic neuroendocrine tumors: HDAC5 as a predictor of poor clinical outcome. *Hum Pathol* **2017**, *65*, 41-52.

SUPPLEMENTAL METHODS

CHROMATIN IMMUNOPRECIPITATION

Snap frozen tissue was crushed and washed with 950 µL PBS supplemented with 1 mM phenylmethylsulfonyl fluoride (PMSF, Thermo Scientific), followed by incubation with formaldehyde for fixation (final concentration of 1%, 10 minutes, room temperature (RT)). To quench the reaction, glycine was added (final concentration of 0.125 M) and the sample was incubated (5 minutes, RT). The sample was washed twice with 950 µL PBS supplemented with 1 mM PMSF (2000 RPM, 5 minutes, 4°C), and the pellet was then resuspended in 500 µL lysis buffer (1 % sodium dodecyl sulphate (SDS), 50 mM tris hydrochloride (Tris-HCl, pH 8.1) and 10 mM ethylenediaminetetraacetic acid (EDTA, pH 8.0) supplemented with 1 mM PMSF). After incubation on ice (10 minutes), the sample was sonified on ice for 5 - 11 times for 20 seconds at 600 microns. The sample was centrifuged (13000 RPM, 10 minutes, 4°C) and the supernatant was used for further analysis. To include a sample for further analysis, the right DNA concentration and fragment size was confirmed. To do so, 50 µL of the supernatant was incubated (30 minutes 37°C) with 100 µL H2O, 6 µL 5 M NaCl and 1 µL RNase A (20 mg/mL). Then 2 µL proteinase K (20 mg/mL) was added and the sample was incubated again (4 hours, 65°C). The DNA was purified with the QIAquick PCR purification kit (Qiagen) according to manufacturer's protocol and subsequently heated (10 minutes, 65°C). The quality of the sample was then confirmed with the NanoDrop 8000 spectrophotometer (Thermo Scientific) and the 4200 TapeStation system (Agilent) (Supplemental Figure 3). For this, 1 µL of 50 ng/µL DNA was loaded into the Genomic DNA ScreenTape (Agilent).

Per antibody of interest, 5 µg chromatin was diluted in CHIP dilution buffer (1.1% Triton X-100, 0.01% SDS, 167 mM NaCl, 16.7 mM Tris-HCl (pH 8.1) and 1.2 mM EDTA supplemented with 1x SIGMAFAST protease inhibitor (Sigma)) to a total volume of 500 µL. Then rabbit anti-mouse IgG antibody (ab46540, Abcam) was added and the mixture was incubated (1 hour, 4°C) to preclear the chromatin, followed by the incubation (2 hours, 4°C) with Dynabeads Protein-G (Invitrogen). Of the precleared chromatin sample, an input sample (10%) was collected. Then, 2.5 µg antibody (H3K27me3 (ab6002, Abcam), H3K9ac (ab4441, Abcam) or IgG (ab46540, Abcam)) was added to each 5 µg chromatin sample, followed by an overnight incubation step (4°C). Dynabeads Protein-G was added followed by an incubation step (2 hours, 4°C). The sample was washed: (1) three times with 20 mM Tris-HCl (pH 8.0), 2 mM EDTA, 1 % Triton X-100 and 150 mM NaCl, (2) once with 20 mM Tris-HCl (pH 8.0), 2 mM EDTA, 1 % Triton X-100, 0.1% SDS and 500 mM NaCl, (3) once with 10 mM Tris-HCl (pH 8.0), 1 mM EDTA, 0.25 M lithium chloride (LiCl), 0.5% IGEPAL and 0.5% sodium deoxycholate and (4) once with 10 mM Tris-HCl (pH 8.0) and 1 mM EDTA. Then, 150 µL elution buffer (25 mM Tris-HCl (pH 7.5) + 10 mM EDTA + 0.5% SDS) was added and the chromatin was eluted by incubation (30 minutes, 65°C, 1200rpm). To both the input sample and the eluted chromatin, 6 µL 5 M NaCl and 2 µL proteinase K (20 mg/ml) were added and the samples were incubated (4 hours, 65°C). The resulting DNA was purified with the QIAquick PCR purification kit (Qiagen) and the

enrichment was measured by RT-qPCR. For this, 2 µL DNA was mixed with 10.5 µL primer mix consisting of 3.5 µL H2O, 0.375 µL 10 µM reverse primer, 0.375 µL 10 µM forward primer and 6.250 µL 2x SensiFAST SYBR Lo-ROX mix (Meridian Bioscience). Primer information can be found in *Supplemental Table 1*. To obtain the CT-values, a threshold of 0.030 was used for all three primer sets (i.e. -2, -1 and TSS).

SUPPLEMENTAL FIGURES AND TABLES

SUPPLEMENTAL TABLE 1

Table S1. (**A**) Primer sequences for RT-qPCR. Primers for housekeeping genes (Thermo Fisher Scientific) were diluted twenty times. For SSTR2, final concentrations were 0.5 pM for both the forward and reverse primer, and 0.1 pM for the SSTR2 probe (Sigma). (**B**) PCR and sequencing primer sequences for pyrosequencing. (**C**) Primer sequences for CHIP analysis [11].

	Primer information	**Efficiency Factor**
(A) RT-qPCR		
GUSB	Hs00939627_m1	1.95
HPRT1	Hs02800695_m1	1.97
B-Actin	Hs01060665_g1	1.96
SSTR2	Forward: 5′-TCGGCCAAGTGGAGGAGAC-3′ Reverse: 5′-AGAGACTCCCCACACAGCCA-3′ Probe: 5′-FAM-CCGGACGGCCAAGATGATCACC-TAMRA-3′	1.91
(B) Pyrosequencing		
PCR	Forward: 5′-[Btn]GGGTTGGTTGGGTTAGTTTT -3′ Reverse: 5′-ATTCCTAACTCCTCCACCCTCTT-3′	
Sequencing	Reverse strand: 5′-ACCTCAAACTAAAACTCTA-3′	
(C) CHIP analysis		
-2	Forward: 5′-TGCTGACTGACGTGGCTACA-3′ Reverse: 5′-CGCACCTGGAGTCCAAGATT-3′	1.96
-1	Forward: 5′-GTCCTTGCCATGAGTCTTGA-3′ Reverse: 5′-CAGGCAGAGCTTACAGACAG-3′	1.99
TSS	Forward: 5′-AGCGAAGCCGCTGTGACGTA-3′ Reverse: 5′-TCTGGGCGCTGGTGGTCTTG-3′	2.00

SUPPLEMENTAL TABLE 2

Table S2. Spearman R values of the correlation analyses between the eight examined CpG positions of the SSTR2 promoter in small intestinal neuroendocrine tumors samples, demonstrating a uniform DNA methylation profile, except for location -1 which did not correlate with any other location. To correct for multiple testing, results were considered statistically significant at $p < 0.002$ and are shown in bold.

	-2	-1	1	2	3	4	5	6
-2		0.06	**0.79**	0.72	**0.75**	**0.74**	**0.75**	0.72
-1			0.29	-0.18	0.27	0.08	0.08	-0.30
1				**0.75**	**0.92**	**0.82**	**0.88**	0.68
2					0.67	**0.79**	**0.88**	**0.82**
3						**0.83**	**0.85**	0.64
4							**0.90**	**0.81**
5								**0.83**
6								

SUPPLEMENTAL TABLE 3

Table S3. Spearman R values of the correlation analyses between the eight examined CpG positions of the SSTR2 promoter in normal small intestinal tissue samples, demonstrating a uniform DNA methylation profile, except for location 6 which did not correlate with any other location. To correct for multiple testing, results were considered statistically significant at $p < 0.002$ and are shown in bold.

	-2	-1	1	2	3	4	5	6
-2		0.79	**0.80**	**0.83**	0.74	**0.89**	**0.80**	0.74
-1			**0.90**	0.73	**0.92**	**0.87**	**0.82**	0.69
1				**0.86**	**0.96**	**0.95**	**0.88**	0.69
2					**0.80**	**0.89**	**0.91**	0.57
3						**0.90**	**0.81**	0.63
4							**0.90**	0.68
5								0.75
6								

SUPPLEMENTAL TABLE 4

Table S4. Spearman R values of the correlation analyses between the three examined locations within the SSTR2 promoter region (i.e. TSS, -2 and -1) in small intestinal neuroendocrine tumor samples, demonstrating a uniform H3K27me3 profile. To correct for multiple testing, results were considered statistically significant at $p < 0.017$ and are shown in bold.

	TSS	-2	-1
TSS		**0.96**	**0.87**
-2			**0.95**
-1			

SUPPLEMENTAL TABLE 5

Table S5. Spearman R values of the correlation analyses between the three examined locations within the SSTR2 promoter region (i.e. TSS, -2 and -1) in small intestinal neuroendocrine tumor samples, demonstrating a uniform H3K9ac profile. To correct for multiple testing, results were considered statistically significant at $p < 0.017$ and are shown in bold.

	TSS	-2	-1
TSS		**0.89**	**0.89**
-2			**0.92**
-1			

SUPPLEMENTAL FIGURE 1

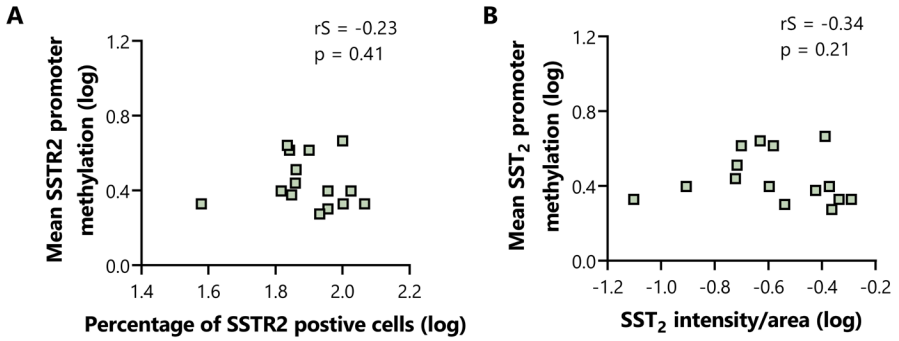

Figure S1. Correlation of the mean level of DNA methylation at CpG positions in the SSTR2 promoter region with (**A**) the percentage of SSTR2 positive cells and (**B**) the SSTR2 intensity/area in small intestinal neuroendocrine tumor samples. Data are log-transformed. rS = Spearman r, SSTR2 = somatostatin receptor subtype 2.

SUPPLEMENTAL FIGURE 2

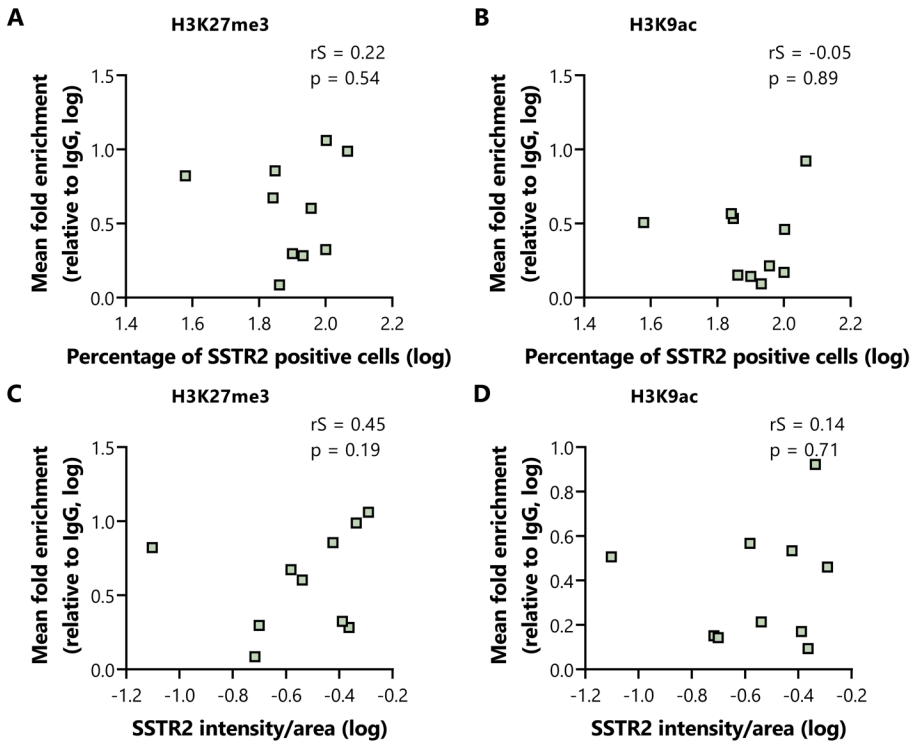

Figure S2. Correlation of (**A, B**) the percentage of SSTR2 positive cells and (**C, D**) the SSTR2 intensity/area with the fold enrichment of (**A, C**) H3K27me3 and (**B, D**) H3K9ac calculated as the mean enrichment on three locations within the SSTR2 promoter (i.e. -2, -1 and TSS) in the small intestinal neuroendocrine tumor samples. All CHiP data are presented as fold enrichment relative to IgG and data are log-transformed. rS = Spearman r, SSTR2 = somatostatin receptor subtype 2.

SUPPLEMENTAL FIGURE 3

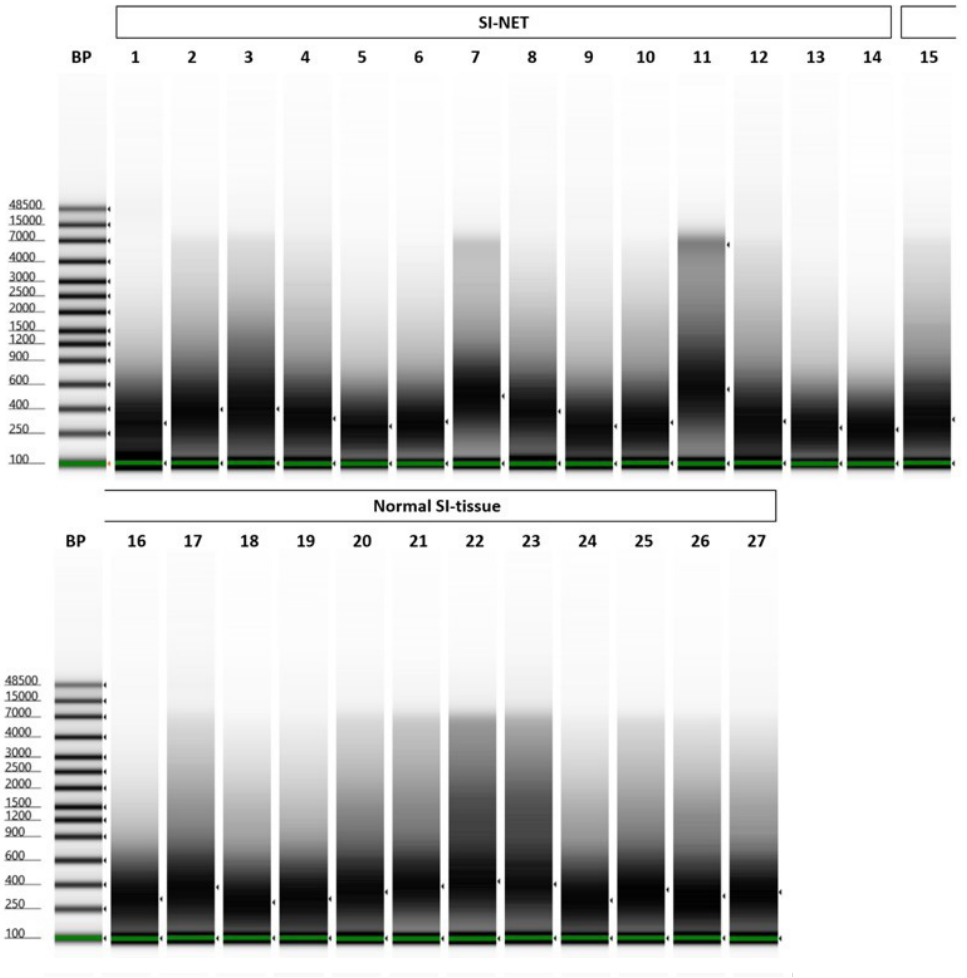

Figure S3. DNA fragment size of small intestinal neuroendocrine tumor samples and normal small intestinal tissue, demonstrating that the majority of the DNA fragments has the desired fragment size between 200 and 1000 base pairs. SI-NET = small intestinal neuroendocrine tumor, Normal SI-tissue = normal small intestinal tissue, BP = base pairs.

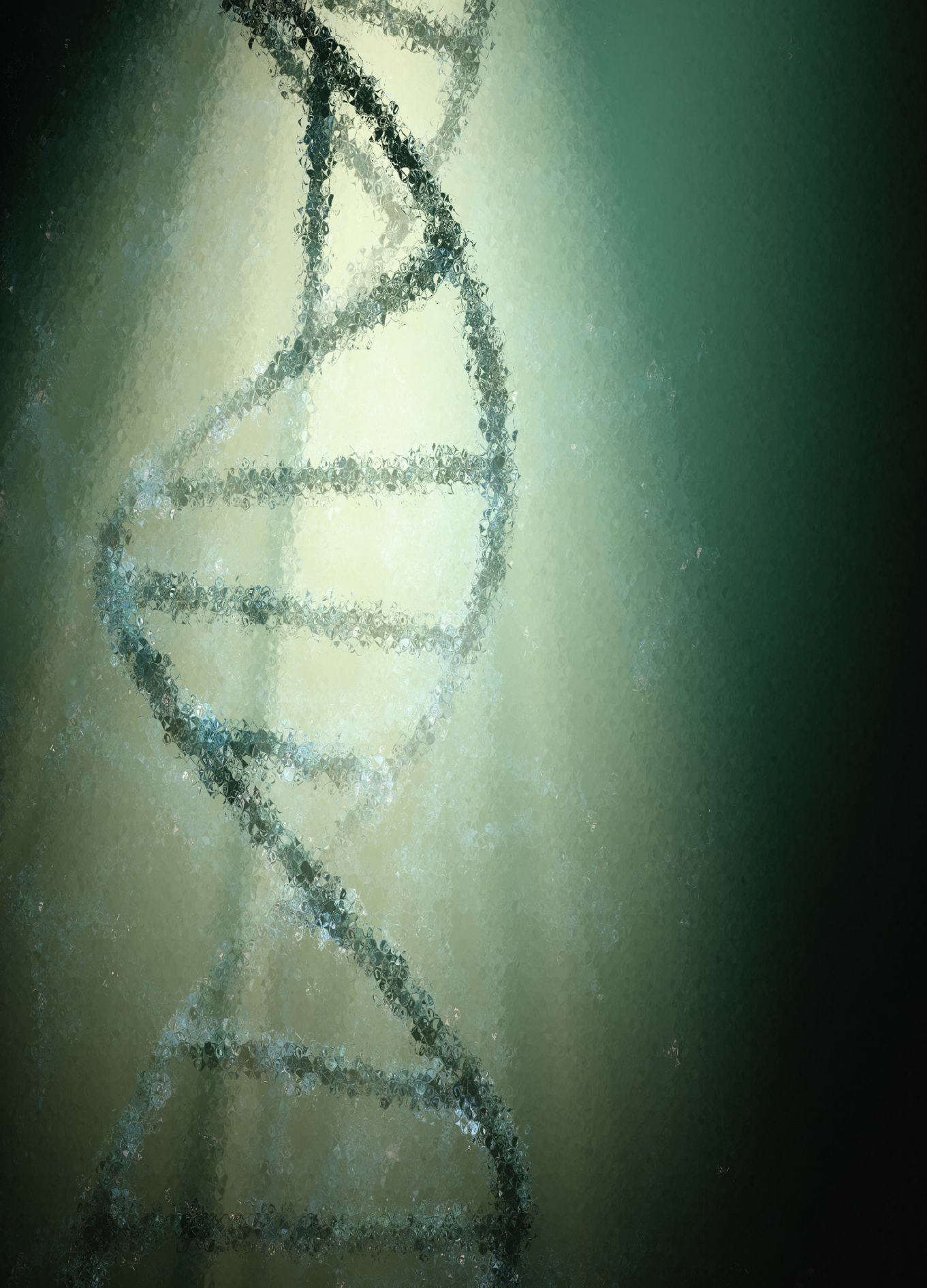

CHAPTER 7

Effect of Epigenetic Treatment on SSTR2 Expression in Neuroendocrine Tumor Patients

Based on[#]:

J. Refardt[1,2], M.J. Klomp[1,3], P.M van Koetsveld[1], F. Dogan[1], M. Konijnenberg[3], T. Brabander[3], R.A. Feelders[1], W.W de Herder[1], L.J. Hofland[1], J. Hofland[1].

[1] ENETS Center of Excellence, Department of Internal Medicine, Section of Endocrinology, Erasmus Medical Center, Rotterdam, The Netherlands. [2] ENETS Center of Excellence, Department of Endocrinology, University Hospital Basel, Basel, Switzerland. [3] ENETS Center of Excellence, Department of Radiology & Nuclear Medicine, Erasmus Medical Center, Rotterdam, The Netherlands.

Clinical and Translational Medicine. 2022 Jul; 12(7):e957

[#] For this chapter, several adjustments were made. For uniformity, SST_2 was changed to SSTR2 and the radiotracer nomenclature has been adjusted. This paper was originally published as letter to the editor. In this thesis, the structure was changed to the structure of an original research article.

1. INTRODUCTION

Several preclinical studies have uncovered that epigenetic drugs can upregulate somatostatin type-2 receptor (SSTR2) expression in neuroendocrine tumor (NET) models [1, 2], which could be of eminent importance for NET patients with low tumoral SSTR expression. In a prospective clinical proof-of-concept trial involving nine advanced NET patients with low SSTR expression, we were able to show that epigenetic treatment with the histone deacetylase inhibitor (HDACi) valproic acid (VPA) and the DNA methyltransferase inhibitor (DNMTi) hydralazine did not lead to an increase in tumor-uptake of [^{68}Ga]Ga-DOTATATE, contradicting the *in vitro* data.

A prerequisite for the treatment of advanced NETs with (radiolabeled) somatostatin analogues (SSA) is the expression of SSTR2 on the tumor cell surface, providing rationale for the inferior outcome in patients with low uptake on functional SSTR imaging [3]. Several previous *in vitro* studies and one *in vivo* study achieved stimulation of SSTR2 expression levels and binding of SSAs by increasing histone acetylation levels and reducing DNA methylation of the SSTR2 gene promoter region in NET cells by epigenetic drugs [1, 2, 4]. Despite these promising results, there are only data from one study showing limited increase of [^{68}Ga]Ga-DOTATOC uptake by HDAC inhibitor vorinostat in five NET patients already expressing SSTR at baseline [5].

2. MATERIALS AND METHODS

In the present study, which was approved by the Ethics Committee of the Erasmus Medical Center Rotterdam and registered at the Netherlands Trial Register (NL7726), nine patients with advanced NETs (Table 1) and low SSTR expression at baseline on [^{68}Ga]Ga-DOTATATE/PET (Table 2), defined as tumor uptake below or equal to the physiological uptake in the liver, were included and provided written informed consent. Patients were treated for 14 days simultaneously with the HDACi VPA (30 mg/kg body weight/day, max. 3000 mg/day) and the DNMT inhibitor hydralazine (150 mg/day). One week after start of treatment, VPA dosage was adjusted to target a serum concentration of 75–120 µg/ml [6]. Hydralazine dosage remained unchanged unless adjusted for tolerability. Treatment effect was evaluated after 2 weeks by the change in [^{68}Ga]Ga-DOTATATE uptake on PET/CT. The last two patients (lung NET, rectum NET) completed the trial without hydralazine due to emerging insights from the *in vitro* studies, which were performed simultaneously in three human NET cell lines BON-1 (pancreatic NET), GOT1 (small intestinal NET) and NCI-H727 (lung NET). Here, effects of VPA and hydralazine on *SSTR2* mRNA and protein levels as well as [^{111}In]In-DOTATATE uptake were assessed (details in the Supplementary Appendix).

3. RESULTS

At the end of the 2-week epigenetic treatment period, none of the NET patients had an increase in [^{68}Ga]Ga-DOTATATE uptake grade (Table 2). No change in median [^{68}Ga]Ga-DOTATATE uptake in any NET sites was observed, and there was even a tendency for reduced

uptake in primary tumors (Figures 1 and S1). These findings were independent of tumor aetiology, metastatic location or drug treatment. Meanwhile, a significant median (IQR) increase of 27% (4.1, 46.4) in uptake was observed in the kidneys (p = 0.02), independent of the study medication. A limitation of our study is the restricted patient number, but given the lack of effects in any of the patients with different NET origins, this protocol is unlikely to affect tumoral SSTR2 expression *in vivo*. All patients reported known side effects of the study medication (details in the Supplementary Appendix), and no serious adverse events occurred during the study.

Table 1. Baseline characteristics of the neuroendocrine tumor patients included in the clinical trial. Values are shown as median (interquartile range [IQR]) or number (%).

Patient characteristics	**Total (n = 9)**
Age, years (IQR)	67 (54, 75)
Sex (male), n (%)	5 (56)
Origin	
Pancreas NET, n (%)	2 (22)
Small intestinal NET, n (%)	1 (11)
Lung NET, n (%)	4 (44)
Rectum NET, n (%)	1 (11)
Thymus NET, n (%)	1 (11)
Metastases	
Lymph nodes, n (%)	9 (100)
Liver, n (%)	5 (56)
Mesenterial, n (%)	1 (11)
Bone, n (%)	3 (33)
Lung, n (%)	1 (11)
Other, n (%)	4 (44)
Ki67 index	
0%–2%, n (%)	3 (33)
5%–10%, n (%)	4 (44)
30% 1 (11)	1 (11)
Unknown	1 (11)
Grading	
G1, n (%)	4 (44)
G2, n (%)	4 (44)
G3, n (%)	1 (11)
Previous treatments	
Surgery, n (%)	3 (33)
Somatostatin analogue, n (%)	2 (22)
Chemotherapy, n (%)	1 (11)
Other, n (%)	3 (33)

Abbreviations: n, number; NET, neuroendocrine tumor; IQR, interquartile range.

Table 2. Change in study parameters of neuroendocrine tumor patients at baseline and after 1 and 2 weeks of epigenetic treatment.

Clinical parameters	**Baseline**	**Week 1**	**Week 2**	***p***
Weight, kg (IQR)	76 (68, 86)	77 (68, 88)	77 (69, 88)	0.05
Blood pressure systolic, mmHg (IQR)	147 (130, 155)	139 (129, 151)	135 (126, 148)	0.14
Heart rate, bpm (IQR)	69 (62, 81)	77 (67, 109)	76 (65, 96)	0.34
Laboratory parameters				
Haemoglobin, mmol/L (IQR)	8.5 (8.1, 9.2)	8.5 (7.7, 9.2)	8.1 (7.6, 8.6)	0.05
Thrombocytes, $\times 10^9$/L (IQR)	247 (195, 282)	233 (173, 255)	177 (148, 271)	0.11
Creatinine, umol/L (IQR)	73 (58, 90)	74 (54, 86)	76 (56, 89)	0.72
ASAT, U/L (IQR)	27 (23, 32)	23 (21, 30)	28 (24, 36)	1
ALAT, U/L (IQR)	26 (17, 35)	17 (16, 25)	21 (13, 26)	0.09
GGT, U/L (IQR)	65 (19, 98)	46 (19, 82)	48 (18, 115)	0.16
VPA drug level, µg/ml (IQR)	NA	102 (84, 126)	95 (90, 117)	NA
Study medication				
VPA dosage, mg/day (IQR) *(n = 9)*	NA	2300 (1900, 2500)	1900 (1763, 2000)	NA
Hydralazine dosage, mg/day (IQR) *(n = 7)*	NA	150 (150, 150)	150 (100, 150)	NA
Tumor uptake of [^{68}Ga]Ga-DOTATATE				
None, n (%)	6 (67)		6 (67)	1
Below liver, n (%)	3 (33)		3 (33)	1
Peak uptake				
Primary tumor, SUV (IQR) *(n = 6)*	8.1 (3.0, 11.4)		6.8 (2.8, 9.9)	0.17
Lymph node metastases, SUV (IQR) *(n = 5)*	4.8 (3.1, 9.0)		5.8 (2.6, 7.8)	0.35
Liver metastases, SUV (IQR) *(n = 5)*	7.5 (5.0, 7.9)		7.3 (4.5, 8.4)	0.29
Bone metastases, SUV (IQR) *(n = 4)*	4.1 (2.6, 5.1)		4.2 (2.7, 5.2)	0.47
Intestinal metastases, SUV (IQR) *(n = 2)*	9 (7.5, 10.5)		8.7 (6.7, 10.6)	0.67
Skin metastases, SUV (IQR) *(n = 1)*	3.5		3.7	NA
Liver, SUV (IQR)	10.5 (8.3, 12.6)		10.7 (8.3, 12.3)	0.95
Kidneys, SUV (IQR)	16.3 (14.3, 19.2)		20.7 (16.1, 26.0)	0.02
Spleen, SUV (IQR)	25.9 (22.7, 32.7)		27.8 (22.0, 31.9)	0.68

Note: Values are shown as median (IQR) or number (%) in nine patients, unless otherwise indicated. Bold writing signifies significance. Abbreviations: Bpm, beats per minute; n, number; NA, not applicable; IQR, interquartile range; SUV, standard uptake values; VPA, valproic acid.

In all cell lines tested, treatment with VPA led to a significant increase of *SSTR2* mRNA levels and [^{111}In]In-DOTATATE uptake, respectively ($p < 0.001$) (Figure 2). An increase in the SSTR2 staining intensity per cell was observed in BON-1 and NCI-H727 cells ($p < 0.01$), but not in GOT1 cells, possibly due to the high baseline SSTR2 expression levels (Figure S2). Meanwhile, an increase in *SSTR2* mRNA levels was seen only for the stronger hydralazine dose in BON-1 cells ($p < 0.001$) and GOT1 cells ($p < 0.05$), but hydralazine decreased mean (SD) *SSTR2* mRNA

expression levels in NCI-H727 cells by 15% (13) (p < 0.05). No changes in SSTR2 protein expression and [^{111}In]In-DOTATATE uptake were seen following incubation with hydralazine in all cell lines. The combined treatment of VPA with the stronger hydralazine dosage led to an additional mean (SD) increase in SSTR2 mRNA expression levels in BON-1 cells of 120% (72) (p < 0.001), whereas no additional effect was seen for GOT1 cells, and even an inhibitory mean effect (SD) of 73% (34) (p < 0.001), was observed in NCI-H727. No synergistic or antagonistic effect on [^{111}In]In-DOTATATE uptake and SSTR2 staining intensity per cell was observed for the combined treatment.

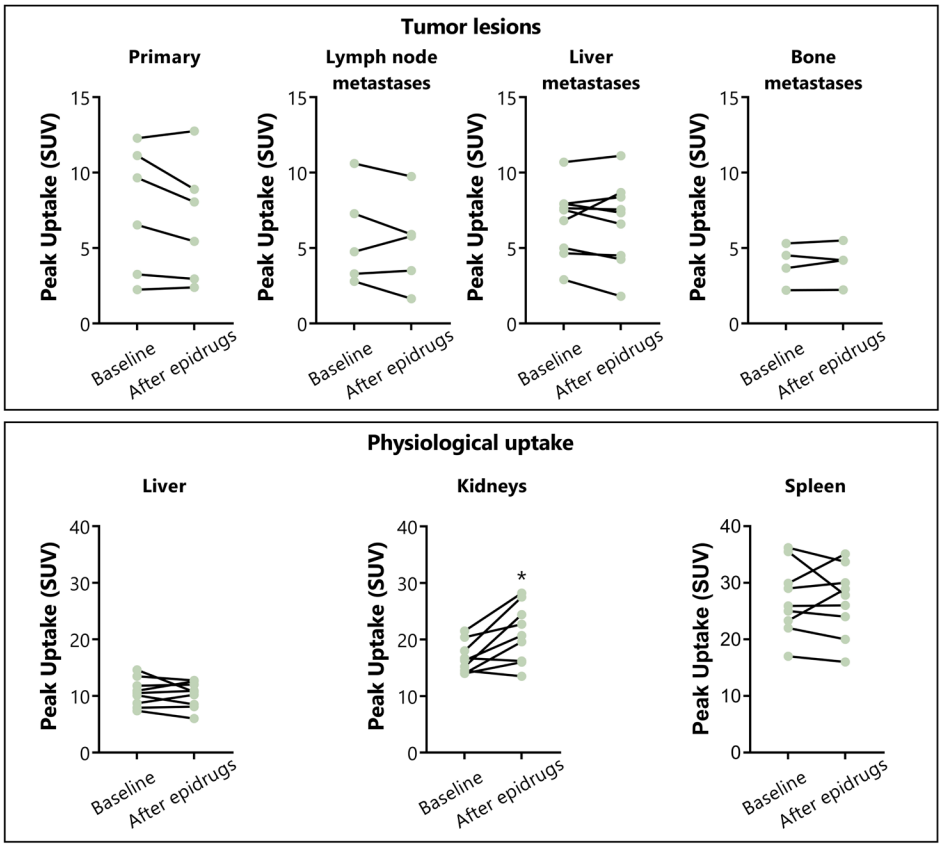

Figure 1. Change in peak uptake of [^{68}Ga]Ga-DOTATATE on PET/CT at baseline and after 2-week epigenetic treatment in patients with neuroendocrine tumors with low somatostatin receptor expression. The upper panel showing changes in tumor lesions, the lower panel showing changes in physiological uptake. Patients were prepared according to our local protocol, which includes the drinking of 1 L of water in 2 h before injection. Imaging was performed from scull base to thighs after median (interquartile range [IQR]) 60 min (59–65) injection with an activity of 118 MBq (103–121) [^{68}Ga]Ga-DOTATATE. For each patient, at least two tumor target lesions, including the primary if applicable, were defined on the initial [^{68}Ga]Ga-DOTATOC PET/CT. Peak standard uptake value (SUV) was calculated for every lesion as well as for the liver, kidneys and spleen. * p < 0.05 according to Wilcoxon signed-rank test.

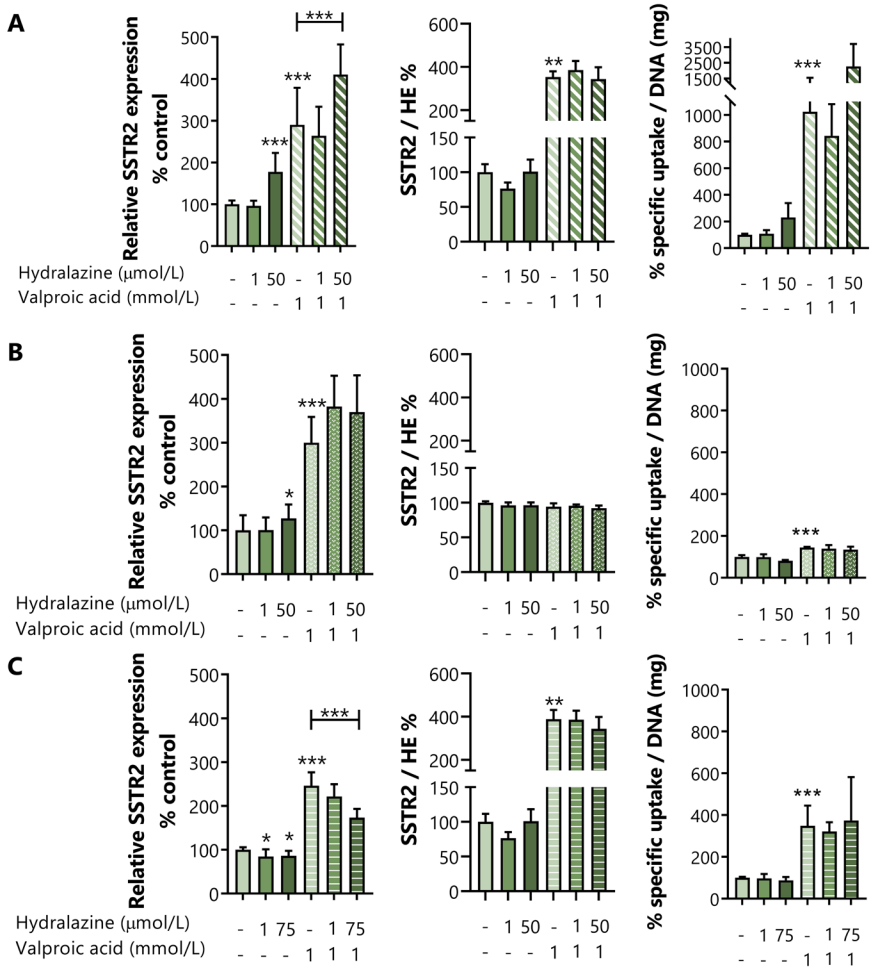

Figure 2. Effect of epigenetic treatment with valproic acid and hydralazine on the human neuroendocrine tumor cell lines (**A**) BON-1, (**B**) GOT1 and (**C**) NCI-H727. Graphs show somatostatin type-2 receptor (SSTR2) mRNA expression levels, SSTR2 protein levels and uptake of radiolabeled [^{111}In]In-DOTATATE as percentage increase or decrease compared to control cells. DNA quantification (as a measure for cell amount in cell growth experiments) was performed with Hoechst 33258 for BON-1 and NCI-H727, whereas Quant-iT PicoGreen dsDNA reagent (Invitrogen, Breda, The Netherlands) was used for GOT1. For mRNA analysis TaqMan Universal PCR Master Mix (Applied Biosystems, Breda, The Netherlands) supplemented with primers and probes was used. SSTR2 expression was determined relative to three housekeeping genes (GUSB, HPRT1 and ACTB) using the QuantStudio 7 Flex RT-qPCR system with QuantStudio Real-Time PCR software v1.5. Immunohistochemistry was performed using rabbit monoclonal anti-SSTR2 IgG (NB-49-015, 1:25 dilution, NeoBiotech, Nanterre, France). Stained cells were visualized with the NanoZoomer 2.0 HT (Hamamatsu Photonics, Hamamatsu City, Japan) and SSTR2 staining intensity per cell was assessed using the CellProfiler software (version 4.0.7, www.cellprofiler.org). Internalization studies were performed with [^{111}In]In-DOTATATE. [^{111}In]InCl_3 (Curium Pharma, Petten, The Netherlands) was used to radiolabel DOTATATE (Bachem AG, Bubendorf, Switzerland) with a molar activity of 50 MBq/nmol. Data are shown as mean with the standard deviation of three (mRNA expression levels and radiolabeled [^{111}In]In-DOTATATE uptake) or two (immunohistochemistry) independent experiments. Data were

normalized to control values, all set at 100%. * $p < 0.05$, ** $p < 0.01$, *** $p < 0.001$ according to one-way ANOVA analysis with Tukey post hoc test after log-transformation of data.

4. DISCUSSION

Our study shows, for the first time, that contrary to the promising *in vitro* and *in vivo* data on epigenetic upregulation of SSTR2 expression, epigenetic treatment did not translate into the stimulation of [^{68}Ga]Ga-DOTATATE uptake in NET patients with low baseline SSTR expression.

This appears to be in contrast to the study with five SSTR-positive patients who received vorinostat treatment for 4 days [5], but their observed change in the maximum standard uptake value (SUVmax) of 1.3 could lack clinical relevance. Combined these studies might imply that either epigenetic upregulation of SSTR2 expression is only effective in patients with sufficient baseline [^{68}Ga]Ga-DOTATATE uptake, or the epigenetic effect depends on the epidrugs used or the drug levels achieved in patients are not sufficient to induce upregulation. The importance of choice and dosage of the epidrugs was shown by the effect of the DNMTi hydralazine, exhibiting only mild effects in pharmacologically unreachable dosages despite good efficiency observed in other tumors [7, 8]. A possible future limitation for epigenetic treatment in NETs could also be the observed non-specific effect of increased renal uptake in our patients. Although changes in uptake measures of up to 25% SUVmax between two scans have been described [9], the increase in renal uptake was seen in 78% of our patients in the second PET/CT. As all patients underwent the same hydration protocol before the scan and no changes in kidney function were noted, this could signify that the epigenetic treatment is not tumor specific and also activates basal expression of SSTR2 in renal tissue [10].

5. CONCLUSION

In conclusion, short-term epigenetic treatment with VPA and hydralazine had no stimulating effect on [^{68}Ga]Ga-DOTATATE uptake in nine patients with well-differentiated NETs of various origins with low baseline SSTR expression, contradicting preclinical findings. Clinical trials with alternative epigenetic drugs or in patients with positive baseline SSTR2 expression may be able to clarify whether epigenetic treatment has a role in the treatment of NETs; however, a potential increase in renal uptake should be closely monitored.

ACKNOWLEDGEMENTS

We would like to thank the Radiopharmaceutical Chemistry group (Radiology and Nuclear Medicine, Erasmus MC, The Netherlands) for radiolabeling [^{111}In]In-DOTATATE used for the uptake experiments performed in this study

REFERENCES

1. Veenstra, M.J.; van Koetsveld, P.M.; Dogan, F.; Farrell, W.E.; Feelders, R.A.; Lamberts, S.W.J.; de Herder, W.W.; Vitale, G.; Hofland, L.J. Epidrug-induced upregulation of functional somatostatin type 2 receptors in human pancreatic neuroendocrine tumor cells. *Oncotarget* **2018**, *9*, 14791-14802.
2. Klomp, M.J.; Dalm, S.U.; van Koetsveld, P.M.; Dogan, F.; de Jong, M.; Hofland, L.J. Comparing the Effect of Multiple Histone Deacetylase Inhibitors on SSTR2 Expression and [(111)In]In-DOTATATE Uptake in NET Cells. *Cancers (Basel)* **2021**, *13*.
3. Refardt, J.; Zandee, W.T.; Brabander, T.; Feelders, R.A.; Franssen, G.J.H.; Hofland, L.J.; Christ, E.; de Herder, W.W.; Hofland, J. Inferior outcome of neuroendocrine tumor patients negative on somatostatin receptor imaging. *Endocr Relat Cancer* **2020**, *27*, 615-624.
4. Taelman, V.F.; Radojewski, P.; Marincek, N.; Ben-Shlomo, A.; Grotzky, A.; Olariu, C.I.; Perren, A.; Stettler, C.; Krause, T.; Meier, L.P., et al. Upregulation of Key Molecules for Targeted Imaging and Therapy. *J Nucl Med* **2016**, *57*, 1805-1810.
5. Pollard, J.H.; Menda, Y.; Zamba, K.D.; Madsen, M.; O'Dorisio, M.S.; O'Dorisio, T.; Bushnell, D. Potential for Increasing Uptake of Radiolabeled (68)Ga-DOTATOC and (123)I-MIBG in Patients with Midgut Neuroendocrine Tumors Using a Histone Deacetylase Inhibitor Vorinostat. *Cancer Biother Radiopharm* **2021**, *36*, 632-641.
6. Dueñas-Gonzalez, A.; Coronel, J.; Cetina, L.; González-Fierro, A.; Chavez-Blanco, A.; Taja-Chayeb, L. Hydralazine-valproate: a repositioned drug combination for the epigenetic therapy of cancer. *Expert Opin Drug Metab Toxicol* **2014**, *10*, 1433-1444.
7. Zambrano, P.; Segura-Pacheco, B.; Perez-Cardenas, E.; Cetina, L.; Revilla-Vazquez, A.; Taja-Chayeb, L.; Chavez-Blanco, A.; Angeles, E.; Cabrera, G.; Sandoval, K., et al. A phase I study of hydralazine to demethylate and reactivate the expression of tumor suppressor genes. *BMC Cancer* **2005**, *5*, 44.
8. Candelaria, M.; Burgos, S.; Ponce, M.; Espinoza, R.; Dueñas-Gonzalez, A. Encouraging results with the compassionate use of hydralazine/valproate (TRANSKRIP™) as epigenetic treatment for myelodysplastic syndrome (MDS). *Ann Hematol* **2017**, *96*, 1825-1832.
9. Menda, Y.; Ponto, L.L.; Schultz, M.K.; Zamba, G.K.; Watkins, G.L.; Bushnell, D.L.; Madsen, M.T.; Sunderland, J.J.; Graham, M.M.; O'Dorisio, T.M., et al. Repeatability of gallium-68 DOTATOC positron emission tomographic imaging in neuroendocrine tumors. *Pancreas* **2013**, *42*, 937-943.
10. Geenen, L.; Nonnekens, J.; Konijnenberg, M.; Baatout, S.; De Jong, M.; Aerts, A. Overcoming nephrotoxicity in peptide receptor radionuclide therapy using [(177)Lu]Lu-DOTA-TATE for the treatment of neuroendocrine tumours. *Nucl Med Biol* **2021**, *102-103*, 1-11.

SUPPLEMENTAL METHODS

1. CLINICAL STUDY

STUDY DESIGN AND PARTICIPANTS

This prospective proof-of-concept study was performed at the Erasmus Medical Center Rotterdam, the Netherlands from 07/2019 until 06/2021. Eligible patients were ≥18 years of age, had an inoperable or metastatic NET with well-differentiated histology grade 1, 2 or 3 and low SST uptake on [^{68}Ga]Ga-DOTATATE PET scan. Patients with hypotension (systolic blood pressure <90 mmHg), heart failure NYHA III-IV, creatinine clearance <50 ml/min, liver transaminases >3 times upper normal range, uncontrolled hormonal symptoms including severe diarrhea, serum albumin concentration <25 g/L, epilepsy or existing drug treatment which could not be stopped and interacted with the study medication were excluded.

STUDY PROCEDURES AND ASSESSMENTS

Patients were recruited from the NET clinic at the ENETS Center of Excellence, Erasmus MC in Rotterdam. After signing the informed consent, screening included a medical questionnaire, physical examination and blood sampling. If [^{68}Ga]Ga-DOTATATE PET/CT had been performed in a different institute or >3 months before inclusion, it was repeated during screening.

The primary endpoint was the percentage of patients with an increase in uptake of ≥1 point [^{68}Ga]Ga-DOTATATE in the tumor lesions according to a predefined uptake scale. Grade 1 uptake was below the liver, grade 2 similar to the liver, grade 3 higher than the liver and grade 4 higher than uptake in spleen/kidneys. Pre-specified secondary endpoints included the change in tumoral [^{68}Ga]Ga-DOTATATE uptake as well as physiological uptake of liver, kidneys and spleen as measured by peak standardized uptake value (SUV), and impact of epigenetic treatment on clinical and laboratory parameters.

Adverse events were registered according to Common Terminology Criteria for Adverse Events (CTCAE) version 5.0.

IMAGING AND RADIOLOGICAL ASSESSMENT

[^{68}Ga]Ga-DOTATATE was prepared locally in our institute. PET images were acquired on a Siemens Biograph mCT PET/CT scanner (Siemens Healthineers, Erlangen, Germany). Quantitative assessment of lesions and physiological uptake was performed on Hermes Hybrid Viewer software (V 2.6D Hermes medical solutions, Stockholm) software.

2. *IN VITRO* EXPERIMENTS WITH NET CELL LINES

For the cell line experiments, the human pancreatic NET cell line BON-1 (kind gift of Dr. Townsend, University of Texas, Medical branch, Galveston, TX, USA), the human midgut NET

cell line GOT1 (kind gift of Ola Nilsson, Sahlgrenska Cancer Center, University of Gothenburg, Sweden) and the human pulmonary carcinoid cell line NCI-H727 (ATCC CRL-5815) were used.

CELL CULTURE

BON-1 cells were cultured in DMEM/F-12 (1:1) supplemented with 10% (v/v) FCS, 2 mM L-glutamine, 1.25 mg/L fungizone, and 100 U/ml penicillin; GOT1 cells were cultured in RPMI medium 1640 supplemented with 10% (v/v) FCS, 2 mM L-glutamine, 100 U/mL penicillin, 100 µg/mL streptomycin, 1.0 g/L insulin, 0.55 g/L transferrin, and 67 µg/L selenite; NCI-H727 cells were cultured in RPMI medium 1640 + L-glutamine supplemented with 10% (v/v) FCS, 100 U/mL penicillin, and 100 µg/mL streptomycin. Once a week, BON-1 and NCI-H727 cells were trypsinized using 0.05% (v/v) trypsin + 0.53 mM EDTA and fresh medium was added on day four. GOT1 cells were trypsinized every two weeks using 0.05% (v/v) trypsin + 0.53 mM EDTA supplemented with DNAse (2 U/mL) with medium refreshment after one week.

EPIGENETIC TREATMENT AND EVALUATION

Valproic acid sodium salt (VPA; Sigma-Aldrich, Zwijndrecht, The Netherlands) and hydralazine (Hydralazine HCl; Selleckchem.com) were dissolved in the according cell line culture media. Dose-response studies were performed based on a 7-day treatment schedule. One day before the start of the epigenetic treatment, cells were plated in 24-well plates.

Epigenetic treatment

Cells were plated in T75 flasks on day zero. VPA and hydralazine, alone or in combination, were added on day 1 at their IC_{50} growth inhibitory concentrations and at the maximum treatment dosage used in patients (equal to IC_{50} dosage for VPA, lower dosage for hydralazine). Medium without or with drugs was refreshed on day 3. On day 5, cells were trypsinized and plated for further analysis. Exactly 4 hours after cell plating, the drugs were added again. On day 7, samples were collected for RT-qPCR analysis (24-well plates) and for internalization studies (12-well plates). For immunohistochemistry, cells were plated in chamber slides after pre-treatment with poly-L-lysine.

mRNA-analysis

After lysis, cells were incubated with oligo$(dT)_{25}$ dynabeads (Invitrogen, Breda, The Netherlands) to isolate poly-A^+ mRNA, as described previously [1]. 23 µL H_2O was added for elution, and 10 µL poly-A^+ mRNA was used in the next steps. Poly-A^+ mRNA was converted into cDNA using the commercial RevertAid First Strand cDNA synthesis kit (Thermo Scientific, Breda, The Netherlands). cDNA was also prepared without the addition of RevertAid Reverse Transcriptase to exclude DNA contamination. Samples were diluted by adding 180 µL H_2O. Afterwards 5 µL sample was mixed with 7.5 µL Taqman Universal PCR mastermix (Applied Biosystems, Breda, The Netherlands) supplemented with primers and probes. SSTR2 expression was determined relative to three housekeeping genes (HKGs). For analysis, the

QuantStudio 7 Flex RT-qPCR system with QuantStudio Real-Time PCR software v1.5 was used. The number of copies for SSTR2 and all HKGs was calculated by the efficiency factor to the power of ΔCt (i.e., 40 minus measured Ct). Subsequently, the relative SSTR2 expression was calculated by dividing the number of SSTR2 copies by the geometric mean of all HKGs.

Immunohistochemistry

Cells were fixed with 4% paraformaldehyde for 20 minutes, before incubating them with 50% methanol for 3 minutes and 100% methanol for 3 minutes. Then, cells were permeabilized (0.1% triton X100 detergent in 1x PBS) for 15 minutes, and blocked (1% BSA) for 1 hour at room temperature (RT). Rabbit monoclonal anti-SSTR2 IgG (NB-49-015, 1:25 dilution, NeoBiotech, Nanterre, France) was added (overnight, 4° C). Finally, the cells were incubated for 30 min at RT with HRP/anti-Rabbit/Mouse (Dako Detection System). Bound antibodies were visualized by incubation with freshly prepared DAB (Dako Detection System). For negative controls, primary antibody was omitted. Slides were counterstained with hematoxylin and mounted. Five locations per slide were used to assess the SSTR2 staining intensity per cell, using a 10x magnification and the CellProfiler software (version 4.0.7, www.cellprofiler.org).

[^{111}In]In-DOTATATE radiolabeling and internalization studies

DOTATATE (Bachem AG, Bubendorf, Switzerland) was radiolabeled with $^{111}InCl_3$ (Curium Pharma, Petten, The Netherlands) as previously described [2]. Internalization studies were performed as previously described [3]. Cells were incubated with internalization medium (DMEM (1x)–GlutaMAX-I, 1% (wt/v) BSA, and 20 mM HEPES (pH 7.4)) supplemented with 10^{-9} M [^{111}In]In-DOTATATE (50 MBq/nmol), with or without 10^{-6} M unlabeled DOTATATE, for 4 hours. Following incubation, the excess of unbound radiotracer was removed, and the membrane-bound and internalized radioactivity were determined. The protocol was adjusted for GOT1 cells due to insufficient cell adherence and included the collection of non-adherent cells (pelleted by centrifugation). For GOT1 cells, the total uptake was determined. Cell pellets of additional wells were collected and DNA content was measured as described above, to correct for possible differences in cell numbers.

3. STATISTICAL ANALYSIS

This proof-of concept clinical trial aimed to include 10 patients. Twelve patients were enrolled in the study. Two patients failed screening because of sufficient uptake on [^{68}Ga]Ga-DOTATATE PET and other tumor diagnosis than NET, respectively. Ten patients started study treatment, but one patient withdrew from the study after one week due to adverse events.

Descriptive statistics were used to characterize clinical, laboratory and radiological data, summarized by median and inter-quartile-range (IQR) or mean and standard deviation (SD), categorical variables by frequency and percentages.

Statistical analyses were performed using SPSS version 25.0 (IBM Corp., Armonk, NY) and GraphPad Prism7. A two-sided significance level of 0.05 was set for every analysis.

SUPPLEMENTAL RESULTS

SAFETY

A total of 18 adverse events occurred during the observation phase in ten patients of the intended to treat analysis set of which 14 were judged to be related to the study intervention. Five events were known effects of valproic acid treatment and involved neurocognitive symptoms, tiredness and/or nausea. Five other adverse events were classified as hydralazine-related and involved palpitations, hypotonia and/or water retention. One patient developed an exanthema and one suffered from glucose dysregulation, requiring adjustment of insulin treatment. The patient who stopped treatment due to side effects suffered from nausea with vomitus, headaches and generalized aches.

CELL LINE EXPERIMENTS

BASAL SSTR2 EXPRESSION, SSTR2 PROTEIN LEVELS AND [^{111}In]In-DOTATATE UPTAKE

BON-1 cells showed the lowest mean (SD) SSTR2 expression level of 0.0046 (0.001) (corrected for the geometric mean of three HKGs), followed by the NCI-H727 cells (0.0054 (0.001)) with the highest levels being measured in the GOT1 cells (0.142 (0.025)). Mean (SD) SSTR2 staining intensity per cell was also lowest for BON-1 cells with 7.95 (7.61), again followed by the NCI-H727 cells with 13.43 (4.72) and showing the highest levels for GOT1 cells with 91.83 (6.89), Figure S2. A similar trend was observed for the mean (SD) uptake of [^{111}In]In-DOTATATE, which was 4.23 (1.86), 21.51 (6.09) and 327.0 (20.95) % added dose per milligram DNA for the three cell lines, respectively.

SUPPLEMENTAL FIGURES AND TABLES

SUPPLEMENTAL FIGURE 1

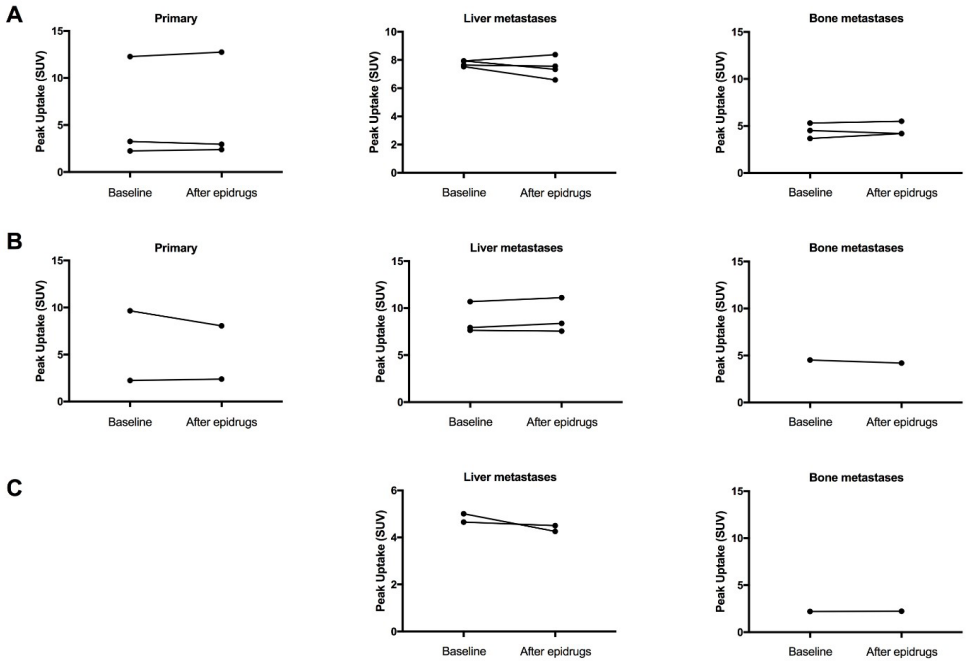

Supplementary Figure S1. Change in peak uptake of [^{68}Ga]Ga-DOTATATE on PET/CT at baseline and after 2-week epigenetic treatment in patients with neuroendocrine tumors with low somatostatin receptor expression according to their origin: (**A**) lung, (**B**) pancreas, (**C**) small-intestine.

SUPPLEMENTAL FIGURE 2

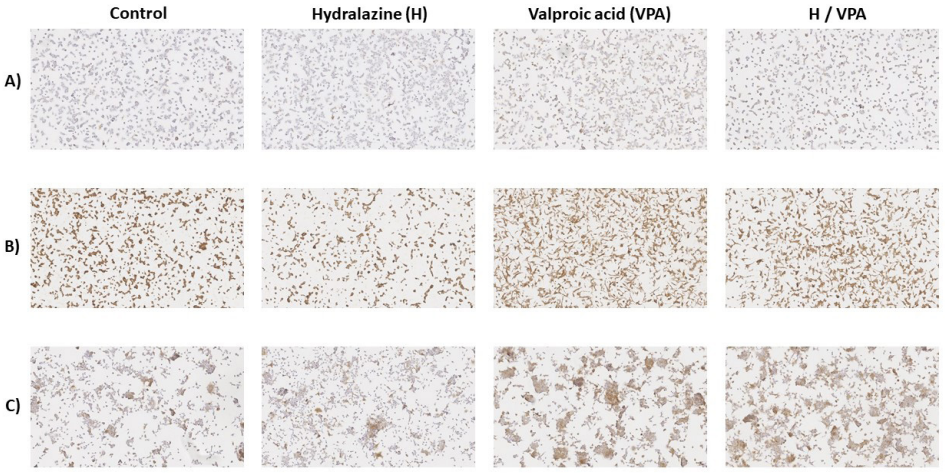

Supplementary Figure S2. Immunohistochemistry of somatostatin receptor subtype 2 in (**A**) BON-1, (**B**) GOT1, (**C**) NCI-H727 shown in an untreated control group (control) and following epigenetic treatment with hydralazine (50 µmol/L), valproic acid (1 mmol/L) or the combined treatment of hydralazine / valproic acid (H / VPA). Pictures were taken at 100x magnification.

SUPPLEMENTAL REFERENCES

1. Klomp, M.J.; Dalm, S.U.; van Koetsveld, P.M.; Dogan, F.; de Jong, M.; Hofland, L.J. Comparing the Effect of Multiple Histone Deacetylase Inhibitors on SSTR2 Expression and [(111)In]In-DOTATATE Uptake in NET Cells. *Cancers (Basel)* **2021**, *13*.
2. de Blois, E.; Chan, H.S.; de Zanger, R.; Konijnenberg, M.; Breeman, W.A. Application of single-vial ready-for-use formulation of 111In- or 177Lu-labelled somatostatin analogs. *Appl Radiat Isot* **2014**, *85*, 28-33.
3. Dalm, S.U.; Nonnekens, J.; Doeswijk, G.N.; de Blois, E.; van Gent, D.C.; Konijnenberg, M.W.; de Jong, M. Comparison of the Therapeutic Response to Treatment with a 177Lu-Labeled Somatostatin Receptor Agonist and Antagonist in Preclinical Models. *J Nucl Med* **2016**, *57*, 260-265.

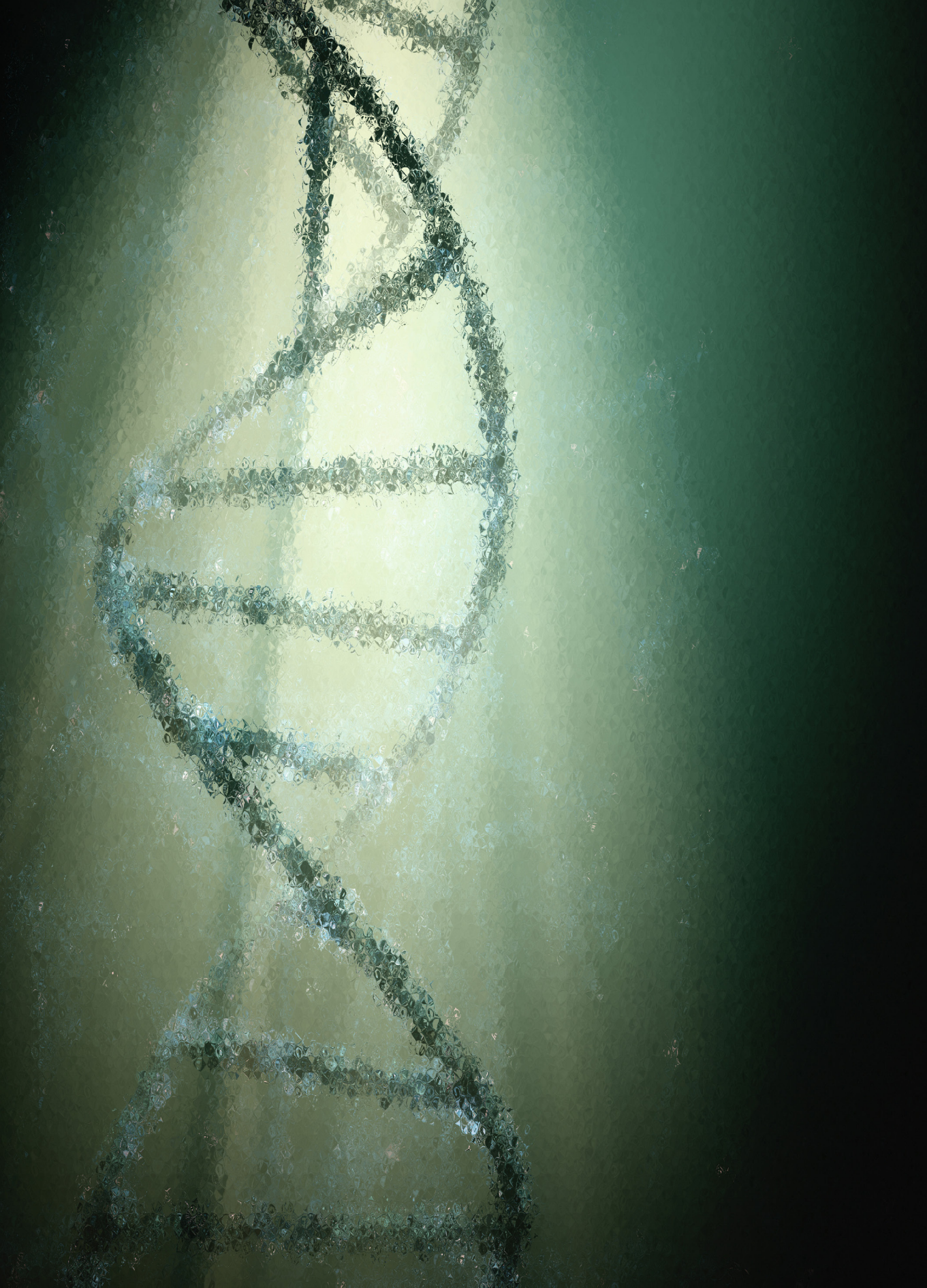

CHAPTER 8

General Discussion and Future Outlook

The previous chapters describe the studies that we have performed with the objective to increase somatostatin type-2 receptor (SSTR2) expression in neuroendocrine tumors (NETs) by epigenetic drug treatment. Moreover, we aimed to gain a better understanding of the role of the epigenetic machinery in the regulation of SSTR2 expression. Our ultimate aim is to increase the uptake of radiolabeled somatostatin analogues (SSAs) on NET cells and hereby improve the response to SSTR2-targeting therapy, better known as peptide receptor radionuclide therapy (PRRT). In this chapter, we provide an overview of the most essential findings of our studies and place these findings into a broader perspective. Moreover, we will discuss our future outlook with the aim of encouraging and directing research on SSTR2 upregulation by the use of epigenetic drugs in NETs.

1. GENERAL DISCUSSION AND FUTURE OUTLOOK

1.1. OPTIMIZING EPIGENETIC DRUG TREATMENT

To modify the epigenetic machinery for increasing SSTR2 expression levels and enhancing the uptake of radiolabeled SSAs (i.e. [^{177}Lu]Lu-, [^{111}In]In- and [^{68}Ga]Ga-DOTATATE), we used epigenetic drugs, i.e. DNA methyltransferase inhibitors (DNMTis) and histone deacetylase inhibitors (HDACis). Our studies were performed preclinically *in vitro* and *in vivo* using several cell lines, i.e. low SSTR2 expressing BON-1 (human pancreatic NET cell line), intermediate SSTR2 expressing NCI-H727 (human pulmonary carcinoid cell line), and the two high SSTR2 expressing cell lines GOT1 (human midgut NET cell line) and NCI-H69 (human small-cell lung carcinoma cell line). Additionally, we used subcutaneous xenografted mouse models derived from these cell lines and NET patient samples. Moreover, the effect of epigenetic drug treatment on the uptake of [^{68}Ga]Ga-DOTATATE was examined in NET patients.

1.1.1. *IN VITRO* RESULTS AFTER EPIGENETIC DRUG TREATMENT

In line with previous data described in literature [1-11], our *in vitro* experiments showed that both SSTR2 expression levels and radiolabeled SSA uptake were efficiently increased after epigenetic drug treatment (**Chapter 3, 4, 5 and 7**).

By screening a panel of six HDACis *in vitro*, we observed convincing stimulatory effects of HDACis on SSTR2 expression and [^{111}In]In-DOTATATE uptake, with the strongest effects observed after HDACi valproic acid (VPA) (**Chapter 3**). Because this HDACi is already clinically applied as an anticonvulsant and mood stabilizer, and, importantly, shown to be well tolerated, VPA is one of the most studied HDACis to increase SSTR2 expression and radiolabeled SSA uptake in NET cells [1-6]. Interestingly, we showed that VPA not only increased SSTR2 expression, but also enhanced the radiosensitivity of NET cells. This epigenetic drug has thus the potential to increase the outcome of PRRT via two mechanisms. The effect of epigenetic drug treatment on the radiosensitivity of tumor cells has previously been investigated for other epigenetic drugs as well. Treatment of QGP-1 pancreatic NET cells with a combination of DNMTi decitabine and HDACi CI-994 increased their radiosensitivity [10]. However, another

study did not find an altered radiosensitivity after epigenetic drug treatment when SSTR2-transfected HEK293 cells were exposed to the combination of decitabine and VPA [6]. This suggests that the radiosensitizing effects might depend on both the cell line and/or the applied epigenetic drug.

In addition to the tested HDACis, the effect of the DNMTi hydralazine was evaluated *in vitro* (**Chapter 7**). Significant changes in SSTR2 protein expression and [^{111}In]In-DOTATATE uptake were not observed after hydralazine monotreatment, whereas significant increased *SSTR2* mRNA expression levels were only shown in BON-1 and GOT1 cells. To the best of our knowledge, the effect of hydralazine on SSTR2 expression has not been evaluated before. In contrast, the effect of other DNMTis has been investigated. Although the observed effects were not univocal as it was not shown for all cell lines, treatment of NET cell lines with DNMTis azacitidine, decitabine or guadecitabine generally induced SSTR2 upregulation and increased radiolabeled SSA uptake [1, 9-11], demonstrating the potential for DNMTi-induced enhanced expression of SSTR2.

We also investigated the effect of combined VPA and hydralazine treatment (**Chapter 7**). Unfortunately, no synergistic effects on radiolabeled SSA uptake or SSTR2 protein expression were found. This is in line with the results reported by others where the DNMTi decitabine was combined with the HDACi trichostatin A [7] or the HDACi CI-994 [10]. However, other studies reported synergistic effects after combining DNMTis and HDACis. The combination of DNMTi decitabine and HDACi VPA [1, 6] and, contradictory to the previously mentioned report, treatment with the combination of DNMTi decitabine and HDACi CI-994 [9] were reported to result in synergistic effects on radiolabeled SSA uptake and/or the cytotoxic response to [^{177}Lu]Lu-DOTATATE. More research is needed to identify the underlying reason for these contradictory results, e.g. the applied epigenetic drugs, the used cell line models and/or the presence of a dose-dependent effect.

When comparing all the *in vitro* results we obtained, it was demonstrated that the increase in SSTR2 expression by epigenetic drug treatment was most evident in BON-1 cells, suggesting that the baseline SSTR2 expression level might be a determinant for the degree of response to epigenetic drug treatment (**Chapter 3 and 7**). This is in line with literature, e.g. the induced effects of CI-994, VPA and decitabine were more potent in low SSTR2-expressing BON-1 cells in comparison to the effects observed in NCI-H727 and/or GOT1 cells, both characterized by higher SSTR2 expression levels [5, 10]. This is further supported by a study by Guenter et al. [2] who described stronger effects of epigenetic drug treatment in low SSTR2 expressing pulmonary carcinoid cell lines and medullary thyroid cancer cell lines in comparison to cell lines with higher SSTR expression.

1.1.2. *IN VIVO* RESULTS AFTER EPIGENETIC DRUG TREATMENT

In addition to our extensive *in vitro* studies, we also performed preclinical *in vivo* studies. VPA, the most potent HDACi *in vitro,* did not alter SSTR2 expression levels *in vivo* (**Chapter 4**). In

contrast, increased SSTR2 expression levels were found in animals xenografted with NCI-H69 cells after treatment with a subset of HDACis (i.e. CI-994, MOC and PAN) (**Chapter 5**). However, in both of the mentioned *in vivo* studies no SSTR2-mediated increase in radiolabeled SSA uptake was observed, and thus further investigations are needed to optimize HDACi treatment to obtain the desired results. Apart from our studies, no preclinical *in vivo* studies are described in literature evaluating the effect of HDACi monotherapy on SSTR2 expression. In contrast, the effect of DNMTis on SSTR2 expression in tumor-bearing animals has been tested in two studies, i.e. the effects after treatment with decitabine [9] and guadecitabine [11] were evaluated in BON-1 tumor-bearing animals. Both these studies demonstrated positive results, in terms of increased tumoral SSTR2 expression levels, enhanced radiolabeled SSA uptake and/or improved tumor-to-background ratios. Moreover, Evans et al. [11] demonstrated that the combination of guadecitabine and [^{177}Lu]Lu-DOTATATE was well tolerated. However, the tumor size and survival rate were not improved in comparison to both monotherapies, requiring the need of further optimizations. The combination of decitabine and HDACi VPA has also been investigated in animals with tumors derived from pheochromocytoma cell lines. This study by Ullrich et al. [12] demonstrated an increased uptake of radiolabeled DOTATATE in a cell line which was characterized by low SSTR2 expression levels, but effects were absent in the studied cell lines characterized by high SSTR2 expression. The positive results observed in the low SSTR2 expressing cell line resulted in a significant decrease in tumor growth when PRRT was combined with the combination of epigenetic drugs in comparison to PRRT alone.

Overall, successful preclinical studies describing the survival rates and tumor growth delays after the combination of epigenetic drugs and PRRT are limited. Therefore, future studies should focus on significantly increasing the tumoral uptake of radiolabeled DOTATATE, followed by efficacy and survival studies for the combination treatment of epigenetic drugs and PRRT. Moreover, as epigenetic drugs might have anti-tumoral activity by themselves [13] and possibly also increase the radiosensitivity of the targeted cells, it is important to include proper controls to confirm the desired mechanism-of-action, i.e. epigenetic drug-induced SSTR2 upregulation.

In parallel, the effect of DNMTi hydralazine and HDACi VPA on [^{68}Ga]Ga-DOTATATE uptake was examined in NET patients (**Chapter 7**). Clinical studies were possible as both the epigenetic drugs and [^{68}Ga]Ga-DOTATATE are clinically approved. A clinical trial was performed in which NET patients with well-differentiated NETs of various origin were treated with hydralazine and VPA. The uptake of [^{68}Ga]Ga-DOTATATE was compared pre- versus post-epigenetic drug treatment. Unfortunately, no significant increase in the tumoral uptake of [^{68}Ga]Ga-DOTATATE was observed in our study. Thus far, only one additional clinical study on this topic has been published. In this study the effect of the HDACi vorinostat in NET patients was evaluated, demonstrating a significant increase in maximum standardized uptake value of the radiolabeled SSA [14]. However, results have to be confirmed in a larger sample size, and the effect of vorinostat on the efficacy of PRRT remains to be evaluated. The two clinical studies

are difficult to compare as different epigenetic drugs and treatment durations were applied. Moreover, another main difference is the patients' inclusion criteria, i.e. insufficient or sufficient baseline SSTR2 expression, respectively. More extensive future studies are therefore required to select the most appropriate epigenetic drug and to investigate which NET patients will benefit from epigenetic drug treatment.

Furthermore, these future studies should monitor the safety of the combination therapy. Of note, our preclinical *in vivo* results in mice showed that the kidneys are at risk when the HDACi VPA is combined with radiolabeled DOTATATE (**Chapter 4**). In line, in a recent systematic review by Anguissola et al. [15], it is described that VPA may also induce renal tubular injury in human. Additionally, we observed an increase in the renal uptake of [^{68}Ga]Ga-DOTATATE in patients after epigenetic drug treatment combining DNMTi hydralazine and HDACi VPA (**Chapter 7**). Moreover, it is known that the kidneys are the dose-limiting organ for PRRT [16]. Therefore, it is needed to pay special attention to potentially undesired renal SSTR2 upregulation and/or renal toxicity.

1.1.3. TRANSLATING *IN VITRO* RESULTS TO *IN VIVO* SETTING

Taken together, in contrast to the results obtained *in vitro*, the effects observed in tumor-bearing animals and NET patients were unsatisfactory. In both latter settings, no effect on tumoral radiolabeled DOTATATE uptake was observed. However, as mentioned above in tumor-bearing animals, a significant increased SSTR2 expression was obtained. Patient material was not analyzed in the clinical study, and thus it remains unknown whether a similar effect was also observed in the studied NET patients. For tumor-bearing animals, the increase in SSTR2 expression was most likely insufficient to enhance radiolabeled DOTATATE uptake. This can be a result of suboptimal HDACi doses reaching the tumor. Another explanation can be suboptimal timing with respect to radiolabeled SSA administration after HDACi treatment. In our *in vitro* studies we observed that effects on SSTR2 expression and radiolabeled SSA uptake were quickly induced after constant HDACi exposure. This constant and stable HDACi exposure is most likely not happening in the *in vivo* situation, which might hamper maximal SSTR2 upregulation. The daily HDACi administration regimen we applied might thus not be adequate to support sufficient SSTR2 upregulation. To achieve stable tumoral doses of the HDACi, it might be required to administer the epigenetic drug several times per day. The above-mentioned reasons might also apply to the clinical situation.

To pinpoint the exact reason why no increased tumoral radiolabeled DOTATATE uptake is observed *in vivo*, additional preclinical animal studies are needed. First, a proof-of-concept *in vivo* study should be performed, where the HDACis are administered intratumorally. This will enable to define the minimal required tumoral dose needed to significantly increase the uptake of radiolabeled DOTATATE *in vivo*. Second, it can be determined whether this tumoral dose can safely be reached after systemic administration.

To enable these experiments, it is required to develop methods to measure intratumoral HDACi drug levels, e.g. methods based on liquid chromatography with tandem mass spectrometry [17]. As alternative, although less straightforward, it may be possible to use radiolabeled HDACis. This has already been described for several HDACis, e.g. for valproic acid using carbon-11 ([^{11}C]VPA) [18] and for panobinostat using fluor-18 ([^{18}F]-panobinostat) [19]. These radiolabeled HDACis might be of use to determine the required tumoral HDACi dose for increased radiolabeled SSA uptake. However, even though the radionuclide is incorporated by a substitution reaction, it should be confirmed that the induced biological effects, HDACi tumor retention time and HDACi distribution are not changed.

Of note, the above-mentioned intratumoral injections can potentially be valuable to deliver a preclinical proof-of-concept, but this approach is not clinically relevant for NET patients with metastatic disease. Moreover, there is a possibility that systemic drug administration of a safe HDACi dose does not lead to sufficient tumoral dosages, e.g. due to the first-pass effect or the insufficient ability to pass through the epithelial membrane thereby lowering the concentration in the bloodstream [20]. Systemic administration might also have several disadvantages, e.g. SSTR2 upregulation in healthy/non-targeted organs. A targeted approach in which the HDACis are specifically delivered to the NET cells might offer a solution. Certain tumor-specific characteristics can be exploited, e.g. the enhanced permeability and retention effect can result into tumor-specific drug delivery, and pH-sensitive particles can release the drug content upon encountering the low pH of the tumor microenvironment [21]. Moreover, HDACis can be targeted to the tumor cells using a NET cell specific receptor characterized by high expression levels in patients showing low SSTR2 expression levels. There are several receptors which can be used for such a targeted approach. First, urokinase plasminogen activator receptor (uPAR), present in many cancers, is expressed on a significant number of neuroendocrine neoplasms (NENs) [22]. In a phase II clinical trial using an uPAR-targeting PET radiotracer, it was demonstrated that 68% of all patients, both low-grade and high-grade NENs, had uPAR-positive tumors [23]. Secondly, the glucose-dependent insulinotropic polypeptide receptor (GIPR) could be exploited for this purpose. Studies have reported a high incidence and density of GIPR in pancreatic, ileal and bronchial NETs [24], i.e. almost 95% of the examined NETs were characterized by GIPR expression [25]. Importantly, 89% of the SSTR negative NETs demonstrated GIPR. Lastly, it is known that cholecystokinin (CCK) receptors, vasoactive intestinal peptide (VIP) receptors and glucagon-like peptide (GLP-1) receptors are frequently overexpressed on NET tissues [26].

Although interesting, thorough investigations will be needed to explore tumor-targeting approaches for HDACi delivery to specifically upregulate SSTR2 expression on NET cells. So far, a few papers have described a tumor-targeting HDACi delivery system. For example, it has been demonstrated that micelles loaded with the HDACi thailandepsin-A and functionalized with SSAs (i.e. KE108 and octreotide) reduced tumor volume of BON-1 tumor-bearing animals with 92% and 74%, respectively, thereby inducing stronger effects in comparison to unloaded micelles [27, 28]. However, this study did not investigate if thailandepsin-A increased SSTR2

expression and whether this could potentiate PRRT efficacy via an enhanced uptake of a radiolabeled SSA. In addition to micelles, also nanoparticles or liposomes can be explored for this purpose [21, 29, 30]. The previously mentioned approaches are based on drug encapsulation, however, antibody-drug conjugates can be explored for an HDACi tumor-targeting method as well. This would entail the conjugation of an HDACi to an antibody directed towards a NET specific receptor [31, 32]. Moreover, the development of such a targeted approach for HDACi delivery might also be of interest for DNMTis or the combination of DNMTis and HDACis.

1.1.4. ELUCIDATING THE ASSOCIATION BETWEEN EPIGENETIC MARKS AND SSTR2

In addition to upregulating SSTR2 expression levels, we also aimed to gain a better understanding of the association between the epigenetic machinery and SSTR2 expression (**Chapter 5 and 6**).

First, we focused on unraveling the association between SSTR2 expression levels and the epigenetic profile in the SSTR2 promoter region in human tissues derived from small-intestinal NETs (SI-NETs) (**Chapter 6**). In this study, we showed that DNA methylation correlated inversely with *SSTR2* mRNA expression, and that this process is thus likely involved in regulating the expression of the receptor. In line with this, a significant relationship between DNA methylation in the SSTR2 promoter region and SSTR2 expression is also described for pancreatic NET samples in literature [33]. Although our study provided insightful information on the role of DNA methylation in SI-NET tissues, the role of histone marks in regulating SSTR2 expression remains unclear. As we did not find an association between SSTR2 expression and two extensively studied histone marks, i.e. histone methylation H3K27me3 and histone acetylation H3K9ac, more studies are required to evaluate the involvement of other histone marks [34]. Moreover, it is of value to focus on NETs of other origin, e.g. bronchial and pancreatic NETs, since NETs of different origin are characterized by different molecular alterations [35] and SSTR2 expression might thus be regulated differently in these subtypes.

Secondly, we focused on *SSTR2* and *HDAC* mRNA expression levels in the four cell lines used in our studies, and demonstrated that HDAC3 had a significant inverse correlation with SSTR2. This suggests that high HDAC3 expression might reduce SSTR2 expression (**Chapter 5**). To the best of our knowledge, there are no other studies in literature describing the direct association between HDACs and SSTR2 expression. Instead, studies focused more on the general role of HDACs in NETs [36, 37]. Obtaining detailed information on the association between HDAC and SSTR2 expression might facilitate the selection of epigenetic drugs which are most potent in increasing SSTR2 expression. Of note, studies should not only focus on HDAC expression levels, but should also study the HDAC enzyme activity.

The above-mentioned analyses would be of most value using human-derived NET tissues. Whereas enrichment at specific residues in the histones and mRNA expression levels might be

measured in fixated tissues, HDAC enzyme activity should be measured on freshly collected material. In addition to this, the use of primary cultures can be of value to validate that the selected HDACi induces strong effects in human tissue, i.e. an increase in SSTR2 expression and an improved response to PRRT. Together, this knowledge that can be obtained from these studies might not only provide basic insight into the association between epigenetic marks and SSTR2 expression, but it might also contribute to selecting the right group of NET patients who, based on their epigenetic profile, would benefit from the combination treatment of epigenetic drugs and PRRT.

1.2. OTHER APPROACHES TO IMPROVE SSTR2-TARGETING PRRT

In addition to epigenetic drug-induced SSTR2 upregulation, more approaches are currently under investigation to improve PRRT outcomes.

First, the potential of different radionuclides is tested, e.g. the α-emitters actinium-225 [38] and lead-212 [39-41]. These radionuclides emit short-range, high-energy particles, thereby potentially inducing more cytotoxic effects than β-particles. Moreover, the β-emitter terbium-161 is currently also under investigation. Terbium-161 can be superior to lutetium-177 as this radionuclide also emits auger electrons and conversion electrons that are characterized by a high linear energy transfer [42-44], whereas the physical properties of the β-particles are comparable [45]. Moreover, the presence of other terbium isotopes only emitting diagnostic radiation supports the use of this radionuclide for pre-therapeutic dosimetry and post-therapeutic imaging [45]. Secondly, structural changes to the radiopharmaceutical might increase the clinical potential, e.g. incorporation of an albumin-binding domain to increase the blood circulation time of the radiolabeled SSA, and thereby enhancing the tumoral uptake [46-48]. However, the increase in the radiation dose delivered to the kidneys and the bone marrow might hamper the clinical translation of this approach and should be monitored closely [49]. Additionally, the use of antagonists instead of agonists might improve PRRT outcomes, as a higher tumoral uptake is reported due to the presence of more binding sites in comparison to the binding sites available for agonists [50-53]. The first-in-human study using a lutetium-labeled SSTR antagonist showed that this radiotracer was generally well tolerated [53]. Lastly, research is focusing on radiosensitizing tumor cells, e.g. by using inhibitors of the DNA damage response such as poly(ADP-ribose) polymerase-1 (PARP) inhibitors, which intensifies the response to [^{177}Lu]Lu-DOTATATE as an increase in both the amount of double-stranded DNA breaks and tumor cell death in preclinical research was observed [54-56]. Clinical trials with the PARP inhibitors olaparib or talazoparib are currently ongoing [57-59].

2. CONCLUDING REMARKS

In conclusion, the studies described in this thesis shed light on the complexity of regulating SSTR2 expression by targeting the epigenetic machinery. Promising *in vitro* results were obtained when HDACis and/or DNMTis were applied for increasing SSTR2 expression levels.

In preclinical *in vivo* studies, we were able to significantly increase tumoral *SSTR2* mRNA and SSTR2 protein expression levels after HDACi treatment, but we did not achieve a significant increase in tumoral radiolabeled DOTATATE uptake. Nevertheless, the results obtained in terms of upregulation of SSTR2 expression in tumor-bearing animals is a first step towards increasing the uptake of radiolabeled SSA. More thorough investigations and optimizations are needed to obtain significant, and more importantly, clinically relevant effects. The complexity of the association between the epigenetic machinery and SSTR2 expression levels was further demonstrated in NET tissues and NET patients, as we only found significant correlations between SSTR2 expression and DNA methylation in the SSTR2 promoter, while correlations with histone marks were lacking, nor did we observe an increase in the tumoral uptake of radiolabeled DOTATATE after epigenetic drug treatment in patients.

Therefore, at present we are unable to give a conclusive answer to the question whether or not the combination of epigenetic drugs and SSTR2-targeted PRRT is a promising therapeutic approach for NET patients. Our studies gave a significant number of novel insights into the epigenetic regulation of SSTR2, but also highlighted the complexity of the epigenetic machinery. As extensively described above, more studies are thus required to further investigate this combination treatment strategy. The future will reveal whether epigenetic drugs can contribute to improve PRRT outcome for NET patients.

REFERENCES

1. Veenstra, M.J.; van Koetsveld, P.M.; Dogan, F.; Farrell, W.E.; Feelders, R.A.; Lamberts, S.W.J.; de Herder, W.W.; Vitale, G.; Hofland, L.J. Epidrug-induced upregulation of functional somatostatin type 2 receptors in human pancreatic neuroendocrine tumor cells. *Oncotarget* **2018**, *9*, 14791-14802.
2. Guenter, R.E.; Aweda, T.; Carmona Matos, D.M.; Whitt, J.; Chang, A.W.; Cheng, E.Y.; Liu, X.M.; Chen, H.; Lapi, S.E.; Jaskula-Sztul, R. Pulmonary Carcinoid Surface Receptor Modulation Using Histone Deacetylase Inhibitors. *Cancers (Basel)* **2019**, *11*.
3. Guenter, R.; Aweda, T.; Carmona Matos, D.M.; Jang, S.; Whitt, J.; Cheng, Y.Q.; Liu, X.M.; Chen, H.; Lapi, S.E.; Jaskula-Sztul, R. Overexpression of somatostatin receptor type 2 in neuroendocrine tumors for improved Ga68-DOTATATE imaging and treatment. *Surgery* **2020**, *167*, 189-196.
4. Sun, L.; Qian, Q.; Sun, G.; Mackey, L.V.; Fuselier, J.A.; Coy, D.H.; Yu, C.Y. Valproic acid induces NET cell growth arrest and enhances tumor suppression of the receptor-targeted peptide-drug conjugate via activating somatostatin receptor type II. *J Drug Target* **2016**, *24*, 169-177.
5. Arvidsson, Y.; Johanson, V.; Pfragner, R.; Wängberg, B.; Nilsson, O. Cytotoxic Effects of Valproic Acid on Neuroendocrine Tumour Cells. *Neuroendocrinology* **2016**, *103*, 578-591.
6. Kotzerke, J.; Buesser, D.; Naumann, A.; Runge, R.; Huebinger, L.; Kliewer, A.; Freudenberg, R.; Brogsitter, C. Epigenetic-Like Stimulation of Receptor Expression in SSTR2 Transfected HEK293 Cells as a New Therapeutic Strategy. *Cancers (Basel)* **2022**, *14*.
7. Torrisani, J.; Hanoun, N.; Laurell, H.; Lopez, F.; Maoret, J.J.; Souque, A.; Susini, C.; Cordelier, P.; Buscail, L. Identification of an upstream promoter of the human somatostatin receptor, hSSTR2, which is controlled by epigenetic modifications. *Endocrinology* **2008**, *149*, 3137-3147.
8. Wanek, J.; Gaisberger, M.; Beyreis, M.; Mayr, C.; Helm, K.; Primavesi, F.; Jager, T.; Di Fazio, P.; Jakab, M.; Wagner, A., et al. Pharmacological Inhibition of Class IIA HDACs by LMK-235 in Pancreatic Neuroendocrine Tumor Cells. *Int J Mol Sci* **2018**, *19*.
9. Taelman, V.F.; Radojewski, P.; Marincek, N.; Ben-Shlomo, A.; Grotzky, A.; Olariu, C.I.; Perren, A.; Stettler, C.; Krause, T.; Meier, L.P., et al. Upregulation of Key Molecules for Targeted Imaging and Therapy. *J Nucl Med* **2016**, *57*, 1805-1810.
10. Jin, X.F.; Auernhammer, C.J.; Ilhan, H.; Lindner, S.; Nolting, S.; Maurer, J.; Spottl, G.; Orth, M. Combination of 5-Fluorouracil with Epigenetic Modifiers Induces Radiosensitization, Somatostatin Receptor 2 Expression, and Radioligand Binding in Neuroendocrine Tumor Cells In Vitro. *J Nucl Med* **2019**, *60*, 1240-1246.
11. Evans, J.S.; Beaumont, J.; Braga, M.; Masrour, N.; Mauri, F.; Beckley, A.; Butt, S.; Karali, C.S.; Cawthorne, C.; Archibald, S., et al. Epigenetic potentiation of somatostatin-2 by guadecitabine in neuroendocrine neoplasias as a novel method to allow delivery of peptide receptor radiotherapy. *European Journal of Cancer* **2022**, *176*, 110-120.
12. Ullrich, M.; Richter, S.; Liers, J.; Drukewitz, S.; Friedemann, M.; Kotzerke, J.; Ziegler, C.G.; Nölting, S.; Kopka, K.; Pietzsch, J. Epigenetic drugs in somatostatin type 2 receptor radionuclide theranostics and radiation transcriptomics in mouse pheochromocytoma models. *Theranostics* **2023**, *13*, 278-294.
13. Eckschlager, T.; Plch, J.; Stiborova, M.; Hrabeta, J. Histone Deacetylase Inhibitors as Anticancer Drugs. *Int J Mol Sci* **2017**, *18*.
14. Pollard, J.H.; Menda, Y.; Zamba, K.D.; Madsen, M.; O'Dorisio, M.S.; O'Dorisio, T.; Bushnell, D. Potential for Increasing Uptake of Radiolabeled (68)Ga-DOTATOC and (123)I-MIBG in Patients with Midgut Neuroendocrine Tumors Using a Histone Deacetylase Inhibitor Vorinostat. *Cancer Biother Radiopharm* **2021**, *36*, 632-641.
15. Anguissola, G.; Leu, D.; Simonetti, G.D.; Simonetti, B.G.; Lava, S.A.G.; Milani, G.P.; Bianchetti, M.G.; Scoglio, M. Kidney tubular injury induced by valproic acid: systematic literature review. *Pediatr Nephrol* **2023**, *38*, 1725-1731.
16. Geenen, L.; Nonnekens, J.; Konijnenberg, M.; Baatout, S.; De Jong, M.; Aerts, A. Overcoming nephrotoxicity in peptide receptor radionuclide therapy using [177Lu]Lu-DOTA-TATE for the treatment of neuroendocrine tumours. *Nuclear Medicine and Biology* **2021**, *102-103*, 1-11.

17. Kiesel, B.F.; Parise, R.A.; Tjørnelund, J.; Christensen, M.K.; Loza, E.; Tawbi, H.; Chu, E.; Kummar, S.; Beumer, J.H. LC-MS/MS assay for the quantitation of the HDAC inhibitor belinostat and five major metabolites in human plasma. *J Pharm Biomed Anal* **2013**, *81-82*, 89-98.
18. Kim, S.W.; Hooker, J.M.; Otto, N.; Win, K.; Muench, L.; Shea, C.; Carter, P.; King, P.; Reid, A.E.; Volkow, N.D., et al. Whole-body pharmacokinetics of HDAC inhibitor drugs, butyric acid, valproic acid and 4-phenylbutyric acid measured with carbon-11 labeled analogs by PET. *Nucl Med Biol* **2013**, *40*, 912-918.
19. Kommidi, H.; Tosi, U.; Maachani, U.B.; Guo, H.; Marnell, C.S.; Law, B.; Souweidane, M.M.; Ting, R. (18)F-Radiolabeled Panobinostat Allows for Positron Emission Tomography Guided Delivery of a Histone Deacetylase Inhibitor. *ACS Med Chem Lett* **2018**, *9*, 114-119.
20. Kim, J.; De Jesus, O. Medication Routes of Administration. **2023**.
21. Yao, Y.; Zhou, Y.; Liu, L.; Xu, Y.; Chen, Q.; Wang, Y.; Wu, S.; Deng, Y.; Zhang, J.; Shao, A. Nanoparticle-Based Drug Delivery in Cancer Therapy and Its Role in Overcoming Drug Resistance. *Frontiers in Molecular Biosciences* **2020**, *7*.
22. Mahmood, N.; Rabbani, S.A. Fibrinolytic System and Cancer: Diagnostic and Therapeutic Applications. *Int J Mol Sci* **2021**, *22*.
23. Carlsen, E.A.; Loft, M.; Loft, A.; Berthelsen, A.K.; Langer, S.W.; Knigge, U.; Kjaer, A. Prospective Phase II Trial of Prognostication by (68)Ga-NOTA-AE105 uPAR PET in Patients with Neuroendocrine Neoplasms: Implications for uPAR-Targeted Therapy. *J Nucl Med* **2022**, *63*, 1371-1377.
24. Reubi, J.C.; Fourmy, D.; Cordomi, A.; Tikhonova, I.G.; Gigoux, V. GIP receptor: Expression in neuroendocrine tumours, internalization, signalling from endosomes and structure-function relationship studies. *Peptides* **2020**, *125*, 170229.
25. Waser, B.; Rehmann, R.; Sanchez, C.; Fourmy, D.; Reubi, J.C. Glucose-dependent insulinotropic polypeptide receptors in most gastroenteropancreatic and bronchial neuroendocrine tumors. *J Clin Endocrinol Metab* **2012**, *97*, 482-488.
26. Reubi, J.C.; Waser, B. Concomitant expression of several peptide receptors in neuroendocrine tumours: molecular basis for in vivo multireceptor tumour targeting. *European Journal of Nuclear Medicine and Molecular Imaging* **2003**, *30*, 781-793.
27. Chen, G.; Jaskula-Sztul, R.; Harrison, A.; Dammalapati, A.; Xu, W.; Cheng, Y.; Chen, H.; Gong, S. KE108-conjugated unimolecular micelles loaded with a novel HDAC inhibitor thailandepsin-A for targeted neuroendocrine cancer therapy. *Biomaterials* **2016**, *97*, 22-33.
28. Jaskula-Sztul, R.; Xu, W.; Chen, G.; Harrison, A.; Dammalapati, A.; Nair, R.; Cheng, Y.; Gong, S.; Chen, H. Thailandepsin A-loaded and octreotide-functionalized unimolecular micelles for targeted neuroendocrine cancer therapy. *Biomaterials* **2016**, *91*, 1-10.
29. Riaz, M.K.; Riaz, M.A.; Zhang, X.; Lin, C.; Wong, K.H.; Chen, X.; Zhang, G.; Lu, A.; Yang, Z. Surface Functionalization and Targeting Strategies of Liposomes in Solid Tumor Therapy: A Review. *Int J Mol Sci* **2018**, *19*.
30. Zhang, Y.; Huang, Y.; Li, S. Polymeric micelles: nanocarriers for cancer-targeted drug delivery. *AAPS PharmSciTech* **2014**, *15*, 862-871.
31. Si, Y.; Kim, S.; Ou, J.; Lu, Y.; Ernst, P.; Chen, K.; Whitt, J.; Carter, A.M.; Markert, J.M.; Bibb, J.A., et al. Anti-SSTR2 antibody-drug conjugate for neuroendocrine tumor therapy. *Cancer Gene Ther* **2021**, *28*, 799-812.
32. Cini, E.; Faltoni, V.; Petricci, E.; Taddei, M.; Salvini, L.; Giannini, G.; Vesci, L.; Milazzo, F.M.; Anastasi, A.M.; Battistuzzi, G., et al. Antibody drug conjugates (ADCs) charged with HDAC inhibitor for targeted epigenetic modulation. *Chem Sci* **2018**, *9*, 6490-6496.
33. Evans, J.S.; Beaumont, J.; Braga, M.; Masrour, N.; Mauri, F.; Beckley, A.; Butt, S.; Karali, C.S.; Cawthorne, C.; Archibald, S., et al. Epigenetic potentiation of somatostatin-2 by guadecitabine in neuroendocrine neoplasias as a novel method to allow delivery of peptide receptor radiotherapy. *Eur J Cancer* **2022**, *176*, 110-120.
34. Alaskhar Alhamwe, B.; Khalaila, R.; Wolf, J.; von Bulow, V.; Harb, H.; Alhamdan, F.; Hii, C.S.; Prescott, S.L.; Ferrante, A.; Renz, H., et al. Histone modifications and their role in epigenetics of atopy and allergic diseases. *Allergy Asthma Clin Immunol* **2018**, *14*, 39.

35. Scarpa, A. The landscape of molecular alterations in pancreatic and small intestinal neuroendocrine tumours. *Ann Endocrinol (Paris)* **2019**, *80*, 153-158.
36. Mafficini, A.; Scarpa, A. Genetics and Epigenetics of Gastroenteropancreatic Neuroendocrine Neoplasms. *Endocr Rev* **2019**, *40*, 506-536.
37. Crabtree, J.S. Epigenetic Regulation in Gastroenteropancreatic Neuroendocrine Tumors. *Front Oncol* **2022**, *12*, 901435.
38. Ballal, S.; Yadav, M.P.; Bal, C.; Sahoo, R.K.; Tripathi, M. Broadening horizons with (225)Ac-DOTATATE targeted alpha therapy for gastroenteropancreatic neuroendocrine tumour patients stable or refractory to (177)Lu-DOTATATE PRRT: first clinical experience on the efficacy and safety. *Eur J Nucl Med Mol Imaging* **2020**, *47*, 934-946.
39. Delpassand, E.S.; Tworowska, I.; Esfandiari, R.; Torgue, J.; Hurt, J.; Shafie, A.; Núñez, R. Targeted α-Emitter Therapy with (212)Pb-DOTAMTATE for the Treatment of Metastatic SSTR-Expressing Neuroendocrine Tumors: First-in-Humans Dose-Escalation Clinical Trial. *J Nucl Med* **2022**, *63*, 1326-1333.
40. *NCT03466216: Phase 1 Study of AlphaMedix™ in Adult Subjects With SSTR (+) NET*. [cited 2023-04-03]; Available from: https://clinicaltrials.gov/ct2/show/NCT03466216.
41. *NCT05153772: Targeted Alpha-emitter Therapy of PRRT Naive Neuroendocrine Tumor Patients (ALPHAMEDIX02)*. [cited 2023- 04-03]; Available from: https://clinicaltrials.gov/ct2/show/NCT05153772.
42. Baum, R.P.; Singh, A.; Kulkarni, H.R.; Bernhardt, P.; Rydén, T.; Schuchardt, C.; Gracheva, N.; Grundler, P.V.; Köster, U.; Müller, D., et al. First-in-Human Application of Terbium-161: A Feasibility Study Using ¹⁶¹Tb-DOTATOC. *Journal of Nuclear Medicine* **2021**, jnumed.120.258376.
43. *NCT05359146: Combined Beta- Plus Auger Electron Therapy Using a Novel Somatostatin Receptor Subtype 2 Antagonist Labelled With Terbium-161 (161Tb-DOTA-LM3) (Beta plus)*. [cited 2023- 04-03]; Available from: https://clinicaltrials.gov/ct2/show/NCT05359146.
44. Borgna, F.; Barritt, P.; Grundler, P.V.; Talip, Z.; Cohrs, S.; Zeevaart, J.R.; Köster, U.; Schibli, R.; van der Meulen, N.P.; Müller, C. Simultaneous Visualization of (161)Tb- and (177)Lu-Labeled Somatostatin Analogues Using Dual-Isotope SPECT Imaging. *Pharmaceutics* **2021**, *13*.
45. Haller, S.; Pellegrini, G.; Vermeulen, C.; van der Meulen, N.P.; Köster, U.; Bernhardt, P.; Schibli, R.; Müller, C. Contribution of Auger/conversion electrons to renal side effects after radionuclide therapy: preclinical comparison of (161)Tb-folate and (177)Lu-folate. *EJNMMI Res* **2016**, *6*, 13.
46. Liu, Q.; Zang, J.; Sui, H.; Ren, J.; Guo, H.; Wang, H.; Wang, R.; Jacobson, O.; Zhang, J.; Cheng, Y., et al. Peptide Receptor Radionuclide Therapy of Late-Stage Neuroendocrine Tumor Patients with Multiple Cycles of (177)Lu-DOTA-EB-TATE. *J Nucl Med* **2021**, *62*, 386-392.
47. *NCT03478358: Treatment Using 177Lu-DOTA-EB-TATE in Patients With Advanced Neuroendocrine Tumors*. [cited 2023- 04-03]; Available from: https://clinicaltrials.gov/ct2/show/NCT03478358.
48. *NCT05475210: 177Lu-DOTA-EB-TATE in Untreated (Naïve) Adult Patients With Advanced, Well-Differentiated Neuroendocrine Tumors*. [cited 2023- 04-03]; Available from: https://clinicaltrials.gov/ct2/show/NCT05475210.
49. Zhang, J.; Wang, H.; Jacobson, O.; Cheng, Y.; Niu, G.; Li, F.; Bai, C.; Zhu, Z.; Chen, X. Safety, Pharmacokinetics, and Dosimetry of a Long-Acting Radiolabeled Somatostatin Analog (177)Lu-DOTA-EB-TATE in Patients with Advanced Metastatic Neuroendocrine Tumors. *J Nucl Med* **2018**, *59*, 1699-1705.
50. Dalm, S.U.; Nonnekens, J.; Doeswijk, G.N.; de Blois, E.; van Gent, D.C.; Konijnenberg, M.W.; de Jong, M. Comparison of the Therapeutic Response to Treatment with a 177Lu-Labeled Somatostatin Receptor Agonist and Antagonist in Preclinical Models. *J Nucl Med* **2016**, *57*, 260-265.
51. Ginj, M.; Zhang, H.; Waser, B.; Cescato, R.; Wild, D.; Wang, X.; Erchegyi, J.; Rivier, J.; Mäcke, H.R.; Reubi, J.C. Radiolabeled somatostatin receptor antagonists are preferable to agonists for in vivo peptide receptor targeting of tumors. *Proc Natl Acad Sci U S A* **2006**, *103*, 16436-16441.

52. Krebs, S.; O'Donoghue, J.A.; Biegel, E.; Beattie, B.J.; Reidy, D.; Lyashchenko, S.K.; Lewis, J.S.; Bodei, L.; Weber, W.A.; Pandit-Taskar, N. Comparison of (68)Ga-DOTA-JR11 PET/CT with dosimetric (177)Lu-satoreotide tetraxetan ((177)Lu-DOTA-JR11) SPECT/CT in patients with metastatic neuroendocrine tumors undergoing peptide receptor radionuclide therapy. *Eur J Nucl Med Mol Imaging* **2020**, *47*, 3047-3057.
53. Baum, R.P.; Zhang, J.; Schuchardt, C.; Müller, D.; Mäcke, H. First-in-Humans Study of the SSTR Antagonist (177)Lu-DOTA-LM3 for Peptide Receptor Radionuclide Therapy in Patients with Metastatic Neuroendocrine Neoplasms: Dosimetry, Safety, and Efficacy. *J Nucl Med* **2021**, *62*, 1571-1581.
54. Cullinane, C.; Waldeck, K.; Kirby, L.; Rogers, B.E.; Eu, P.; Tothill, R.W.; Hicks, R.J. Enhancing the anti-tumour activity of (177)Lu-DOTA-octreotate radionuclide therapy in somatostatin receptor-2 expressing tumour models by targeting PARP. *Sci Rep* **2020**, *10*, 10196.
55. Nonnekens, J.; van Kranenburg, M.; Beerens, C.E.; Suker, M.; Doukas, M.; van Eijck, C.H.; de Jong, M.; van Gent, D.C. Potentiation of Peptide Receptor Radionuclide Therapy by the PARP Inhibitor Olaparib. *Theranostics* **2016**, *6*, 1821-1832.
56. Feijtel, D.; Reuvers, T.G.A.; van Tuyll-van Serooskerken, C.; de Ridder, C.M.A.; Stuurman, D.C.; de Blois, E.; Verkaik, N.S.; de Bruijn, P.; Koolen, S.L.W.; de Jong, M., et al. In Vivo Efficacy Testing of Peptide Receptor Radionuclide Therapy Radiosensitization Using Olaparib. *Cancers (Basel)* **2023**, *15*.
57. *NCT04086485: Lu-177-DOTATATE (Lutathera) in Combination With Olaparib in Inoperable Gastroenteropancreatico Neuroendocrine Tumors (GEP-NET)*. [cited 2023- 04-03]; Available from: https://clinicaltrials.gov/ct2/show/NCT04086485.
58. *NCT04375267: 177Lu-DOTA-TATE and Olaparib in Somatostatin Receptor Positive Tumours (LuPARP)*. [cited 2023- 04-03]; Available from: https://clinicaltrials.gov/ct2/show/NCT04375267.
59. *NCT05053854: PARP Inhibitor With 177Lu-DOTA-Octreotate PRRT in Patients With Neuroendocrine Tumours (PARLuNET)*. [cited 2023- 04-03]; Available from: https://clinicaltrials.gov/ct2/show/NCT05053854.

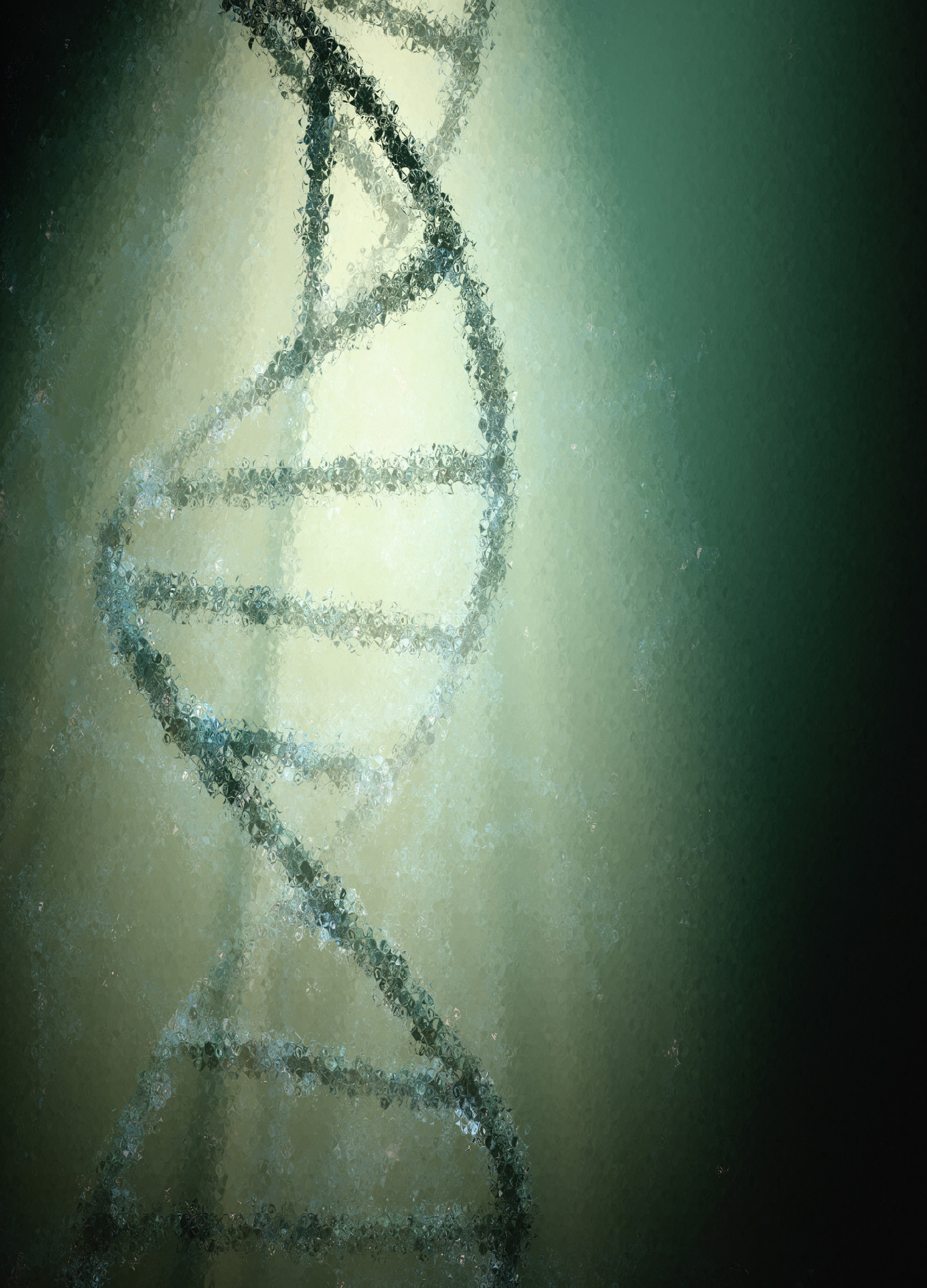

APPENDIX

SUMMARY

The overexpression of somatostatin type-2 receptors (SSTR2) on neuroendocrine tumor (NET) cells forms a pivotal biomarker for theranostic approaches. Radiolabeled somatostatin analogues (SSAs), most frequently [^{68}Ga]Ga-DOTATATE and [^{177}Lu]Lu-DOTATATE for PET nuclear imaging and therapy, respectively, have shown to be of great importance for NET disease management. [^{177}Lu]Lu-DOTATATE treatment, known as peptide receptor radionuclide therapy (PRRT), is EMA and FDA approved for SSTR2-positive gastroenteropancreatic NET patients. However, complete responses are rare and progressive disease after treatment is often observed. Approaches to further improve PRRT efficacy are thus of great need. In this thesis, we aim to upregulate SSTR2 on NET cells by modulating the epigenetic machinery, in order to increase radiolabeled SSA uptake and ultimately improve treatment response. Furthermore, we aimed to gain more insights into the interaction between epigenetic marks and the regulation of SSTR2 expression.

In **Chapter 2** we provide an overview of the involvement of the epigenetic machinery in regulating the expression of the neuropeptide somatostatin (SST) and somatostatin receptors (SSTRs). Our main focus was on NETs, but the involvement of the epigenetic machinery in regulating SST and SSTRs in other cancer types was also discussed. Additionally, we described how the epigenetic machinery can be modulated to alter the expression of both the neuropeptide and the corresponding receptors.

Next, in **Chapter 3** we evaluated the effects of several histone deacetylase inhibitors (HDACis) on *SSTR2* mRNA expression level and uptake of [^{111}In]In-DOTATATE. The effects of these epigenetic drugs were tested in three NET cell lines, i.e. the human pancreatic NET cell line BON-1, the pulmonary carcinoid cell line NCI-H727 and the human midgut NET cell line GOT1, which are characterized by low, intermediate and high SSTR2 baseline expression levels, respectively. Our studies demonstrated that HDACi treatment increased both *SSTR2* mRNA expression levels and the uptake of [^{111}In]In-DOTATATE in all three cell lines. The strongest effects were observed for the BON-1 cell line, which had lowest SSTR2 expression, suggesting that baseline SSTR2 expression levels might be a determinant for the extent of SSTR2 upregulation by the HDACis. Additionally, we showed that the induced effects were generally reversible within seven days after HDACi withdrawal, showing the strongest reduction within the first day. Of the tested HDACis, the most promising effects were observed after valproic acid (VPA) treatment. This HDACi not only increased SSTR2 expression, but also increased the radiosensitivity of the NET cells, and thus has the potential to increase PRRT efficacy via two mechanisms.

Subsequently, we investigated the effect of VPA in mice xenografted with the human small cell lung carcinoma cell line NCI-H69, which is characterized by a relatively high baseline SSTR2 expression level (**Chapter 4**). First, we confirmed the effect of VPA on SSTR2 expression *in vitro* and demonstrated that, as expected, SSTR2 expression was enhanced and that this occurred

quickly after the start of HDACi treatment. On the basis of the positive results obtained in the *in vitro* study, we evaluated the effect of a single injection of VPA (low or high dose) on the uptake of radiolabeled SSA *in vivo*, following two treatment schedules with regards to the time between VPA and [^{177}Lu]Lu-DOTATATE injection (four and eight hours). When VPA was administered four hours prior to [^{177}Lu]Lu-DOTATATE injection, no significant increase in the tumoral uptake of [^{177}Lu]Lu-DOTATATE was observed. A significantly increased tumoral uptake was observed when VPA was administered eight hours prior to radiolabeled SSA injection, independent of the VPA dose administered. However, we found that this was not caused by an increased tumoral SSTR2 expression level. Instead, this was likely the consequence of renal toxicity observed in HDACi-treated animals, which, in turn, leads to an increase in blood circulation time of [^{177}Lu]Lu-DOTATATE. We hypothesize that the observed toxicity was caused by the combination of VPA and (radiolabeled) SSA, ultimately leading to an increased tumoral radiolabeled SSA uptake.

As VPA treatment did not result in SSTR2 upregulation *in vivo* in NCI-H69 xenografted mice and a higher VPA dose was not feasible due to the observed renal toxicity, a panel of five other HDACis was tested in this animal model. The results of these studies are described in **Chapter 5**. Animals were injected with the HDACis three times on three consecutive days, following radiolabeled SSA injection two hours after the last HDACi injection. Although HDACis mocetinostat, CI-994 and panobinostat (PAN) increased tumoral *SSTR2* mRNA expression levels, and SSTR2 protein expression levels were enhanced significantly after CI-994 treatment, a significant increase in the tumoral uptake of [^{177}Lu]Lu-DOTATATE was lacking. To confirm these findings, and to overcome model-dependent outcomes, the effect of PAN was also tested in BON-1 tumor-bearing animals. Even though PAN induced stronger effects in BON-1 cells in comparison to NCI-H69 cells cultured *in vitro*, BON-1 tumor-bearing animals treated with PAN also did not show a significant increase in tumoral uptake of the radiolabeled SSA. In line with what was observed in NCI-H69 xenografts, *SSTR2* mRNA expression levels were upregulated significantly in PAN-treated BON-1 xenografts, and no statistically significant effects on SSTR2 protein expression levels were observed. To better interpret and understand our findings, NCI-H69 and BON-1 xenografts and cell lines were further evaluated in terms of *SSTR2* and *HDAC* mRNA expression levels. Our analysis showed that six out of the eleven tested HDACs were significantly higher expressed in BON-1 xenografts. Moreover, analysis of the mRNA expression levels of these six HDACs and SSTR2 in NCI-H69, BON-1, NCI-H727 and GOT1 cells showed that the expression of HDAC3 was inversely correlated with the levels of SSTR2 expression, suggesting that HDAC3 may be involved in regulating SSTR2 expression. Despite this HDAC being significantly higher expressed in BON-1 xenografts than in NCI-H69 xenografts, the uptake of radiolabeled DOTATATE was not changed in response to PAN, emphasizing the need to optimize the HDACi treatment regimen, e.g. changing dose and/or timing, or by the development of a tumor-targeting approach. Moreover, a further unraveling of the association between SSTR2 and HDACs might give novel insights facilitating these future studies.

In **Chapter 6**, we used primary well-differentiated small-intestinal NET (SI-NET) tissues to gain better insight in which epigenetic marks are involved in regulating SSTR2 expression levels. It was demonstrated that DNA methylation levels and histone methylation levels were significantly decreased in SI-NET tissue in comparison to normal SI-tissue. Moreover, for both SI-NET and SI-tissues, a significant inverse correlation was found between *SSTR2* mRNA expression levels and the mean level of DNA methylation on CpG positions within the SSTR2 promoter region. No significant correlations were found between SSTR2 expression levels and enrichment of the suppressive histone methylation mark H3K27me3 and the activating histone acetylation mark H3K9ac. In summary, our data suggests that DNA methylation is involved in regulating SSTR2 expression in both SI-NET tissue and SI-tissue. The exact role of histone modifications remains to be further elucidated.

In **Chapter 7**, the results of a prospective clinical proof-of-concept trial are described in which the effect of VPA (HDACi) and hydralazine (DNA methyltransferase inhibitor) on the uptake of radiolabeled DOTATATE was evaluated in nine NET patients with low baseline SSTR2 expression levels. No significant difference was observed in the tumoral peak uptake of radiolabeled DOTATATE on the PET/CT scan pre- versus post-epigenetic drug treatment. The reason for the absent effects remains unclear, and stresses the need for further investigations. In this future research, the safety of the combination treatment should be monitored closely, as we observed an increase in radioactivity in the kidneys post-epigenetic drug treatment.

To conclude, **Chapter 8** provides an overview of the most essential findings of the above-mentioned studies and places these findings into a broader perspective. Moreover, possible future perspectives and recommendations are discussed with the aim to encourage and direct research on relevant questions regarding SSTR2 upregulation using epigenetic drugs.

NEDERLANDSE SAMENVATTING

De somatostatine receptor subtype-2 (SSTR2) komt sterk tot expressie op neuro-endocriene tumor (NET) cellen, en is daarmee een interessante biomarker voor de ontwikkeling van anti-kanker interventies voor patiënten met deze tumoren. Radioactief gelabelde somatostatine analogen (SSAs) worden dan ook succesvol toegepast voor de beeldvorming en behandeling van NETs. Hierbij wordt [^{68}Ga]Ga-DOTATATE gebruikt om met behulp van positron emissie tomografie (PET) tumoren in beeld te brengen, en wordt [^{177}Lu]Lu-DOTATATE gebruikt voor de behandeling. De laatstgenoemde behandeling staat ook wel bekend als peptide receptor radionuclide therapie (PRRT), en is goedgekeurd door de EMA en FDA voor de behandeling van patiënten met SSTR2-positieve gastro-enteropancreatische NETs. Volledige genezing na PRRT is echter zeldzaam en progressieve ziekte wordt vaak waargenomen na behandeling. Er is dus noodzaak om de effectiviteit van PRRT te verbeteren. Het overkoepelende doel van de studies beschreven in dit proefschrift is om de SSTR2 expressie op NET cellen te verhogen zodat de opname van radioactief-gelabeld SSA toeneemt en de tumoren aan een hogere dosis radioactiviteit worden blootgesteld. De verwachting is dat dit uiteindelijk zal resulteren in een verbeterde response op PRRT. Om de SSTR2 expressie te verhogen hebben we ons gericht op de epigenetica, n.l. het modificeren van het epigenetische profiel gebruikmakende van epigenetische medicijnen. Tevens hebben we ons gericht op het beter inzichtelijk maken van de interactie tussen het epigenetische profiel en SSTR2 expressie in NETs.

In **Hoofdstuk 2** geven we een overzicht van de bestaande literatuur waaruit blijkt dat epigenetische mechanismen betrokken zijn bij het reguleren van zowel de somatostatine receptoren (SSTRs), als het natuurlijke ligand van deze receptoren; somatostatine (SST). De focus van de literatuurstudie lag vooral op NETs, maar ook de betrokkenheid van epigenetische mechanismen in andere kankersoorten wordt besproken. Daarnaast wordt beschreven hoe epigenetische mechanismen gemoduleerd kunnen worden voor het reguleren van de expressie van zowel SST als SSTRs.

In **Hoofdstuk 3** hebben we getest hoe verschillende epigenetische medicijnen, genaamd histon deacetylase remmers (HDACis), de hoeveelheid *SSTR2* mRNA en de opname van radioactief-gelabeld SSA beïnvloeden. De effecten van deze epigenetische medicijnen werden *in vitro* geëvalueerd in drie humane NET cellijn modellen; BON-1 ontstaan uit een pancreas NET, NCI-H727 ontstaan uit een pulmonale carcinoïd en GOT1 ontstaan uit een middendarm NET. Deze drie cellijnen worden gekenmerkt door een respectievelijk lage, intermediaire en hoge SSTR2 expressie. In alle drie de cellijnen verhoogde HDACi behandeling zowel de hoeveelheid *SSTR2* mRNA als de opname van radioactief-gelabeld SSA. In BON-1 cellen, gekenmerkt door een lage SSTR2 expressie, werd de grootste toename in zowel *SSTR2* expressie als opname van radioactief-gelabeld SSA waargenomen, wat kan suggereren dat de hoeveelheid SSTR2 expressie voor de start van behandeling bepalend kan zijn voor de mate waarin er een effect optreedt na HDACi behandeling. Ook bleken de geïnduceerde effecten grotendeels reversibel en werd de sterkste afname in de hoeveelheid *SSTR2* mRNA

waargenomen in de eerste dag na het beëindigen van HDACi behandeling. Uit resultaten van de bovengenoemde studie bleek valproïnezuur (VPA) de meest veelbelovende HDACi te zijn. Naast het verhogen van de SSTR2 expressie, zorgde VPA ook voor een verhoogde radiosensitiviteit. VPA kan hiermee mogelijk de effectiviteit van PRRT via twee mechanismen verhogen; (1) door de opname van radioactief-gelabeld SSA te verhogen en (2) door de NET cellen gevoeliger te maken voor straling.

Volgend op de positieve resultaten verkregen in **Hoofdstuk 3**, richt **Hoofdstuk 4** zich op het effect van VPA op SSTR2 expressie levels en de daaruit volgende verhoogde opname van [^{177}Lu]Lu-DOTATATE in muizen met een tumor afgeleid van de humane kleincellig longcarcinoom cellijn NCI-H69. Deze cellijn wordt gekenmerkt door hoge SSTR2 expressie. Eerst hebben wij bevestigd dat VPA behandeling leidt tot een verhoogde expressie van SSTR2 in deze cellijn *in vitro.* Deze verhoging werd snel na start van de behandeling geïnduceerd. Volgend op de positieve *in vitro* resultaten, werd het effect van een enkele VPA injectie *in vivo* in NCI-H69-tumordragende muizen onderzocht, waarbij de voornaamste focus lag op de opname van [^{177}Lu]Lu-DOTATATE in de tumor. In deze studie hebben we een lage en een hoge dosis VPA getest en deze volgens twee behandelingsschema's toegediend. Het verschil in de behandelingsschema's was de variatie in de tijd tussen VPA en [^{177}Lu]Lu-DOTATATE injectie, n.l. vier en acht uur. Wanneer VPA vier uur voorafgaand aan het radioactief-gelabeld DOTATATE werd toegediend was de opname niet significant verhoogd in de tumor. De tumoropname van [^{177}Lu]Lu-DOTATATE was wel significant verhoogd wanneer VPA acht uur voor het radioactief-gelabeld SSA werd toegediend. Dit was het geval voor zowel de lage als de hoge VPA dosis. De oorzaak bleek echter geen verhoging van de SSTR2 expressie, maar waarschijnlijk was dit het gevolg van nierschade en een daarmee geassocieerde verlengde [^{177}Lu]Lu-DOTATATE bloedcirculatietijd.

Aangezien VPA niet resulteerde in verhoging van SSTR2 *in vivo* bij muizen met NCI-H69 afgeleide tumoren en een hogere VPA dosis niet haalbaar was vanwege de waargenomen nierschade, hebben we vijf andere HDACis getest in ditzelfde diermodel. De resultaten van deze studie worden beschreven in **Hoofdstuk 5**. Muizen ontvingen drie keer op drie opeenvolgende dagen een HDACi injectie, gevolgd door een injectie met radioactief-gelabeld SSA twee uur na de laatste HDACi injectie. Hoewel behandeling met de HDACis mocetinostat, CI-994 en panobinostat (PAN) de tumorale *SSTR2* mRNA expressie verhoogde, en de SSTR2 eiwitexpressie significant verhoogd was na CI-994 behandeling, resulteerde dit in geen van de gevallen in een verhoogde tumoropname van radioactief-gelabeld DOTATATE. Om deze bevindingen te bevestigen en om uit te sluiten dat de resultaten afhankelijk zijn van het gebruikte muismodel, werd het effect van PAN ook getest in BON-1-tumordragende dieren. De *in vitro* effecten geïnduceerd na PAN behandeling waren duidelijk sterker in BON-1 cellen dan in NCI-H69 cellen. Desondanks vertoonden BON-1-tumordragende dieren behandeld met PAN ook geen significante toename in tumoropname van het radioactief-gelabeld DOTATATE. In overeenstemming met de resultaten waargenomen in de NCI-H69-tumordragende muizen, was de *SSTR2* mRNA expressie ook verhoogd in BON-1-

tumordragende dieren na HDACi behandeling, maar waren er geen effecten op eiwitniveau. Om deze bevindingen beter te interpreteren, onderzochten we de *SSTR2* en *HDAC* mRNA expressie in NCI-H69 en BON-1 xenograften. Ons onderzoek wees uit dat BON-1 tumoren zes van de elf onderzochte HDACs significant hoger tot expressie brengen dan NCI-H69 tumoren. Vervolgens werden expressieniveaus van deze zes HDACs en SSTR2 gemeten in NCI-H69, BON-1, NCI-H727 en GOT1 cellen. Een correlatieanalyse tussen de hoeveelheid HDAC en SSTR2 expressie resulteerde in een significant negatieve correlatie tussen *HDAC3* en *SSTR2* mRNA, wat suggereert dat HDAC3 mogelijk betrokken is bij het reguleren van SSTR2 expressie. Ondanks het feit dat deze HDAC significant hoger tot expressie werd gebracht in BON-1 tumoren in vergelijking tot het expressieniveau gevonden in NCI-H69 tumoren, werd er geen verhoogde opname van radioactief-gelabeld SSA gevonden na PAN behandeling, wat benadrukt dat verder onderzoek nodig is, zoals het verder optimaliseren van het HDACi behandelingsschema door de dosis en/of de tijdsduur van de behandeling aan te passen, of een aanpak te ontwikkelen waarbij de epigenetische medicijnen gericht naar de tumor worden gebracht. Bovendien zou het verder ontrafelen van de relatie tussen SSTR2 en HDACs nieuwe inzichten kunnen geven die deze toekomstige studies vereenvoudigen.

In **Hoofdstuk 6** is geprobeerd een beter inzicht te krijgen in de epigenetische markers die betrokken kunnen zijn bij het reguleren van de SSTR2 expressie in goed gedifferentieerde dunne darm NETs. Hiervoor is gekeken naar de mate van DNA methylatie, en histon methylatie en acetylatie in de SSTR2 promoter regio van zowel normaal dunne darmweefsel als dunne darm NETs. In vergelijking tot normaal dunne darmweefsel, werd in NET weefsel een lager niveau DNA methylatie en histon methylatie gevonden. Bovendien werd er, voor zowel gezond dunne darmweefsel als voor dunne darm NETs, een significante negatieve correlatie gevonden tussen *SSTR2* mRNA expressie levels en de gemiddelde DNA methylatie op CpG posities in de SSTR2 promoter regio. Er werd geen correlatie gevonden tussen SSTR2 expressie en de remmende histon methylatie marker H3K27me3 of de stimulerende histon acetylatie marker H3K9ac. Dit suggereert dat vooral DNA methylatie van de SSTR2 promoter regio betrokken is bij het reguleren van SSTR2 expressie in zowel normaal dunne darmweefsel als in dunne darm NETs. De rol van histon modificaties in het reguleren van SSTR2 expressie in dunne darm NETs moet echter nog verder onderzocht worden.

Hoofdstuk 7 beschrijft de resultaten van een prospectieve klinische *proof-of-concept* studie. In deze studie is het effect van de epigenetische medicijnen VPA (HDACi) en hydralazine (DNA-methyltransferase remmer) getest op de tumorale opname van radioactief-gelabeld SSA in negen NET patiënten met tumoren gekarakteriseerd door een lage opname van radioactief-gelabeld DOTATATE. Met behulp van een PET/CT scan werd de opname van [^{68}Ga]Ga-DOTATATE voor en na behandeling met de epigenetische medicijnen vergeleken. Er was geen significant verhoogde opname meetbaar in de tumoren na epigenetische behandeling. De reden voor de afwezigheid van een effect blijft onduidelijk en vervolgonderzoek is nodig om dit te ontrafelen. In dit toekomstig onderzoek moet rekening gehouden worden met de

veiligheid van bovenbeschreven combinatie aangezien een significante toename in het radioactieve signaal werd gemeten in de nieren na epigenetische behandeling.

Hoofdstuk 8 is een samenvatting van de meest essentiële bevindingen van de bovengenoemde onderzoeken en plaatst deze bevindingen in een breder perspectief. Ook worden toekomstperspectieven en aanbevelingen voor vervolgonderzoek besproken.

CURRICULUM VITAE

Maria Johanna (Ilva) Klomp was born on December 23rd, 1993 in 's-Hertogenbosch. In 2012, she graduated from her pre-university education at the Sint Janslyceum, 's-Hertogenbosch, and started with her B.Sc. studies in Molecular Life Sciences at the Radboud University, Nijmegen. After obtaining her B.Sc. degree in 2015, she continued with the M.Sc. education Molecular Life Sciences specializing in Clinical Biology. During this two-year education program, she performed two internships. The first internship was at the Department of Urology at the Radboud University Medical Center, Nijmegen, under the supervision of Dr. Silvia Mihaila and Dr. Egbert Oosterwijk. The objective of this project was to obtain and characterize cell-made extracellular matrices, followed by investigating the cellular responses to these matrices in the context of urinary tissue engineering. Her second internship was at the Biological Soft Matter group at the AMOLF institute, Amsterdam, under the supervision of Prof. dr. Gijsje Koenderink, Dr. Federica Burla and Dr. Christina Martinez Torres. Here, she focused on cell-matrix interactions in tunable fibrin-collagen hybrid networks in order to obtain information about the fibroblast-mediated remodeling of these networks, to gain a better insight into this process taking place during wound healing. During these internships, she discovered a great interest for translational, biology-oriented research. For this reason, she started as a Ph.D. student at the Erasmus Medical Center, Rotterdam, in December 2018. Her work was carried out at the Department of Internal Medicine, under the supervision of Prof. dr. Leo Hofland, and at the Department of Radiology and Nuclear Medicine, under the supervision of Prof. dr. ir. Marion de Jong, Dr. Simone Dalm and Prof. dr. Clemens Löwik. This project focused on elucidating the role of the epigenetic machinery in regulating somatostatin type-2 receptor expression, which forms an important target for peptide receptor radionuclide therapy in neuroendocrine tumor patients. The overall aim was to enhance the expression of the target receptor by modulating the epigenetic machinery. This thesis describes the findings of this research.

LIST OF PUBLICATIONS

Applying HDACis to Increase SSTR2 Expression and Radiolabeled DOTATATE Uptake: From Cells to Mice.
(Submitted, Life Sciences)
Klomp MJ, van den Brink, L, van Koetsveld PM, de Ridder CMA, Stuurman DC, Löwik CWGM, Hofland LJ, Dalm SU.

Epigenetic Regulation of SST2 Expression in Small Intestinal Neuroendocrine Tumors.
(Frontiers in Endocrinology, 2023)
Klomp MJ*, Refardt J*, van Koetsveld PM, Campana C, Dalm SU, Dogan F, van Velthuysen MF, Feelders RA, de Herder WW, Hofland J, Hofland LJ.
* Contributed equally and share first authorship

Effect of Epigenetic Treatment on SST_2 Expression in Neuroendocrine Tumour Patients.
(Clinical and Translational Medicine, 2022)
Refardt J, Klomp MJ, van Koetsveld PM, Dogan F, Konijnenberg M, Brabander T, Feelders RA, de Herder WW, Hofland LJ, Hofland J.

The Effect of VPA Treatment on Radiolabeled DOTATATE Uptake: Differences Observed *In Vitro* and *In Vivo*.
(Pharmaceutics, 2022)
Klomp MJ, Hofland LJ, van den Brink L, van Koetsveld PM, Dogan F, de Ridder CMA, Stuurman DC, Clahsen-van Groningen MC, de Jong M, Dalm SU.

Comparing the Effect of Multiple Histone Deacetylase Inhibitors on SSTR2 Expression and [^{111}In]In-DOTATATE Uptake in NET Cells.
(Cancers, 2021)
Klomp MJ, Dalm SU, van Koetsveld PM, Dogan F, de Jong M, Hofland LJ.

Epigenetic Regulation of Somatostatin and Somatostatin Receptors in Neuroendocrine Tumors and other Types of Cancer.
(Reviews in Endocrine and Metabolic Disorders, 2021)
Klomp MJ, Dalm SU, de Jong M, Feelders RA, Hofland J, Hofland LJ.

PORTFOLIO

Courses and Workshops	Year	ECTS
Radiation Protection Course	2018	0.5
Workshop on Photoshop and Illustrator CS6	2019	0.3
Introduction in GraphPad Prism Version 7	2019	0.3
Translational Imaging Workshop by AMIE: from Mouse to Man	2019	1.4
Nederlandse Klinisch Radiochemische Vereniging Workshop	2019	0.3
Biomedical English Writing Course	2021	2.5
Research Integrity	2021	0.3
Excel Visual Basic	2021	0.3
Personal Leadership and Communication	2021	1.0
Gene Expression Data Analysis using R: How to Make Sense out of your RNA-Sequencing/Microarray Data	2021	2.0

Congresses	Presentation	Year	ECTS
Molecular Medicine Molmed Day	-	2019	0.3
Internal Medicine Science Days	-	2019	2.0
	Poster presentation	2020	
	Poster presentation	2022	
European Association of Nuclear Medicine, EANM	Poster	2019	6.0
	Oral (online) presentation	2021	
	Oral (Online) presentation	2020	
	Oral presentation	2022	
European Society of Endocrinology, ECE	-	2020	0.3
The Neuroendocrine Tumor Research Foundation Research Symposium, NETRF	-	2020	0.3
The European Neuroendocrine Tumor Society, ENETS	Poster	2020	2.0
	-	2022	
Biomedical Science Day	-	2022	0.3

Other activities	Year	ECTS
Organizing Erasmus MC PhD day	2019	0.5
Supervising students	2020 – 2022	10
Journal Club, Radiology and Nuclear Medicine	2020 - 2023	0.6
Blog writing for RPO Scientific, "Episode 3, Radionuclides of choice"	2021	0.2
PhD Wellbeing Working Group, Radiology and Nuclear Medicine	2021 - 2022	0.6

Total ECTS: **32**

A

DANKWOORD

En dan is het nu tijd voor het laatste gedeelte van dit proefschrift, het dankwoord. Ik heb de afgelopen jaren als bijzonder, leuk en heel leerzaam ervaren, en daar wil ik een aantal mensen graag voor bedanken.

Als eerste wil ik graag mijn promotoren **prof. dr. Leo Hofland, prof. dr. ir. Marion de Jong** en **prof. dr. Clemens Löwik** bedanken.

Beste Leo, ik kan me het begin van het eerste sollicitatiegesprek nog goed herinneren. Ondanks dat ik een glas water over de tafel omgooide en vervolgens vroeg of er gerenoveerd werd, maar dit gewoon de staat van het EE-gebouw bleek te zijn, kreeg ik toch de kans om te starten aan dit PhD traject. Ik wil je natuurlijk bedanken voor deze mogelijkheid, en jouw begeleiding en betrokkenheid. Je bent altijd goed op de hoogte geweest van de resultaten. Verder vind ik het bewonderenswaardig hoe je achter jouw ideeën staat en hierin gelooft. Bedankt voor alles de afgelopen jaren!

Beste Marion, via een sollicitatie op een ander project binnen de afdeling kwam het huidige PhD project op mijn pad. Ik heb veel van je mogen leren, zowel over het uitvoeren van onderzoek als over de onderzoekswereld in het algemeen. Helaas hebben we maar tweeënhalf jaar in deze samenstelling mogen werken, ik had gehoopt dat dit langer had mogen duren. Bedankt voor het verwelkomende gevoel en de prettige sfeer in jouw groep, jouw eerlijkheid en betrokkenheid, en grappige anekdotes.

Beste Clemens, bedankt voor jouw bijdrage in de laatste fase van mijn promotieperiode. Ik heb het contact dat we hebben gehad als prettig ervaren. Bedankt voor de input en jouw bijdrage aan dit proefschrift.

Natuurlijk wil ik ook mijn copromotor **dr. Simone Dalm** bedanken. Beste Simone, wat was het fijn om vanaf het begin iemand te hebben om bij terecht te kunnen! Ik heb onze interactie en samenwerking altijd als enorm prettig ervaren. Niet alleen heb je me alles geleerd rondom de nucleaire technieken en het uitvoeren van dierexperimenten, je hebt me met veel meer geholpen dan dat. Er was altijd ruimte om twijfels en onzekerheden te uiten, en de aandacht voor het individuele persoon heeft zeker aan mijn persoonlijke ontwikkeling bijgedragen. Ik hoop dat meer mensen dit in de toekomst binnen jouw groep mogen ervaren! Verder creëerden bepaalde vragen, ook al vond ik ze niet altijd even leuk, soms toch een stuk bewustwording of trok het mijn kop, die diep, diep in het zand zat, eruit. Bedankt voor de afgelopen jaren, en natuurlijk ook voor de mogelijkheid om voorlopig nog even binnen jouw groep te blijven.

Ook wil ik de leden van mijn leescommissie, **prof. dr. John Martens**, **prof. dr. Annemarie Dingemans** en **dr. Daniëlle Vugts**, bedanken voor het beoordelen van mijn proefschrift. Additionally, I would like to thank **prof. dr. Melpomeni Fani**, **prof. dr. Wouter de Herder** en

dr. Sophie Veldhuijzen van Zanten for participating in the committee. I'm looking forward to discuss the results of this thesis with all of you.

Marjolein en Marleen, wat vind ik het bijzonder dat jullie mijn paranimfen zijn! Lieve **Marjolein**, we zijn dit 'avontuur' gelijktijdig gestart, en nu zullen we ook beide dit hoofdstuk binnenkort afsluiten. Alhoewel deze gelijktijdige start zorgde voor een 'gemakkelijke connectie', ben ik blij dat we over de jaren heen bevriend zijn geraakt. Jouw zorgzame, sociale en sterke karakter zorgde ervoor dat ik altijd bij je terecht kon om te sparren of te ventileren. Ook de twee schrijfweekenden waren een welkome afwisseling. Maar daarnaast kijk ik ook met een grote glimlach terug het jaarlijkse VVAL (ik hoop dat we deze erin kunnen houden!) of gewoonweg een simpele spelletjesavond. Je bent een topper, en ik wens je het beste! Lieve **Marleen**, we leerden elkaar kennen tijdens de introductie van de studie. We vonden elkaar snel en konden lang speculeren of we wel de juiste studie gekozen hadden. Gelukkig hebben we ondertussen op deze vraag eindelijk een antwoord. Voor mijn gevoel zit het altijd goed tussen ons, en ik vind het fijn dat we kunnen lachen met elkaar! Hoop dat er nog vele weekendjes weg, vakanties en feestjes zullen volgen, en wie weet zit een congres er ook nog wel in nu we in hetzelfde vakgebied zitten. Ik ben heel blij met onze vriendschap en hoop dat dit nooit zal veranderen!

Dan wil ik ook graag collega's van de afdeling Interne Geneeskunde bedanken.

Peter, we hebben de afgelopen jaren veel contact gehad over het onderzoek. Dank voor jouw input en het delen van al jouw ervaring. Na een overleg waarbij we data bespraken die niet naar wens of verwachting waren, waarbij ik soms wat gedemotiveerd kon raken, vertelde je me vaak dat dit onderdeel was van het proces. Ik kan de afbeelding die boven jouw bench hangt met de hoge pieken en diepe dalen zo voor de geest halen. Verder zorgt jouw aanwezigheid voor een gezellige sfeer op het lab! **Fadime**, je bent altijd bereid om iets uit te leggen of mee te denken. Ik heb bewondering voor hoe secuur je te werk gaat. Bedankt voor al jouw hulp! **Rosanna**, onze gedeelde voorliefde voor ABBA zorgde ervoor dat ik altijd wist welke muziek op te zetten! Ook hebben we, voornamelijk de eerste twee jaar, veel naast elkaar in de kweek gezeten en hier hebben we aardig wat gekletst. Bedankt voor de gezelligheid. **Anand**, jouw antwoorden op mijn PCR-gerelateerde vragen en jouw hulp rondom de problemen met de gelelektroforese tijdens de CHIP-analyse hebben enorm geholpen, bedankt daarvoor! **Annelies**, ook jou wil ik bedanken, zowel voor hulp bij praktische zaken, als voor de organisatie van allerlei sociale activiteiten!

Dear **Ticiana** and **Julie**, the three of us together shared the office for about two and a half years. In the beginning, because of our age difference, I was a bit afraid that both of you would not be in for fun. But, damn.. I was wrong haha! We quickly developed a personal connection and I could share everything with the two of you. Ticiana, you taught me a great lesson in hospitality. You have a warm personality and besides that, you are a great, hardworking scientist with a keen eye for detail as well. I also think it is admirable how you decided to move

with your entire family to The Netherlands and the US. I hope a trip to Boston will happen soon! Julie, I can still remember how we were learned the ropes in the lab together. You have an energetic and attentive personality, and with that you could sometimes put the finger on the sore spot. But I feel like that helped me grow! I'm also very happy that we could work together with the project on epigenetics in SI-NETs, and that we were able to finish that never-ending study. So exciting that you decided to come back to the Netherlands again! Dear **Claudia**, you are a kind, honest and curious person. I feel that we became even closer when we started sharing the office. I feel like we could talk about everything, both work-related and about personal life. It really made my time on EE5 much better. You also showed me that personal growth can be much more than you may think yourself. Crazy enough, I have never visited Italy before, so I will visit you soon for sure! Dear **Noémie**, whether it is with an Aperol Spritz on your balcony at the beginning of COVID or during a cringy word joke, you always bring lots of cheerfulness and energy with you! You are super powerful and I really appreciate how you step up for your opinion. To all of you, I will forever cherish the memories we created together, whether it was a Brazilian BBQ combined with dancing and singing, a music "quiz" on your favorite genre (*"What is your favorite music?!"*) or guessing the title of the song ("*Noémie, this one you know for sure!"*), Swiss Raclette, a trip to Basel with a near-death experience on a mountain, karaoke or a visit to the Gorinchem Castle. When I first panicked a bit when this topic was discussed ("*I have to find my AH plastic bag"*), I can now easily say that I'm super grateful that we became friends! Thank you all for everything!

Daarnaast wil ik ook graag alle andere (ex)collega's van de 5e bedanken. **Anela** en **Amber**, ik heb jullie leren kennen aan het begin van mijn PhD. Bedankt voor het verwelkomende gevoel, het delen van jullie ervaringen, en de gezelligheid op het lab en tijdens de lunch! **Merijn**, ook wij hebben lange tijd het kantoor gedeeld. Al duurde het misschien even voordat we een band kregen, de sfeer is altijd goed geweest. Bedankt daarvoor, ook voor het bieden van een luisterend oor wanneer nodig. En natuurlijk succes met het afronden van jouw PhD! **Charlotte** en **Eva**, de tijd die we samen op het lab rond hebben gebracht is relatief kort geweest, maar jullie frisse energie heeft de groep goed gedaan. Ik wens jullie beiden succes met jullie carrière. **Robin**, bedankt voor jouw gezelligheid, zowel op het lab als tijdens de lunch. Je hebt een hartelijke, lieve persoonlijkheid, en wij vonden elkaar vaak in onze wensen en leerdoelen. Én ik weet bij wie ik terecht kan voor input voor een tattoo artiest haha! Ook de overige collega's op de 5e etage, **Susanne, Eline** en **Mostafa**, dank jullie wel, het gaat jullie allen goed!

Ook wil ik graag iedereen aanwezig bij het voormalige **NETwerk overleg** en het huidige **NET PhD overleg** bedanken, in het bijzonder **prof. dr. Wouter de Herder**, **dr. Hans Hofland**, **dr. Richard Feelders** en **dr. Julie Nonnekens**. Jullie input en kritische vragen hebben zeker bijgedragen! Ook vond ik het heel leerzaam om in deze overleggen vanuit een meer klinisch perspectief naar de huidige problematiek rondom NETs en het lopende onderzoek te kijken.

Naast alle fijne contacten bij de afdeling Interne Geneeskunde, heb ik het geluk gehad ook bij de afdeling Radiologie en Nucleaire Geneeskunde veel mensen te leren kennen.

Allereerst wil ik alle collega's binnen de **Radiotracer Interactions Group** bedanken. Ik heb me altijd bij jullie thuis gevoeld en ik besef me goed dat ik hier heel dankbaar voor mag zijn. Heel erg bedankt voor de gezelligheid, alle lunchpauzes, de nuttige input en de open werksfeer. **Lilian**, wat heb jij me vaak geholpen, eerst als stagiair op het project en later als analist. Je bent een toegewijde en betrouwbare collega, en niks is je te gek! Het hielp enorm om soms, nadat de H69 uptake wéér onverwachte problemen gaf, samen even te balen om vervolgens weer met frisse moed verder te gaan. Ik wil je enorm bedanken, je bent een kanjer! **Lisette**, je bent een enorm lieve en behulpzame collega. Ik vind het fijn dat we altijd kunnen kletsen, en ik hoop dat je nog veel jaren met heel veel plezier op het CIL zult werken. **Circe**, wat was het aangenaam om, nadat jij bij de groep kwam, niet meer de grootste chaoot te zijn haha. Bedankt voor alle leuke borreltjes, je open houding en kritische blik, en de zangsessies in het CIL! **Tyro**, ik vind het tof hoe jij vaak je eigen plan trekt, daar zou menig ander nog iets van kunnen leren. Succes met de laatste loodjes en veel plezier met de mooie plannen die voor het komende jaar gepland staan! **Marjolein**, dat je paranimf bent zegt denk ik al genoeg! **Eline**, ik heb altijd bewondering gehad voor hoe je jouw sterke mening zelfverzekerd en vastberaden kunt communiceren. En wat was het leuk om paranimf bij jouw promotie te zijn. Als ik ervoor zou kunnen tekenen om het net zoals jou te doen, doe ik dat zonder twijfel. Ik ben benieuwd wat de toekomst je gaat brengen, maar ik ben ervan overtuigd dat dit heel veel moois gaat zijn! **Joana**, I'm happy that we have gotten to know each better during the (short) period we shared the same office. I wish you all the best with your career.

Corrina en **Debra**, wat had ik zonder jullie gemoeten tijdens de *in vivo* studies. Ik kijk met enorm veel plezier op deze dagen terug, zelfs de squats door de gehele gang van het CIL zullen niet vergeten worden. Enorm bedankt voor jullie harde werk, jullie geduld wanneer ik het tijdschema op de minuut nauwkeurig wilde volgen én natuurlijk de gezelligheid! Jullie zijn twee toppers!

Thom en **Danny**, ik ben vaak bij jullie geweest voor hulp bij bepaalde technieken of voor NET-specifiek advies, dank daarvoor! Verder hebben jullie zelfverzekerde houding en de kritische vragen tijdens het voormalige TRACER overleg mij ook geholpen om keuzes te verdedigen en zelfverzekerder te worden over mijn eigen onderzoek en resultaten. **Stefan**, ook jou moet ik hiervoor bedanken! Bedankt voor al jullie hulp, maar natuurlijk ook de gezelligheid tijdens borrels! **Nina**, ook jij bedankt, onder andere voor de leuke tijd tijdens de ENETS in Barcelona en de Interne Wetenschapsdagen!

Ook wil ik graag de gehele **Radiopharmaceutical Chemistry Group** bedanken voor de DOTATATE labelingen die heel wat experimenten mogelijk hebben gemaakt. To everyone of this group, a big thanks, especially to **Erika** and **Maryana**, both for the frequent labelings and interactions during social events. **Savanne,** ik vind het fijn dat wij het laatste jaar regelmatig gelijktijdig in het CIL hebben gestaan! En je wijze les, iets met min en min maakt plus, zal ik onthouden haha!

Dr. Erik de Blois, beste Erik, je was altijd bereid mee te denken over *in vivo* experimenten of te helpen bij berekeningen als het weer eens niet zo soepel ging, bedankt hiervoor!

Jan, bedankt voor alle lunchgesprekken en jouw aanwezigheid in het CIL. **Monique**, **Sandra** en **Joost**, jullie wil ik ook bedanken voor de hulp vanuit de **AMIE**, maar ook zeker voor de gezelligheid, onder andere tijdens de EANM congressen! Verder zal ik ook niet snel vergeten hoe warm het welkom voelde op de 25e aan de start van mijn PhD. Dank jullie wel hiervoor!

Additionally, I would also like to thank all other (ex)colleagues for creating a nice ambience in the CIL, for their valuable input during the Joint meeting and for all the fun during social events. Verder wil ik natuurlijk ook alle overige co-auteurs bedanken voor jullie bijdrage en input aan het onderzoek.

Naast de vele collega's zijn er natuurlijk ook vrienden en familieleden die ik hier graag wil bedanken.

Allereerste, lieve **mama**, **papa**, **Jesse**, **Jante** en **oma**, het is altijd fijn om weer even in Vught te zijn, alhoewel het ook niet te lang moet duren haha! Ma en pa, jullie hebben me altijd gestimuleerd om ergens voor te gaan en er iets moois van te maken, een erg waardevolle eigenschap! Jesse en Jante, jullie zijn twee lieverds, en ik vind het altijd fijn om bij jullie te zijn! Oma, ik vind het heel bijzonder dat je ondanks je leeftijd toch goed op de hoogte bent van wat er allemaal speelt. Ik kijk uit naar de promotie om jullie allemaal een inkijkje te geven waar ik de afgelopen jaren aan heb gewerkt. Ik zeg dit eigenlijk nooit omdat jullie het tóch wel weten, maar ik hou van jullie!

Dan mijn lieve vrienden en vriendinnen. Vughtse en Bossche vriendinnen, **Britt**, **Eline**, **Lotte**, **Marleen** en **Nicole**, ik ken jullie al heel erg lang, jullie hebben allemaal een speciaal plekje in mijn hart! Lieve (ex)Nijmegenaren **Anne**, **Annika**, **Irene**, **Jolanda**, **Jorryt**, **Marleen** en **Sander**, we kennen elkaar al sinds de bachelor en ik ben blij dat we nog steeds contact met elkaar hebben. Ik kan altijd bij jullie terecht en jullie begrijpen als geen andere de struggles die soms bij een PhD komen kijken. Wat is het fijn om het daar over te kunnen hebben met mensen uit een (net iets) ander veld. Ik hoop jullie nog lang in mijn leven te hebben! Lieve **Daniëlle**, **Karlijn**, **Marleen**, **Merel** en **Saskia**, onze eerste kipburger tijdens Expeditie Robinson is ondertussen al zo'n zeven, of misschien zelfs wel acht jaar geleden, dat zegt denk ik al genoeg! Of het nu om een oud-en-nieuw feestje gaat, een simpel etentje of ons jaarlijkse weekendje weg, het zit altijd goed! Heel erg bedankt voor jullie vriendschap!